An original deliverable submitted to the

Florida Department of Transportation

by the

Texas A&M Transportation Institute

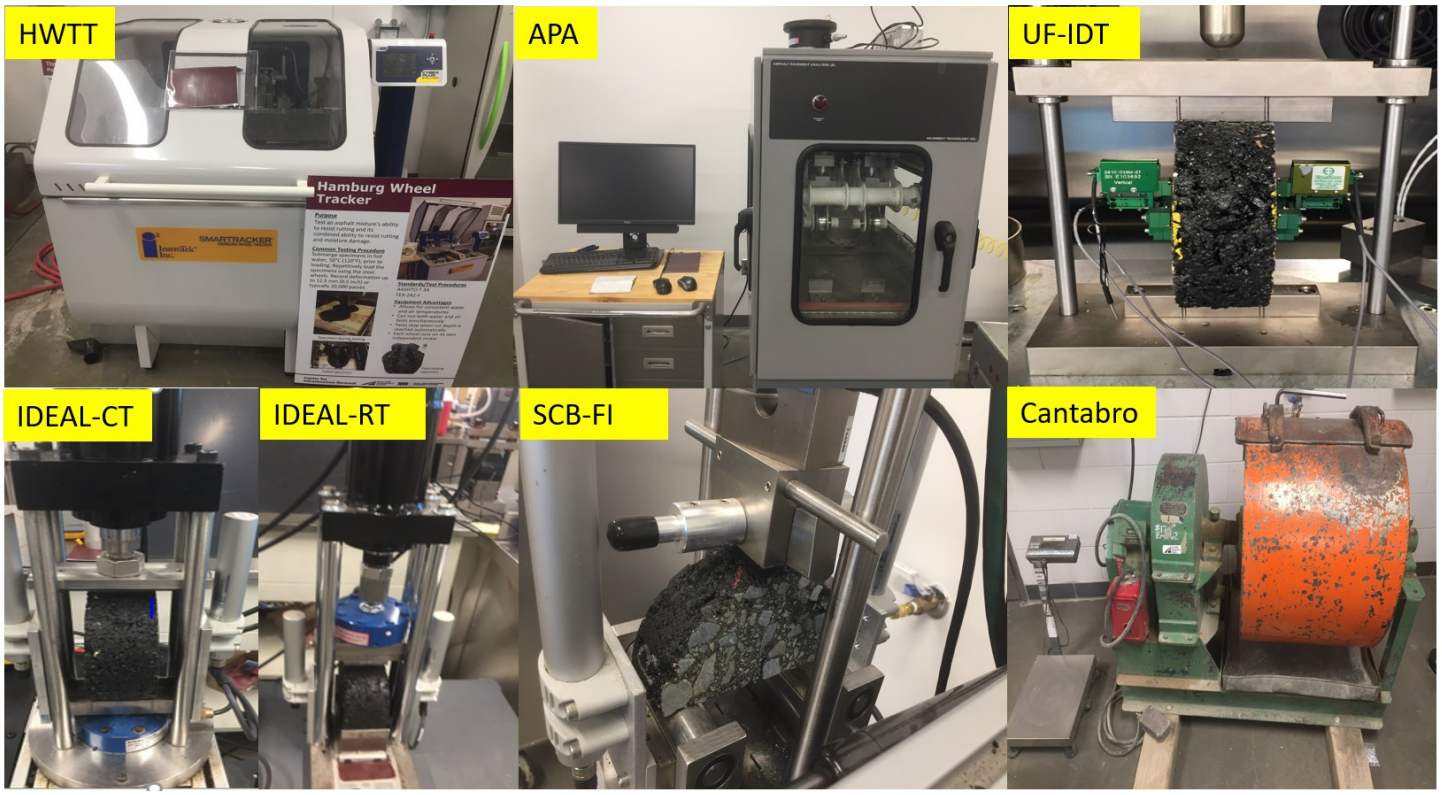

BE928
PERFORMANCE EVALUATION OF SP-9.5 AND SP-12.5 SUPERPAVE MIXTURES

Deliverable 5: Final Report
June 30, 2022

Authors:

Sheng Hu, Ph.D., P.E.
Fujie Zhou, Ph.D., P.E.

Texas A&M Transportation Institute

DISCLAIMER

The opinions, findings, and conclusions expressed in this publication are those of the authors and not necessarily those of the Florida Department of Transportation.

METRIC CONVERSION CHART

SI* (MODERN METRIC) CONVERSION FACTORS

APPROXIMATE CONVERSIONS TO SI UNITS

Symbol	When You Know	Multiply By	To Find	Symbol
		LENGTH		
in	inches	25.4	millimeters	mm
ft	feet	0.305	meters	m
yd	yards	0.914	meters	m
mi	miles	1.61	kilometers	km
		AREA		
in^2	square inches	645.2	square millimeters	mm^2
ft^2	square feet	0.093	square meters	m^2
yd^2	square yard	0.836	square meters	m^2
ac	acres	0.405	hectares	ha
mi^2	square miles	2.59	square kilometers	km^2
		VOLUME		
fl oz	fluid ounces	29.57	milliliters	mL
gal	gallons	3.785	liters	L
ft^3	cubic feet	0.028	cubic meters	m^3
yd^3	cubic yards	0.765	cubic meters	m^3
	NOTE: volumes greater than 1000 L shall be shown in m^3			
		MASS		
oz	ounces	28.35	grams	g
lb	pounds	0.454	kilograms	kg
T	short tons (2000 lb)	0.907	megagrams (or "metric ton")	Mg (or "t")
		TEMPERATURE (exact degrees)		
°F	Fahrenheit	5 (F-32)/9 or (F-32)/1.8	Celsius	°C
		ILLUMINATION		
fc	foot-candles	10.76	lux	lx
fl	foot-Lamberts	3.426	candela/m^2	cd/m^2
		FORCE and PRESSURE or STRESS		
lbf	poundforce	4.45	newtons	N
lbf/in^2	poundforce per square inch	6.89	kilopascals	kPa

APPROXIMATE CONVERSIONS FROM SI UNITS

Symbol	When You Know	Multiply By	To Find	Symbol
		LENGTH		
mm	millimeters	0.039	inches	in
m	meters	3.28	feet	ft
m	meters	1.09	yards	yd
km	kilometers	0.621	miles	mi
		AREA		
mm^2	square millimeters	0.0016	square inches	in^2
m^2	square meters	10.764	square feet	ft^2
m^2	square meters	1.195	square yards	yd^2
ha	hectares	2.47	acres	ac
km^2	square kilometers	0.386	square miles	mi^2
		VOLUME		
mL	milliliters	0.034	fluid ounces	fl oz
L	liters	0.264	gallons	gal
m^3	cubic meters	35.314	cubic feet	ft^3
m^3	cubic meters	1.307	cubic yards	yd^3
		MASS		
g	grams	0.035	ounces	oz
kg	kilograms	2.202	pounds	lb
Mg (or "t")	megagrams (or "metric ton")	1.103	short tons (2000 lb)	T
		TEMPERATURE (exact degrees)		
°C	Celsius	1.8C+32	Fahrenheit	°F
		ILLUMINATION		
lx	lux	0.0929	foot-candles	fc
cd/m^2	candela/m^2	0.2919	foot-Lamberts	fl
		FORCE and PRESSURE or STRESS		
N	newtons	0.225	poundforce	lbf
kPa	kilopascals	0.145	poundforce per square inch	lbf/in^2

*SI is the symbol for the International System of Units. Appropriate rounding should be made to comply with Section 4 of ASTM E380.
(Revised March 2003)

TECHNICAL REPORT DOCUMENTATION PAGE

1. Report No.	2. Government Accession No.	3. Recipient's Catalog No.
4. Title and Subtitle PERFORMANCE EVALUATION OF SP-9.5 AND SP-12.5 SUPERPAVE MIXTURES		5. Report Date June 2022 6. Performing Organization Code
7. Author(s) Sheng Hu and Fujie Zhou		8. Performing Organization Report No.
9. Performing Organization Name and Address Texas A&M Transportation Institute The Texas A&M University System 3135 TAMU College Station, TX 77843-3135		10. Work Unit No. (TRAIS) 11. Contract or Grant No. BE928
12. Sponsoring Agency Name and Address Florida Department of Transportation 605 Suwannee Street, MS 30 Tallahassee, FL 32399		13. Type of Report and Period Covered Final Report July 2020–June 2022 14. Sponsoring Agency Code
15. Supplementary Notes		

16. Abstract

Current Florida Department of Transportation specifications allow the use of Superpave (SP)-12.5/Friction Course (FC)-12.5 mixtures in heavy traffic levels (e.g., level E), but not SP-9.5/FC-9.5 mixtures. The main goal of this project is to compare the performance of SP-9.5/FC-9.5 to SP-12.5/FC-12.5 Superpave asphalt mixtures and then determine if SP-9.5/FC-12.5 mixtures are at least equivalent to SP-12.5/FC-12.5 mixtures in terms of cracking, rutting resistance, and durability. To achieve this goal, a full factorial experiment was designed and executed. This experiment includes 24 mixture designs (i.e., two gradations [SP-9.5 and SP-12.5], two aggregate types [granite and limestone], two binder grades [PG 67-22 and PG 76-22], and three design gyrations [50, 75, and 100]). For each mixture, specimens were prepared at two compaction levels (or air voids [5 percent and 7 percent]), and seven performance tests were conducted. The test results were summarized in tables and bar charts, showing their averages and standard deviations. Statistical analysis was performed based on the paired t-test to compare the performance between SP-9.5 and SP-12.5 mixtures. The results show only limestone SP-9.5 PG 67-22 mixtures have worse rutting performance than the corresponding SP-12.5 mixtures. Other SP-9.5 mixtures, such as granite (PG 67-22 or PG 76-22) and limestone (PG 76-22), show equivalent or better performance (rutting, cracking, and durability) than the corresponding SP-12.5 mixtures.

17. Key Words Asphalt Mixture Stability; Anti-Strip Agents	18. Distribution Statement No restrictions.		
19. Security Classif. (of this report)	20. Security Classif. (of this page)	21. No. of Pages 175	22. Price

Form DOT F 1700.7 (8-72) Reproduction of completed page authorized.

ACKNOWLEDGMENTS

The authors would like to extend their gratitude to Florida Department of Transportation project manager Wayne Rilko, panel members Howard Moseley, Greg Sholar, and Jesus Caballero for their great support and guidance throughout the execution of this project. Gratitude is also extended to Pravat Karki for his serving as Co-PI, contributions to the literature review, and other invaluable supports when working at TTI.

Appreciation is also extended to TTI researchers Zeinab Mraiza, Ethan Karnei, Tony Barbosa, and Rick Canatella for their assistance in laboratory-related activities. Finally, the authors are thankful to the suppliers of aggregates, asphalt binder, and anti-strip agents used to execute the experimental plan of this project.

EXECUTIVE SUMMARY

Current Florida Department of Transportation (FDOT) specifications allow the use of Superpave (SP)-12.5/Friction Course (FC)-12.5 mixtures in heavy traffic levels (e.g., level E), but not SP-9.5/FC-9.5 mixtures. In contrast, the Georgia Department of Transportation allows SP-9.5 (Type II) and SP-12.5 mm mixtures in medium to heavy traffic levels. The fact that the neighboring department of transportation allows the use of the SP-9.5 mix for medium to heavy traffic levels suggests a similar possibility in Florida. In addition, FDOT contractors often use aggregates from Georgia.

Previous studies have compared the rutting and cracking performance of several SP-9.5/FC-9.5 and SP-12.5/FC-12.5 mixtures using different laboratory tests. These studies in literature showed that the SP-9.5 mixtures could have equivalent, if not better, performance than those SP-12.5 mixtures, but these studies are limited in different ways. It becomes important to conduct a comprehensive study considering different factors (aggregate types, aggregate gradation, binder grades, binder contents, design gyrations, and compaction levels) to determine if SP-9.5/FC-9.5 mixtures and SP-12.5/FC-12.5 mixtures have equivalent performance.

The main goal of this project is to compare the performance of SP-9.5/FC-9.5 to SP-12.5/FC-12.5 Superpave asphalt mixtures and then determine if SP-9.5/FC-12.5 mixtures are at least equivalent to SP-12.5/FC-12.5 mixtures in terms of cracking and rutting resistance, including durability. The project's qualitative and quantitative benefits are below:

- *Validation of currently imposed limitations:* If the performance and durability of the SP-9.5/FC-9.5 mixtures are not even equivalent to the performance and durability of SP-12.5/FC-12.5 mixtures, it will validate the limitation imposed on the use of SP-9.5/FC-9.5 mixtures and require no change in the specifications.
- *Better use of resources and saving cost:* If the performance and durability of the SP-9.5/FC-9.5 mixtures are equivalent to or even better than the performance and durability of SP-12.5/FC-12.5 mixtures, it will invalidate and therefore require the removal of the limitation imposed on the use of SP-9.5/FC-9.5 mixtures. This removal will allow less expensive, smaller aggregates in heavy traffic level applications, which make up 30 percent of FDOT's network, thereby facilitating better use of natural resources and lowering construction costs. The removal of the above restrictions will save not only the construction costs but also the maintenance costs if the durability of the SP-9.5/FC-9.5 mixtures is proved to be better than that of SP-12.5/FC-12.5 mixtures.

To achieve this goal, the researchers conducted a literature search on national, international, and local practices and specifications of SP-9.5/FC-9.5 and SP-12.5/FC-12.5 mixtures and associated pavement rutting, cracking, and durability requirements. The active American Association of State Highway and Transportation Officials and American Society for Testing and Materials test standards, including some recently developed performance tests related to asphalt mixture rutting, cracking, and durability, were collected and reviewed.

The in-depth literature review revealed that there are multiple test methods proposed to evaluate the same type of performance of asphalt binders and asphalt mixtures. Based on the minimum

required features such as simplicity and sensitivity to mixture design variables, including the effect of practicality, repeatability, reproducibility, cost-effectiveness, and field performance correlation, the researchers designed and executed a full factorial experiment. This experiment included 24 mixture designs, i.e., the full factorial combinations of two gradations (SP-9.5 and SP-12.5), two aggregate types (granite and limestone), two binder grades (PG 67-22 and PG 76-22), and three design gyrations (50, 75, and 100). For each mixture, specimens were prepared at two compaction levels (or air voids [5 percent and 7 percent]), and seven performance tests were conducted. The seven performance tests are:

- Ideal cracking tolerance test.
- University of Florida indirect tensile test.
- Semi-circular bending flexibility index test.
- Asphalt pavement analyzer test.
- Hamburg wheel-track test.
- Ideal rutting tolerance test.
- Cantabro abrasion loss test.

The test results were summarized in tables and bar charts, showing their averages and standard deviations. Statistical analysis was performed based on the paired t-test to compare the performance between SP-9.5 and SP-12.5 mixtures.

The test and analysis results show only limestone SP-9.5 PG 67-22 mixtures have worse rutting performance than the corresponding SP-12.5 mixtures. Other SP-9.5 mixtures, such as granite (PG 67-22 or PG 76-22) and limestone (PG 76-22), show equivalent or better performance (rutting, cracking, and durability) than the corresponding SP-12.5 mixtures. Based on this conclusion, the researchers recommended changes to the current FDOT specifications.

TABLE OF CONTENTS

LIST OF FIGURES

LIST OF TABLES

LIST OF ACRONYMS

A

AASHTO American Association of State Highway and Transportation Officials
ADT Annual daily traffic
ALDOT Alabama Department of Transportation
ALF Accelerated loading facility
AMPT Asphalt mixture performance tester
ARZ Above restricted zone
ASTM American Society for Testing and Materials
APA Asphalt pavement analyzer
APT Accelerated pavement test
AV Air void

B

BBR Bending beam rheometer
BRZ Below restricted zone

C

CAL Cantabro abrasion loss
COV Coefficient of variation
CRI Cracking resistance index
CT_{index} Cracking tolerance index

D

$DCSE_f$ Dissipated creep strain energy
DCT Disc-shaped compact tension
DGA Dense-graded asphalt
DOT Department of transportation
DSR Dynamic shear rheometer

E

ER Energy ratio
ESAL Equivalent single axle load

F

FAA Fine aggregate angularity
FC Friction course
FDOT Florida Department of Transportation
FHWA Federal Highway Administration
FI Flexibility index
FN Flow number
FPBBF Four-point bending beam fatigue
FSCH Frequency sweep at constant height
FTIR Fourier transform infra-red

G
GDOT Georgia Department of Transportation
G_f Fracture energy
G_{mm} Theoretical maximum specific gravity
G_{mb} Bulk specific gravity
G_{sb} Aggregate specific gravity
GTR Ground tire rubber
H
HMA Hot-mix asphalt
HVS Heavy-vehicle simulator
HWT Hamburg wheel tracking
I
IDEAL-CT Ideal cracking tolerance test
IDEAL-RT Ideal rutting tolerance test
iRLPD Incremental RLPD
ITS Indirect tensile strength
L
LaDOTD Louisiana Department of Transportation and Development
LVE Linear viscoelastic
M
MDOT Mississippi Department of Transportation
ML Mass loss
M_R Resilient modulus
MSCR Multiple stress creep recovery
MSR Minimum strain rate
N
NAPA National Asphalt Pavement Association
NCAT National Center for Asphalt Technology
NCHRP National Cooperative Highway Research Program
NMAS Nominal maximum aggregate size
O
OGFC Open-graded friction course
OT Overlay tester
P
PAV Pressure aging vessel
Pb Optimum binder content
Pbe Effective binder content
PEM Porous European mix
PG Performance Grade
PMA Polymer-modified asphalt

R
RAP Recycled asphalt pavement
RAS Recycled asphalt shingle
RBBF Repeated bending beam fatigue
RLPD repeated load permanent deformation
RSCH Repeated shear at constant height
RTFO Rolling thin-film oven
RT_{index} Rutting tolerance index
S
SBS Styrene-butadiene-styrene
SCB Semi-circular bending
SCB-FI Semi-circular bending flexibility index
SCB-Jc Semi-circular bending strain energy release rate
SCDOT South Carolina Department of Transportation
SGC Superpave gyratory compactor
SHRP Strategic Highway Research Program
SMA Stone matrix asphalt
SP Superpave
SSCH Simple shear at constant height
SST Simple shear test
SVECD Simplified viscoelastic continuum damage
T
TDOT Tennessee Department of Transportation
TP Product of temperature and pressure
TSR Tensile strength ratio
TTI Texas A&M Transportation Institute
U
UF-IDT University of Florida indirect tensile
V
V_a Air void
VFA Voids filled with asphalt
VMA Voids in mineral aggregates

1. INTRODUCTION

1.1 Background

Superpave (SP)-based dense-graded asphalt (DGA) mixtures can be designed as SP-4.75, SP-9.5, SP-12.5, SP-19.0, SP-25.0, or SP-37.5 mixtures by blending aggregates such that the passing percentages of aggregates in each sieve size, including the nominal maximum aggregate size (NMAS), comply with the lower and upper limits and the mixtures so produced meet the volumetric requirements specified in American Association of State Highway and Transportation Officials (AASHTO) M 323 (2017a). The NMAS refers to the sieve size above the first sieve that retains more than 10 percent aggregate. For example, the NMAS of SP-9.5 and SP-12.5 mix types are 9.5 and 12.5, respectively. The departments of transportation (DOTs) in the United States use more or less the same aggregate gradation (maximum and minimum passing percentages) and mix volumetric requirements as specified in AASHTO M 323 to design their mix types. For example, the Florida Department of Transportation (FDOT) uses the same gradation specified in AASHTO M 323 to design its SP mixtures (FDOT 2020). Section 334-1.1 of the *Standard Specifications for Road and Bridge Construction* (FDOT 2020) lists three mix types. These mix types include Type SP-9.5, Type SP-12.5, and Type SP-19.0 mixtures, which refer to SP mixtures produced with the NMAS of 9.5, 12.5, and 19.0 mm, respectively, that satisfy air void contents of 4.0 percent at the design number of gyrations (N_{design}).

FDOT's *Standard Specifications for Road and Bridge Construction* requires that the friction courses (FCs) with an NMAS of 9.5 and 12. 5 mm (FC-9.5 and FC-12.5, respectively) meet the design (gradation) requirements for SP-9.5 and SP-12.5 mixtures (Sections 337-3.3.2 and 337-3.3.3) (FDOT 2020). Since SP and FC mixtures with the same NMAS are designed with the same requirements of aggregate gradation, this document refers to them together as SP/FC-9.5 and SP/FC-12.5 or simplified as SP-9.5 and SP-12.5.

1.2 Motivation

FDOT's specification (Section 334-1.4.1) (FDOT 2022a) allows the use of Type SP-9.5 mix only in two traffic levels (i.e., traffic levels B and C) and Type SP-12.5 mix in all traffic levels (i.e., traffic levels B, C, and E). Note that the previous version of this specification (FDOT 2020) included traffic levels A and D. Traffic Level A is now combined with B, and Traffic Level D is now combined with E.

However, the Georgia Department of Transportation (GDOT) already allows contractors to use SP-9.5 (Type II) in medium to heavy traffic levels (GDOT 2013). The fact that the neighboring DOT already allows the use of SP-9.5 mix in medium to heavy traffic-level applications and that FDOT gets many of the aggregates from Georgia suggests that a similar use of SP-9.5 might be possible in Florida as well.

Previous studies have suggested that a finer NMAS mix (e.g., SP-4.75 or SP-9.5) might perform equivalent to or better than a coarser NMAS mix (e.g., SP-12.5 mix). For example, Kandhal and Cooley (2002) evaluated the rutting resistance of SP-9.5 and SP-12.5 mixes designed with several combinations of aggregate types and gradations. Based on test results, the authors

reported that the SP-9.5 mix produced with coarse aggregates of granite and fine aggregates of limestone together performed the best among these combinations.

Similarly, Ahmad et al. (2012) showed that the SP-9.5 mixtures exhibited lower rut depths than the SP-12.5 mixtures regardless of whether the mixtures were designed with the Marshall or SP mix design method, underscoring the fact that some SP-9.5 mixtures might have better rutting performance than SP-12.5 mixtures.

Likewise, Greene and Choubane (2016) previously compared the performance of varying thicknesses of the fine-graded SP-4.75 mix with an SP-12.5 (control) mix in FDOT's Accelerated Pavement Test facility. They reported that the SP-4.75 mix had better rutting and cracking resistance than the SP-12.5 mix. The fact that even the SP-4.75 mix performed better than the SP-12.5 mix suggests that a certain thickness of the SP-9.5 mix might perform equivalent to or better than the SP-12.5 mix.

Moreover, West et al. (2018a) investigated low-temperature cracking, intermediate-temperature cracking, and rutting performances of one SP-9.5 mix (Mix 1) and five SP-12.5 mixtures (Mix 2 to Mix 6). The authors reported that the SP-9.5 mix exhibited mostly equivalent low-temperature cracking performance, always better intermediate-temperature cracking performance, and mostly worse rutting performance in comparison to the SP-12.5 mixtures.

All these previous studies showed that there is a possibility for designing some SP-9.5 mixtures that perform at least equivalent to SP-12.5 mixtures. These studies underscore a simple question: can SP-9.5 be equivalent to or better than an SP-12.5 mix?

However, the studies that can unequivocally answer this question are limited in both number and scope. Therefore, a comprehensive study was needed to consider possible factors such as aggregate types, binder grades, mixture design gyrations, compaction levels, and performance tests to address FDOT's concerns.

1.3 Objective

This project's main objective is to compare the performance of SP-9.5 with SP-12.5 asphalt mixtures and then determine if SP-9.5 mixtures are at least equivalent to SP-12.5 mixtures in terms of cracking and rutting resistance, including durability. A full factorial experiment was designed and executed to achieve this objective. The experimental design is as follows:

- Eight mix combinations:
  - Two gradation types (SP-9.5 ad SP-12.5).
  - Two aggregate types (Georgia granite and Florida limestone).
  - Two binder grades (Performance Grade [PG] 67-22 and PG 76-22).
- Three design numbers of gyrations targeting 4 percent air voids (AV):
  - 50 gyrations (corresponding to Traffic Level A).
  - 75 gyrations (corresponding to Traffic Level C).
  - 100 gyrations (corresponding to Traffic Levels D and E).
- Two compaction levels:

  - 93 percent theoretical maximum specific gravity (G_{mm}).
  - 95 percent G_{mm}.
- Seven performance tests:
  - Ideal cracking tolerance (IDEAL-CT) test.
  - University of Florida indirect tensile (UF-IDT) test.
  - Semi-circular bending flexibility index (SCB-FI) test.
  - Asphalt pavement analyzer (APA) test.
  - Hamburg wheel tracking (HWT) test.
  - Ideal rutting tolerance (IDEAL-RT) test.
  - Cantabro abrasion loss (CAL) test.

Thus, there are 24 mixture designs (i.e., eight mix combinations × three design gyrations). For each of the 24 mixtures, two sets of performance test specimens are required—each set represents a different field compaction level: 93 percent G_{mm} (7 percent AV) and 95 percent G_{mm} (5 percent AV). The seven performance test results were summarized, and statistical analysis was performed to compare the performance between SP-9.5 and SP-12.5 mixtures.

1.4 Report Organization

This report is organized in the following:

- Chapter 1 introduces the background and objectives of this project.
- Chapter 2 conducts the literature review, focused on the performance of finer (i.e., SP-9.5/FC-9.5) mixtures compared to coarser (i.e., SP-12.5/FC-12.5) mixtures. Both the test procedures and the results from these tests were reviewed and discussed.
- Chapter 3 describes the full factorial experimental design, material acquisition, and material evaluation.
- Chapter 4 presents the mixture designs.
- Chapter 5 demonstrates the performance test results, performs statistical analysis, and draws conclusions based on the test and analysis results.
- Chapter 6 provides the conclusions and recommendations.
- Appendix A includes the Mixture Design Data Sheets.

2. LITERATURE REVIEW

The researchers searched the literature on national, international, and local practices and specifications of SP-9.5/FC-9.5 and SP-12.5/FC-12.5 mixtures and associated pavement rutting, cracking, and durability requirements. The active AASHTO and American Society for Testing and Materials (ASTM) test standards, including some recently developed performance tests related to asphalt mixture rutting, cracking, and durability, were also collected and reviewed.

2.1 State of Knowledge of SP-9.5 and SP-12.5 Mixtures

This chapter summarizes the types of hot-mix asphalt (HMA) mixtures used in Florida or similar mixtures in its neighboring states, focusing on mixtures similar to FDOT's SP/FC-9.5 and SP/FC-12.5. The chapter also includes the most common asphalt mixture performance (rutting, cracking, and durability) tests in these states. These summaries are directly based on the specifications, test methods, and other official documents published by FDOT and its six neighboring DOTs.

2.1.1 Florida

FDOT's *Standard Specifications for Road and Bridge Construction* (FDOT 2020) specifies in Section 334-1.1 three Superpave DGA mix types for use in its contracts—(a) Type SP-9.5 mix, (b) Type SP-12.5, and (c) Type SP-19.0 mix. The specification also specifies in Section 337-1 three mix types for use in its FC contracts—(a) FC-5 mix, (b) FC-9.5 mix, and (c) FC-12.5 mix. FDOT requires that both SP and FC mixtures with the same NMAS (i.e., SP/FC-9.5 and SP/FC-12.5) follow the same gradation of Superpave mixtures as specified in AASHTO M 323 (Section 334-1.1, Sections 337-3.3.2 and 337-3.3.3).

Traffic level–wise, FDOT's specification (Section 334-1.4.1) (FDOT 2020) allows the use of Type SP-9.5 mix only in two traffic levels (i.e., traffic levels B and C) and Type SP-12.5 mix in all five traffic levels (i.e., traffic levels B, C, and E). Note that the previous version of this specification (FDOT 2020) included traffic levels A and D. Traffic Level A is now combined with B, and Traffic Level D is now combined with E.

Pavement layer-wise, FDOT allows the use of Type SP-9.5 mix only on the top two structural layers of pavement; it can be the first, the second, or both top layers but not any other underlying layers. FDOT does not have any restrictions on the use of SP-12.5 mm.

2.1.2 Neighboring States

2.1.2.1 Alabama

Alabama Department of Transportation's (ALDOT's) *Standard Specifications for Highway Construction* (ALDOT 2018) specifies:

- Two open-graded friction course (OGFC) mixtures designed using ALDOT-395 (ALDOT 2008a) meet the requirements listed in Section 420: 9.5 mm and 2.36 mm OGFC mixtures.

- Five stone matrix asphalt (SMA) (Marshall) mixtures designed using ALDOT-289 (ALDOT 1999) meet the requirements listed in Section 423 (not the focus of this study): 9.5 mm, 12.5 mm, 19.0 mm, 25.0 mm, and 37.5 mm SMA mixtures.
- Five Superpave (DGA) mixtures designed using ALDOT-384 (ALDOT 2016) meet the requirements listed in Section 424: 9.5 mm, 12.5 mm, 19.0 mm, 25.0 mm, and 37.5 mm mixtures.

The specification allows the use of a 9.5 mm Superpave mix with maximum voids in mineral aggregates (VMA) of 16.5 percent in streets or highways with an equivalent single axle load (ESAL) range of A/B (ESAL ≤ 1.0 million) and 9.5 mm Superpave mix with a maximum VMA of 18.0 percent in streets or highways with ESAL range greater than A/B (ESAL > 1.0 million). The specification allows the 12.5 mm mix with a maximum VMA of 15.5 percent in streets or highways with an ESAL range of A/B. These facts show that ALDOT allows a 9.5 mm with a maximum VMA of 16.5 percent or a 12.5 mm mix with a maximum VMA of 15.5 percent as an alternative in roads with the same ESAL range (i.e., A/B).

In terms of performance testing, the specification (ALDOT 2018) requires that Section 420 (OGFC) and Section 424 (Superpave) mixtures are subject to the following tests and meet the associated criteria tabulated in Section 106:

- AASHTO T 305 (2014) draindown test for all mixtures (≤ 0.30 percent).
- ALDOT-361 (ALDOT 2008b) tensile strength ratio for SMA and Superpave mixtures (≥ 0.80).
- ALDOT-401 (ALDOT 2001) APA rutting test for SMA (≤ 4.50 mm) and Superpave mixtures (≤ 4.50 mm for Traffic Level E).

2.1.2.2 Georgia

GDOT's *Standard Specifications for the Construction of Transportation Systems* (GDOT 2013) specifies:

- Three open-graded surface mixtures that are designed using GDT 114 (GDOT 2020a) and conform to the gradation and volumetric limits provided in Section 828.2.01: 9.5 mm, 12.5 mm, and 12.5 mm porous European mix (PEM) (which refers to a European equivalent OGFC mix).
- Five Superpave mixtures that conform to the gradation and volumetric limits (separate for standard paving and parking lot paving) as provided in Section 828.2.02, AASHTO 312, and AASHTO R30: 9.5 mm Type I, 9.5 mm Type II, 12.5 mm, 19.0 mm, and 25.0 mm mixtures.
- Three SMA mixtures that conform to the gradation and volumetric limits as provided in Section 828.2.03: 9.5 mm, 12.5 mm, and 19.0 mm SMA mixtures.
- One fine-graded mixture that conforms to the gradation and volumetric limits as listed in Section 828.2.04, AASHTO 312 and AASHTO R30: 4.75 mm mix.

Among Superpave mixtures, 9.5 mm Type I and 9.5 mm Type II mixtures differ mainly in terms of lower and upper limits of (a) cumulative passing percentages at sieve sizes 4.75 mm and 2.36 mm and (b) asphalt binder content limits.

In an inter-department correspondence, GDOT's Office of Materials and Testing recently revised the criteria for using asphalt concrete layer and mix types for maintenance projects based on two-way annual daily traffic (ADT) volume (GDOT 2018). The revisions include using:

- 9.5 mm Type I mix of standard asphalt binder in off-system routes, parking lots, and GDOT-selected state highways with 0–2,000 ADT.
- 9.5 mm Type I mix of standard asphalt binder in state and off-system roads with up to 10,000 ADT.
- 9.5 mm Type II mix of polymer-modified asphalt (PMA) binder in GDOT-selected pavements.
- 12.5 mm mix of standard asphalt binder in state highways and interstate system shoulders with 10,000–25,000 ADT.
- 12.5 mm mix of PMA binder in all flexible pavement interstate ramps, all flexible pavement roundabouts, and GDOT-selected interstate.

This revision shows the recommended use of Superpave 9.5 Type I mix of standard binder and Superpave 9.5 Type II mix of PMA binder II in GDOT-selected routes with medium to heavy traffic levels. In terms of performance testing, the specification (GDOT 2013) requires that the mixtures designed for its contracts meet several performance criteria (see Table 2-1).

Table 2-1. Performance and Durability Tests (GDOT 2013, 2019)

Test (Standard)	OGFC	Superpave and Fine-Graded (4.75 mm)	SMA
Permeability: GDT 1 (GDOT 2011a)	n/a	Air void (V_a) content = 6.0 ± 1.0 % Permeability = 3.60 ft/day (125 × 10^{-5} cm/sec)	
Moisture Damage: GDT 66 (GDOT 2011b) and GDT 56 (GDOT 2020b)	n/a	V_a = 7.0 ± 1.0% Indirect tensile strength (ITS) ≥ 60 psi (415 kPa) Tensile strength ratio (TSR) ≥ 0.80 if ITS < 100 psi (690 kPa) TSR ≥ 0.70 if TSR ≥ 100 psi (690 kPa) Coating ≥ 95%	V_a = 6.0 ± 1.0%
Rutting: GDT 115 (GDOT 2020c) or AASHTO T 340 (AASHTO 2010a)	n/a	V_a = 5.0 ± 1.0% APA rut depth (d): ≤ 8.0 mm for 4.75 mm mix at 64°C (147°F) ≤ 8.0 mm for 9.5 mm Type I mix at 64°C (147°F) ≤ 6.0 mm for 9.5 mm Type II mix at 64°C (147°F) ≤ 5.0 mm for 12.5 mm mix at 64°C (147°F) ≤ 5.0 mm for 19.0 mm mix at 49°C (120°F) ≤ 5.0 mm for 25.0 mm mix at 49°C (120°F)	n/a
Fatigue: AASHTO T 321 Beam Fatigue Test (AASHTO 2017b) or other approved procedure	n/a	GDOT may verify DGA mix designs by fatigue testing according to AASHTO T 321 or other procedure approved by the department.	n/a
Durability/ Draindown: AASHTO T 305 (AASHTO 2014)	< 0.3%	n/a	
Hamburg Wheel-Tracking Test: AASHTO T 324 (AASHTO 2017c)	Warm mix asphalt, DGA mixtures, or other mixtures that have polyphosphoric acid (PPA) in the asphalt binders.		

2.1.2.3 Mississippi

Mississippi Department of Transportation's (MDOT's) *Standard Specifications for Road and Bridge Construction* (MDOT 2017) specifies:

- Five Superpave mixtures that are designed using MT-78 (MDOT 2010a) and satisfy gradation and volumetric requirements listed in Section 401: 4.75 mm mix, 9.5 mm mix, 12.5 mm mix (surface lift and underlying lift), 19.0 mm mix, and 25.0 mm mix.
- Two OGFC mixtures that are designed using MT-83 (MDOT 2010b) and satisfy gradation and volumetric requirements listed in Section 402: 9.5 mm and 12.5 mm mix.
- Three SMA mixtures that are designed using MT-80 (MDOT 2010c) and satisfy gradation and volumetric requirements listed in Section 405: 9.5 mm mix, 12.5 mm mix, and 19.0 mm mix.

The specification also specifies the types of Superpave mixtures that can be used with different levels of mixtures (see Table 2-2). The table clearly shows that MDOT has medium- and high-type mixtures with NMAS 4.75 mm and 9.5 mm.

Table 2-2. Superpave Mix Design Options (MDOT 2017)

Mix Type	Standard Type: N_initial = 6 N_design = 50 N_maximum = 75	Medium Type: N_initial = 7 N_design = 65 N_maximum = 100	High Type: N_initial = 7 N_design = 85 N_maximum = 130
Traffic	< 1.0 million ESALs	1.0 to 3.0 ESALs	> 3.0 million ESALs
4.75 mm mix	Yes	Yes	Yes
9.5 mm mix	Yes	Yes	Yes
12.5 mm mix	Yes	Yes	Yes
19.0 mm mix	Yes	Yes	Yes
25.0 mm mix	Yes	No	No

In terms of performance testing, the specification (MDOT 2017) requires that these mixtures are subjected to various testing and associated criteria:

- MT-82 draindown test for OGFC and SMA mixtures (MDOT 2010d): draindown ≤ 0.30 percent.
- MT-84 permeability test for OGFC mixtures (MDOT 2010e): permeability ≥ 30 meters/day.
- MT-85 abrasion loss test for OGFC mixtures (MDOT 2010f): abrasion loss ≤ 30 percent (unaged), ≤ 40 percent (aged).
- MT-63 TSR test for all mixtures (MDOT 2010g): TSR ≥ 85 percent, interior face coating ≥ 95 percent.
- MT-59 boiling water test for all mixtures (MDOT 2010h): coating ≥ 95 percent.

2.1.2.4 Louisiana

Louisiana Department of Transportation and Development's (LaDOTD's) *Standard Specifications for Roads and Bridges* (LaDOTD 2016) specifies:

- Three thin layer mixtures (less than 1.5 inches thick) that meet the requirements of mix design, aggregate physical properties, and the extracted aggregate gradation listed in Tables 501-1, 501-2, and 501-3 of Section 501:
  - "Dense" mix—allowed for less than 3,500 ADT volume.
  - "Coarse" mix—allowed for all traffic volumes.
  - "OGFC" mix—required in the Interstate Highway System and allowed for all traffic volume levels.
- Four Superpave mixtures that are designed using AASHTO M 323 and meet the criteria set for aggregate properties, asphalt binder properties, mix volumetric properties, and mix rutting and cracking properties listed in Table 502-6 of Section 502:

    - 12.5 mm mix—incidental paving course, level 1 wearing course, and level 2 wearing course.
    - 19.0 mm mix—level 2 wearing course, level 1 binder course, and level 2 binder course.
    - 25.0 mm mix—level 1 binder course, level 2 binder course, level 1 base course, and level 1 asphalt-treated binder (ATB) course.
    - 37.5 mm mix—level 1 base course.
- One SMA mix that is designed using AASHTO M 325 and meets the requirements listed in Table 502-6 of Section 502:
    - SMA mix—level 2 wearing courses.

As the list above shows, the specification does not specify any 9.5 mm Superpave mix. LaDOTD's *Supplemental Specifications Part V—Asphalt Pavements* (LaDOTD 2018) mentions that each mixture can be designated for level 1F or 2F as long as the mixtures meet (a) each requirement of the corresponding level and (b) the friction rating requirements in Table 502-3 for travel lane wearing courses.

In terms of performance testing, the specifications (LaDOTD 2016) specify that the Superpave and SMA mixtures are subjected to various tests and must pass their associated criteria:

- AASHTO T 305 draindown test for thin layer mixtures; draindown:
    - ≤ 0.15 percent for "Coarse" mix.
    - ≤ 0.30 percent for OGFC mix.
- DOTD TR 317 water susceptibility test for thin layer mixtures; percent coating:
    - ≥ 90 percent ("Coarse" mix).
- AASHTO T 324 HWT test for rut depth at 50°C:
    - ≤ 10 mm @ 10,000 wheel passes:
        - 12.5 mm incidental paving course.
    - ≤ 10 mm @ 20,000 wheel passes:
        - 12.5 mm level 1 wearing course.
        - 19.0 mm level 1 binder course.
        - 25.0 mm level 1 binder course.
        - 25.0 mm level 1 ATB course.
    - ≤ 6 mm @ 20,000 wheel passes:
        - 12.5 mm level 2 wearing course.
        - 19.0 mm level 2 wearing course.
        - 19.0 mm level 2 binder course.
        - 25.0 mm level 2 binder course.
        - 37.5 mm level 1 ATB course.
        - SMA level 2 wearing course.
    - ≤ 12 mm @ 12,000 wheel passes:
        - "Dense" mix.
    - ≤ 12 mm @ 5,000 wheel passes:
        - OGFC mix.
    - ≤ 12 mm @ 20,000 wheel passes:
        - "Coarse" mix.

    - 25.0 mm level 1 base course.
- Semi-circular bending beam test for Superpave and SMA mixtures; J_c at 25°C:
    - ≥ 0.5 KJ/m^2 (level 1).
    - ≥ 0.6 KJ/m^2 (level 2).

2.1.2.5 South Carolina

South Carolina Department of Transportation's (SCDOT's) *Standard Specifications for Highway Construction* (SCDOT 2007) specifies:

- Five HMA surface course mixtures that meet the criteria set for (a) aggregate gradation, (b) asphalt binder, (c) mix design properties, and (d) aggregate properties in Section 402 (SCDOT 2007) and *SC-M-402 Supplemental Technical Specification for Hot-Mix Asphalt Material Properties* (SCDOT 2018a):
    - Type A—for interstate/intersections.
    - Type B—for high volume primary roads.
    - Type C—for high volume secondary roads.
    - Type D—for low volume secondary roads.
    - Type E—for seal coats.
- Five HMA base course mixtures that meet the criteria set for (a) aggregate gradation, (b) asphalt binder, (c) mix design properties, and (d) aggregate properties in Section 400 (SCDOT 2007) SC-M-402 (SCDOT 2018a):
    - Type A—for interstate and primary roads.
    - Type B—for specialty roads.
    - Type C—for specialty roads.
    - Type D—for specialty roads.
    - Shoulder widening—for specialty roads.
- Three HMA intermediate course mixtures that meet the criteria set for (a) gradation, (b) asphalt binder grade and limits, (c) mixture design properties, and (d) aggregate properties in Section 402 (SCDOT 2007) and SC-M-402 (SCDOT 2018a):
    - Type A—for new construction.
    - Type B—for interstates, high volume primary roads.
    - Type B Special—for rehabilitation, repairs, interstates, and high-volume primary roads.
    - Type C—for low-volume and other roads.
- Two OGFC mixtures that meet the requirements of Section 409 (SCDOT 2007) and additional requirements of the *Supplemental Specification for Open-Graded Friction Course* (SCDOT 2019a):
    - 9.5 mm OGFC mixture.
    - 12.5 mm OGFC mixture.

These specifications show that Type B, Type C, and Type D surface course mixtures; Type B, Type B Special, and Type C intermediate course mixtures; and Type C base course mixtures can be designed with two different NMAS sizes. For example, Type B surface course mixtures can be designed with NMAS 9.5 mm or NMAS 12.5 mm, which is relevant to this project. The specification does not specify where a certain type of OGFC mixture is preferred.

In terms of performance tests, the specification requires that the mixtures used in contracts pass the criteria set for the following tests:

- SC-T-90 draindown test (SCDOT 2019b) for OGFC mixtures: coating ≥ 95 percent.
- SC-T-127 CAL test (SCDOT 2013) for OGFC mixtures: loss < 15 percent.
- SC-T-70 moisture susceptibility test (SCDOT 2018b) for Type A, B, and C surface and all intermediate mixtures.
- AASHTO T 340 (AASHTO 2010a) APA rutting test for HMA surface and intermediate mixtures; rut depth:
    - ≤ 3 mm for Type A surface and Type A intermediate.
    - ≤ 5 mm for Type B surface mixture, Type B, and Type B intermediate mixtures.

2.1.2.6 Tennessee

Tennessee Department of Transportation's (TDOT's) *Standard Specifications for Road and Bridge Construction* (TDOT 2015) specifies:

- Five hot surface mixtures that are designed using the Marshall Method of Mix Design (Asphalt Institute 2015) and meet mixture design requirements, such as Marshall stability, flow, design void content, production void content, VMA, and dust-asphalt ratio, listed in Section 411 and the gradation listed in Section 903: 411-D, 411-E, 411-E-Shoulder, 411-TL, and 411-TLD.
- One OGFC mixture that is designed using the National Asphalt Pavement Association (NAPA) Publication IS-115 (NAPA 2002), except where modified by TDOT, meets mixture design requirements listed in Section 411 and the gradation listed in Section 903: 411-OGFC.

The prefix "411' in these designations refers to Section 411 of the specification, and the suffixes "D," "E," "TL" (Thin Lift), "TLD" (Thin Lift D), and "OGFC" refer to aggregate gradation listed in Table 903-11-2 of Section 903. Though not specified, Section 903 suggests that 411-D and 411-E refer to 12.5 mm mixtures, 411-E-Shoulder mixture refers to 4.75 mm mixtures, 411-TL and 411-TLD refer to 9.5 mm mixtures, and 411-OGFC refers to 12.5 mm mixtures.

To ensure performance, Section 411.03 of the specification (TDOT 2015) requires the following tests:

- AASHTO T 305 draindown test (AASHTO 2014) for OGFC mixture: draindown ≤ 0.3 percent.
- CAL for OGFC mixture: loss ≤ 20 percent.
- Marshall stability test of hot surface mixtures; Marshall stability:
    - ≥ 1,500 lb/ft. for 411E.
    - ≥ 2,000 lb/ft. for others.

The specification review did not indicate that TDOT allows (or does not allow) any 9.5 mm mixture as an alternative to a 12.5 mm mixture in its pavements.

2.1.3 Summary

This review revealed that FDOT's neighboring state agencies had not imposed any specific restrictions on using a 9.5 mm mixture in place of a 12.5 mm mixture. However, few have specific designs for 9.5 mm for heavy traffic volume roads. In terms of performance tests, the neighboring state agencies mainly use the draindown and CAL tests for the durability of OGFC (and SMA) tests, either APA or HWT test for rutting, and TSR for moisture damage tests; only LADOTD requires a semi-circular bending cracking test to determine the strain energy release rate, and GDOT mentions a beam fatigue test as an optional verification test.

2.2 Rutting Performance

Rutting is one of the major distresses and it accelerates asphalt pavement failures, adds maintenance and rehabilitation costs, and elevates wet weather accidents, sometimes leading to loss of lives and properties (Fwa et al. 2012; Zhou et al. 2019a). Therefore, researchers have studied different aspects of rutting over the years. These include factors that can cause or accelerate rutting (Button et al. 1990), such as:

- Use of an excessive amount of rounded (less shear-resistant) aggregates or inadequate crushed (angular) aggregates.
- Use of an excessive amount of fine (or sand-like) particles.
- Use of an excessive amount of asphalt binders.
- Use of too-soft asphalt binders.
- Presence of excessive moisture in the mixture.
- Relatively low temperature in drum mixture plants.
- Elimination of multiple stockpile requirements.
- Use of a control-strip density requirement over a reference-type density requirement.
- Paving at cold weather, which would lead to lower density.

Among these factors, aggregate characteristics (e.g., their gradation roundness and fineness) have been recognized as the most influencing factors that can dictate the occurrence and severity of rutting in asphalt pavements (Ahlrich 1996; Button et al. 1990; Golalipour et al. 2012). Similarly, asphalt binder characteristics (e.g., asphalt binder grade, type, chemistry, and content) and asphalt mixture characteristics (e.g., workability and compaction density) are other important factors that need to be dealt with from the very beginning of the mixture design phase.

Over the years, researchers have developed different types of laboratory tests to determine the rutting resistance of the asphalt mixtures produced. These tests include but are not limited to the stability tests developed in the 1920s (Huber 2013), the wheel-track tests and SP simple shear tests developed in the 1970s through 1990s, and the IDEAL (shear) rutting tests developed as recently as 2019 (Zhou et al. 2019a).

However, not all DOTs use the same test or parameter to evaluate the rutting resistance of asphalt mixtures. A recent survey conducted of DOTs that had specified a given rutting test in their mixture design specifications revealed that the APA test ranks the highest, followed by the

HWT test, the flow number (FN) test, and the Hveem stability test, in that order (West et al. 2018b).

The appropriateness of a given test for a specific purpose depends on several factors (Zhou et al. 2019a), such as:

- **Simplicity:** minimal specimen preparation steps (coring, cutting, gluing, or notching) and minimal instrumentation.
- **Efficiency:** minimum test completion time.
- **Practicality:** minimal training for operation and suitable for both laboratory-molded specimens and field cores.
- **Low cost:** use of existing test equipment with minimal modification or purchase of a brand new but low-cost test equipment.
- **Repeatability:** low coefficient of variation (COV).
- **Manifesting primary mechanism:** rutting testing should be based on shear (and cracking testing should be based on tension).
- **Correlation with field performance:** measured parameters must have a very good correlation with measured field data.
- **Sensitivity:** sensitive to the change in the:
    - Gradation, NMAS, and type of aggregates.
    - Grade, type, and content of asphalt binders.
    - Type and percentage of recycled materials.
    - Mixture design density (or air void content) and aging.

The following sections briefly describe each of the major rutting tests developed over the years with their features and limitations and provide some examples of their use in previous studies similar to this one.

2.2.1 Hveem Stability Test

Before the development of SP performance tests through the Strategic Highway Research Program (SHRP), the DOTs in the United States mainly relied on stability tests (e.g., Hveem stability tests) to evaluate the rutting resistance of asphalt mixtures and the associated mixture design methods (e.g., Hveem mixture design method) to design asphalt pavement mixtures. The Hveem stability test involves loading cylindrical asphalt mixture samples (102 mm or 4.0 inches in diameter by 64 mm or 2.5 inches in height) at selected levels of confinement and measuring its stability number (*S*), which is an indicator of internal friction within the test sample. The test can be conducted following ASTM D1560 (ASTM 2015) and AASHTO T 246 (AASHTO 2010b).

However, studies have shown the stability number does not correlate well with field rutting performance (Chowdhury and Button 2002). Therefore, only two DOTs (Hawaii and Nevada) now use this test to evaluate rutting performance in its mixture design specification (West et al. 2018b).

2.2.2 Superpave Simple Shear Test

During SHRP, the SP simple shear test (SST) was developed to provide a mechanistic testing approach compared to previous empirical rutting tests, including the stability tests (Monismith and Tayebali 1994). The SST involves loading cylindrical samples of asphalt mixtures in four different modes and determining parameters that help in evaluating rutting performance:

- **Frequency sweep at constant height (FSCH):** complex shear modulus and shear phase angle.
- **Simple shear at constant height (SSCH):** maximum deformation, permanent deformation, and elastic recovery.
- **Repeated shear at constant height (RSCH):** permanent shear strain.
- **Repeated shear at constant stress ratio:** permanent shear strain.

The main strength of the SST is that this test evaluates the rutting resistance of asphalt mixtures in terms of shear, which is identified as the driving force behind rutting; however, researchers have found that this test has several limitations. These limitations include the requirement of relatively expensive instruments, complex specimen preparation and testing steps, and inconclusive correlation with field rutting performance.

Furthermore, researchers also came to different, sometimes contrary, conclusions. For example, Romero and Mogawer (1998) compared the properties obtained from the SST and the performance observed at the Federal Highway Administration's (FHWA's) accelerated loading facility (ALF). They reported that the FSCH test was "able," the SSCH test was "not able," and the RSCH test was not reliable ("extremely variable") in discriminating between well-performing and poorly performing asphalt mixtures. However, Tayebali et al. (1999) reported that the RSCH test had a good correlation with field performance and could discriminate between well-performing and poorly performing asphalt mixtures. Additionally, Anderson et al. (2000) suggested that the SSCH and the FSCH tests could rank pavement rutting performance correctly. Because of these limitations, none of the DOTs in the United States currently specify the SST as a routine test in their mixture design specifications (West et al. 2018b).

2.2.3 Repeated Load Permanent Deformation Test

The repeated load permanent deformation (RLPD) test refers to a permanent deformation test that involves the application of multiple load cycles. In this test, cylindrical asphalt mixture samples (100 mm in diameter by 150 mm in height) are subjected to Haversine load cycles of certain values (138 kPa or 20 psi at 40°C and 69 kPa or 10 psi at 50°C) at a frequency of 1.0 Hz (0.1-second loading followed by 0.9-second rest periods) until 10,000 load repetitions or 25,000 microstrain. The analysis of these test data includes the determination of axial permanent deformation, permanent and resilient strains (ε_p, ε_r), stress, the number of load passes, time, temperature, frequency, permanent deformation properties (α, μ), and resilient modulus, along with their correlation with the field rutting performance.

Researchers have reported a fair to good correlation of RLPD parameters with field rutting performance and empirical wheel-track testers (Walubita et al. 2012a; Walubita et al. 2014). For example, Walubita et al. (2012b) reported that the accumulated permanent microstrain obtained

from the RLPD test successfully discriminated the rutting resistance of 10 different mixtures, including rich bottom layer, heavy-duty stone mastic asphalt, and stone-filled HMA concrete, with different NMASs (Figure 2-1).

However, several limitations have also been identified over the years (Walubita et al. 2014), such as:

- A laborious and long sample fabrication process.
- High variability at higher temperatures.
- Instrumentation issues, especially related to linear variable differential tensor use at higher temperatures.
- The need for trained personnel.
- The need for expensive instruments such as a universal testing machine.

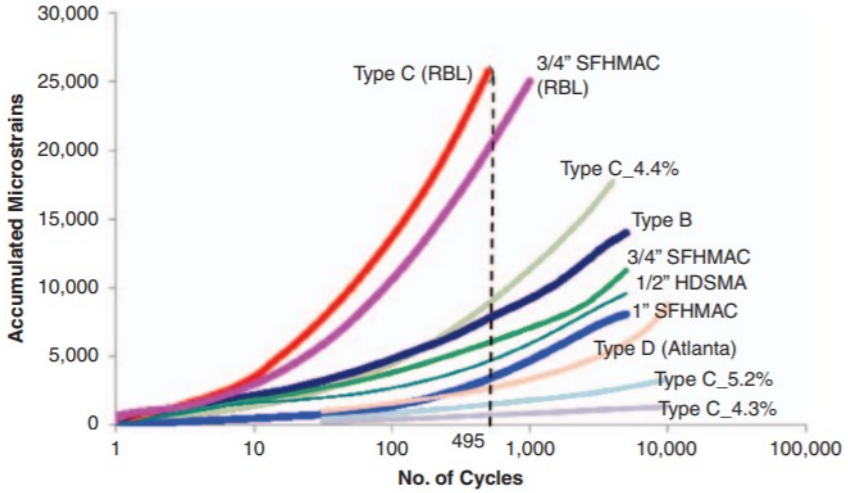

Figure 2-1. RLPD Test Results (Walubita et al. 2012a)

Azari and Mohseni (2013) developed a modified version of RLPD, called the incremental RLPD (iRLPD) test, in which asphalt mixture samples are subjected to several increments of repeated load cycles at multiple stress levels. The analysis of iRLPD involves the determination of permanent or minimum strain rate (MSR) at the end of each test increment, construction of the master curve for MSR versus the product of temperature and pressure (TP), and their correlation with field rutting performance. The authors used this test to evaluate the rutting resistance of nine different asphalt mixtures selected by the FHWA Expert Task Group to appraise several existing rutting determination protocols. The researchers compared the results of the iRLPD test to three different FN tests conducted with the same confining stress but different deviatoric stresses. Test results showed the strain rates obtained from the relatively slower FN tests coincided with the MSR master curves from results obtained from the comparatively faster iRLPD test.

Based on this comparison, the researchers highlighted several advantages of the iRLPD test over the FN test:

- Shorter duration of testing.

- Creation of a more informative master curve.
- Straightforward calculation of the MSR.
- Use of the shear mode of loading.
- Well-defined input variables.
- Criteria for discrimination of asphalt mixtures.
- Wider application.

However, the iRLPD test shares several limitations of the RLPD test.

As of 2018, no DOT in the United States has implemented either the RLPD or iRLPD test as a routine rutting test in the mixture design process (West et al. 2018b).

2.2.4 Flow Number Test

The FN test is one of the simple performance tests developed through the National Cooperative Highway Research Program (NCHRP) 9-19 (Witczak et al. 2002). The test involves repeatedly loading the cylindrical asphalt mixture specimens (with a haversine load for 0.1 seconds followed by 0.9-second rest periods [i.e., a frequency of 1.0 Hz]) at a given temperature (usually 50°C) until 10,000 load repetitions or 30,000microstrain (Zhang et al. 2013; Walubita et al. 2014). The FN test is a variation of the RLPD test (Bonaquist 2012). The load versus displacement data obtained from this test are used to determine the *FN* value (i.e., the number of load cycles at the minimum rate of change in the permanent strain), permanent strain at FN ($\varepsilon_{p_{\mathrm{FN}}}$), and flow time ($t_{FN}$). The tests can be conducted with or without confinement. NCHRP 9-19 recommended using a stress level between 69 and 207 kPa without confinement and between 483 and 966 kPa with confinement.

Research has shown that the FN value correlates well with the rutting resistance of asphalt mixtures used in field test sections at MnROAD, WesTrack, and the FHWA Pavement Testing Facility (Witczak et al. 2002). Generally, the higher FN value implies better resistance to rutting. Research has also shown that the test is sensitive to mixture design variables such as binder grade, binder modification, in-place air voids, and voids in mineral aggregates (Bonaquist 2012). The test was also included as a routine rutting test in the HMA mixture design manual with tentative criteria (NCHRP 2011).

Research has also shown that the test is sensitive to aggregate gradation and density levels. For example, Mogawer et al. (2010) compared the rutting performance of an SP-9.5 mixture and an SP-12.5 mixture (containing 4.8 and 5.8 percent binder, respectively) with target density levels of 88, 91, 94, and 97 percent G_{mm} (i.e., 12, 9, 6, and 3 percent air void levels). The authors reported that SP-9.5 and SP-12.5 mixtures had equivalent performances at various density ranges regardless of the difference in binder content and NMAS (Figure 2-2). The authors also reported that the FN value increased exponentially in the SP-9.5 mixture at densities above 98 percent G_{mm} (Figure 2-2a).

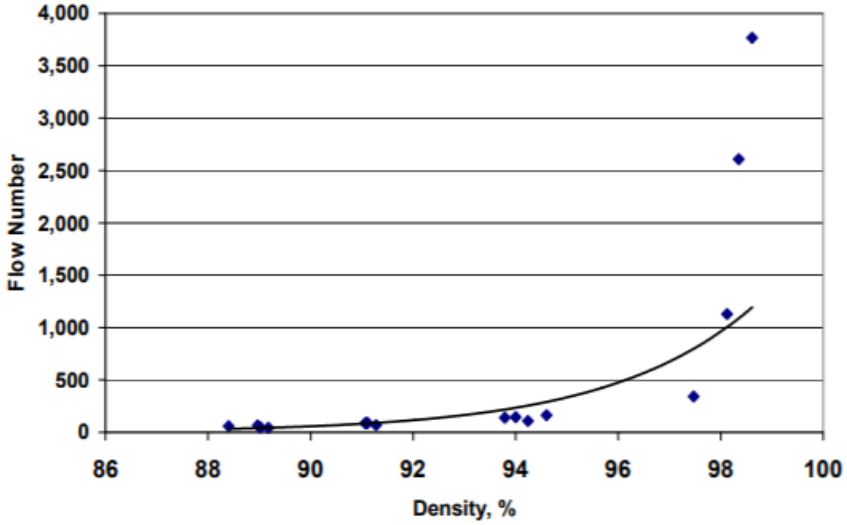

(a) SP-9.5 FN Results

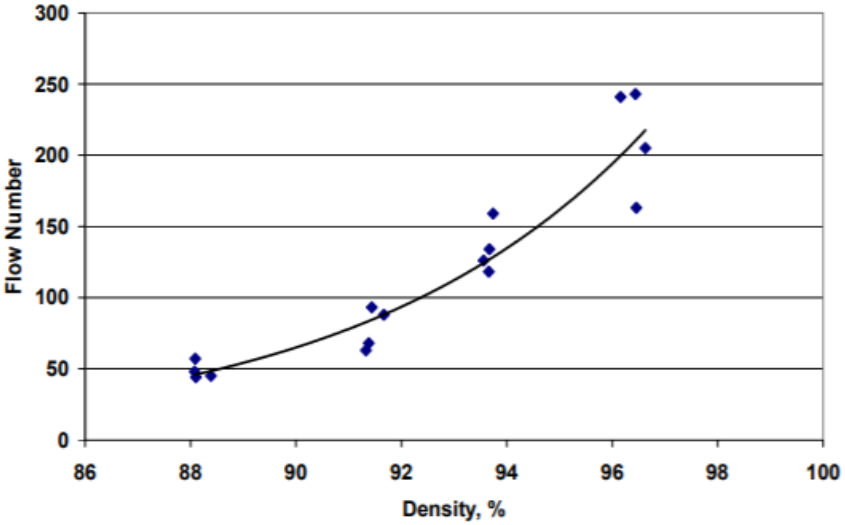

(b) SP-12.5 FN Results

Figure 2-2. FN Test Results (Mogawer et al. 2010)

Despite some promising reports, the FN test has several limitations (Azari and Mohseni 2013), such as:

- Lack of criteria that can be reliably used for discriminating asphalt mixtures.
- Inability of some asphalt mixtures to show tertiary flow.
- Variation in testing time to reach the tertiary flow.
- Use of only one stress level and only one temperature.
- Use of primary and secondary stages of deformation for evaluating rutting resistance instead of shear strength parameters.

Additionally, this test does not always correlate well with commonly used rutting tests such as the APA test (Mogawer et al., 2010) and HWT test (Mogawer et al. 2010; Willis et al. 2014).

The sample preparation requirements (coring and cutting) and instrumentation are inherent limitations of this test (Zhou et al. 2019a). Because of these limitations, the test has not been implemented as a routine test in the mixture design specification by more than one DOT in the United States (West et al. 2018b).

2.2.5 Hamburg Wheel-Track Test

The HWT test was developed in the 1970s through 1990s (Lai 1986; Williams and Prowell 1999). The test involves the application of continuous passes of a heavily loaded (705 N or 158 lb) steel wheel directly on 38- to 100-mm-thick (1.5- to 4.0-inch-thick) cylindrical asphalt mixture specimens submerged in water at a certain temperature (usually 40–70°C; 50°C in Texas) until the number of wheel passes reaches a DOT-specified value (usually 20,000 wheel passes) or until the tracks just under these wheels rut by a certain depth (usually 12.5 mm or 0.50 inches).

The HWT test is conducted underwater; therefore, it can also evaluate the stripping potential of asphalt mixtures. Furthermore, the specimen preparation and test procedure itself is very simple, and the HWT test results correlate well with field performance. Therefore, the test has been implemented as a routine rutting test by at least 10 DOTs in the United States: California, Iowa, Illinois, Louisiana, Massachusetts, Maine, Montana, Texas, Utah, and Washington (West et al. 2018b).

Several researchers have used this test to evaluate the effect of mixture design parameters (the type and gradation of aggregates; the type, grade, and percentage of asphalt binder; and the mixture density) on rutting performance. Kandhal and Cooley (2002) tested mixtures produced with fine and coarse gradations using three different rutting performance tests, including the HWT test, but observed no significant difference between gradations.

Golalipour et al. (2012) evaluated the rutting resistance of three types of mixtures, each produced with a different gradation variation, using the HWT test as one of the primary tests. The authors reported that mixtures produced along the upper limits of gradations (fine gradations) were better in rutting resistance.

Ahmad et al. (2012) evaluated the rutting resistance of eight different mixtures with different gradations using the Wessex wheel-track test—the original predecessor of the HWT test in the United Kingdom (Powell 2006). The authors used two different asphalt binder grades (PG 64 and PG 70, referred to as B1 and B2, respectively), two different gradations of granite aggregates obtained from a quarry named QS (QS 9.5 and QS 12.5), and two different mixture design methods (SP and Marshall, referred to as QS Superpave and QS Public Works Department criteria, respectively) to produce these mixtures. Their test results revealed that the SP-9.5 mixture had better rutting resistance (or lower rut depth) than the corresponding SP-12.5 mixture, regardless of the selected mixture design method (Figure 2-3). Additionally, the test results also revealed that the SP mixtures performed better than the Marshall mixtures, and the PG 64 and PG 70 (i.e., B2) mixtures performed better than the PG 64 (i.e., B1) mixtures. Though the Wessex wheel-track test, but not the HWT test or accelerated pavement test (APT), was used in this study, the proof that SP-9.5 performed better than SP-12.5, irrespective of the selected mixture design method, is relevant to this study.

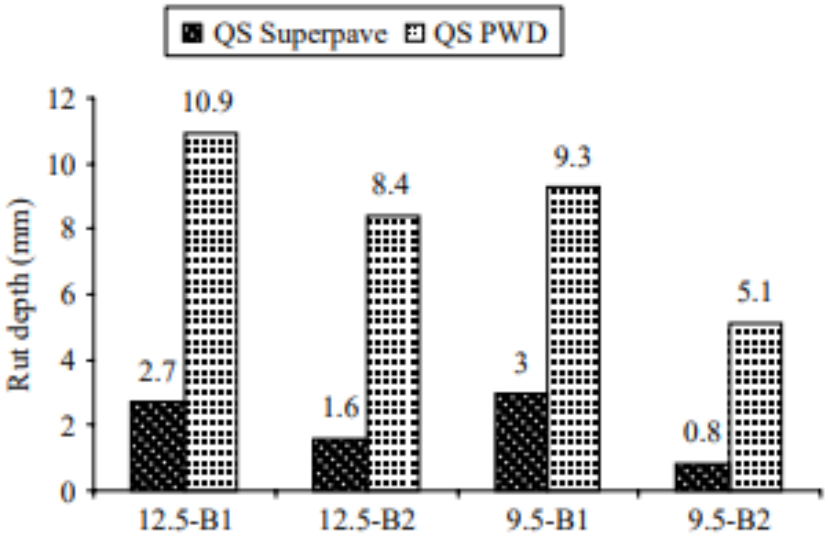

Figure 2-3. Wheel Tracking Test Results (Ahmad et al. 2012)

That said, this test has its limitations. Unlike some new tests, this test needs cutting on at least one edge and sometimes might take longer than six hours to complete a test (especially for polymer-modified binder). Additionally, the test might not always show any stripping phase, especially with the polymer-modified binder, and therefore might not be able to evaluate stripping potential.

2.2.6 Asphalt Pavement Analyzer Test

Research from the 1970s through 1990s also led to the development of the Georgia loaded wheel test, which later became the current form of the APA test (Lai 1986; Williams and Prowell 1999). The APA test involves the application of continuous passes of heavily loaded steel wheels on 75-mm-thick (2.95-inch-thick) cylindrical specimens at a certain high temperature (usually 64°C such as in the case of Florida) through pressurized rubber hoses until the total number of wheel cycles reaches a DOT-specified number (usually 8,000 cycles as in Florida) or until the rut depths along the tracks of these wheels reach a certain value (usually 4.5 mm or 0.178 inches as in Florida).

Several researchers have validated the use of the APA test as a rutting performance test. Kandhal and Cooley (2002) conducted APA tests on SP-9.5 and SP-19.0 mixtures produced with different combinations of aggregate types, gradations, and binder contents. The mixtures were produced with binder contents corresponding to 4.0 percent air void content and density corresponding to 6.0 percent air void content. The authors found that the rut depth was smallest in the 9.5-mm mixture produced with coarse granite aggregates–fine limestone aggregates and largest in the 19.0-mm mixture produced with crushed gravel coarse aggregates–fine granite aggregates, which highlights the possibility of producing a more rut-resistant mixture even with finer gradation choice (Figure 2-4.).

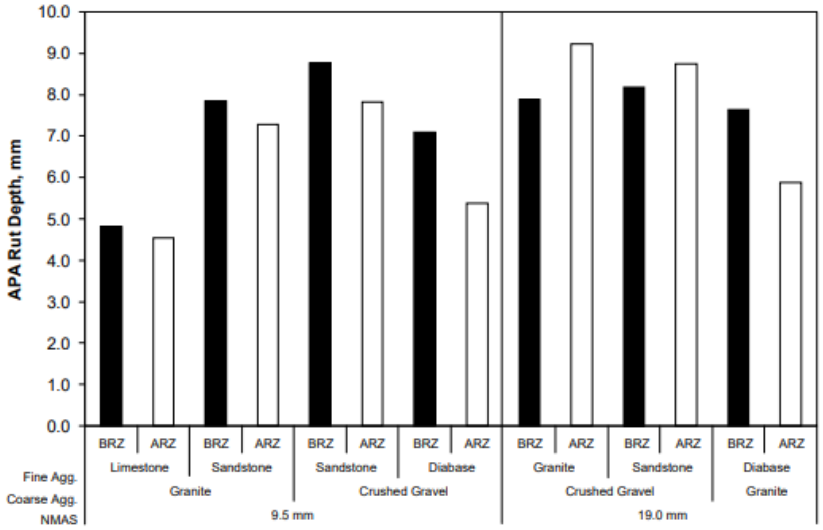

Figure 2-4. APA Test Results (Kandhal and Cooley 2003)
[Note: BRZ = Below Restricted Zone and ARZ = Above Restricted Zone]

Choubane et al. (2006) assessed the correlation of the rutting performance of fine-graded and coarse-graded SP mixtures under the APT with APA results obtained from two different sample thicknesses (3 inches or 75 mm, and 4.5 inches or 115 mm). For this study, the authors produced two different asphalt mixtures using the same binder type, grade, and content (unmodified, 8.2 percent PG 67-22 binder) and the same aggregate type (granite aggregate and local sand) and paved their tracks on the heavy-vehicle stimulator (HVS) for the APT. The recovered samples from both tracks measured 92–93 percent in situ. Based on the APA (not shown here) and the HVS test results, the fine-graded mixture performed slightly better than the coarse-graded mixture in terms of rutting resistance (Figure 2-5).

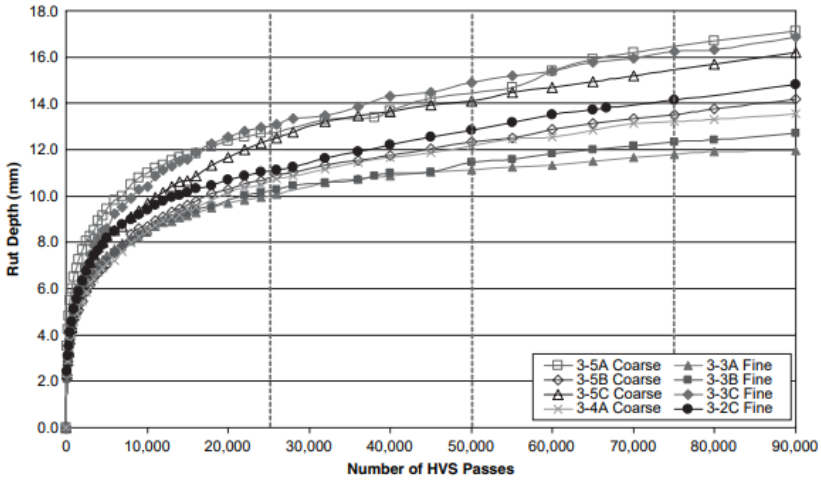

Figure 2-5. HVS Results (Choubane et al., 2006)

Greene and Choubane (2016) compared the performance of varying thicknesses (i.e., 0.5, 0.75, and 1.0 inches) of the FC-4.75 overlays with the performance of fine-graded SP-12.5 (control)

structural courses with either PG 67-22 or PG 76-22 under accelerated load in FDOT's HVS facility (Figure 2-6). The authors reported that adequate rutting resistance was observed with all three thicknesses of the FC-4.75 layer in the case of lower-volume roadways but only with a 0.75-inch-thick FC-4.75 layer in the case of higher-volume roadways. The fact that a certain thickness of FC-4.75 mixture could provide enough rutting resistance for higher-volume roadways strongly suggests that an even thinner SP-9.5 layer might provide adequate rutting resistance.

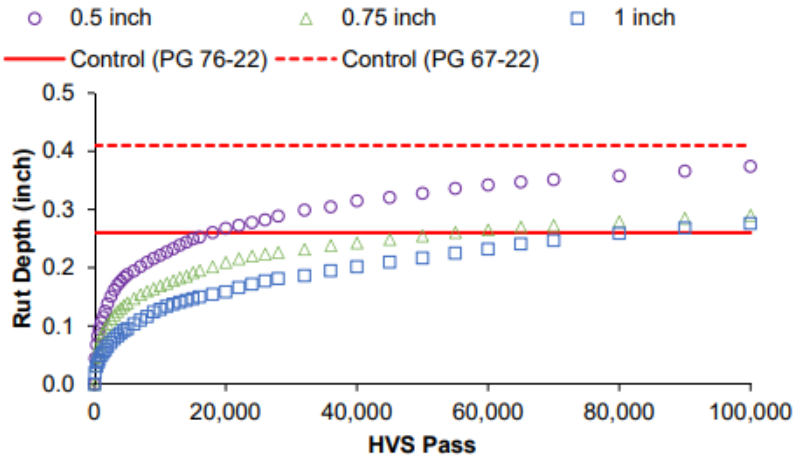

Figure 2-6. HVS Results (Greene and Choubane 2016)

Several DOTs have adopted the APA as the routine test in their mixture design specifications: Alaska, Alabama, Arkansas, Georgia, Idaho, North Carolina, New Jersey, Oregon, South Carolina, South Dakota, and Virginia (West et al. 2018b). FDOT also uses this test to evaluate the rutting performance of some mixture types in one region of the state.

2.2.7 IDEAL Shear Rutting Test

Zhou et al. (2019a) recently developed yet another test, IDEAL-RT, for evaluating the rutting resistance of asphalt mixtures. The new test involves the application of a load on cylindrical specimens (same as the standard HWT test sample without cutting and coring: 150 mm in diameter and 62 mm in thickness, 7.0 ± 0.5 percent in air void content) at a rate of 50 mm/minute (2 inches/minute) at a high temperature (usually the temperature used for the HWT or APA) and the determination of a rutting parameter through the relationship of the shear strength (τ) and the peak contact stress (p) (Figure 2-7):

$$\tau = 0.356 \, . \, p \qquad (2\text{-}1)$$

The larger the shear strength, the better the rutting resistance of asphalt mixtures.

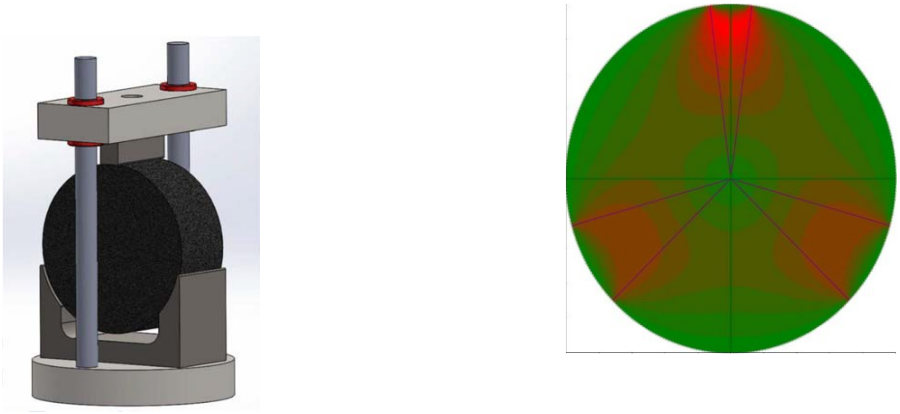

(a) Test Setup (b) Shear Stress Distribution

Figure 2-7. IDEAL-RT Setup (Zhou et al. 2019a)

Through a rigorous experimental design, the authors showed that the IDEAL-RT has the following advantages over other conventional tests:

- **Simple:** uses 62-mm-thick by 150-mm-diameter cylindrical samples without coring, cutting, and gluing.
- **Practical:** requires minimal training.
- **Economic:** requires the least amount of modification of common test equipment.
- **Efficient:** completes within one minute.
- **Sensitive:** uses an IDEAL-RT parameter (or shear strength [τ]) that increases with higher binder grade, lower asphalt binder content, higher recycled asphalt pavement (RAP)/recycled asphalt shingle (RAS) content, more angular aggregates, more severe aging, and lower air void content (Figure 2-8a).
- **Repeatable:** has less than 10 percent COV among three replicates.
- **Truly representative:** uses the shear mode of damage as the driving force of rutting.
- **Correlation with conventional tests:** correlates well with HWT and RLPD tests.
- **Field validation:** has very good correlations with rutting data collected from MnROAD, WesTrack, and in-service Texas test sections (Figure 2-8b).

Because the test was developed only recently, no DOT in the United States has yet fully implemented the test. However, the test has been increasingly included in several research projects sponsored by different DOTs, such as Texas and Florida.

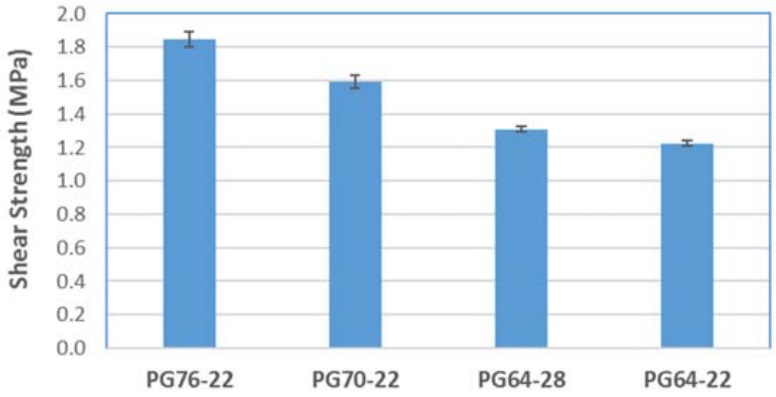

(a) Sensitivity to Asphalt Binder Grade

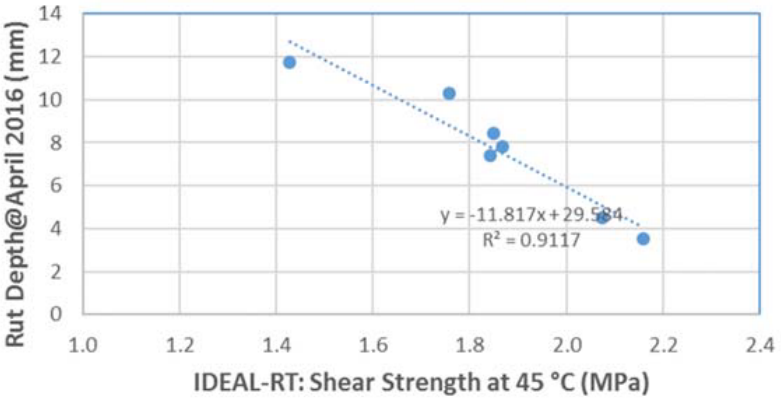

(b) Validation with Minnesota DOT Performance

Figure 2-8. IDEAL-RT Sensitivity (Zhou et al. 2019a)

2.2.8 Summary

Table 2-3 lists the rutting performance tests and their advantages and limitations.

Table 2-3. Common Asphalt Mixture Rutting Performance Tests (Al-Qadi et al. 2015; West et al. 2018b; West et al. 2018c; Zhou et al. 2019a)

Test	Standard	Conditioning	Loading	Parameters	Limitations
Superpave shear test	AASHTO T320 (2016a)	High temperature	Varies	Frequency sweep test: G^*, δ Simple shear test: γ_{max}, $\%Recovery$ Reheated shear test: γ_p	• Preparation: complex • Instrument: expensive • Testing time: moderate (in minutes to hours) • Variability: depends
Repeated load permanent deformation test	AASHTO TP116-15 (2015a)	High temperature	Repeated load cycles at multiple stress levels	Master curve of minimum strain rate and product of temperature and pressure (MSR × TP)	• Preparation: complex • Instrument: expensive • Testing time: depends • Variability: moderate
Flow number test	AASHTO T378 (2017e)	High temperature	Load: 0.1 seconds Rest: 0.9 seconds	Flow number: FN	• Not a shear test • Sample preparation: complex • Instrument: expensive • Testing time: depends on tertiary flow • Variability: depends on tertiary flow
Asphalt pavement analyzer test	AASHTO T340 (2010a)	High temperature; dry air	60 wheel passes/ minute (max. 8,000 wheel passes on rubber hose); dry	Rut depth: d No. of wheel passes: N	• Preparation: No cutting • Instrument: expensive, separate • Testing time: depends • Variability: moderate
Hamburg wheel tracking test	AASHTO T324 (2017c)	High temperature (usually 50°C); submerged in water	52 wheel passes/ minute (max. 20,000 passes)	Rut depth: d No. of wheel passes: N Secondary inflection point: SIP	• Preparation: cutting, submergence • Instrument: expensive, separate • Testing time: depends • Variability: moderate
IDEAL-RT	N/A	High temperature (the HWT or APA test temperature); dry	50 mm/ second	Shear strength: τ	• Preparation: no cutting • Instrument: inexpensive • Testing time: short (in minutes) • Variability: low, COV < 10%

2.3 Cracking Performance

Cracking is another major distress that can cause early structural and serviceability failures of asphalt pavements. Based on the primary cause, two types of cracking can occur in asphalt pavements (Underwood and Braham 2019): the first type involves cracking in asphalt pavement layers due to traffic load, and the second type involves cracking due to temperature change.

Load-associated cracking can exhibit itself in the form of bottom-up fatigue cracking, top-down cracking (i.e., cracking that occurs due to accumulation of microcracks under repeated traffic loads), or reflective cracking (i.e., cracking that initiates from existing flaws in underlying layers and propagates toward the newly constructed layers under traffic loads). This cracking category indicates issues with pavement structural capacity, material properties, and truck loading (Al-Qadi et al. 2019). Non-load-associated cracking can exhibit itself in the form of transverse cracking (i.e., cracking that occurs when the temperature fluctuates drastically and the stress so developed overcomes the strength of the materials (Al-Qadi et al. 2019).

Over the years, researchers have made efforts to understand the mechanism by which cracking initiates and propagates in asphalt pavement layers and to devise laboratory methods that can measure parameters on cracking performance of asphalt mixtures in the field (Kaseer et al. 2018; Lytton et al. 1993; Ozer et al. 2016a; Underwood and Kim 2012; Zhou and Scullion, 2005). However, these methods differ in several aspects, including but not limited to:

- Loading frequency:
  - Cyclic:
    - Repeated bending beam fatigue (RBBF).
    - Asphalt mixture performance tester (AMPT) cyclic fatigue test.
    - (Modified) (Texas) overlay tester (OT).
  - Monotonic:
    - UF-IDT test.
    - (Louisiana) semi-circular bending strain energy release rate (SCB-Jc).
    - (Illinois) SCB-FI.
    - Disc-shaped compact tension (DCT).
    - IDEAL-CT.
- Working principle:
  - Empirical (uses correlations: RBBT, Texas OT):
    - Number of load cycles to failure: $N_f = N_{50\%stiffness}$.
    - Strain as a function of the number of cycles at failure: $\varepsilon = f(N_f)$.
  - Dissipated energy(uses strain versus strain history: UF-IDT, SCB-J_c, and SCB-FI):
    - Dissipated creep strain energy (DCSE): UF-IDT.
    - Energy ratio (ER): UF-IDT.
    - Plateau value (not discussed in this report).
  - Continuum damage mechanics (uses work potential theory: AMPT cyclic fatigue):
    - Simplified viscoelastic continuum damage (SVECD): $C = f(S)$.
  - Fracture damage mechanics (uses the Paris's law):
    - Fracture energy: UF-IDT, SCB-J_c, IDEAL-CT, and Texas OT.
    - Tensile strength: UF-IDT, SCB-J_c, and SCB-FI.
    - Strain energy release rate: SCB-J_c.
    - Flexibility index: SCB-FI.
    - Cohesive zone models (not discussed in this report).
- Loading mode:

    - Flexural tension: RBBF.
    - Tension-compression: AMPT cyclic fatigue and OT.
    - Indirect tension: UF-IDT, SCB-J_c, SCB-FI, and IDEAL-CT.
    - Direct tension: DCT.
- Cracking mode:
    - Opening (tension) or Mode I: DCT, SCB-J_c, SCB-FI, and Texas OT.
    - Sliding in-plane (shear) or Mode II (not discussed in this report).
    - Sliding out-of-plane or Mode III (not discussed in this report).
    - Mixed mode (not discussed in this report).
- Specimen shape:
    - Four-point bending (rectangular) beams: RBBF.
    - Semi-circular bending beams: SCB-$J_c$and SCB-FI.
    - Circular/cylindrical:
        - Loaded parallel to compaction direction: AMPT cyclic fatigue.
        - Loaded perpendicular to compaction direction: UF-IDT and IDEAL-CT.
    - Specialized:
        - Texas OT.
        - DCT.
- Presence of pre-crack or notch:
    - Present: SCB-J_c, SCB-FI, and DCT.
    - Absent: IDEAL-CT.

These test methods, each with different features and limitations, can characterize the cracking resistance of asphalt mixtures. Before selecting a test method, it must be considered whether the parameters obtained from the prospective test method truly represent the performance of asphalt mixtures in the field. Like the selection of an appropriate rutting test, the selection of an appropriate cracking test also has to consider several other equally important parameters such as simplicity in sample preparation and testing, confidence in repeatability, cost-effectiveness in terms of equipment cost or modification, sensitivity to asphalt mixture composition, practicality in terms of its use in mixture design, and quality control and quality assurance processes (Zhou et al. 2019a). The next sections present brief introductions of major asphalt mixture cracking tests focused on intermediate temperature cracking (which is the primary mode of pavement cracking in Florida) and provide some examples of their use in evaluating the cracking resistance of asphalt mixtures designed with different asphalt binder type/content/grade, aggregate type/gradation/NMAS, and design/in-situ density (which is the primary focus of this study). Tests such as the DCT test run at low temperatures are not discussed here.

2.3.1 Repeated Bending Beam Fatigue Test

The RBBF test is one of the earliest cracking tests of asphalt mixtures (Underwood and Braham 2019). The test uses the classical, empirical definition of fatigue failure to determine the cracking resistance of asphalt pavements (Hernandez-Fernandez et al. 2020). This definition presents fatigue life (N_f) (the number of cycles at 50 percent reduction in stiffness) as a function of either the tensile strain (ε_t) alone (Monismith et al. 1961) or both tensile strain and stiffness (S_{mix}) (Kingham 1972), where a, b, and c are empirical constants (Underwood and Braham 2019):

$$N_f = a \times \left(\frac{1}{\varepsilon_t}\right)^b \quad (2\text{-}2)$$

or

$$N_f = a \times \left(\frac{1}{\varepsilon_t}\right)^b \times (S_{mix})^c \quad (2\text{-}3)$$

The standardized versions of this test or the four-point bending beam fatigue (FPBBF) test involve the application of cyclic loading to four-point bending beam specimens at a certain linear frequency, and a constant conditioning/testing temperature until sometime after the flexural stiffness (S) drops by a certain percentage (usually when $\Delta S \geq 50$ percent) or the normalized stiffness and normalized cycle ($\hat{S}\ x\ \hat{N}$) reach their peak values by following AASHTO T 321 (2017b) or ASTM D8237 (2018). The test can extract parameters like a, b, and c, which can be used to estimate the fatigue life of asphalt mixtures under similar loading conditions.

Over the years, many researchers have used the parameters obtained from the different versions of RBBF tests to evaluate the fatigue cracking resistance of asphalt mixtures with different mixture design parameters (Deacon 1965; Monismith et al. 1961; Tayebali et al. 1994). For example, Mogawer et al. (2011) used the FPBBF test to evaluate the fatigue cracking resistance of plant-produced, laboratory-compacted SP-9.5 and SP-12.5 mixtures, each with 88, 91, 94, and 97 percent Gmm (i.e., two mix types × four densities = eight mixtures). The researchers reported that SP-9.5 mixtures generally exhibited longer fatigue life (i.e., better cracking resistance) than SP-12.5 mixtures and that fatigue life did not change significantly with mixture density (Figure 6-1). The authors attributed the longer fatigue lives of SP-9.5 mixtures to 1 percent higher asphalt binder content than SP-12.5 mixtures (5.8 percent versus 4.8 percent binder content, respectively). More importantly, their results showed that there is a possibility of designing SP-9.5 mixtures equivalent to or even better than SP-12.5 mixtures—the focus of this study.

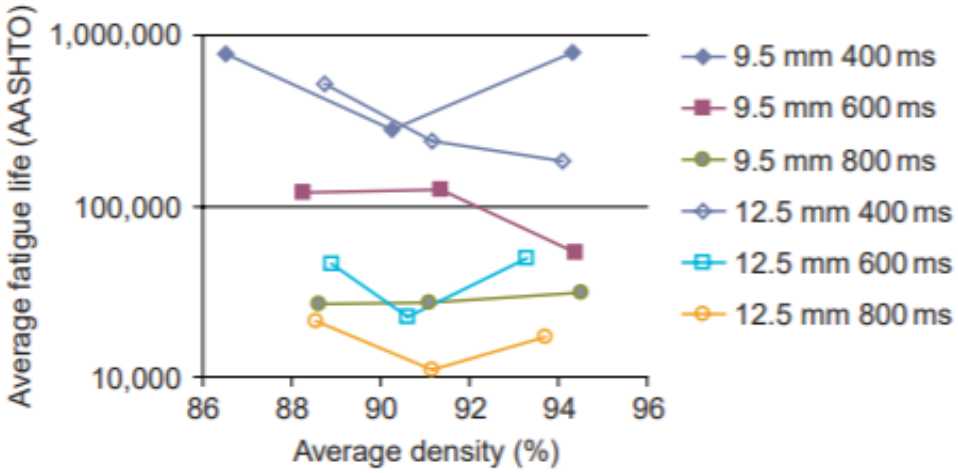

(a) Failure Criterion: 50 Percent Drop in Flexural Stiffness

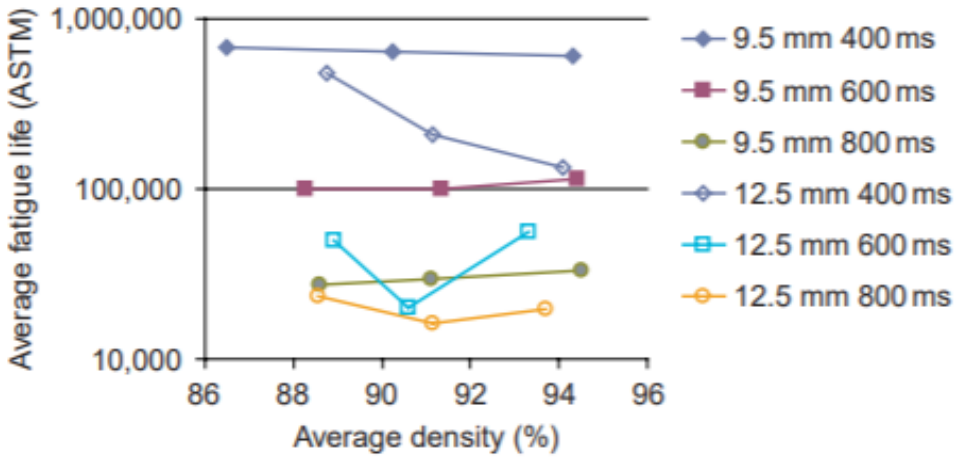

(b) Failure Criterion: Peak Value of $\hat{S} \times \hat{N}$

Figure 2-9. Repeated Bending Beam Fatigue Test Results (Mogawer et al. 2011)

However, this test has several limitations that bar it from being accepted as a routine test (Kim et al. 2012; Zhou et al. 2019b):

- Difficulty in sample preparation:
  - Size: large.
  - Cutting: four cuts per specimen.
  - Gluing: one stud.
- Not efficient: minimum 1 hour to several days to complete the tests.
- Expensive equipment: over $100,000.

2.3.2 AMPT Cyclic Fatigue

The AMPT cyclic fatigue is a uniaxial fatigue test for asphalt mixtures (Underwood and Braham 2019). Previous versions of this test involved repeatedly applying haversine pull (tension) or sinusoidal push-pull (compression-tension) load cycles on cylindrical samples until certain conditions were met (usually until the dynamic modulus dropped by 50 percent or more) and

correlating this failure criterion to stress/strain at the bottom of the asphalt concrete layer. These versions included Transport and Road Research Laboratory, Pennsylvania State University, Delft University of Technology, North Carolina State University, Advanced Asphalt Technologies, and Arizona State University versions. Unlike these previous versions, the AASHTO TP 107-18 (2018a) version of this test, developed under FHWA project DTFH61-08-H-00005 and specifically for AMPT, involves two major steps:

1. Subjecting the cylindrical sample to a series of frequency sweep tests at various loading frequencies and temperatures within its linear viscoelastic (LVE) range (Wang et al. 2020).
2. Subjecting the same specimen to a haversine function of tensile load at a constant loading frequency (usually 10 Hz), a constant testing temperature (usually 25°C or lower), and a constant stress or strain level, which can cause damage upon repetition (Wang et al. 2020).

The specimens used for this test are prepared by coring and cutting each Superpave gyratory compactor (SGC) specimen (150 mm or 6 inches in diameter by 178 mm or 7 inches in height) (Figure 2-10) into either:

- One specimen that measures 100 mm or 3.93 inches in diameter by 130 mm or 5.11 inches in height by following AASHTO TP 107-18 (AASHTO 2018a).
- Three specimens that measure 38 mm or 1.50 inches in diameter by 110 mm or 4.33 inches in height by following AASHTO TP 133-19 (AASHTO 2019a).

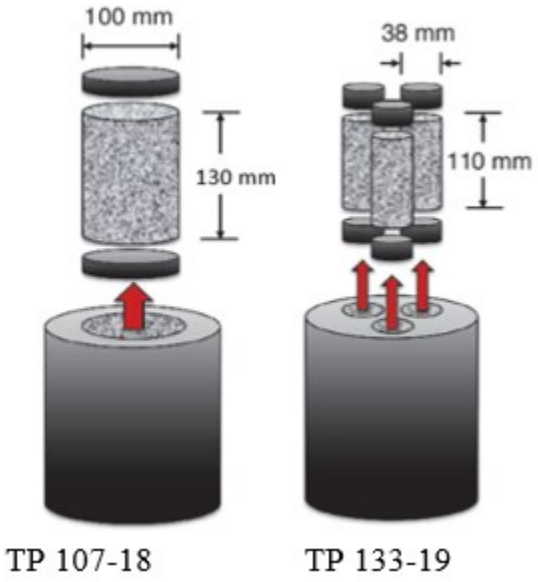

(a) Geometry

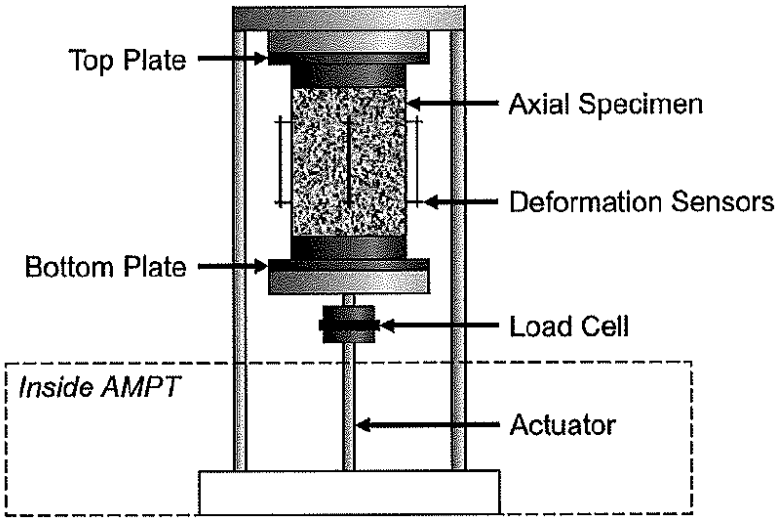

(b) Setup

Figure 2-10. Schematic of AMPT Cyclic Fatigue Test

The data from the first step are used to obtain the LVE dynamic modulus ($|G^*|_{LVE}$) and the damage parameter (α). These two parameters, together with the dynamic modulus, are analyzed using SVECD to obtain the characteristic pseudo-stiffness versus damage evolution ($C \times S$) curve (Underwood and Braham 2019). The SVECD mechanics describe the rate of damage evolution (dS/dt) as a α^{th} function of dissipated pseudo-strain energy (W^R) (Schapery 1984):

$$\frac{dS}{dt} = \left(-\frac{\partial W^R}{\partial S}\right)^{\alpha} \quad (2\text{-}4)$$

The main advantage of the uniaxial fatigue test over other alternative tests is the inherent nature of the SVECD model itself. The characteristic fatigue damage evolution model (C versus S) is

independent of loading frequency, loading strain/strain level, rest period, and test temperature (Karki et al. 2016, 2014; Underwood et al. 2012; Xie et al. 2015).

Researchers have used this test as an alternative to fracture damage–based monotonic tests in evaluating the fatigue cracking resistance of asphalt mixtures (Chehab 2002; Hernandez-Fernandez et al. 2020; Kim et al. 1995; Kutay et al. 2008; Underwood et al. 2010; Underwood and Kim 2012; Xie et al. 2015).

Among them, Tavakol et al. (2018) used the direct tension fatigue test and SVECD model to evaluate the fatigue-cracking resistance of nine different mixtures:

- Three SP-9.5 mixtures obtained from a US-59 surface course.
- Three SP-9.5 mixtures obtained from a US-59 intermediate course.
- Three SP-19.0 mixtures obtained from a US-36 intermediate course.

Each contained 15, 20, or 35 percent RAP and different binder contents. The authors concluded that the US-59 mixtures that contained the same aggregate type and binder source had similar SVECD-predicted fatigue lives, irrespective of the aggregate size (i.e., NMAS). In contrast, the US-36 mixtures showed a considerably different fatigue behavior (Figure 2-11). Though not directly stated, the observed similarity in fatigue life pattern between the two mixtures, whose only difference was aggregate size (NMAS), implies the possibility of using the SP-9.5 mixture in place of the SP-19.0 mixture in some cases. However, not many studies could be found that directly compared the fatigue damage resistance of asphalt mixtures prepared with different NMASs.

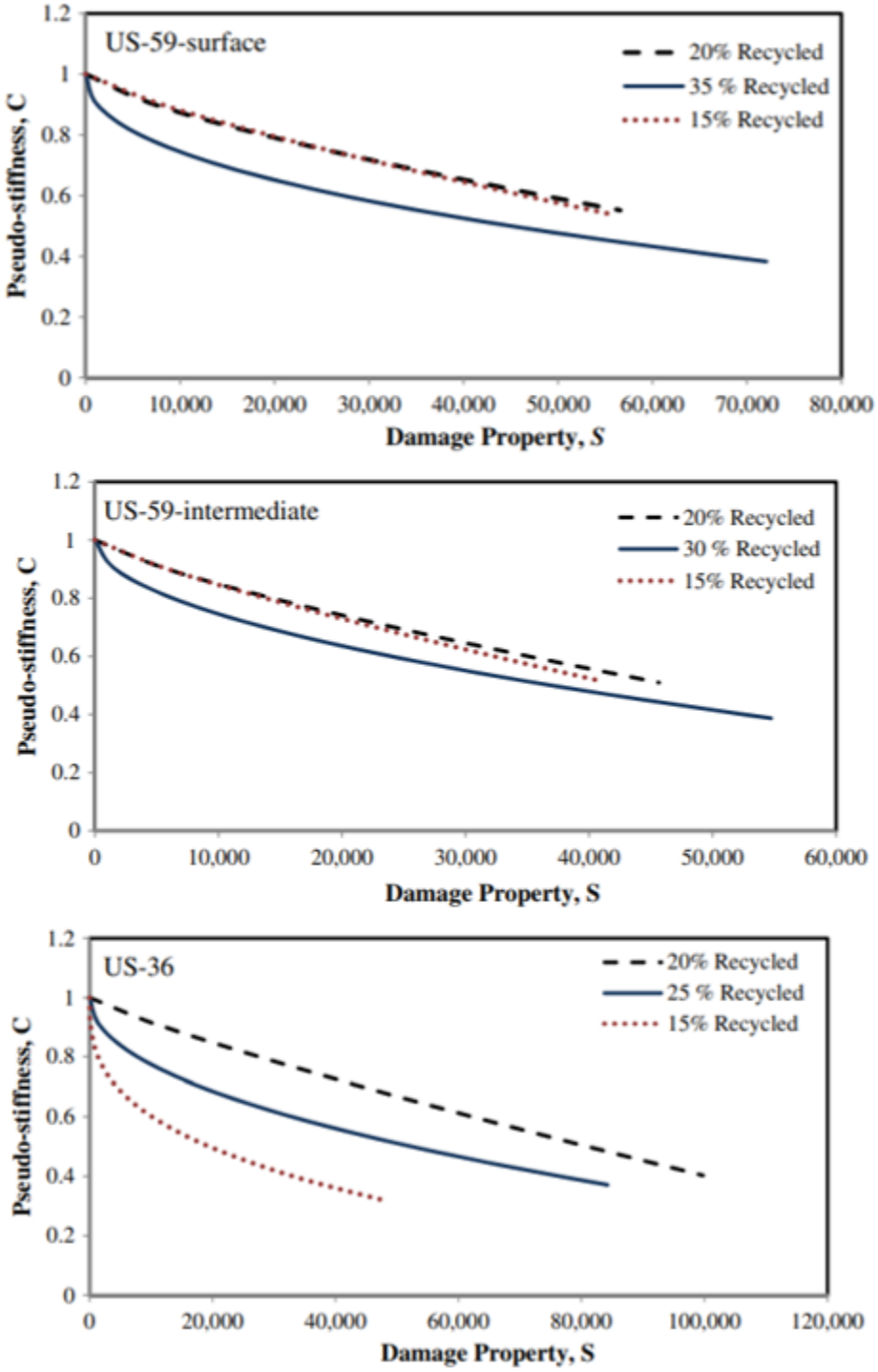

Figure 2-11. Characteristic C versus S curves (Tavakol et al. 2018)

Despite the attested correlation of these tests with field performance, researchers have also highlighted some limitations of this test method, such as:

- Requirement of a highly skilled technician for:
  - Sample preparation: 1 × coring + 2 cuttings per specimen.
  - Instrumentation: gluing the samples to the loading platen parallelly and vertically.
  - Selecting the appropriate loading strain levels for fatigue damage.
  - Estimating fatigue life using a relatively complex (or not user-friendly) model instead of direct measurement.
- Lengthy conditioning and testing time:
  - 3–4 days for conditioning and testing in Step 1.
  - 3–4 days for conditioning and testing in Step 2.
- Use of relatively expensive test instruments such as the AMPT.
- Questions about repeatability:
  - Hard to know if the test results are repeatable or not looking at C versus S curves.
  - Cannot compare the parameters themselves to tell good or bad.

2.3.3 Texas Overlay Test

The Texas OT is a modified version of the asphalt-over-cement concrete overlay tests developed in the 1970s (Germann and Lytton 1979). Unlike the original version, the OT is used to evaluate the cracking resistance of asphalt-over-asphalt overlays (Zhou and Scullion 2003, 2005). The standardized version of this test, Tex-248-F (TxDOT 2017), involves gluing one half of an asphalt mixture specimen to a moveable plate and the other half to a stationary metal plate (Figure 2-12) and applying horizontal movements on the moveable metal plate back and forth, with a maximum opening displacement of 0.635 mm (0.025 inches). The test is run at room temperature (25°C or 77°F) in a controlled displacement mode at a rate of one cycle per 10 sec (5 sec to the maximum opening displacement and 5 sec back to the original position). The peak load of each cycle reduces because the crack propagates (bottom-up) after each loading cycle. The number of cycles to failure is defined in relation to the reduction of the peak load of each cycle (currently, a 93 percent reduction from the peak load of the first cycle is used).

Other state agencies have adopted this test as a routine test. They have set criteria to prevent reflective cracking in asphalt mixture overlays based on the correlation of the OT results of local materials with field performance. For example, New Jersey requires overlay samples produced with PG 64-22 or high RAP content to not fail before 150 cycles and those produced with PMA binders to not fail before 175 cycles.

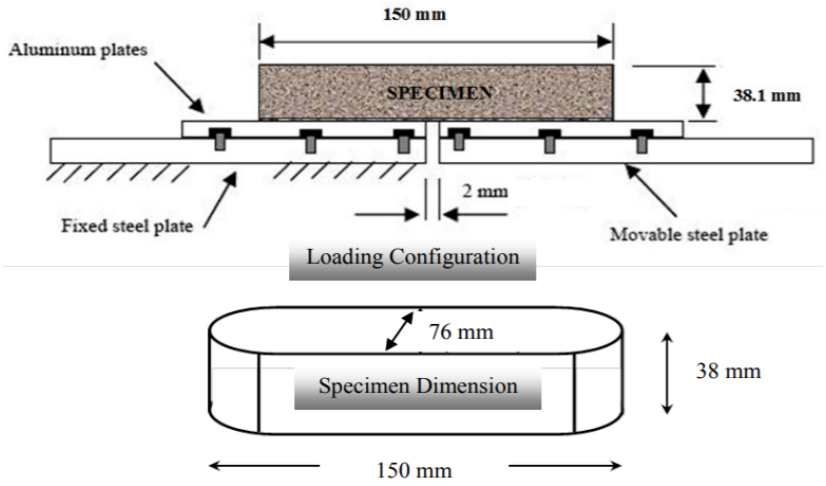

Figure 2-12. Schematic of Texas Overlay Tester

Karki et al. (2019) used this test to evaluate the cracking performance of asphalt mixtures produced with 10 PG 58-XX asphalt binders. The researchers produced these asphalt binders by blending unmodified PG 58-28 asphalt binder with type R1 and type R4 re-refined engine oil bottom, PPA, and RAP-extracted binder together or separately at different proportions. Test results showed that asphalt mixtures performed very differently in cracking resistance (Figure 2-13).

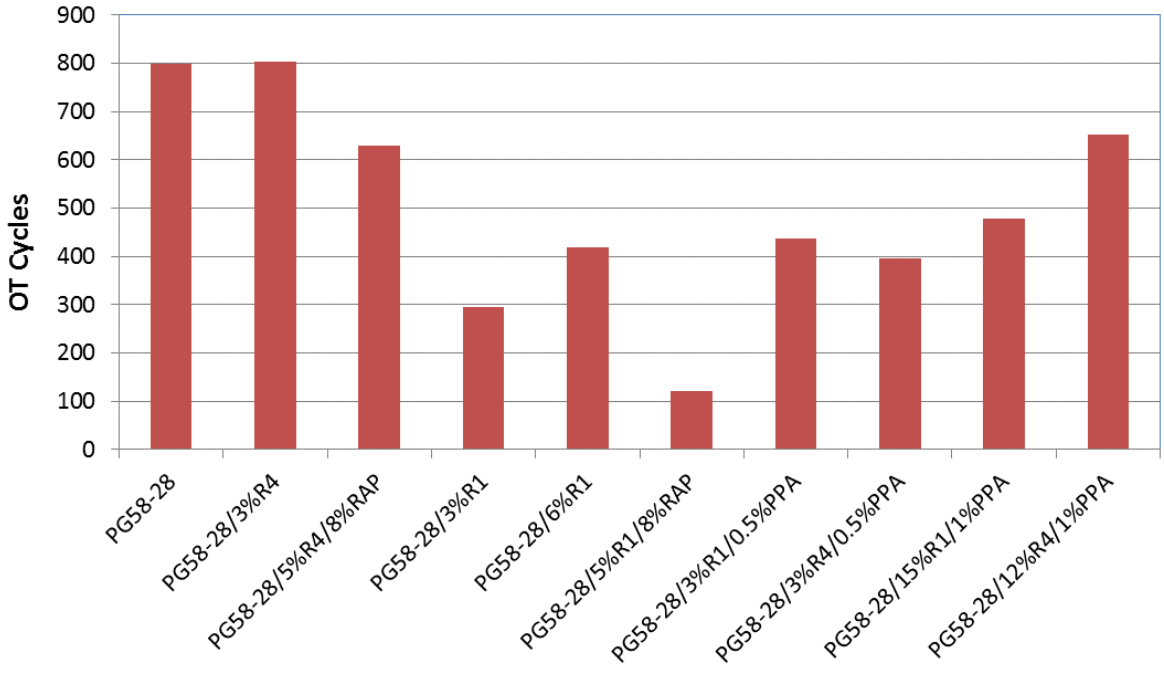

Figure 2-13. OT Results (Karki et al. 2019)

Despite its well-reported effectiveness, the test has several limitations:

- Difficulty:
  - Sample preparation: four cuts per specimen; gluing of the specimen to bottom plates.
- Not efficient:
  - 30 minutes to 3 hours of testing time.
- Not repeatable:
  - 30 to 50 percent COV.
  - Subjective selection of three closest results out of five minimum tests to deal with this COV.
- Expensive:
  - Requires separate conditioning and testing equipment.
  - Total cost of $40,000–$50,000.

Several modifications have been proposed to address these limitations (especially the high variability). Texas A&M Transportation Institute (TTI) researchers (Walubita et al. 2012a) recommended more clearly specifying the sample drying method, glue quantity, number of sample replicates, air voids, sample age at the testing time, and temperature variation to minimize the variability of OT results. Similarly, National Center for Asphalt Technology (NCAT) researchers (Ma 2014) mentioned lowering the COV value, reducing the total duration of the loading and unloading cycle from 10 seconds to 1 second, reducing the maximum displacement from 0.635 mm to 0.381 mm, and using a peak value of the maximum load multiplied by the load cycle instead of 93 percent reduction from the initial peak load since the failure criterion would lower the COV value from 30–50 percent to 20–30 percent. Nevertheless, these improvements only address the repeatability issue.

2.3.4 Louisiana Semi-circular Bending Test

The Louisiana SCB-Jc test is a monotonic fracture test developed after the works of Abdulshafi and Majidzadra (1985), who used notched rectangular beams; Little and Mahboub (1985), who used notched indirect tensile (IDT) tests; and Mull et al. (2002), who used notched semi-circular bending (SCB) specimens, to evaluate the cracking resistance of asphalt mixtures. As the name suggests, the test involves monotonically loading the notched SCB specimens with thickness (b) until failure and using the linear elastic fracture mechanics–based relationship of dissipated energy (U) with notched depth (a) to determine the critical strain energy release rate, or the J-integral (J_c) under opening mode (Mode I) of cracking (Mull et al. 2002; Wu et al. 2005):

$$J_c = -\frac{1}{b}\left(\frac{dU}{da}\right) \quad (2\text{-}5)$$

As an energy parameter, a higher J_c value refers to materials that need more energy for crack initiation and propagation. The test has been standardized to evaluate the cracking resistance of asphalt mixtures at both low and intermediate temperatures.

The SCB-Jc test, ASTM D8044 (2016), involves fabricating SCB specimens with 25-, 32-, and 38-mm-deep notches (narrower than 3.5 mm) at the center of the flat side of the specimens and loading them at a constant displacement rate of 0.5 mm/minute (0.02 inches/minute). The

analysis part of this test involves calculating the fracture energy for each notch depth following loading (Mull et al. 2002).

Unlike the SCB-Jc test, the low-temperature SCB test (i.e., AASHTO TP 105-13 [AASHTO 2015b]) involves testing SCB specimens with 15-mm-deep notches (narrower than 1.5 mm) at a crack mouth opening displacement rate of 0.0005 mm/sec (0.00002 inches/sec) and measuring the cracking resistance of asphalt mixtures in terms of fracture energy (G_f) and fracture toughness (K_{IC}). Since low-temperature cracking was not the focus of this study, this review focused on the intermediate-temperature SCB (i.e., SCB-Jc) test only.

Several researchers have used the SCB-Jc test to evaluate the cracking resistance of asphalt mixtures at an intermediate temperature (the focus of this study) because the method can be used to test both gyratory-compacted and field-cored samples, and multiple specimens can be obtained from a single core/compacted sample, and there is less error due to the self-weight of the specimen.

Most relevant to this study, Wu et al. (2005) used this test to evaluate the fracture resistance of 13 different asphalt mixtures in terms of four different parameters, including peak load, vertical displacement at peak load, U_f, and J_c, and to determine the parameter that was most sensitive to mixture design variables. The mixtures included:

- Two aggregate NMASs: 3 × SP-19.5 + 10 × SP-25.
- Two gradation types: 2 × fine graded + 11 × coarse graded.
- Three aggregate types: 11 × limestone + 1 × granite + 1 × rhyolite.
- Four asphalt binder types: 3 × AC-30 or PG 64-22 (unmodified) + 4 × PAC-30 or PG 70-22 (unmodified) + 3 × PG 70-22M + 3 × PG 76-22M).
- Three design levels for binder contents: 3 × 75 gyrations + 3 × 97 gyrations + 3 × 109 gyrations + 4 × 125 gyrations.

The authors fabricated SGC specimens with 25-, 32-, and 38-mm-deep notches and 7 percent air void content for the study. A two-way analysis of variance of mixture design variables showed that—compared to peak value, vertical displacement at peak load, and strain energy at failure—the J_c-value was more sensitive to mixture design variables. Of particular interest for this study was the fact that the SP-25 mixtures had larger J_c values than the SP-19 mixtures did, which implies that SP mixtures with larger NMASs have better aggregate structure (and stone-to-stone contact) and therefore need more energy for fracture than the SP mixtures with smaller NMASs. It indicates that asphalt mixtures with larger NMASs tend to have stronger aggregate structures than smaller NMASs. Of interest for this study was the fact that SP mixtures with stiffer asphalt binders such as PG 76-22M and PG 70-22M showed smaller J_c values than SP mixtures with softer asphalt binders such as PG 64-22 and PG 70-22.

Though not stated directly in the text, the authors' test results clearly showed that an SP-19 mixture produced with PG 70-22M or AC-30 has higher J_c values (or better fracture resistance) than SP-25 mixtures produced with PAC-40 (Figure 2-14), which underscores the possibility of producing mixtures with higher J_c values (or better fracture resistance) using smaller NMASs.

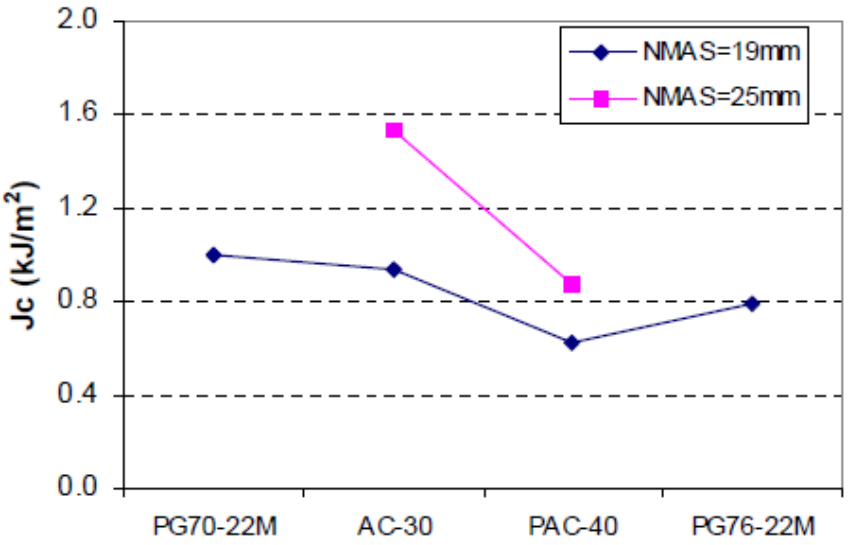

Figure 2-14. SCB Test Results (Wu et al. 2005)

However, the test is not without limitations (West et al. 2018c; Zhou et al. 2019b):

- Sample preparation involves several cutting and notching steps, which adds variability.
- Cutting a minimum of 12 specimens (a minimum of four replicates for each of the three notch depths) needs a longer sample preparation time.
- The critical J_c value is a single value derived from the correlation of the J-integral and notch depth, making it hard to capture its variation and conduct a statistical comparison.
- The cost of equipment is higher than that of the IDEAL-CT test.
- Studies have revealed a poor correlation with other tests and field performance.

2.3.5 Illinois Semi-circular Bending Flexibility Index Test

The Illinois SCB-FI test is another monotonic fracture test developed with the same type of loading configuration as the SCB-Jc test but with only one notch depth instead of three. Al-Qadi et al. (2015) developed the test based on better sensitivity of the post-peak slope of the load versus the displacement curve to material properties and loading conditions than fracture energy. Unlike the intermediate-temperature SCB-Jc test that requires three notch depths (25, 32, and 28 mm) and that yields critical J-integral as an index of cracking resistance, the standardized version of SCB-FI (i.e., AASHTO TP 124-16 [2018b]) requires the use of only one notch depth (25 mm) and yields a new index for fracture resistance, which is called the flexibility index (FI). This index is determined by the following steps:

1. Calculating the work done for fracture (W_f) by integrating the area under load (P) versus displacement (u) curve until failure:

$$W_f = \int P.du \tag{2-6}$$

2. Calculating the fracture energy (G_f) by dividing W_f by the effective ligament area:

$$G_f = \frac{W_f}{A} \quad (2\text{-}7)$$

where:

$$A = t\,(r - a) \quad (2\text{-}8)$$

t = thickness
$r - a$ = ligament length
a = notch depth
r = radius

3. Calculating the FI value by dividing the G_f value by the absolute value of the post-peak slope at the inflection point (m) and multiplying by a unit conversion or scaling factor (C):

$$FI = \frac{G_f}{|m|} \quad (2\text{-}9)$$

AASHTO TP 124-16 also specifies that the SCB specimens can be prepared from either one 160-mm-tall SGC sample to get two discs (four SCB specimens) or one 115-mm-tall SGC sample to get one disc (two SCB specimens).

In their study, Al-Qadi et al. (2015) evaluated the FI value of asphalt mixtures produced with 6.0 percent PG 70-22 styrene-butadiene-styrene (SBS), PG 64-22, PG 58-28, or PG 52-34 and 0–40 percent RAP and/or 0–7 percent RAS by weight. Test results showed that the FI captured the effect of the asphalt binder grade (positive), field aging (negative), and RAP/RAS use (negative) on the cracking resistance of asphalt mixtures. Test results also exhibited a good correlation between the FI and field performance. Similarly, Ozer et al. (2016b) determined that asphalt mixtures with excellent cracking resistance had an FI value of 10.0 or above, while those with poor cracking resistance had an FI value of 6.0 or below. Al-Qadi et al. (2017) later found the minimum value of 8.0 for the FI to distinguish well-performing from poorly performing asphalt mixtures.

Several recent studies have since used this test and the FI value of 8.0 to determine the fracture resistance of asphalt mixtures produced with different mixture design variables including but not limited to design and compaction densities, aggregate gradation, and NMAS.

Among them, Ali (2018) used this test to evaluate the cracking resistance of two mixtures. The first (control) mixture was designed with 4 percent air void content at 70 gyrations; its samples contained 7 percent air void content. Since it also contained 10 percent reclaimed materials, the name was N70-10. The second mixture was designed with 5 percent air void content at 70 gyrations; its samples too contained 5 percent air voids, and the name was Superpave 5. Test results showed that the new mixture (Superpave 5) exhibited higher fracture energy, fracture strength, and post-peak slope but a lower FI value (lower cracking resistance) than the N70-10 mixture (Figure 2-15). The authors attributed the lower FI value of the new mixture to a higher brittleness resulting from lower air void content and higher stiffness. The study showed the sensitivity of FI values to mixture volumetric design properties, including air void content.

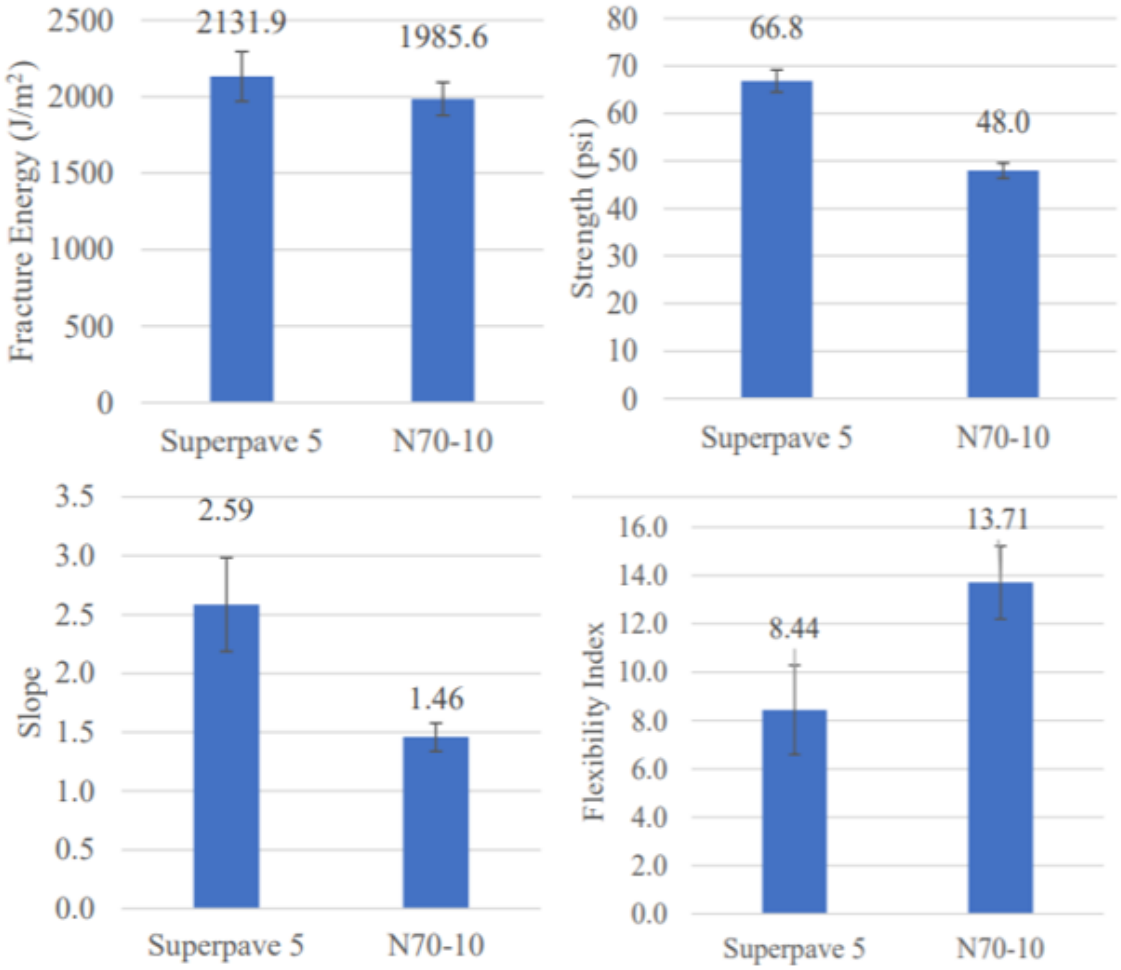

Figure 2-15. SCB-FI Test Results (Ali 2018)

Additionally, West et al. (2018a) used this test to investigate the resistance to fracture of six different SP mixtures: one SP-9.5 mixture (Mix 1) and five SP-12.5 mixtures (Mix 2 to Mix 6). The authors designed mixtures with target air voids of 4, 3.5, and 3 percent by changing asphalt binder content. The authors fabricated samples with a target of 7 percent air voids for each designed mixture. Test results showed that mixtures with lower design air voids (higher asphalt binder content) performed with better fracture resistance (or had a higher FI value) than mixtures designed with higher design air void content. Test results also showed that SP-9.5 mixtures had higher intermediate-temperature cracking resistance (or higher FI values) than SP-12.5 mixtures in all but two cases, a promising premise concerning this FDOT study.

Recently, Kaseer et al. (2018) used a new parameter called the cracking resistance index (CRI), obtained by dividing G_f with peak load (P_{max}) to evaluate the cracking resistance of field-collected asphalt mixtures obtained from three states in the United States:

$$CRI = \frac{G_f}{P_{max}} \quad (2\text{-}10)$$

The asphalt mixtures contained different combinations of PG 58-22, PG 64-22, and PG 70-22 unmodified asphalt binders, recycled materials, and recycling agents. The mixtures showed the CRI was more sensitive to the recycled material content.

In a study sponsored by the Indiana Department of Transportation, Batioja-Alvarez et al. (2019) used both FI and CRI parameters to evaluate the fracture resistance of the plant-mixed, laboratory-compacted specimens and the plant-mixed, field-compacted specimens of asphalt mixtures. The asphalt mixtures used in this study contained different combinations of asphalt binders (PG 64-22 and PG 70-22), aggregate NMASs (9.5 mm and 12.5 mm), and recycled material content (up to 32 percent). The test results revealed that FI and CRI parameters were sensitive to these mixture design variables, including NMAS and recycled material content. More importantly, the results showed that CRI was more repeatable than FI values and less sensitive to sample variability (Figure 2-16), and therefore the authors recommended using CRI over FI.

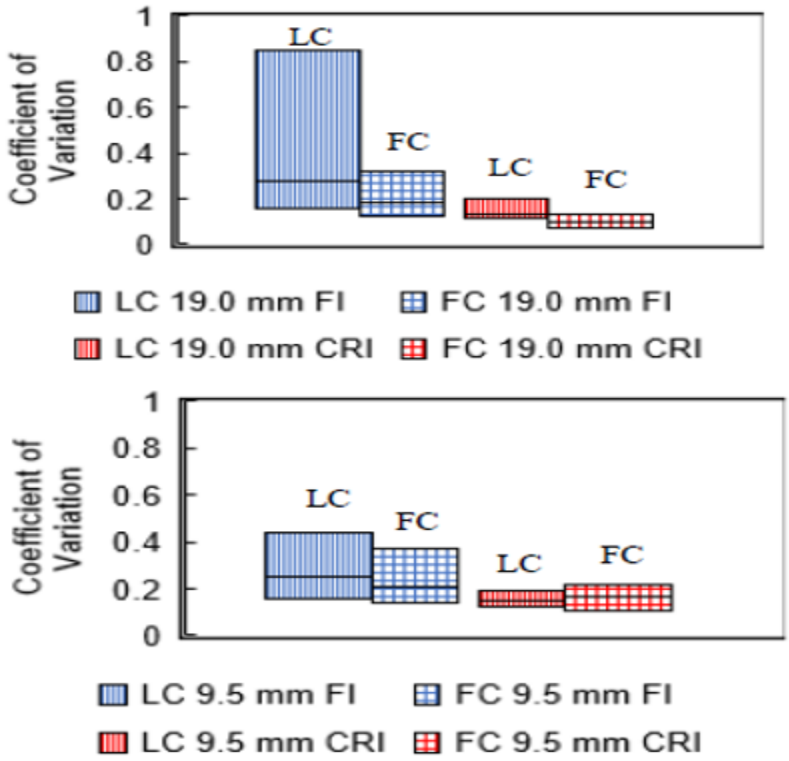

Figure 2-16. Distribution of CRI and FI (Batioja-Alvarez et al. 2019)
[Note: LC = Laboratory-Compacted; FC = Field-Compacted]

In addition to describing the benefits and various options of SCB-FI tests, previous studies have also revealed some issues with this test, such as:

- Difficulty in calculating the post-peak slope (and FI) when asphalt mixtures undergo brittle failure due to either a higher-than-normal percentage of recycled materials (Barry 2016; Zhou et al. 2017a) or severe aging of asphalt binders/mixtures (Kaseer et al. 2018).

- A higher coefficient of variation (or less repeatability) when the load-displacement curves are not smooth and therefore lack well-defined inflection points (Kaseer et al. 2018).
- Insufficient sensitivity to some mixture design parameters, such as asphalt binder content (Kaseer et al. 2018).
- The need for correction factors for air void content and specimen thickness, especially for field samples (Kaseer et al. 2018).
- A high COV due to variability in post-peak slopes (Batioja-Alvarez et al. 2019).

2.3.6 University of Florida Indirect Tensile Test

The UF-IDT procedure includes three tests:

- A resilient modulus test.
- A creep test.
- A tensile fracture test.

Dr. Rey Roque developed a draft procedure for FDOT in early 2015. The energy ratio concept worked well to predict the top-down cracking of virgin mixtures at the NCAT 2006 test track (Timm et al. 2009) but failed to differentiate mixtures with RAP/RAS at the NCAT 2016 test track (Taylor, 2018). The NCHRP 9-57A project evaluated the UF-IDT test and fine-tuned some test parameters according to the ruggedness testing results.

The parameter ER is used to distinguish asphalt mixtures with different resistance to top-down cracking (surface-initiated longitudinal wheel-path cracking). Roque et al. (Roque et al. 2004) recommended determining the total amount of energy required to fail, also called dissipated creep strain energy ($DCSE_f$) by running UF-IDTs on cylindrical specimens of asphalt mixtures at 10°C. The authors also recommended determining the minimum dissipated creep strain energy ($DCSE_{min}$) by running the creep compliance test. The ER parameter is defined as the ratio of these two energies as an index that represents the resistance of asphalt mixtures to cracking:

$$ER = \frac{DCSE_f}{DCSE_{min.}} \quad (2\text{-}11)$$

In their study, Roque et al. (2004) conducted these tests on asphalt mixtures obtained from several field test sections and compared their $DCSE_{min}$ and ER values. Test results showed that asphalt mixtures with a record of early cracking had a lower value of ER than asphalt mixtures with a record of fewer or no cracks. Based on these results, the authors recommended using the minimum value of 1.0 for ER and 0.75 $kJ/m3$ for $DCSE_{min.}$ as thresholds for differentiating well-performing asphalt mixtures from poorly performing asphalt mixtures.

Willis et al. (2014) also used this test to evaluate the cracking resistance of rubber and PMA mixtures. Test results showed that asphalt rubber binder mixtures had a higher ER (6.68) than PMA mixtures (5.42). Though both asphalt mixtures passed the minimum criteria of ER recommended for a traffic volume of 1,000,000 ESALs per year or less, the results showed the ER could differentiate two asphalt mixtures from each other.

Similarly, Yan et al. (2017) used this test to evaluate the cracking resistance of dense-graded structural friction course asphalt mixtures produced with SBS-modified PG 76-22 PMA, two different sources of virgin aggregates, three different dosages, and two different sources of RAP following FDOT's FC-12.5 design. Test results showed that the ER value decreased differently with an increase in RAP content (20, 30, and 40 percent by total weight of mixture) depending on the source of aggregates. The authors also reported that each of the seven asphalt mixtures (one control and six RAP-modified) passed the minimum criteria of $DCSE_{min.}$ and ER, signifying the effectiveness of the use of PMA asphalt binders.

2.3.7 IDEAL Cracking Test

TTI researchers (Zhou et al. 2017b) recently developed a new cracking test, IDEAL-CT, to determine asphalt mixtures' cracking resistance. It is the key product of the NCHRP-IDEA 20-30/IDEA 195 project. The test has been recently standardized as ASTM D8225 (2019). The test involves loading the 38- to 75-mm-thick SGC specimens with indirect tension at a constant displacement rate of 50 mm/minute (2 inches/minute) diametrically (Figure 2-17). An index for cracking called the cracking tolerance index (CT_{index}) can be determined based on the load-displacement curve. Ideally, asphalt mixtures with a higher CT_{index} are more tolerant to cracking and perform better than their counterparts. The researchers conducted these tests using 17 different asphalt mixtures and determined that the test offered the following attributes:

- Simple: no instrumentation, cutting, gluing, drilling, or notching.
- Repeatable/reproducible: COV < 20 percent.
- Efficient: test completion within minutes.
- Less expensive: existing or inexpensive equipment or parts.
- Practical: minimum training needed for routine operation.
- Sensitive: sensitive to asphalt mixture characteristics (Figure 2-18a).
- Representative: good correlation with field test sections (Figure 2-18b).

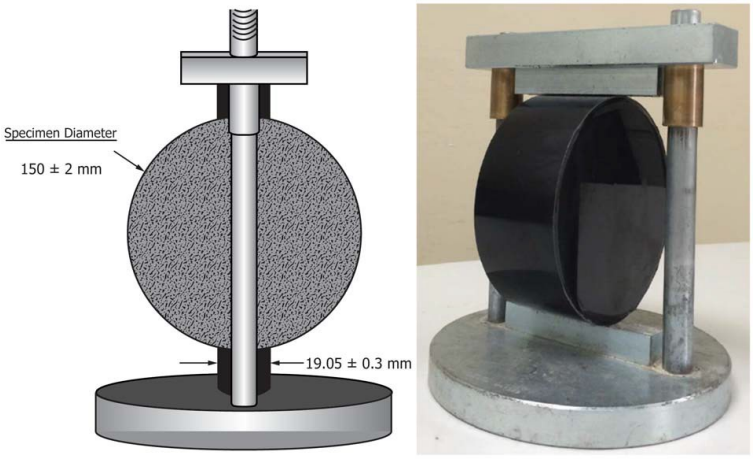

Figure 2-17. IDEAL-CT Setup (Zhou et al. 2017b)

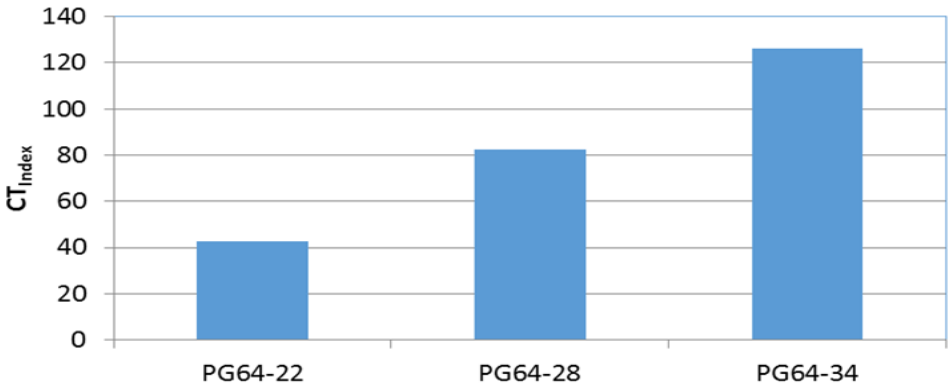

(a) Sensitivity to Asphalt Binder Grade

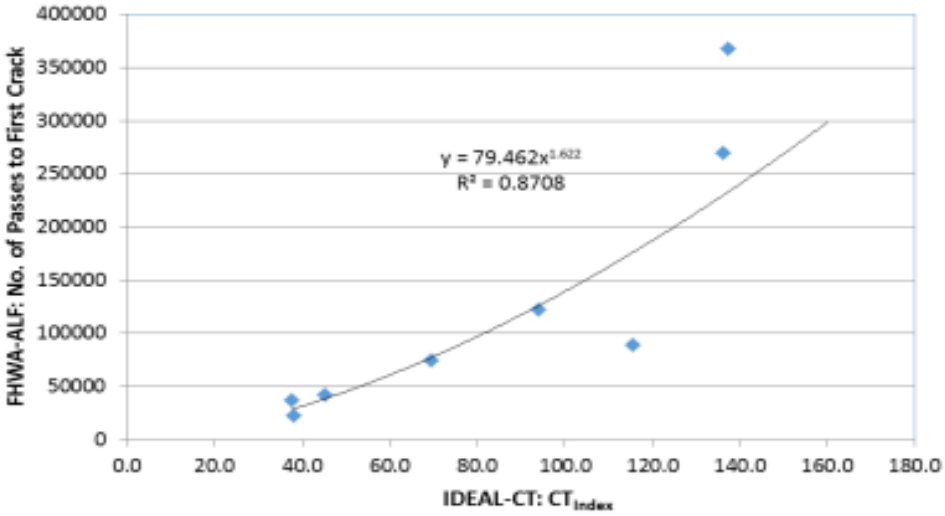

(b) Validation with FHWA-ALF Performance

Figure 2-18. IDEAL-CT Sensitivity and Field Validation (Zhou et al. 2017b)

TTI researchers (Zhou et al. 2017a) confirmed its sensitivity to the binder and mixture design variables and validated its correlation to FHWA's ALF fatigue cracking test (Figure 2-18). In addition, during the NCHRP 9-57A project, the research team performed the ruggedness testing on the IDEAL-CT and confirmed the current test parameter settings were reasonable. The ruggedness testing also pointed out that the IDEAL-CT result is sensitive to specimen air void, and the researchers recommended the air void tolerance be ± 0.5 percent. Therefore, lab-compacted specimens with air void beyond this range were not used for IDEAL-CT.

West et al. (2018c) recently reported that the IDEAL-CT and the SCB-FI tests ranked asphalt mixtures similarly, owing to the use of post-peak analysis in both methods. The authors also reported comparable COVs for seven different reheated plant-produced mixtures. Based on the Pearson correlation analysis, the authors determined that IDEAL-CT results were closely correlated to Texas OT and SCB-FI test results. Furthermore, the authors found that sample preparation was faster in the IDEAL-CT test than in the other five cracking tests because IDEAL-CT does not require cutting and notching the samples. The authors also found that

IDEAL-CT and SCB-FI were equivalent but better than the other four cracking tests in terms of equipment cost and testing time.

2.3.8 Summary

Table 2-4 summarizes the cracking performance tests.

Table 2-4. Common Asphalt Mixture Cracking Performance Tests (Al-Qadi et al. 2015; West et al. 2018b; West et al. 2018c; Zhou et al. 2019b)

Test	Standard	Conditioning	Loading	Parameters	Limitations
RBBF	AASHTO T321 (2017d)	Int. temp.: 20 ± 0.5°C	10 Hz	Measured failure cycle: N_f	• Preparation: cutting • Instrument: separate, expensive • Testing time: long (in hours or days) • Variability: high; self-weight errors
AMPT cyclic fatigue	AASHTO TP107 (2018a), TP133 (2019a)	Int. temp.: max. of 21°C, $\frac{PG_{HT} + PG_{LT}}{2} - 3$	10 Hz	$C \times S$ curve pseudo strain energy-based fatigue criterion	• Preparation: coring, cutting, gluing, curing • Instrument: expensive, separate • Testing time: long (in hours) • Variability: high; eccentricity errors
Texas OT	TxDOT Tex-248-F (2017)	Int. temp.	0.1 Hz	Load cycles to 93% initial load (N_f)	• Preparation: cutting, gluing, curing • Instrument: expensive, separate • Testing time: variable (in minutes to hours) • Variability: high; 30–50% COV
SCB-J_c	ASTM D8044 (2016)	Int. temp.: $\frac{PG_{HT} + PG_{LT}}{2} + 4$	50 mm/ minute	Critical strain energy release rate (J_c)	• Preparation: cutting, notching • Instrument: inexpensive, adaptable • Testing time: short (in minutes) • Variability: high
SCB-FI	AASHTO TP124 (2018b)	Int. temp. 25 ± 0.5°C	50 mm/ minute	FI CRI	• Preparation: cutting, notching • Instrument: inexpensive, adaptable • Testing time: short (in minutes) • Variability: high; 10–20% COV; depends on post-peak data quality
UF-IDT	N/A	Int. temp.	Varies	DCSE ER	• Preparation: simple; cutting • Instrument: inexpensive, adaptable • Testing time: short (in minutes) • Variability: depends
IDEAL-CT	ASTM D8225 (2019)	Int. temp.: 25°C or $\frac{PG_{HT} + PG_{LT}}{2} + 4$	50 mm/ minute	Cracking tolerance index (CT_{index})	• Preparation: simple; no cutting • Instrument: inexpensive, adaptable • Testing time: short (in minutes) • Variability: low, COV < 20%

2.4 Durability Performance

Durability can be broadly defined as the ability to withstand deterioration tendencies over time (Cox et al. 2017).

2.4.1 Durability Tests

The CAL test is the primary test used to evaluate the durability of asphalt mixtures. The test involves placing an SGC specimen in the Los Angeles abrasion drum without steel spheres at a temperature of 18 or 25°C and then rotating the drum for 300 revolutions at the rate of 30–33 revolutions/minute. The analysis part of the test involves the calculation of mass lost due to abrasion during this process from the difference in specimen mass before and after the test (AASHTO 2018c). More-durable asphalt mixtures usually have lower mass loss compared to less-durable asphalt mixtures.

The CAL test has been mostly used for evaluating the durability (or raveling resistance) of OGFC, or simply FC, mixtures (Arámbula-Mercado et al. 2019, 2016; Cooley et al. 2009; Tsai et al. 2012). Among the ones that evaluated the durability of mixtures with two different NMASs, a study sponsored by the South Carolina Department of Transportation recently evaluated the influence of aggregate gradation and NMAS on the durability of OGFC mixtures using CAL tests (Nekkanti et al. 2019). The study incorporated two NMASs (9.5 and 12.5 mm) and four different percentages passing the No. 4 sieve (10, 20, 30, and 40 percent). The test results revealed that the NMAS did not influence the mixture durability as much as the passing percentage of the No. 4 sieve did (Figure 2-19).

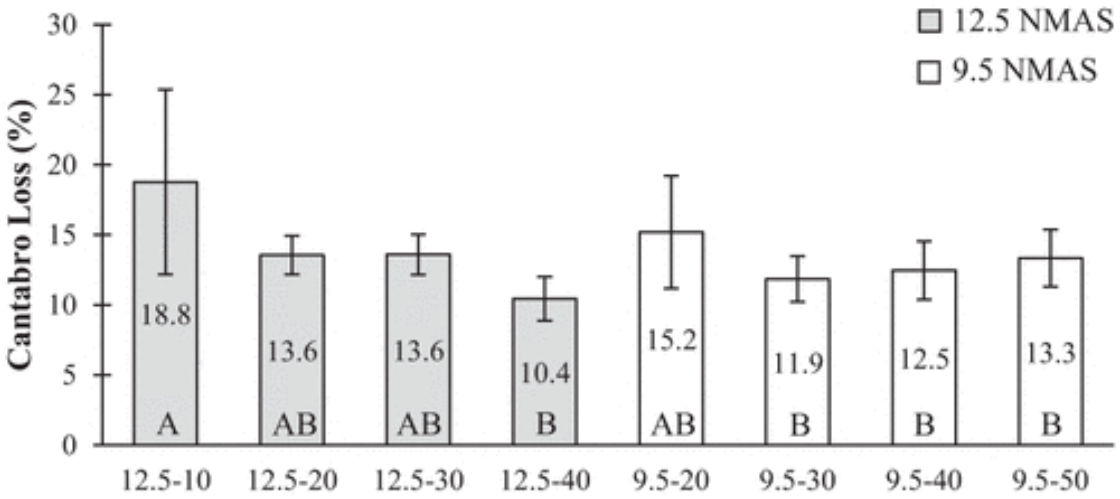

Figure 2-19. CAL Test Results (Nekkanti et al. 2019)

The CAL test has also been used to evaluate the effect of dryness on the durability of DGA mixtures (Baumgardner et al. 2012; Doyle and Howard 2016). The dryness of asphalt mixtures refers to the decrease in asphalt binder content to improve rutting resistance and the increase in recycled material percentage to increase sustainability (Cox et al. 2017). Since the applicability of this test to FC mixtures has been well documented, the review primarily focused on the applicability of this test to the SP DGA mixtures.

Doyle and Howard (2011) were some of the first researchers to study the applicability of the CAL test to evaluate the durability of DGA mixtures. In their study, researchers used six 9.5-mm mixtures (No. 1, 3, 4, 5a, 5b, and 5c), three 12.5-mm mixtures (No. 2, 6, and 7), and one 19.0-mm mixture (No. 8) prepared with different percentages of gravel, limestone, and sand. Out of these 10 mixtures, two contained 0 percent RAP (No. 1 and 2), and the rest contained 15 percent RAP. Mixtures 5a, 5b, and 5c are NMAS 9.5-mm mixtures produced with different asphalt binder types and contents. Test results revealed that mass loss (ML) was sensitive to binder content, binder type, NMAS, and RAP use. Based on these results, the authors concluded that the CAL test was a good candidate to compare the durability of conventional mixtures to that of high RAP-content mixtures (Figure 2-20).

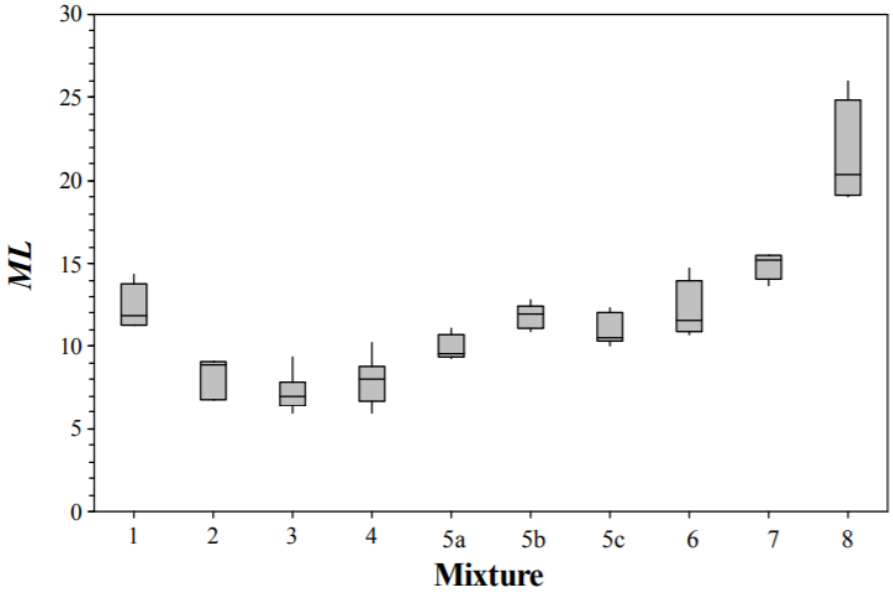

Figure 2-20. Mass Loss Content (Doyle and Howard 2011)

Similarly, Baumgardner et al. (2012) used the CAL test to evaluate the effect of adding ground tire rubber (GTR) additives to asphalt binders on the durability of DGA. The authors used three types of mixtures for this study: wet-processed GTR-modified, dry-processed GTR-modified, and wet-processed SBS-modified asphalt mixtures. The CAL test results showed that wet-processed SBS-modified and GTR-modified asphalt mixtures lost relatively less mass than the dry-processed GTR-modified asphalt mixtures, highlighting the effectiveness of wet-processing asphalt binders.

Doyle and Howard (2016) again evaluated whether the CAL test could be used to evaluate the durability of DGA mixtures. For this study, the authors evaluated the CAL test's sensitivity to mixture design parameters, asphalt mixture oven aging, RAP content in warm-mix asphalt, and its specimen-to-specimen variability. Statistical analysis of the test results revealed that ML was sensitive to several mixture design parameters such as aggregate NMAS (9.5, 12.5, and 19.0), aggregate type, mixture aging, and RAP content. More importantly, the study showed that ML generally decreased with smaller NMAS, which highlights the possibility that the 9.5-mm DGA mixture has more durability than the 12.5-mm DGA mixture.

Similarly, Cox et al. (2017) evaluated the effectiveness of the CAL test in assessing the durability of DGA asphalt mixtures by analyzing 1,200 CAL test data. The study found that the test was sensitive to various factors, such as:

- RAP content: ML increased with higher RAP content.
- Aging: ML increased with higher aging.
- Aggregate type: ML changed with a change in aggregate type.
- Asphalt binder grade: ML increased with an increase in high temperature in unmodified asphalt binders until the polymer was used.
- Additives: the test successfully discriminated asphalt mixtures containing GTR-modified asphalt binders from SBS-modified asphalt binders and hybrid (GTR- and SBS-modified) asphalt binders.

2.4.2 Summary

Based on the literature review, the CAL test is the most widely used durability test for asphalt mixtures. It has been used for evaluating the durability of mainly OGFC mixtures and, more recently, DGA mixtures, which are the mixtures of interest in this project.

2.5 Conclusions and Recommendations

The researchers conducted an in-depth review of literature that evaluated the performance of smaller (i.e., SP-9.5/FC-9.5) and larger NMAS (i.e., SP-12.5/FC-12.5) mixtures and compared them to each other. Specifically, the researchers reviewed FDOT specifications regarding the use of SP-9.5/FC-9.5 and SP-12.5/FC-12.5 mixtures in its contracts; the peer-reviewed articles and technical reports that describe the current state of knowledge on the use of SP-9.5/FC-9.5 and SP-12.5/FC-12.5 mixtures; and the AASHTO and ASTM standards used to evaluate the mixtures' associated rutting, cracking, and durability performance.

The review revealed multiple test methods proposed to evaluate the same type of performance of asphalt binders and asphalt mixtures. The review also revealed that all test methods have some limitations. Based on the minimum required features such as simplicity and sensitivity to mixture design variables, including the effect of practicality, repeatability, reproducibility, cost-effectiveness, and field performance correlation, the researchers have made several conclusions and recommendations on this project.

2.5.1 Asphalt Mixture Rutting Performance Tests

Below are the conclusions and recommendations for the rutting performance tests. The IDEAL-RT was recommended as an additional rutting test in the BE928 project.

- Wheel-track tests (e.g., APA and HWT tests) are the most popular and well-studied rutting tests.
- The APA test is a dry rutting test already implemented by FDOT. The HWT test is a wet rutting test studied by FDOT as part of various projects. The HWT test can characterize rutting and the moisture susceptibility of asphalt mixtures.

- The IDEAL-RT test is a new dry rutting test developed by TTI researchers. This test does not need cutting, correlates well with other tests and field performance, and takes only a few seconds to complete after conditioning. Since the test has been incorporated into FDOT's BE585 and BE719 projects, researchers recommend adding this test as an additional rutting test in this project.

2.5.2 Asphalt Mixture Cracking Performance Tests

Below are the conclusions and recommendations for the cracking performance tests. The SCB-FI test was recommended as an additional cracking test in the BE928 project.

- Cyclically loaded cracking tests (e.g., RBBF, AMPT cyclic fatigue, and Texas OT) require relatively long sample preparation, instrumentation, conditioning, and testing time (in hours or days) and more expensive, separate instruments (e.g., bending beam machine, AMPT, and overlay tester) and have high variability. Therefore, researchers do not recommend adding these cyclic tests to this project.
- Monotonically loaded cracking tests (e.g., SCB-Jc, SCB-FI, UF-IDT, and IDEAL-CT) are based on fracture mechanics and require shorter testing times and less-expensive instruments. Their analyses mainly yield energy-index parameters (e.g., J_c, FI, CRI, ER, and CT_{index}). However, the notch(es) requirement in some of these tests makes them prone to higher sample-to-sample variation.
- Among them, UF-IDT, IDEAL-CT, and SCB-FI have proven to be effective asphalt mixture fracture tests in several recent studies.
- UF-IDT was essentially developed and validated using local materials in Florida. IDEAL-CT was developed as part of the NCHRP-IDEA project and is being increasingly used by several DOTs in the United States. Therefore, researchers second FDOT's decision to include these two tests as required tests in this project.
- Likewise, the SCB-FI test needs SCB samples with one notch and is increasingly used by several DOTs in the United States. Therefore, researchers recommend adding this test as an additional cracking test. Researchers also recommend analyzing both FI and CRI parameters from this test.

2.5.3 Asphalt Mixture Durability Tests

The CAL test is the most widely used durability test for asphalt mixtures. The test has been used for evaluating the durability of mainly OGFC mixtures and, more recently, DGA mixtures, which are the mixtures of interest in this project. FDOT has already selected the CAL test for this project. Based on its simplicity and wide use, researchers strongly second this selection.

3. MATERIAL ACQUISITION AND EVALUATION

This chapter presents the full factorial experimental design, material acquisition, and initial testings for material evaluation.

3.1 Introduction

With the literature review findings and inputs from FDOT's project panel, two additional performance tests—the IDEAL-RT test and the SCB-FI test—were recommended.

A full factorial experimental design was developed based on the literature review results. The experimental design focused on the mixture performance comparison of SP-9.5 and SP-12.5 produced by varying several factors, such as two aggregate gradations, two aggregate types, two asphalt binder types, three mixture design gyration levels, two field compaction levels, and tests employing seven different performance tests (five FDOT-selected and two TTI-recommended tests).

3.2 Full Factorial Experimental Design

The research team performed a full factorial experimental design, which considered the effects of each factor and their interaction on performance test results (cracking, rutting, and durability). Based on the test results of the full factorial design, the research team can draw unequivocal conclusions about the performance of SP-9.5 mixtures when compared to SP-12.5 mixtures. FDOT can then make an informed decision on the use of SP-9.5/FC-9.5 mixtures. The experimental design is as follows:

- Eight mix combinations:
  - Two gradation types (SP-9.5 ad SP-12.5).
  - Two aggregate types (Georgia granite and Florida limestone).
  - Two binder grades (PG 67-22 and PG 76-22).
- Three design numbers of gyrations targeting 4 percent air voids:
  - 50 gyrations (corresponding to traffic level A).
  - 75 gyrations (corresponding to traffic level C).
  - 100 gyrations (corresponding to traffic levels D and E).
- Two compaction levels:
  - 93 percent G_{mm}.
  - 95 percent G_{mm}.
- Seven Performance Tests:
  - IDEAL-CT.
  - UF-IDT.
  - SCB-FI.
  - APA.
  - HWT.
  - IDEAL-RT.
  - CAL.

Table 3-1 shows the mix type numbers and their corresponding combinations.

Table 3-1. Mix Combinations

Mix Type No.	Gradation	Aggregate Type	Binder Type
1	SP-9.5	Georgia granite	PG 67-22
2	SP-12.5	Georgia granite	PG 67-22
3	SP-9.5	Georgia granite	PG 76-22
4	SP-12.5	Georgia granite	PG 76-22
5	SP-9.5	Florida limestone	PG 67-22
6	SP-12.5	Florida limestone	PG 67-22
7	SP-9.5	Florida limestone	PG 76-22
8	SP-12.5	Florida limestone	PG 76-22

In this project, for each mix type, three laboratory design gyration numbers—50, 75, and 100—were used for mixture design, and correspondingly each mixture had a different optimum binder content. There were 24 mixture designs (i.e., eight mix types × three design gyrations).

For each of the 24 mixtures, the team prepared two sets of performance test specimens, each set representing a different field compaction level—93 percent G_{mm} (7 percent air voids) and 95 percent G_{mm} (5 percent air voids). The research team conducted seven different performance tests on each mixture at each compaction level: three cracking tests (IDEAL-CT, UF-IDT, and SCB-FI tests); three rutting tests (APA, HWT, and IDEAL-RT tests); and one durability test (CAL test). Figure 3-1 shows the performance testing specimens preparation flowchart, using Mix Type 1 as an example. The total number of SGCs required for performance tests is 1056 ([22 + 22] × 3 × 8).

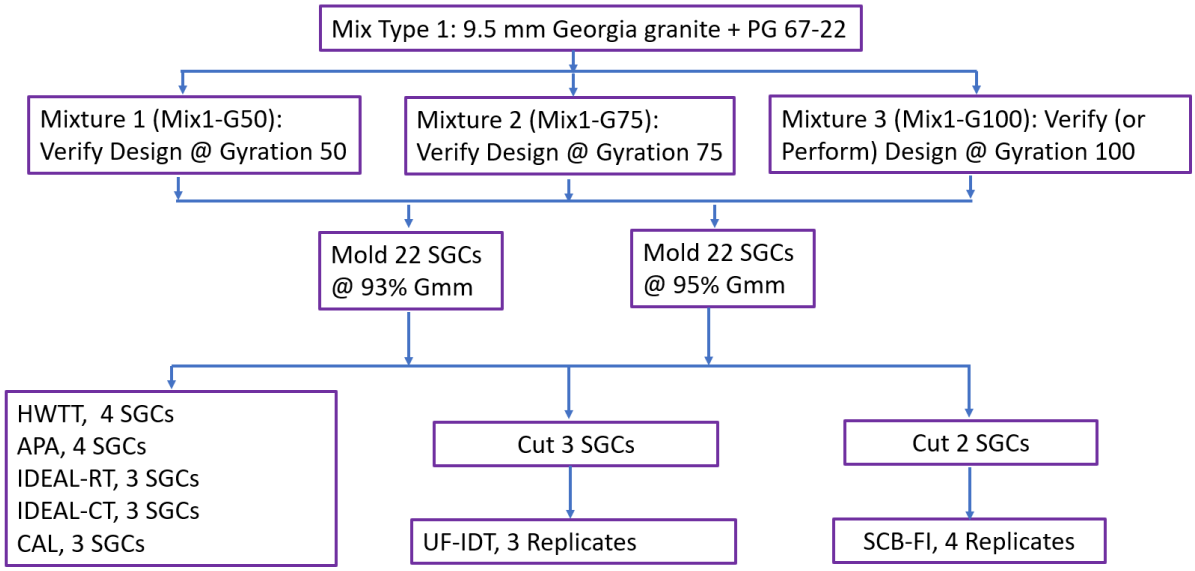

Figure 3-1. Flowchart of Performance Testing Specimens Preparation

3.3 Material Quantity Determination and Acquisition

The FDOT project panel queried Florida suppliers and selected four aggregate mixes based on Florida typical mixtures. The corresponding stockpile names, percentages, gradations, and locations are shown in Figure 3-2 (Granite SP-9.5), Figure 3-3 (Granite SP-12.5), Figure 3-4 (Limestone SP-9.5), and Figure 3-5 (Limestone SP-12.5).

Product Description	Product Code	Producer Name	Product Name	Plant/Pit Number	Terminal
1. S1B Stone	C53	Junction City Mining	S1B Stone	GA553	
2. Screenings	F22	Junction City Mining	Screenings	GA553	
3. Screenings	F23	Junction City Mining	Screenings	GA553	
4. Sand	334-LS	Peavy & Son Construction Company	Hwy 267		
5.					
6.					
7. HP Binder	916-HP		High Polymer		

PERCENTAGE BY WEIGHT TOTAL AGGREGATE PASSING SIEVES

	Blend Number	36% 1	34% 2	15% 3	15% 4	5	6	JOB MIX FORMULA	CONTROL POINTS	PRIMARY CONTROL SIEVE
SIEVE SIZE	3/4" 19.0mm	100	100	100	100			100		
	1/2" 12.5mm	100	100	100	100			100	100	
	3/8" 9.5mm	100	100	100	100			100	90 - 100	
	No. 4 4.75mm	35	100	100	100			77	- 89	
	No. 8 2.36mm	5	76	78	100			54	48 - 67	47
	No. 16 1.18mm	4	50	56	98			42	35	
	No. 30 600µm	3	34	41	85			32	26	
	No. 50 300µm	3	24	32	31			19	19	
	No. 100 150µm	2	13	23	5			9		
	No. 200 75µm	1.0	5.8	15.1	3.0			5.5	2 - 10	
	G_{SB}	2.764	2.730	2.730	2.630			2.727		

Figure 3-2. Florida Granite SP-9.5 Aggregate Mix

	Product Description	Product Code	Producer Name	Product Name	Plant/Pit Number	Terminal
1.	S1A Stone	C47	Junction City Mining	S1A	GA553	
2.	S1B Stone	C53	Junction City Mining	S1B	GA553	
3.	Screenings	F22	Junction City Mining	Screenings	GA553	
4.	Sand	334-LS	Pit. # 267	Sand		
5.						
6.						
7.	HP Binder	916-HP		High Polymer		

PERCENTAGE BY WEIGHT TOTAL AGGREGATE PASSING SIEVES

	Blend Number	26% 1	19% 2	37% 3	18% 4	5	6	JOB MIX FORMULA	CONTROL POINTS	PRIMARY CONTROL SIEVE
SIEVE SIZE	3/4" 19.0mm	100	100	100	100			100	100	
	1/2" 12.5mm	96	100	100	100			99	90 - 100	
	3/8" 9.5mm	60	98	100	100			89	- 89	
	No. 4 4.75mm	7	31	97	100			62		
	No. 8 2.36mm	2	5	74	100			47	40 - 58	39
	No. 16 1.18mm	1	3	47	99			36	29 -	
	No. 30 600µm	1	2	32	88			28	22 -	
	No. 50 300µm	1	2	21	41			16	16 -	
	No. 100 150µm	1	1	13	6			6		
	No. 200 75µm	1.0	1.0	6.0	3.0			3.6	2 - 10	
	G_{SB}	2.775	2.764	2.730	2.626			2.728		

Figure 3-3. Florida Granite SP-12.5 Aggregate Mix

	Product Description	Product Code	Producer Name	Product Name	Plant/Pit Number	Terminal
1.	S1B Stone	C51	White Rock Quarries	S1B Stone	87339	
2.	S1B Stone	C54	White Rock Quarries	S1B Stone	87339	
3.	Screenings	F22	White Rock Quarries	Screenings	87339	
4.						
5.						
6.						
7.	PG Binder	916-76PMA		PG 76-22 (PMA)		

PERCENTAGE BY WEIGHT TOTAL AGGREGATE PASSING SIEVES

	Blend Number	9% 1	40% 2	51% 3	4	5	6	JOB MIX FORMULA	CONTROL POINTS	PRIMARY CONTROL SIEVE
SIEVE SIZE	3/4" 19.0mm	100	100	100				100		
	1/2" 12.5mm	100	100	100				100	100	
	3/8" 9.5mm	89	100	100				99	90 - 100	
	No. 4 4.75mm	35	84	100				88	- 89	
	No. 8 2.36mm	10	24	91				57	48 - 67	47
	No. 16 1.18mm	5	12	74				43	35	
	No. 30 600µm	5	10	57				34	26	
	No. 50 300µm	4	7	36				22	19	
	No. 100 150µm	3	2	13				8		
	No. 200 75µm	2.5	2.0	5.0				3.6	2 - 10	
	G_{SB}	2.412	2.480	2.527				2.497		

Figure 3-4. Florida Limestone SP-9.5 Aggregate Mix

	Product Description	Product Code	Producer Name	Product Name	Plant/Pit Number	Terminal
1.	S1A Stone	C41	White Rock Quarries	S1A Stone	87339	
2.	S1B Stone	C51	White Rock Quarries	S1B Stone	87339	
3.	S1B Stone	C54	White Rock Quarries	S1B Stone	87339	
4.	Screenings	F22	White Rock Quarries	Screenings	87339	
5.						
6.						
7.	PG Binder	916-76PMA		PG 76-22 (PMA)		

PERCENTAGE BY WEIGHT TOTAL AGGREGATE PASSING SIEVES

SIEVE SIZE	Blend Number	15% 1	28% 2	10% 3	47% 4	5	6	JOB MIX FORMULA	CONTROL POINTS	PRIMARY CONTROL SIEVE
	3/4" 19.0mm	100	100	100	100			100	100	
	1/2" 12.5mm	74	100	100	100			96	90 - 100	
	3/8" 9.5mm	40	93	100	100			89	- 89	
	No. 4 4.75mm	16	54	89	100			73		
	No. 8 2.36mm	11	15	20	92			51	28 - 58	39
	No. 16 1.18mm	9	11	16	72			40		
	No. 30 600µm	6	8	8	55			30		
	No. 50 300µm	4	6	6	39			21		
	No. 100 150µm	3	5	5	15			9		
	No. 200 75µm	2.0	3.5	3.5	4.0			3.5	2 - 10	
	G_{SB}	2.407	2.412	2.480	2.527			2.471		

Figure 3-5. Florida Limestone SP-12.5 Aggregate Mix

Table 3-2 lists the total aggregate and binder quantity estimated: 5586 kg aggregate and 294 kg binder.

Table 3-2. Aggregate and Binder Quantity Estimation

Item	Number
Number of SGCs for performance tests	1,056
Number of SGCs for air void trial	528
Number of SGCs for mixture design verification	96
Weight of 1 SGC sample (Φ 150 mm, H 76.4 mm), kg	3.5
Total mixture weight [(1056 + 528 + 96) * 3.5], kg	5,880
Total binder weight (assuming 5% binder content), kg	294
Total aggregate weight, kg	5,586

Note: SGC = Superpave gyratory compactor.

Because of the material wastage caused by specimen remolding or other unforeseen reasons, some redundancy factors need to be introduced into the quantity estimation. A larger factor (e.g., close to 2.0) is considered for coarse aggregates if there is a gradation discrepancy between the sampled material and the original stockpile. A smaller factor (e.g., close to 1.5) is considered for fine aggregates such as screenings and sand. Table 3-3 lists the quantity of each stockpile aggregate according to the four Florida mixture designs and their corresponding redundancy factors.

Table 3-3. Aggregate Quantity According to Florida Mixture Designs

Aggregate Mixes	Stockpile	Product Code	Plant/Pit Number	Percent (%)	Redundancy Factor	Quantity (5-gallon bucket)
Limestone SP-12.5	S1A Stone	C41	87339	15	1.9	16
	S1B Stone	C51	87339	28	1.6	26
	S1B Stone	C54	87339	10	1.4	8
	Screenings	F22	87339	47	1.4	37
Limestone SP-9.5	S1B Stone	C51	87339	9	1.6	9
	S1B Stone	C54	87339	40	1.4	32
	Screenings	F22	87339	51	1.4	40
Granite SP-12.5	S1A Stone	C47	GA553	26	1.75	26
	S1B Stone	C53	GA553	19	1.5	16
	Screenings	F22	GA553	37	1.4	29
	Sand	334-LS	Pit #267	18	1.4	15
Granite SP-9.5	S1B Stone	C53	GA553	36	1.5	31
	Screenings	F22	GA553	34	1.4	27
	Screenings	F23	GA553	15	1.4	12
	Sand	334-LS	Pit #267	15	1.4	12

Note: The final quantities for each stockpile are summarized in Table 3-4.

Table 3-4. Aggregate Quantity of Each Stockpile

Aggregate Mixes	Stockpile	Product Code	Plant/Pit Number	Quantity (5-gallon bucket)
Limestone, total 168 buckets	S1A Stone	C41	87339	16
	S1B Stone	C51	87339	35
	S1B Stone	C54	87339	40
	Screenings	F22	87339	77
Granite, total 168 buckets	S1A Stone	C47	GA553	26
	S1B Stone	C53	GA553	47
	Screenings	F22	GA553	56
	Screenings	F23	GA553	12
	Sand	334-LS	Pit #267	27

According to the optimum binder contents (P_b) in the Florida mixture designs, the binder quantity estimations and the corresponding redundancy factors are listed in Table 3-5. Thus, 36 buckets of PG 67-22 and 36 buckets of PG 76-22 were required for this project.

Table 3-5. Binder Quantity Estimations

Mixture Type	Optimum Binder Content (%)	Redundancy Factor	Quantity (5-gallon bucket)
Limestone SP-12.5	6.2	1.8	18
Limestone SP-9.5	7	1.7	18
Granite SP-12.5	5.5	2	18
Granite SP-9.5	5.6	2	18

After the aggregate type and quantity were decided, TTI sent the buckets to FDOT (in mid-November 2020). The FDOT panel made great efforts to collect this huge quantity of materials. In early January 2021, all the buckets were filled, organized, and labeled carefully by FDOT, as Figure 3-6 shows.

(a) (b)

Figure 3-6. Collected Aggregates on FDOT Site (a) Before Packing and (b) After Packing

Following FDOT's help packing and loading the material, TTI arranged for shipping and received all the aggregate material on January 20, 2021, as Figure 3-7 displays.

Figure 3-7. Aggregates Received by TTI

3.4 Evaluation of Aggregates

After receiving the Florida aggregate, the research team performed the sieving analysis according to AASHTO T 27 (AASHTO 2020a) and AASHTO T 11 (AASHTO 2020c). In total, there were nine stockpiles (five stockpiles from granite mixes and four stockpiles from limestone mixes) of aggregates to be tested. The research team randomly picked two buckets of aggregates for each aggregate stockpile and mixed them. Then, based on AASHTO R 76 (AASHTO 2016b), the research team used a mechanical splitter to reduce the portion until obtaining the appropriate mass for two replicates of sieving analysis (see Figure 3-8).

Figure 3-8. Use of Mechanical Splitter to Reduce the Mass

The sieving analysis work was repeated two or three times for each stockpile aggregate to ensure the gradation results were not biased. Table 3-6 and Table 3-7 show the gradation results for the granite stockpiles and limestone stockpiles, respectively. The numbers from the Florida mixture design spreadsheets are also listed for comparison. In these tables, “FL” means the original Florida measurements, and “TTI” means the TTI measurements on the received aggregates.

Table 3-6. Granite Stockpile Gradation Comparisons between Florida Measurements and TTI Measurements

Sieve Size	Granite -C47		Granite -C53		Granite – F22 (GA553)		Granite – F23		Sand	
	FL	TTI	FL	TTI	FL	TTI	FL	TTI	FL	TTI
3/4 in.	100.0	100.0	100.0	100.0	100.0	100.0	100.0	100.0	100.0	100.0
1/2 in.	96.0	93.0	100.0	100.0	100.0	100.0	100.0	100.0	100.0	100.0
3/8 in.	60.0	61.4	98.0	96.3	100.0	100.0	100.0	100.0	100.0	100.0
No. 4	7.0	12.0	31.0	23.1	97.0	97.3	100.0	97.8	100.0	100.0
No. 8	2.0	2.3	5.0	2.8	74.0	68.5	78.0	78.8	100.0	99.7
No. 16	1.0	0.8	3.0	0.8	47.0	41.8	56.0	54.9	98.0	94.5
No. 30	1.0	0.7	2.0	0.6	32.0	26.7	41.0	40.1	85.0	67.4
No. 50	1.0	0.7	2.0	0.6	21.0	16.6	32.0	29.5	31.0	20.4
No.100	1.0	0.6	1.0	0.6	13.0	9.8	23.0	22.1	5.0	4.4
No.200	1.0	0.5	1.0	0.5	6.0	5.0	15.1	15.2	3.0	1.9

Table 3-7. Limestone Stockpile Gradation Comparison between Florida Measurements and TTI Measurements

Sieve Size	Limestone C41		Limestone C51		Limestone C54		Limestone F22 (87339)	
	FL	TTI	FL	TTI	FL	TTI	FL	TTI
3/4 in.	100.0	100.0	100.0	100.0	100.0	100.0	100.0	100.0
1/2 in.	74.0	76.7	100.0	100.0	100.0	100.0	100.0	100.0
3/8 in.	40.0	35.7	93.0	94.2	100.0	100.0	100.0	100.0
No. 4	16.0	8.1	54.0	28.6	89.0	70.6	100.0	99.7
No. 8	11.0	6.0	15.0	9.1	20.0	15.4	92.0	91.8
No. 16	9.0	5.3	11.0	5.6	16.0	7.7	72.0	80.0
No. 30	6.0	4.9	8.0	4.8	8.0	5.9	55.0	69.1
No. 50	4.0	4.5	6.0	4.2	6.0	5.1	39.0	46.1
No. 100	3.0	3.8	5.0	3.4	5.0	4.2	15.0	10.0
No. 200	2.0	3.0	3.5	2.6	3.5	3.4	4.0	2.7

Figure 3-9 and Figure 3-10 plot the stockpile aggregate gradation curves for granite and limestone, respectively. Overall, the TTI-measured gradation for granite stockpiles was close to Florida's measurements except for the sand. The TTI-measured percentage of passing No. 50 for sand was around 20, while the numbers shown in the Florida mixture design spreadsheet were 31 (Granite SP-9.5) and 41 (Granite SP-12.5), which means the sand from the original Florida stockpile might have been finer than the sample TTI received.

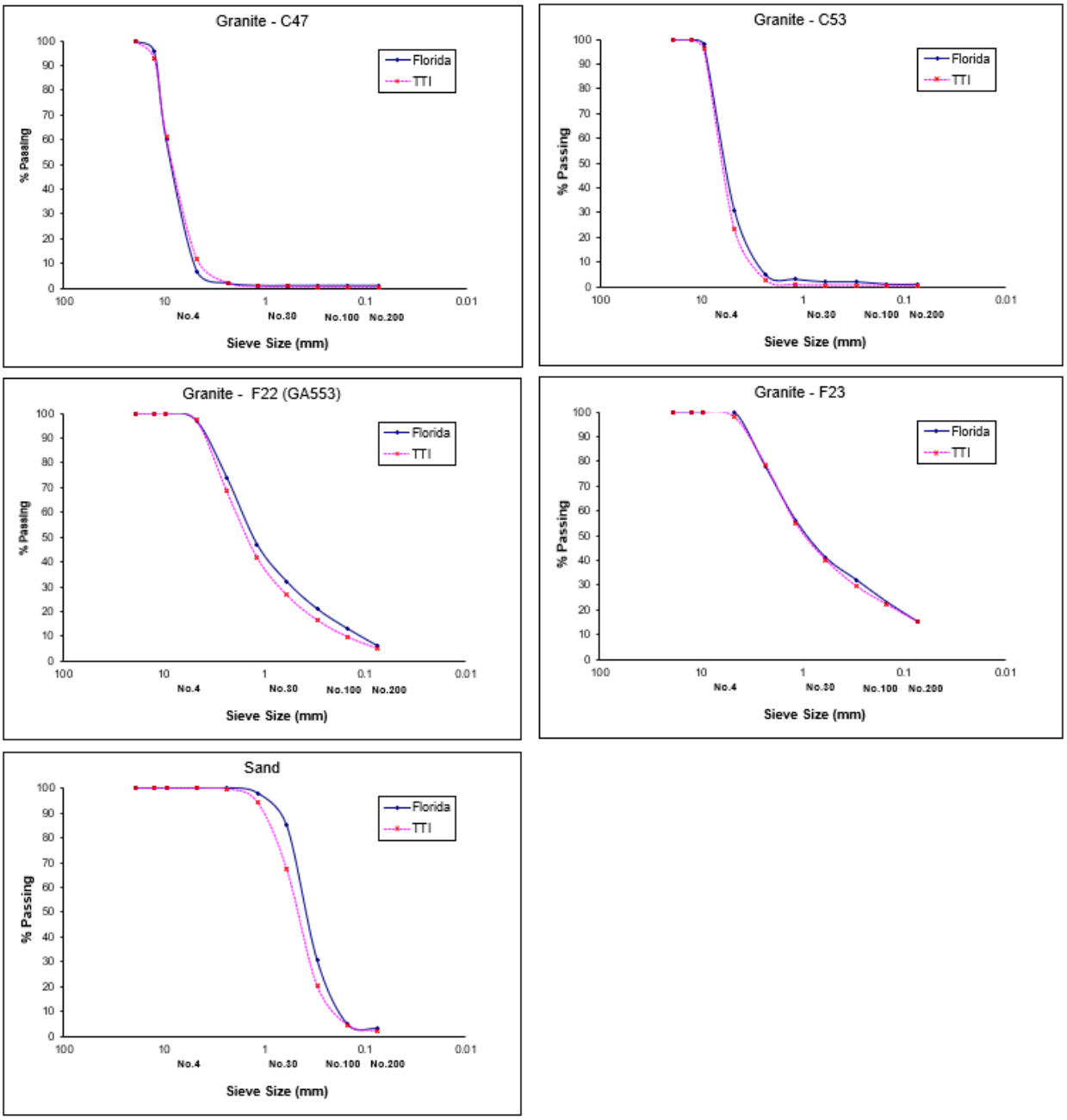

Figure 3-9. Granite Stockpile Gradation Curve

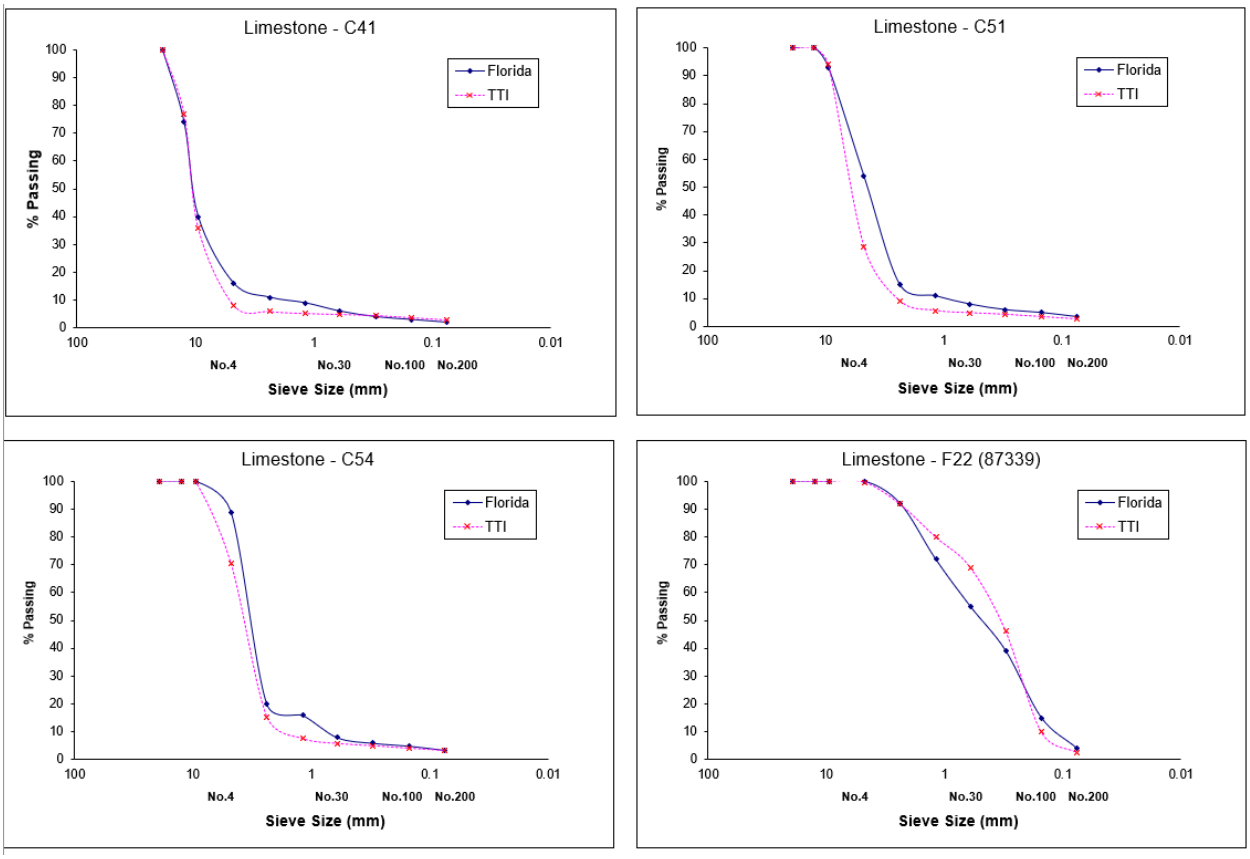

Figure 3-10. Limestone Stockpile Gradation Curve

After inserting the TTI-measured aggregate stockpile gradation numbers into the corresponding Florida mixture design spreadsheets, the final blended gradations for each mix (Granite SP-9.5, Granite SP-12.5, Limestone SP-9.5, and Limestone SP-12.5) were determined and are listed in Table 3-8. Again, the original Florida blended gradation numbers for each mix are also listed in the table for comparison.

Table 3-8. Blended Gradation Comparison between Florida Measurements and TTI Measurements

Sieve Size	Granite SP-9.5		Granite SP-12.5		Limestone SP-9.5		Limestone SP-12.5	
	FL	TTI	FL	TTI	FL	TTI	FL	TTI
3/4 in.	100.0	100.0	100.0	100.0	100.0	100.0	100.0	100.0
1/2 in.	100.0	100.0	99.0	98.0	100.0	100.0	96.0	97.0
3/8 in.	100.0	99.0	89.0	89.0	99.0	99.0	89.0	89.0
No. 4	77.0	71.0	62.0	62.0	88.0	82.0	73.0	63.0
No. 8	54.0	51.0	47.0	44.0	57.0	54.0	51.0	48.0
No. 16	42.0	37.0	36.0	33.0	43.0	44.0	40.0	41.0
No. 30	32.0	25.0	28.0	22.0	34.0	38.0	30.0	35.0
No. 50	19.0	*13.0**	16.0	*10.0***	22.0	26.0	21.0	24.0
No. 100	9.0	8.0	6.0	5.0	8.0	7.0	9.0	7.0
No. 200	5.0	4.0	3.0	2.0	3.6	2.5	3.5	2.8

* Minimum requirement is 19
** Minimum requirement is 16

Figure 3-11 shows the blended gradation curves for Granite SP-9.5, Granite SP-12.5, Limestone SP-9.5, and Limestone SP-12.5.

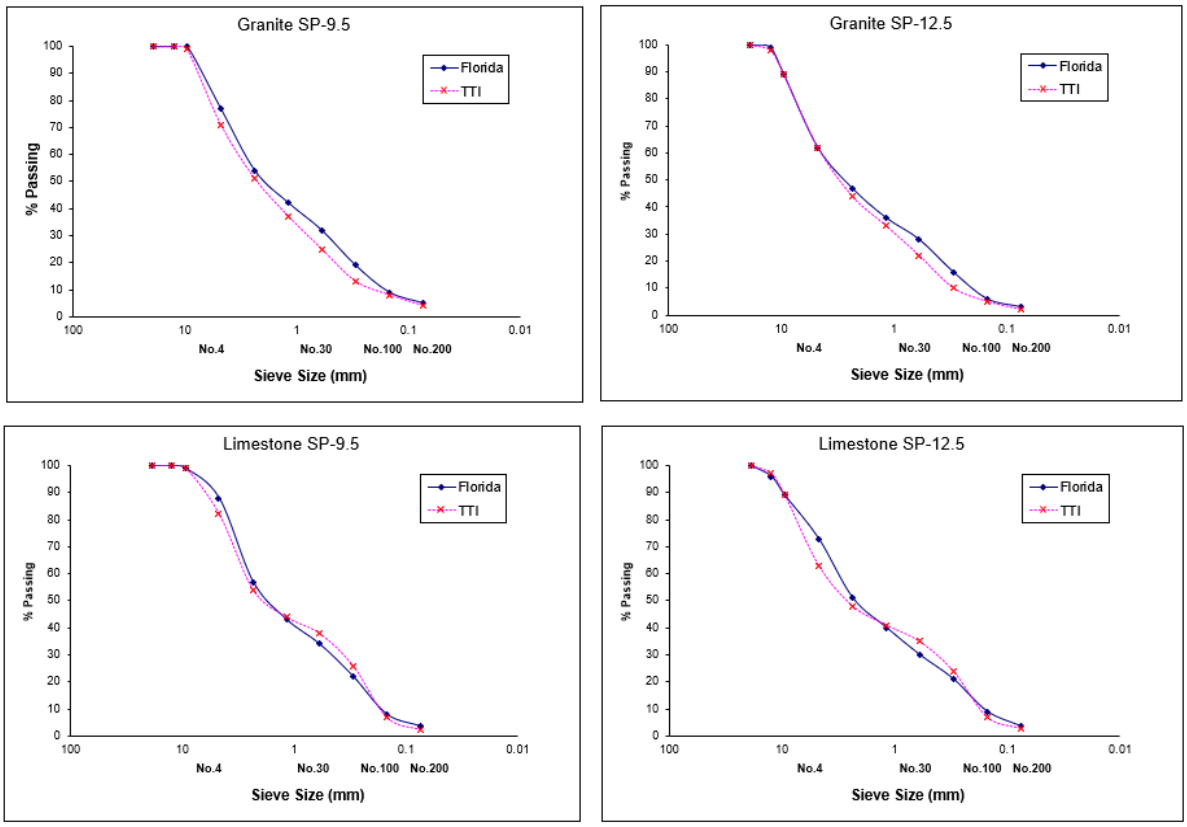

Figure 3-11. Blended Gradation Curves

Based on the results shown in Table 3-8 and Figure 3-11, the research team noted the following:

- *Granite Mixes:* The combined percentages of passing No. 50 sieve are 13 and 10 for Granite SP-9.5 and Granite SP-12.5, respectively. However, the minimum required numbers are 19 and 16 for Granite SP-9.5 and Granite SP-12.5, respectively. The main reason for these measurements is that the TTI-measured percentage of passing No. 50 is smaller than the Florida measurements. The research team may need to add some finer sand to address this issue.
- *Limestone Mixes:* The combined percentages of dust (passing No. 200 sieve) for limestone aggregates (Limestone SP-9.5 and Limestone SP-12.5) are smaller than the numbers in the original Florida mixture design (2.5 versus 3.6 for Limestone SP-9.5, and 2.8 versus 3.5 for Limestone SP-12.5). The dust/binder ratio may not meet the criteria (minimum 0.6) during mixture design.

After discussion with the FDOT project panel, the research team tried replacing part of the Florida sand with one type of Texas sand (finer). Originally, the sand percentages were 15 percent and 18 percent for Granite SP-9.5 and Granite SP-12.5, respectively. The trials use 3 percent Florida sand plus 12 percent Texas sand for Granite SP-9.5 and 4 percent Florida sand plus 14 percent Texas sand for Granite SP-12.5 (see Figure 3-12 and Figure 3-13).

Product Description	Product Code	Producer Name	Product Name	Plant/Pit Number	Terminal
1. S1B Stone	C53	Junction City Mining	S1B Stone	GA553	
2. Screenings	F22	Junction City Mining	Screenings	GA553	
3. Screenings	F23	Junction City Mining	Screenings	GA553	
4. Florida Sand	334-LS	Peavy & Son Construction Company	Hwy 267		
5. Texas Sand					
6.					
7. PG Binder	916-67		PG 67-22		

PERCENTAGE BY WEIGHT TOTAL AGGREGATE PASSING SIEVES

	Blend	36%	34%	15%	3%	12%		JOB MIX	CONTROL	PRIMARY
	Number	1	2	3	4	5	6	FORMULA	POINTS	CONTROL SIEVE
SIEVE	3/4" 19.0mm	100	100	100	100	100		100		
	1/2" 12.5mm	100	100	100	100	100		100	100	
	3/8" 9.5mm	96.3	100	100	100	100		99	90 - 100	
	No. 4 4.75mm	23.1	97.3	97.8	100	100		71	- 89	
	No. 8 2.36mm	2.8	68.5	78.8	99.7	98.6		51	48 - 67	47
	No. 16 1.18mm	0.8	41.8	54.9	94.5	97.7		37	35	
	No. 30 600µm	0.6	26.7	40.1	67.4	94.5		29	26	
	No. 50 300µm	0.7	16.6	29.5	20.4	64.6		19	19	
	No. 100 150µm	0.6	9.8	22.1	4.4	17.3		9		
	No. 200 75µm	0.5	5.0	15.2	1.9	4.5		5	2 - 10	
	G_{sb}	2.764	2.730	2.730	2.630	2.615		2.725		

Figure 3-12. Trial Granite SP-9.5 Aggregate Mix with Texas Sand

Product Description	Product Code	Producer Name	Product Name	Plant/Pit Number	Terminal
1. S1A Stone	C47	Junction City Mining	S1A	GA553	
2. S1B Stone	C53	Junction City Mining	S1B	GA553	
3. Screenings	F22	Junction City Mining	Screenings	GA553	
4. Florida Sand	334-LS	Pit. # 267	Sand		
5. Texas Sand					
6.					
7. HP Binder	916-HP		High Polymer		

PERCENTAGE BY WEIGHT TOTAL AGGREGATE PASSING SIEVES

	Blend	26%	19%	37%	4%	14%		JOB MIX	CONTROL	PRIMARY
	Number	1	2	3	4	5	6	FORMULA	POINTS	CONTROL SIEVE
SIEVE SIZE	3/4" 19.0mm	100	100	100	100	100		100	100	
	1/2" 12.5mm	93	100	100	100	100		98	90 - 100	
	3/8" 9.5mm	61.4	96.3	100	100	100		89	- 89	
	No. 4 4.75mm	12	23.1	97.3	100	100		62		
	No. 8 2.36mm	2.3	2.8	68.5	99.7	98.6		44	40 - 58	39
	No. 16 1.18mm	0.8	0.8	41.8	94.5	97.7		33	29 -	
	No. 30 600µm	0.7	0.6	26.7	67.4	94.5		26	22 -	
	No. 50 300µm	0.7	0.7	16.6	20.4	64.6		16	16 -	
	No. 100 150µm	0.6	0.6	9.8	4.4	17.3		6		
	No. 200 75µm	0.5	0.5	5.0	1.9	4.5		3.6	2 - 10	
	G_{sb}	2.775	2.764	2.730	2.626	2.615		2.727		

Figure 3-13. Trial Granite SP-12.5 Aggregate Mix with Texas Sand

Since the majority of the original Florida sand was replaced by Texas sand (finer sand) in the gradation design, the research team also performed a fine aggregate angularity (FAA) test (AASHTO 2020b) to determine if rutting potential was advertently introduced in the mix.

The FAA tests were performed for four mixes: Granite SP-9.5 with 15 percent Florida sand, Granite SP-9.5 with 3 percent Florida sand plus 12 percent Texas sand, Granite SP-12.5 with 18 percent Florida sand, and Granite SP-12.5 with 4 percent Florida sand plus 14 percent Texas sand. To determine the FAA number, specific gravities of the fine aggregates (passing No. 4 sieve) were determined for the four mixes (AASHTO 2017f).

In the AASHTO T 304 specification (AASHTO 2020b), there are three ways (Methods A, B, and C) to determine the FAA number. In Florida, Method A is used for blended samples, and Method C is only for testing individual aggregates. The difference is that Method A specifies individual weight retaining on each sieve, while Method C only specifies a total weight (190 g) of passing No. 4 sieve. Figure 3-14 and Figure 3-15 show the fine aggregate specific gravity test, FAA test—Method A, and FAA test—Method C.

Figure 3-14. Fine Aggregate Specific Gravity Test

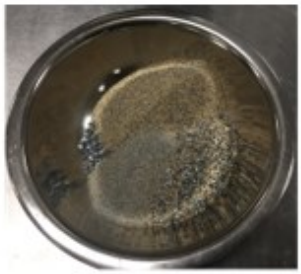

Individual Size Fraction	Mass, g
2.36 mm (No. 8) to 1.18 mm (No. 16)	44
1.18 mm (No. 16) to 600 µm (No. 30)	57
600 µm (No. 30) to 300 µm (No. 50)	72
300 µm (No. 50) to 150 µm (No. 100)	17
	190

(a)

Method C—As-Received Grading—Pass the sample (dried in accordance with T 27) through a 4.75-mm (No. 4) sieve. Obtain a 190 ± 1-g sample of the material passing the 4.75-mm (No. 4) sieve for test.

(b)

Figure 3-15. FAA Test: (a) Method A and (b) Method C

Table 3-9 lists the four mixes' fine aggregate specific gravity (G_{sb}) and FAA numbers. Both Method A and Method C were performed. As seen in the table, after replacing Florida sand with Texas sand, the FAA number gets smaller, indicating a smaller VMA.

Table 3-9. Fine Aggregate Specific Gravity G_{sb} and FAA Test Results

Test	Granite SP-9.5 (15% Florida sand)	Granite SP-9.5 (3% Florida sand + 12% Texas sand)	Granite SP-12.5 (18% Florida sand)	Granite SP-12.5 (4% Florida sand + 14% Texas sand)
Fine Aggregate G_{sb}	2.707	2.740	2.717	2.739
FAA, % (Method A)	46.1	45.8	45.4	45.1
FAA, % (Method C)	38.3	38.0	40.0	39.2

3.5 Evaluation of Binder

The project panel selected Martin Asphalt Company as the binder supplier and asked that PG 67-22 and PG 76-22 samples be sent to the research team for initial tests. After obtaining the binder samples (one gallon of PG 67-22 and one gallon of PG 76-22) from Martin Asphalt, the research team performed the PG tests following Section 916 (Bituminous Materials) of FDOT's *Standard Specifications for Road and Bridge Construction* (FDOT 2020). Table 3-10 and Table 3-11 show the test results for PG 67-22 and PG 76-22, respectively. The binder test specifications include AASHTO T 313 (AASHTO 2016c), AASHTO T 315 (AASHTO 2016d), and AASHTO M 332 (AASHTO 2019b).

Table 3-10. Initial Test Results of PG 67-22 Sample

Aging	Test	Geometry	Temp. (°C)	Parameter	Criteria	Test Result	Pass/ Fail
Original	DSR	25 mm x 1 mm	67	G*/Sin (Delta)	≥ 1.0 kPa	1.1	Pass
RTFO	MSCR	25 mm x 1 mm	67	Jnr_3.2	≤ 4.5 kPa^{-1} "S"	2.8	Pass
RTFO + PAV	BBR	Beams	−12	m @ 60 sec	≥ 0.300	0.314	Pass
				S @ 60 sec	≤ 300 MPa	159	Pass
				ΔTc	≥ −5.0°C	−3.5	Pass
	DSR	8 mm x 2 mm	26.5	G* Sin (Delta)	≤ 5000 kPa	3341.9	Pass

Note: DSR = dynamic shear rheometer; MSCR = multiple stress creep recovery; RTFO = rolling thin-film oven; BBR = bending beam rheometer; PAV = pressure aging vessel.

Table 3-11. Initial Test Results of PG 76-22 Sample

Aging	Test	Geometry	Temp. (°C)	Parameter	Criteria	Test Result	Pass/ Fail
Original	DSR	25 mm x 1 mm	76	G*/Sin (Delta)	≥ 1.0 kPa	1.6	Pass
				Delta	≤ 75.0 deg.	64.8	Pass
RTFO	MSCR	25 mm x 1 mm	67	Jnr_3.2	≤ 1.0 kPa^{-1} "V"	0.14	Pass
				%Jnr_diff	≤ 75% (n/a if Jnr_3.2 ≤ 0.50)	11.6	n/a
				%Rec_3.2	≥ 29.37 $(Jnr\_3.2)^{-0.2633}$	73.2	Pass
RTFO + PAV	BBR	Beams	−12	m @ 60 sec	≥ 0.300	0.3	Pass
				S @ 60 sec	≤ 300 MPa	191	Pass
				ΔTc	≥ −5.0 °C	−4.2	Pass
	DSR	8 mm x 2 mm	26.5	G* Sin (Delta)	≤ 6000 kPa	3765.4	Pass

In addition, the research team performed the high-temperature true grade test and Fourier transform infra-red (FTIR) spectroscopy test for the PG 76-22 sample. The results are shown in Table 3-12 and Figure 3-16.

Table 3-12. PG 76-22 High-Temperature True Grade

	Test Temp. (°C)	G*/sinδ (kPa)		High Temp. of True PG (°C)
		Measured	Criteria	
PG 76-22 Original Binder	76	1.582	1.0	83.5
	82	1.098		
PG 76-22 RTFO Binder	82	2.698	2.2	84.2
	88	1.551		

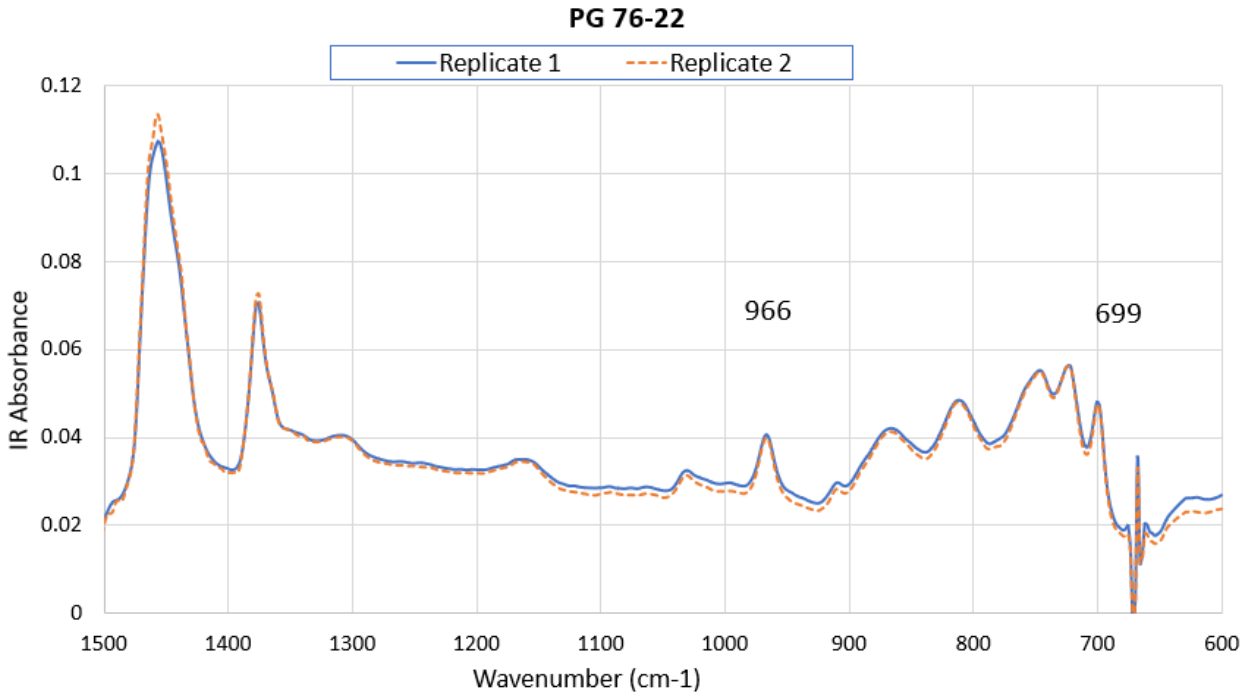

Figure 3-16. FTIR Spectrum of PG 76-22 Sample

According to the information in Table 3-12, the high temperature of the true grade test is 83.5°C, which indicates it is closer to a PG 82-22 binder, although it meets FDOT PG 76-22 specifications. Martin Asphalt also admitted that this sample ran "harder than normal." On February 8, 2021, the company sent another PG 76-22 sample to TTI. The research team repeated all the initial tests on this new sample, including the high-temperature true grade and FTIR tests. The results are shown in Table 3-13, Table 3-14, and Figure 3-17.

Table 3-13. Initial Test Results of PG 76-22 Sample (New)

Aging	Test	Geometry	Temp. (°C)	Parameter	Criteria	Test Result	Pass/ Fail
Original	DSR	25 mm x 1 mm	76	G*/Sin (Delta)	≥ 1.0 kPa	1.3	Pass
				Delta	≤ 75.0 deg.	71.2	Pass
RTFO	MSCR	25 mm x 1 mm	67	Jnr_3.2	≤ 1.0 kPa^{-1} "V"	0.27	Pass
				%Jnr_diff	≤ 75% (n/a if Jnr_3.2 ≤ 0.50)	19.4	n/a
				%Rec_3.2	≥ 29.37 $(Jnr\_3.2)^{-0.2633}$	64	Pass
RTFO + PAV	BBR	Beams	−12	m @ 60 sec	≥ 0.300	0.308	Pass
				S @ 60 sec	≤ 300 MPa	151	Pass
				ΔTc	≥ −5.0 °C	−4.6	Pass
	DSR	8 mm x 2 mm	26.5	G* Sin (Delta)	≤ 6000 kPa	1539.4	Pass

Table 3-14. PG 76-22 High-Temperature True Grade (New Sample)

	Test Temp. (°C)	G*/sinδ (kPa)		High Temp. of True PG (°C)
		Measured	Criteria	
PG 76-22 Original Binder	76	1.3	1.0	81.5
	82	0.96		
PG 76-22 RTFO Binder	76	2.965	2.2	79.1
	82	1.669		

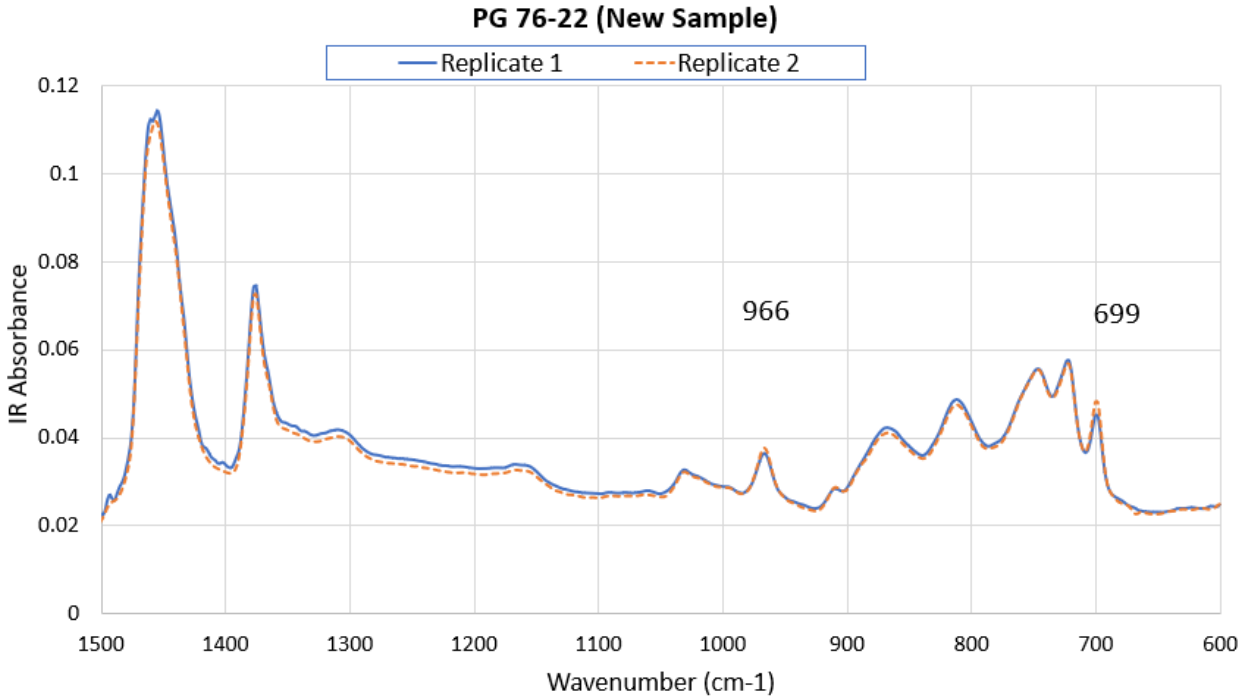

Figure 3-17. FTIR Spectrum of PG 76-22 Sample (New)

The results show that the new sample meets FDOT PG 76-22 specifications. In addition, the high temperature of the true grade test is 79.1°C, which indicates it is truly a PG 76-22 binder. The FDOT project panel accepted these binder's initial test results and contacted Martin Asphalt to coordinate the collection and shipment of the binder (36 buckets of PG 67-22 and 36 buckets of PG 76-22).

3.6 Summary

This chapter presents the full factorial experimental design, material acquisition, and initial testing for material evaluation.

There were eight mix type combinations (two gradation types, two aggregate types, and two binder types). For each mix type, there were three mixtures due to the three design gyrations (or optimum binder contents). Therefore, there were a total of 24 asphalt mixtures.

For each of the 24 mixtures, two sets of performance test specimens were fabricated at two compaction levels, corresponding to 7 percent and 5 percent air voids, respectively. Then, seven performance tests (HWT, APA, IDEAL-RT, IDEAL-CT, UF-IDT, SCB-FI, and CAL) were conducted on these specimens.

Four types of mixes were identified utilizing aggregates commonly used in FDOT mixes: Granite SP-9.5, Granite SP-12.5, Limestone SP-9.5, and Limestone SP-12.5. According to the stockpile percentages of these mixes, the quantity of each stockpile was determined. Due to testing requirements, the material quantity was huge (336 buckets of aggregates and 72 buckets of binder). The FDOT project panel put great effort into collecting and preparing these materials for shipping.

After receiving the Florida aggregates, the research team performed the aggregate sieving analysis tests. In total, there were nine stockpiles (five stockpiles from granite mixes and four stockpiles from limestone mixes) of aggregates to be tested. There were some discrepancies between TTI and the Florida measurements, especially for the sand gradation (used in granite mixes) and the percentage of dust (passing No. 200 sieve) for limestone mixes. To meet the requirement of granite mixes, the research team tried Texas sand (finer sand) to replace part of the Florida sand. FAA tests were conducted to see if rutting potential was advertently introduced in the mix by introducing the Texas sand.

The research team conducted the initial test for the binders (PG 67-22 and PG 76-22) after receiving samples from Martin Asphalt. Since the first PG 76-22 sample ran “harder than normal,” a new PG 76-22 sample was received and tested. The initial test results of the PG 67-22 and the new PG 76-22 samples met FDOT criteria and were accepted by the FDOT project panel.

4. MIXTURE DESIGN

As mentioned in previous chapters, 24 mixture designs (i.e., eight mix types × three design gyrations) needed to be conducted. This chapter describes the process and presents the design results.

4.1 Trial Mixture Designs

Since there were some discrepancies between the TTI measurements and the numbers in the Florida mixture design spreadsheets for the sand gradation, the research team tried to use Texas sand (finer sand) to replace part of Florida sand to meet the final gradation requirement. The aggregate tests indicated that after replacing Florida sand with Texas sand, the FAA number got smaller, indicating a smaller VMA. To further investigate the feasibility of using Texas sand in the Florida granite mixes, the research team performed trial mixture designs for Granite SP-9.5 (15 percent Florida sand) and Granite SP-9.5 (3 percent Florida sand + 12 percent Texas sand). The binder was the PG 76-22 from Martin Asphalt, and the antistrip additive was Evotherm M14, with the dosage at 0.4 percent (by weight) of the asphalt binder, as Figure 4-1 displays.

Figure 4-1. Binder and Antistrip Additive

Specification AASHTO M323 (AASHTO 2017a) and AASHTO R 35 (AASHTO 2017b) were followed during the mixture design. Three trial binder contents—4.8 percent, 5.3 percent, and 5.8 percent—were selected for the mixture design. Two replicates of the specimen (115 ± 5 mm high) for each binder content were compacted under 75 gyrations. Figure 4-2 shows the specimens fabricated for the mixture Granite SP-9.5 (15 percent Florida sand) and the mixture Granite SP-9.5 (3 percent Florida sand + 12 percent Texas sand).

Figure 4-2. Granite SP-9.5 Specimens with and without Texas Sand (75 Gyrations)

Figure 4-3 and Figure 4-4 show the mixture design data sheets of Granite SP-9.5 (15 percent Florida sand) and Granite SP-9.5 (3 percent Florida sand + 12 percent Texas sand). The figures show that the G_{mm} values are very close for each binder content between the mixtures with 15 percent Florida sand and 3 percent Florida sand + 12 percent Texas sand. However, the bulk specific gravity (G_{mb}) values are quite different: the mixture with Texas sand has significantly larger G_{mb} values. This finding indicated that after introducing the Texas sand (finer sand), the mixture was easier to compact and had less VMA.

HOT MIX DESIGN DATA SHEET

SPH 19-17409A (TL-C)

P_b	G_{mb} @ N_{des}	G_{mm}	V_a	VMA	VFA	P_{be}	$P_{0.075}$ / P_{be}	%G_{mm} @ N_{ini}	%G_{mm} @ N_{max}
4.8	2.412	2.576	6.4	15.8	59	4.0	1.4		
5.3	2.443	2.553	4.3	15.2	72	4.6	1.2		
5.8	2.432	2.531	3.9	16.0	76	5.1	1.1		

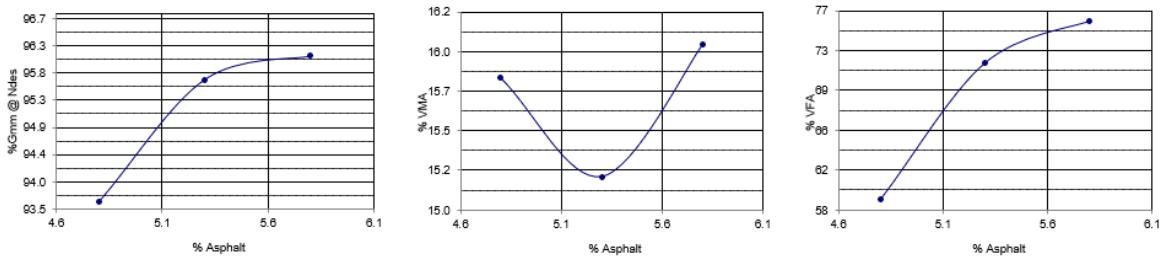

Figure 4-3. Mixture Design Data Sheet of Granite SP-9.5 (15 Percent Florida Sand)

SPH 19-17409A (TL-C)

P_b	G_{mb} @ N_{des}	G_{mm}	V_a	VMA	VFA	P_{be}	$P_{0.075}$ / P_{be}	%G_{mm} @ N_{ini}	%G_{mm} @ N_{max}
4.8	2.441	2.573	5.1	14.7	65	4.0	1.4		
5.3	2.473	2.555	3.2	14.1	77	4.5	1.2		
5.8	2.485	2.533	1.9	14.1	87	5.1	1.1		

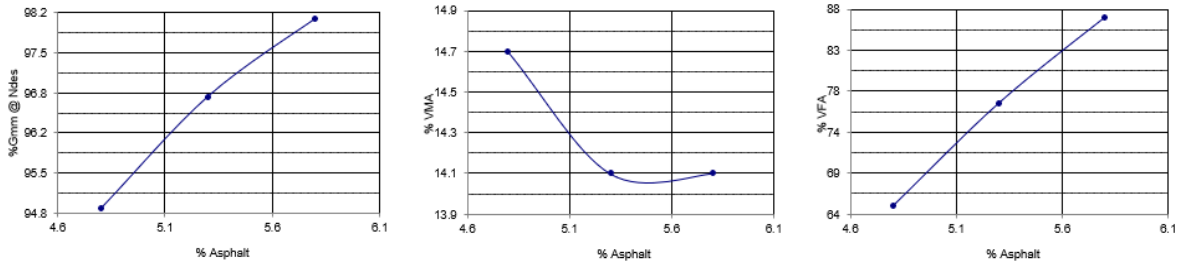

Figure 4-4. Mixture Design Data Sheet of Granite SP-9.5 (3 Percent Florida Sand + 12 Percent Texas Sand)

By interpolation, the optimum binder content was determined to be 5.6 percent for the Granite SP-9.5 (15 percent Florida sand) and 5.1 percent for the Granite SP-9.5 (3 percent Florida sand + 12 percent Texas sand). The VMAs are determined to be 15.6 percent and 14.3 percent at their optimum binder contents. According to AASHTO M 323, the minimum allowed VMA for an

SP-9.5 mixture is 15 percent, which means the mixture with Texas sand does not meet the VMA requirement. Thus, the FDOT project panel decided to stick with the original Florida gradation designs for granite mixes (Granite SP-9.5 and Granite SP-12.5), and no Texas sand was introduced.

Subsequently, the research team performed the mixture designs at 75 gyrations for Granite SP-12.5, Limestone SP-9.5, and Limestone SP-12.5. The corresponding design data sheets are shown in Figure 4-5, Figure 4-6, and Figure 4-7, respectively.

HOT MIX DESIGN DATA SHEET

SPH 19-17110A (TL-C)

P_b	G_{mb} @ N_{des}	G_{mm}	V_a	VMA	VFA	P_{be}	$P_{0.075}$ / P_{be}	%G_{mm} @ N_{ini}	%G_{mm} @ N_{max}
4.8	2.416	2.573	6.1	15.7	61	4.1	0.9		
5.3	2.431	2.553	4.8	15.6	69	4.6	0.8		
5.8	2.453	2.533	3.2	15.3	79	5.1	0.7		

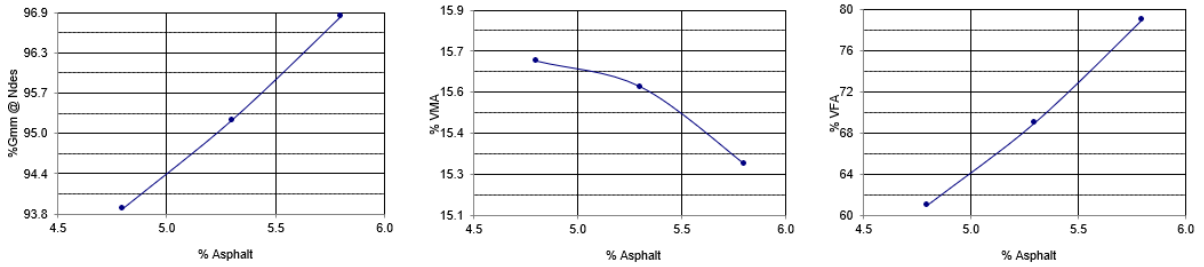

Figure 4-5. Mixture Design Data Sheet of Granite SP-12.5 (18 Percent Florida Sand)

HOT MIX DESIGN DATA SHEET

SPM 17-15834A (TL-C)

P_b	G_{mb} @ N_{des}	G_{mm}	V_a	VMA	VFA	P_{be}	$P_{0.075}$ / P_{be}	%G_{mm} @ N_{ini}	%G_{mm} @ N_{max}
6.3	2.210	2.357	6.3	17.1	63	5.0	0.6		
6.8	2.228	2.336	4.6	16.8	73	5.6	0.5		
7.3	2.232	2.317	3.7	17.1	78	6.2	0.5		

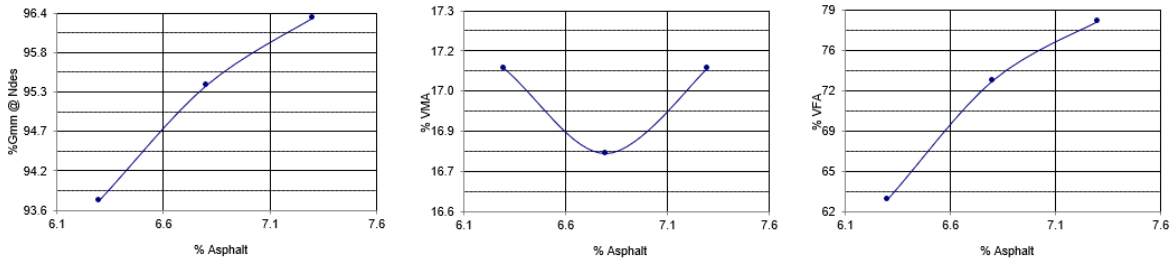

Figure 4-6. Mixture Design Data Sheet of Limestone SP-9.5

HOT MIX DESIGN DATA SHEET

SPM 14-13202B (TL-D)

P_b	G_{mb} @ N_{des}	G_{mm}	V_a	VMA	VFA	P_{be}	$P_{0.075}$ / P_{be}	%G_{mm} @ N_{ini}	%G_{mm} @ N_{max}
6.0	2.244	2.352	4.6	14.6	68	4.6	0.6		
6.5	2.251	2.344	4.0	14.8	73	5.0	0.6		
7.0	2.271	2.313	1.8	14.5	88	5.8	0.5		

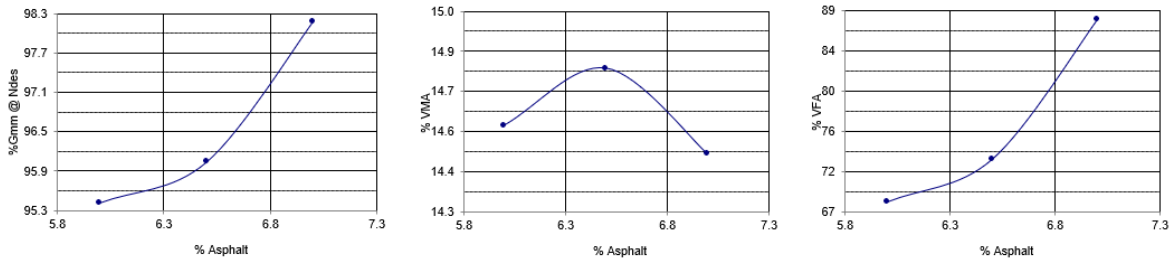

Figure 4-7. Mixture Design Data Sheet of Limestone SP-12.5

By interpolation, the final optimum binder contents P_b and the corresponding volumetric properties for each mixture are listed in Table 4-1. The original Florida design results are also listed in the table for comparison.

Table 4-1. Optimum Binder Content and Volumetric Properties (75 Gyrations)

Mixture Type	Design Provider	P_b	G_{mb} @ N_{des}	G_{mm}	V_a	VMA	VFA	P_{be}	$P_{0.075}/P_{be}$
Granite SP-9.5	TTI	5.6	2.439	2.541	4	15.6	74	4.9	1.1
	Florida	5.6	2.438	2.540	4	15.6	74	4.9	1.1
Granite SP-12.5	TTI	5.5	2.442	2.543	4	15.4	74	4.8	0.8
	Florida	5.5	2.442	2.544	4	15.4	74	4.8	0.8
Limestone SP-9.5	TTI	7.1	2.230	2.323	4	17.0	76	6.0	*0.5***
	Florida	7.0	2.248	2.341	4	16.3	75	5.6	0.6
Limestone SP-12.5	TTI	6.4	2.249	2.342	4	14.8	73	5.0	0.6
	*Florida**	6.2	2.266	2.361	4	14.0	71	4.5	0.8

* For Limestone SP-12.5, the original Florida design is based on 100 gyrations.
** Minimum requirement is 0.6.
Note: P_{be} = effective binder content.

According to Table 4-1, the TTI-designed optimum binder content and the corresponding volumetric properties are almost the same as the original Florida designs for Granite SP-9.5 and Granite SP-12.5. For Limestone SP-9.5, the TTI-designed optimum binder content is 7.1 percent, while the original Florida design is 7.0 percent; the dust/binder ratio ($P_{0.075}/P_{be}$) is 0.5 (minimum 0.6) because the TTI-measured number of passing No. 200 sieve is smaller than the original Florida measurements. For Limestone SP-12.5, the TTI-designed optimum binder content is 6.4 percent at 75 gyrations. In comparison, the original Florida design is 6.2 percent at 100 gyrations, which is reasonable since the optimum binder content is usually a little larger at fewer design gyrations.

The research team suggested adding extra (0.5 percent) dust into the Limestone SP-9.5 mixes to meet the dust/binder ratio requirement and received the FDOT project panel's approval.

4.2 Mixture Design Results

After the aggregate and binder evaluation and mixture design trials, the final aggregate components were decided and ready. As mentioned before, 24 mixture designs (i.e., eight mix types × three design gyrations) needed to be conducted. For simplicity, the researchers used "GA" to represent granite aggregate, "L" to represent limestone aggregate, "P" to represent binder PG, and "G" to represent "Gyration." For example, "GA95P67G50" represents a mixture of Granite SP-9.5 PG 67-22 designed at 50 Gyrations, and "L125P76G100" represents a mixture of Limestone SP-12.5 PG 76-22 designed at 100 Gyrations.

Specification AASHTO M323 (AASHTO 2017a) and AASHTO R 35 (AASHTO 2017b) were followed during the mixture design. According to FDOT's specifications, the mixing temperatures were 163°C (325 °F) for PG 76-22 (PMA) and 157 °C (315 °F) for PG 67-22. Mixtures were aged and compacted at the same temperatures as the mixing temperatures, and the conditioning time was two hours.

Three trial binder contents were selected for each mixture design. For each trial binder content, two replicates were prepared for the rice tests to determine the G_{mm} and two replicates (115 ±

5mm high) were compacted under specified gyrations. Taking the mixture design of Granite SP-9.5 PG 67-22 at 50 Gyrations (GA95P67G50) as an example, Figure 4-8 shows the G_{mm} and G_{mb} samples for each trial binder content, and Figure 4-9 shows the test results. The averaged G_{mm} values were determined to be 2.572, 2.542, and 2.521 for the three trial binder contents of 5.0 percent, 5.5 percent, and 6.0 percent, respectively. Accordingly, the averaged G_{mb} values are 2.403, 2.440, and 2.466. Thus, the volumetric properties such as V_a, VMA, voids filled with asphalt (VFA), P_{be}, and the dust/binder ratio ($P_{0.075}/P_{be}$) for each trial binder content can be determined. The P_b can be determined by interpolation at $V_a = 4$ percent. In Figure 4-9, the V_a corresponding to the trial binder content of 5.5 percent happened to be 4 percent, then the P_b for this mixture is 5.5 percent.

If none of the V_a values is 4 percent for all the trial binder contents, interpolation must be conducted to determine the P_b. In addition, the G_{mb}, VMA, VFA, P_{be}, and $P_{0.075}/P_{be}$ also need to be determined by interpolation and checked if they meet the requirements in the specifications AASHTO M323 (AASHTO 2017a) and AASHTO R 35 (AASHTO 2017b).

The rice test Gmm and bulk specific gravity Gmb samples for each trial binder content.

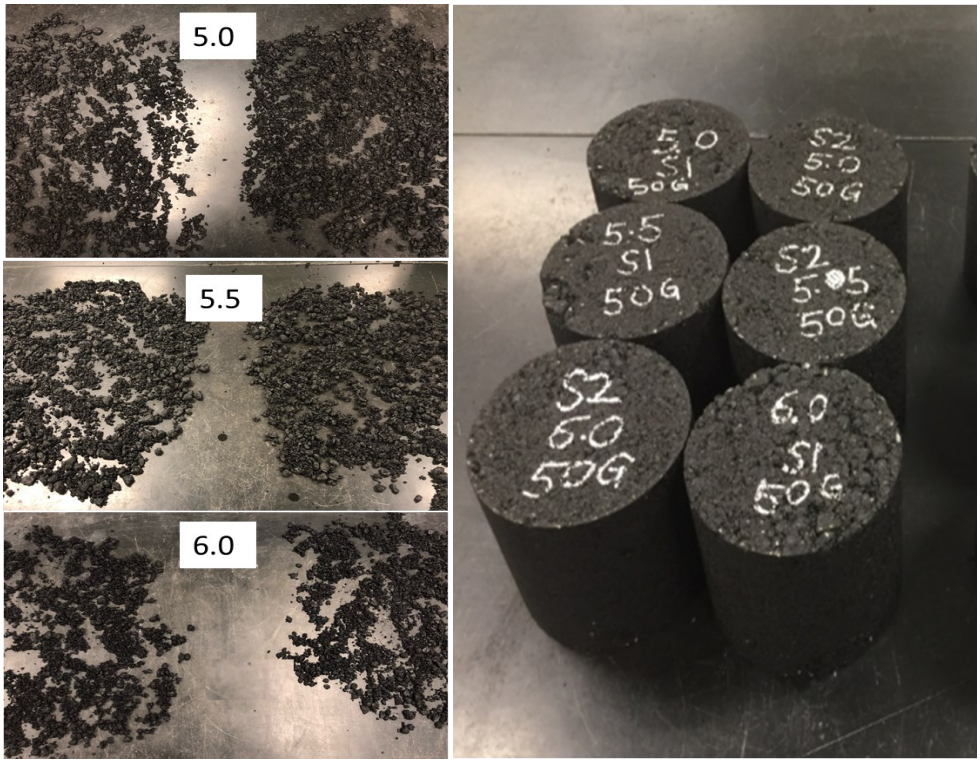

(a) (b)

Figure 4-8. Design of Mixture GA95P67G50 (a) Rice Test G_{mm} Samples and (b) G_{mb} Samples

P_b	G_{mb} @ N_{des}	G_{mm}	V_a	VMA	VFA	P_{be}	$P_{0.075}$ / P_{be}	%G_{mm} @ N_{ini}	%G_{mm} @ N_{max}
5.0	2.403	2.572	6.6	16.3	60	4.2	1.3		
5.5	2.440	2.542	4.0	15.4	74	4.8	1.1		
6.0	2.466	2.521	2.2	15.0	85	5.4	1.0		

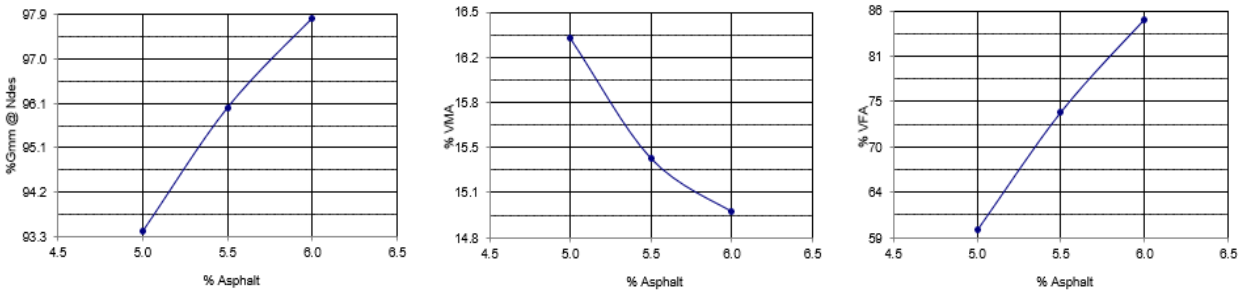

Figure 4-9. Mixture Design Data Sheet of GA95P67G50

Table 4-2 lists the design results for all 24 mixtures. More details such as the trial binder contents and their corresponding G_{mm} and G_{mb} values for each mixture can be found in Appendix A: Mixture Design Data Sheets.

According to AASHTO M323 (AASHTO 2017a), the minimum allowed VMA numbers are 15 percent for SP-9.5 mixtures and 14 percent for SP-12.5 mixtures. In Table 4-2, three mixtures could not meet the requirements: GA95P67G100 (14.7 percent), GA95P76G100 (14.9 percent), and L125P67G100 (13.8 percent). The project panel agreed to proceed since they were only slightly out of tolerance, which often happens during production. In addition, it was worthwhile to compare and investigate the performance of the mixtures, which were slightly off the VMA requirements.

Table 4-2. Optimum Binder Content and Volumetric Properties

Mixture	No.	P_b (%)	G_{mb} @ N_{des}	G_{mm}	VMA (%)	VFA (%)	Pbe (%)	$P_{0.075}/P_{be}$
GA95P67G50	1	5.5	2.440	2.542	15.4	74	4.8	1.1
GA95P67G75	2	5.4	2.447	2.548	15.1	74	4.7	1.2
GA95P67G100	3	5.3	2.455	2.556	***14.7***	73	4.5	1.2
GA125P67G50	4	5.3	2.448	2.549	15.0	73	4.7	0.8
GA125P67G75	5	5.1	2.456	2.559	14.6	73	4.4	0.8
GA125P67G100	6	5.0	2.462	2.564	14.3	72	4.3	0.8
L95P67G50	7	7.0	2.242	2.336	16.5	76	5.7	0.6
L95P67G75	8	6.9	2.248	2.341	16.2	75	5.6	0.6
L95P67G100	9	6.8	2.251	2.346	16.0	75	5.5	0.6
L125P67G50	10	6.3	2.258	2.351	14.4	72	4.8	0.7
L125P67G75	11	6.1	2.263	2.357	14.0	71	4.6	0.8
L125P67G100	12	6.0	2.267	2.361	***13.8***	71	4.5	0.8
GA95P76G50	13	5.8	2.434	2.535	15.9	75	5.1	1.1
GA95P76G75	14	5.6	2.439	2.541	15.6	74	4.9	1.1
GA95P76G100	15	5.3	2.450	2.553	***14.9***	73	4.6	1.2
GA125P76G50	16	5.7	2.435	2.536	15.8	75	5.0	0.7
GA125P76G75	17	5.5	2.442	2.543	15.4	74	4.8	0.8
GA125P76G100	18	5.2	2.455	2.556	14.7	73	4.5	0.8
L95P76G50	19	7.1	2.237	2.329	16.8	76	5.9	0.6
L95P76G75	20	7.0	2.242	2.335	16.5	76	5.7	0.6
L95P76G100	21	6.8	2.247	2.341	16.1	75	5.6	0.6
L125P76G50	22	6.3	2.252	2.347	14.6	73	4.8	0.6
L125P76G75	23	6.2	2.258	2.353	14.3	72	4.7	0.6
L125P76G100	24	6.1	2.263	2.358	14.0	71	4.5	0.7

4.3 Summary

The trial mixture designs showed that mixtures using Texas sand (finer sand) could not meet the VMA requirement. Thus, the FDOT project panel decided to stay with the original Florida gradation designs for granite mixtures (Granite SP-9.5 and Granite SP-12.5), which meant no Texas sand would be introduced. In addition, the trial mixture designs showed that Limestone SP-9.5 mixtures could not meet the dust/binder ratio requirement. The research team suggested adding extra (0.5 percent) dust into the Limestone SP-9.5 mixtures and received the FDOT project panel's approval.

Based on these decisions, 24 mixtures were designed. Their optimum binder contents and volumetric properties were tabulated. More details about the design information, such as the trial binder contents and their corresponding G_{mm} and G_{mb} values for each mixture, can be found in Appendix A: Mixture Design Data Sheets.

5. PERFORMANCE TESTS

Seven performance tests were required in this research: IDEAL-CT, UF-IDT, SCB-FI, APA, HWT, IDEAL-RT, and CAL. For each of the 24 mixtures, two sets of performance test specimens were required—each set represented a different field compaction level: 93 percent G_{mm} (7 percent AV) and 95 percent G_{mm} (5 percent AV).

Table 5-1 lists the specimen size and replicates for each performance test. The corresponding specifications, brief test conditions, and outputs are also listed in the table.

Table 5-1. Performance Test Specification and Specimen Information

Test	Test Standards	Test Conditions	Test Outputs
IDEAL-CT	ASTM D8225-19 (ASTM 2019)	• 3 replicates, Φ 150 mm, H 62 mm • 50 mm/minute • 25°C	• Cracking tolerance index: CT_{index}
UF-IDT	Roque (2015)	• 3 replicates, Φ 150 mm, H 38 mm • Resilient modulus test: 0.1 seconds loading followed by 0.9 seconds rest period • Creep test: 1,000 seconds • Fracture test: 50 mm/minute • 10°C	• Resilient modulus: M_R • Creep compliance: D and m • Dissipated creep strain energy density: $DCSE_f$ • Energy ratio: ER
SCB-FI	AASHTO TP 124 (AASHTO 2018b)	• 4 replicates, Φ 150 mm, H 50 mm • 15 mm notch • 50 mm/minute • 25°C	• Flexibility index: FI
APA	AASHTO T 340 (AASHTO 2010a)	• 4 replicates, Φ 150 mm, H 75 mm • No water • 60 passes/minute • 64°C	• Rut depth at a certain number of allowed passes: d • Number of passes at certain rut depth or failure: N
HWT	AASHTO T 324 (AASHTO 2017c)	• 4 replicates, Φ 150 mm, H 62 mm • Submerged • 52 passes/minute • 50°C	• Rut depth at a certain number of allowed passes: d • Number of passes at certain rut depth or failure: N • Stripping point: SP
IDEAL-RT	Zhou et al. (2019a)	• 3 replicates, Φ 150 mm, H 62 mm • 50 mm/minute • 50°C	• Rutting tolerance index: RT_{index}
CAL	AASHTO TP 108-14 (AASHTO 2018c)	• 3 replicates, Φ 150 mm, H 115 mm • 300 cycles, 30–33 cycles/minute • 25°C	*%Mass Loss*

5.1 Sample Preparation

Each performance test specimen was obtained from a SGC sample, except for SCB-FI tests. One SGC sample yielded two separate semi-circular bending test specimens.

Figure 5-1 shows the samples prepared for mixture GA95P67G50. For each compaction level (95 percent and 93 percent G_{mm}), 22 SCG cylinders were fabricated. These cylinders have the same diameter (150 mm) but different heights, including 115 mm for 3 CAL samples; 75 mm for 4 APA samples; 62 mm for 4 HWT, 3 IDEAL-CT and 3 IDEAL-RT samples; 38 mm for 3 UF-IDT samples (cut from 115 mm SGC samples); and 50 mm for SCB-FI samples (cut from 115 mm SGC samples and then cut into halves and notched).

AV has a significant influence on most performance test results. The AV of each sample was in the tolerance of ± 0.5 percent (AVs are 4.5–5.5 percent for the 95 percent compaction level, and 6.5–7.5 percent for the 93 percent compaction level).

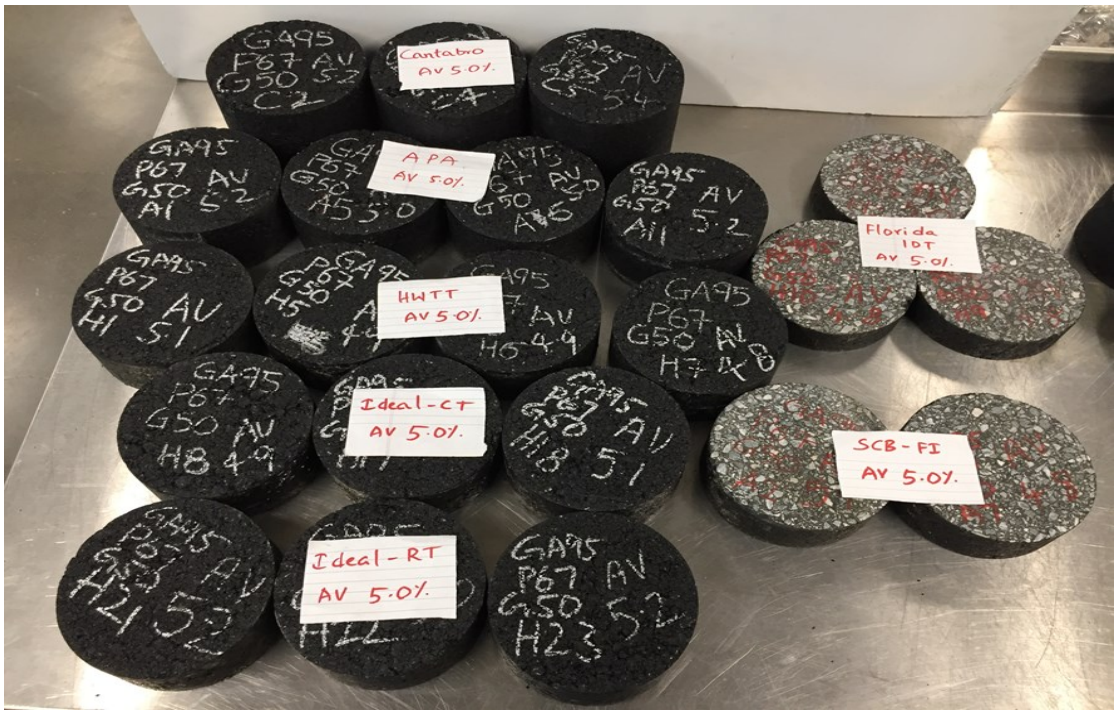

(a)

(b)

Figure 5-1. Performance Test Samples for Mixture GA95P67G50 at (a) 95 percent and (b) 93 percent G_{mm} Compaction Levels

More details of each performance test are provided below.

5.2 IDEAL-CT

TTI researchers (Zhou et al. 2017a) developed this method as the key product of the NCHRP-IDEA 20-30/IDEA 195 project. The test has been standardized as ASTM D8225 (ASTM 2019). The IDEAL-CT sample is subjected to indirect tension at the rate of 50 mm/min (2 in./min) in terms of cross-head displacement. Figure 5-2 shows the test equipment and the samples (GA95P76G75, AV 7 percent) before and after the test.

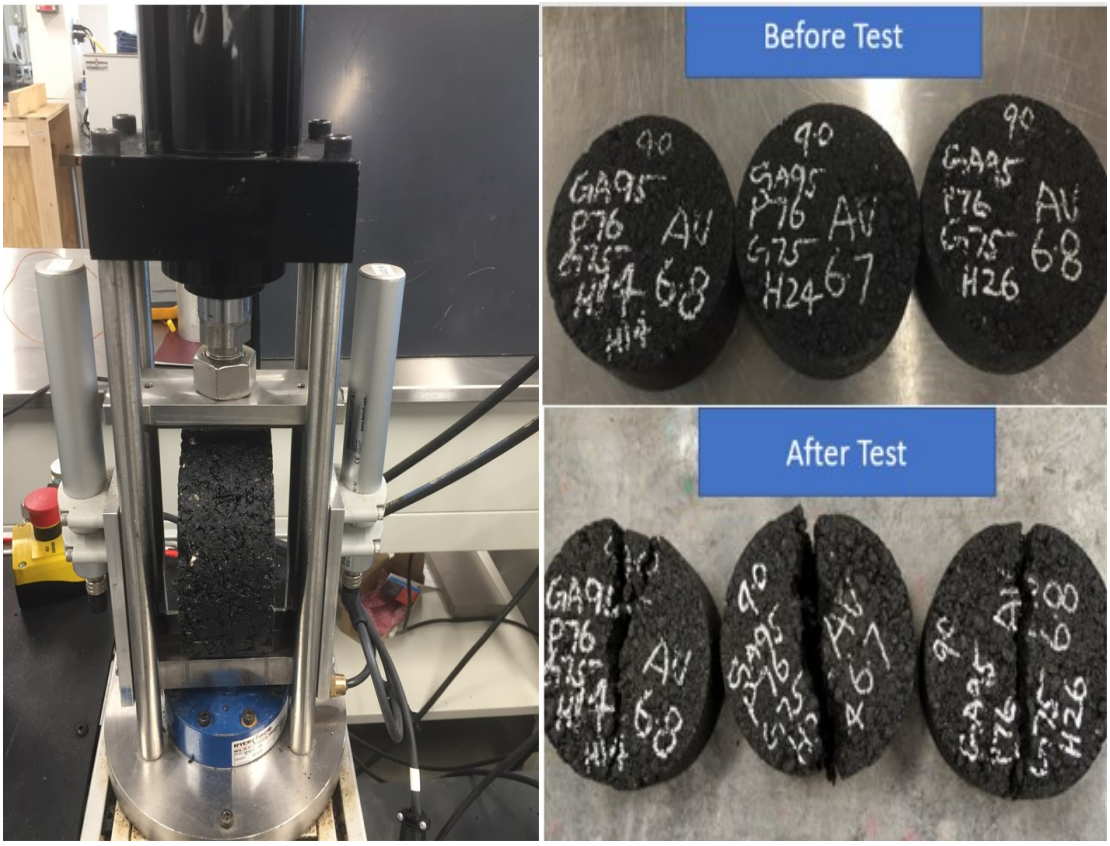

(a) (b)

Figure 5-2. IDEAL-CT (a) Test Equipment and (b) Samples Before and After Test

Figure 5-3 shows a typical IDEAL-CT test curve. The fracture energy (G_f) is determined from the total area under the load-displacement curve. The absolute post-peak load slope of this curve at 75 percent peak load (m_{75}) and the post-peak displacement at 75 percent peak load (l_{75}) can also be determined by the curve. Then these individual parameters can be combined into an index called cracking tolerance index (CT_{index}), as seen in Equation 5-1. The larger the CT_{index}, the better the cracking resistance of the mix and vice versa.

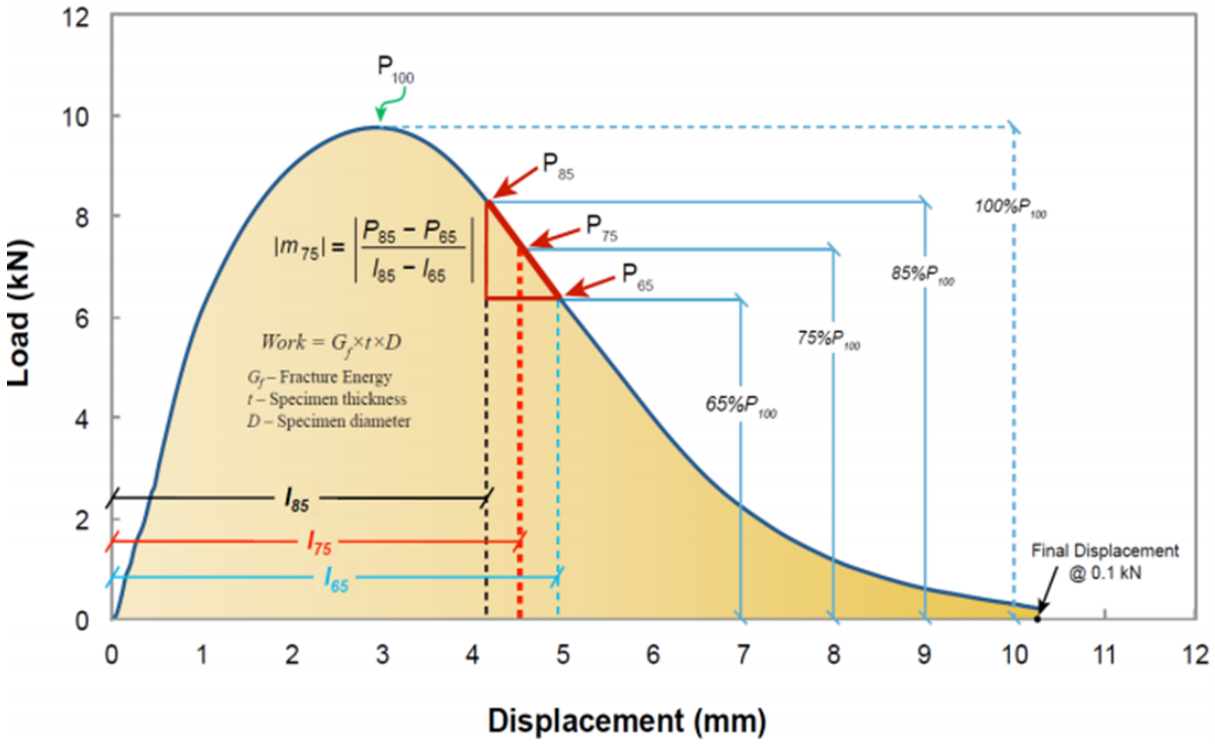

Figure 5-3. IDEAL-CT Typical Test Curve

$$CT_{Index} = \frac{t}{62} \times \frac{G_f}{|m_{75}|} \times \left(\frac{l_{75}}{D}\right) \times 10^6 \qquad (5\text{-}1)$$

where:

t = the sample thickness (mm)

D = the sample diameter (mm)

Figure 5-4 shows the load-displacement curves and CT_{index} results for the samples of GA95P76G75, AV 7%.

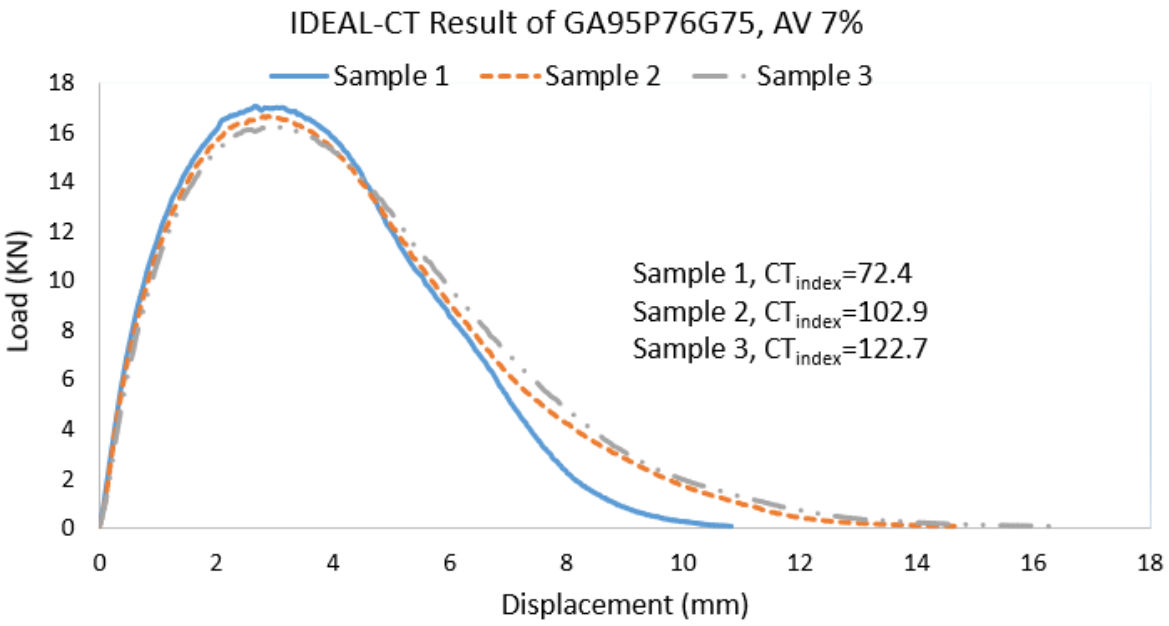

Figure 5-4. IDEAL-CT Result Curves of GA95P76G75, AV 7% Samples

5.3 UF-IDT

The UF-IDT test procedure includes a resilient modulus (M_R) test, a creep test, and a tensile fracture test. A draft procedure was developed for FDOT by Dr. Rey Roque (2015). In 2020, NCHRP 9-57A evaluated the UF-IDT test and fine-tuned some test parameters according to the ruggedness testing results.

The parameter ER is used to distinguish asphalt mixtures with different resistances to top-down cracking (surface-initiated longitudinal wheel-path cracking). Roque et al. (2004) recommended determining the total energy required to fail, also called $DCSE_f$, by running the fracture tensile test. The authors also recommended determining the $DCSE_{min}$ by running the creep compliance test. The ER parameter is defined as the ratio of these two energies as an index representing the resistance of asphalt mixtures to cracking, as seen in Equation 5-2.

$$ER = \frac{DCSE_f}{DCSE_{min.}} = \frac{DCSE_f}{\frac{m^{2.98} \times D_1}{A}} \quad (5\text{-}2)$$

where:

ER = energy ratio (dimensionless).

D_1, m = tensile creep compliance parameters.

A = parameter that takes into account the tensile strength and the tensile stress in the pavement structure. If the tensile stress is unknown, a value of 1 MPa is suggested.

Test results (Roque et al. 2004) showed that asphalt mixtures with a record of early cracking had a lower ER value than asphalt mixtures with fewer or no cracks. Based on these results, the authors recommended using the minimum value of 1.0 for ER and 0.75 kJ/m^3 for $DCSE_f$ as

thresholds for differentiating well-performing asphalt mixtures from poorly performing asphalt mixtures.

Figure 5-5 shows the test equipment and the samples (GA95P76G75, AV 7%) before and after the test. For each specimen, four gage points were centered at the middle quartile of both faces along with two perpendicular directions, at a gage length of 38 mm (1.5 inches). The placement and location of the gage points on each face produced a mirror image of each other. The loading heads were perfectly aligned with a pair of gage points on each face. This action defined the vertical diametral axis along which load was applied. The built-in magnets-extensometer system attaching to the steel gage points was used to measure horizontal and vertical deformations on both faces of a test specimen.

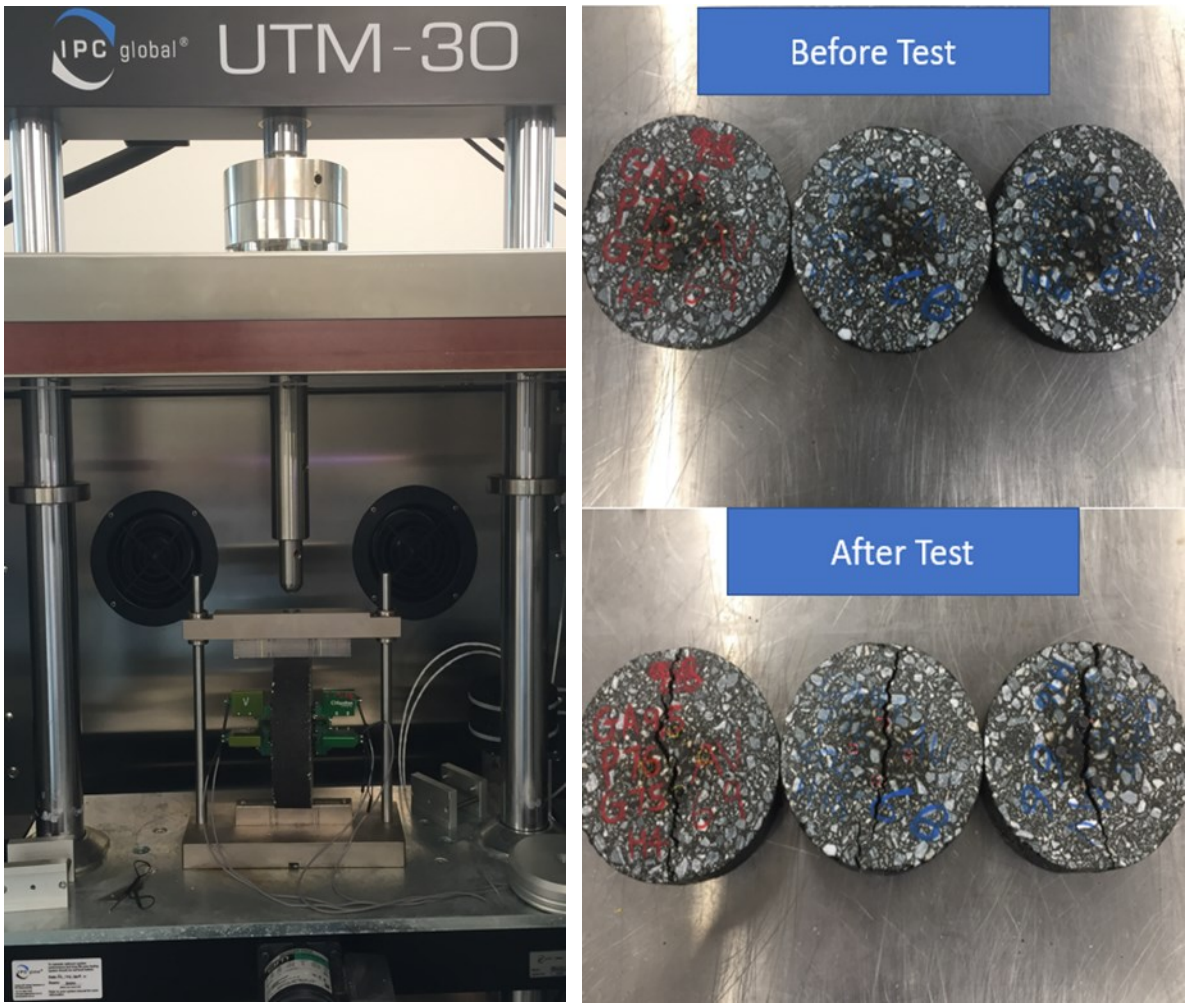

(a) (b)

Figure 5-5. UF-IDT (a) Test Equipment and (b) Samples Before and After Test

There were six sets of data (three specimens, two faces per specimen) for each deformation and loading cycle. A “trimming average process” was followed to determine the resilient modulus, creep compliance parameters, DCSE, and ER. In this process, deformation data are sorted, the

highest and the lowest deformation values are removed, and the remaining four deformation values are averaged. Figure 5-6 shows the UF-IDT results for the samples of GA95P76G75, AV 7%.

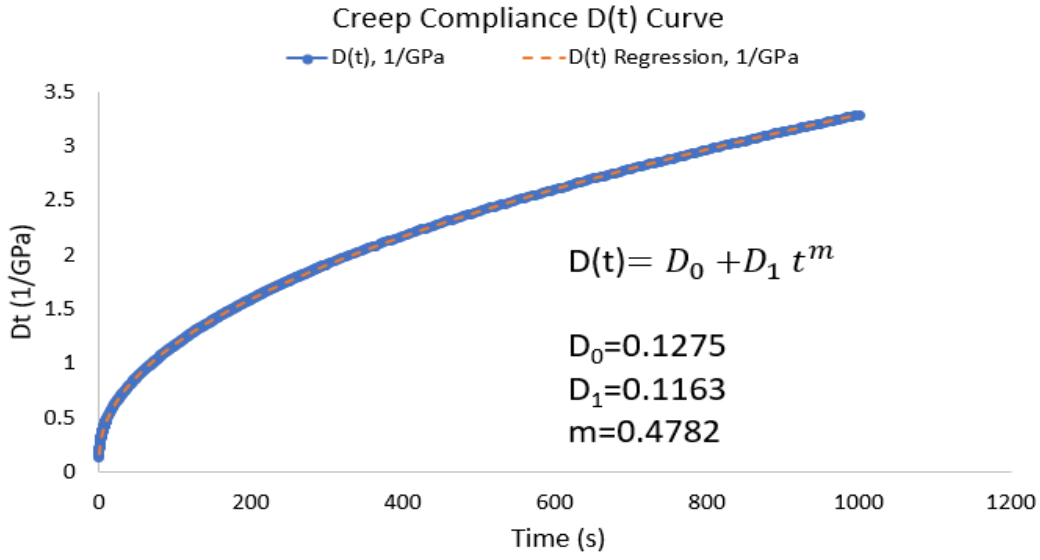

(a)

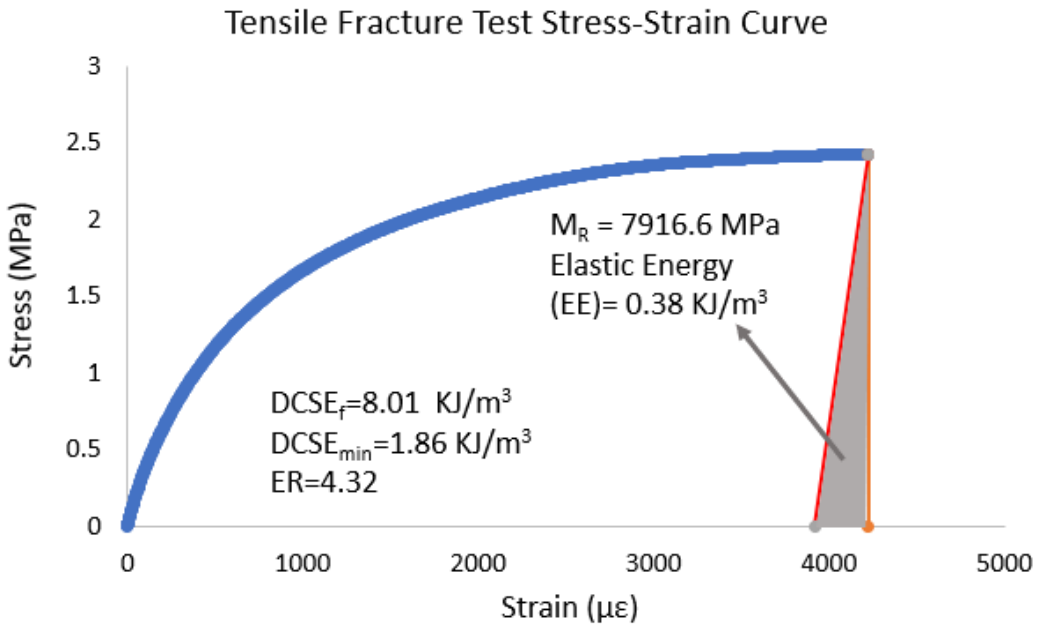

(b)

Figure 5-6. UF-IDT (a) Creep Compliance and (b) Tensile Fracture Results of GA95P76G75, AV 7% Samples

5.4 SCB-FI

SCB-FI test was conducted following AASHTO TP124-18 (2018b). Two cylindrical specimens (Φ150 mm x 115 mm) can be cut into four SCB specimens (Φ150 mm x 50 mm). Each specimen was notched with a 15-mm-long depth at the center. The specimen would be under a monotonic load at 50 mm/min (or 2 in./min) from the top in a three-point bending beam configuration at 25°C (77°F). Figure 5-7 shows the test equipment and the samples (GA95P76G75, AV 7%) before and after the test.

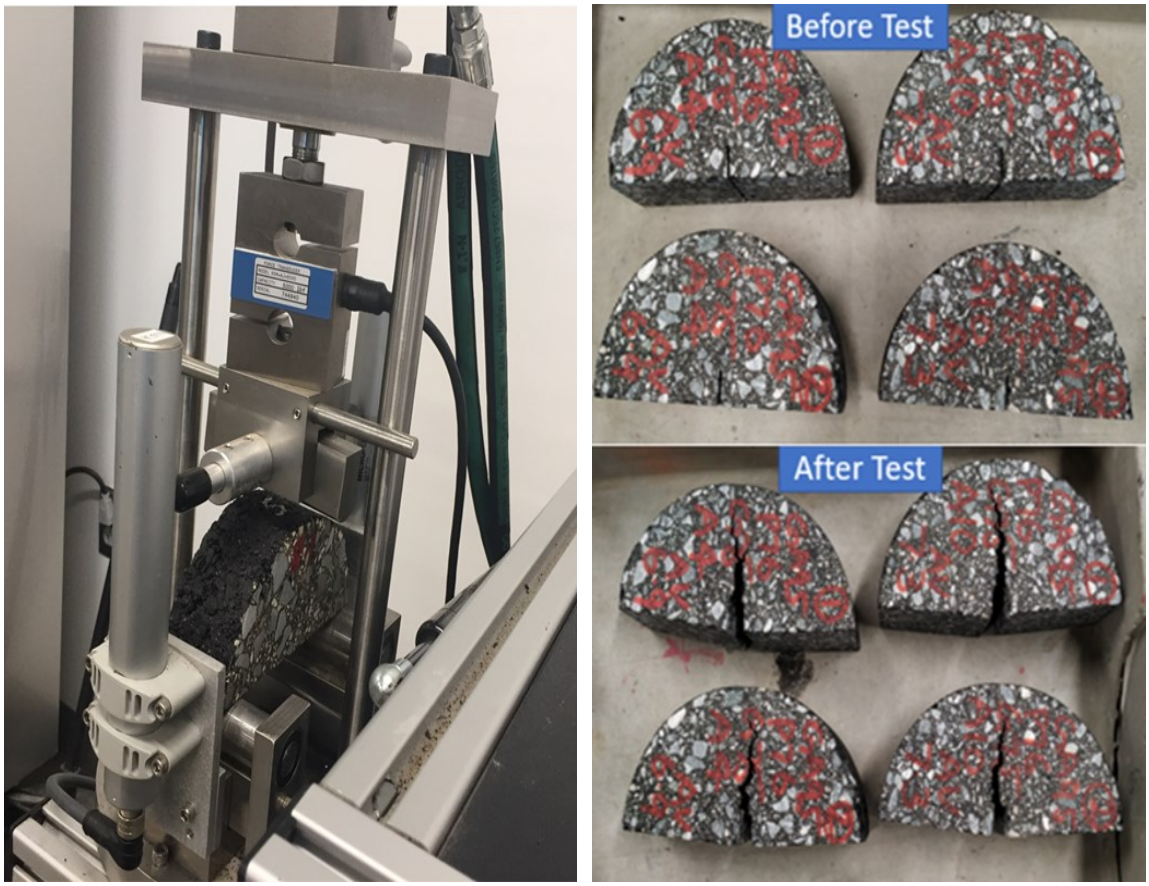

(a) (b)

Figure 5-7. SCB-FI (a) Test Equipment and (b) Samples Before and After Test

Figure 5-8 shows a typical SCB-FI test curve. The flexibility index (FI) can be calculated by Equation 5-3. The G_f is calculated by dividing the work of fracture (the area under the load-displacement curve) by the ligament area (the product of the ligament length and the thickness of the specimen). The |m| is the absolute slope at the inflection point on the load-displacement curve.

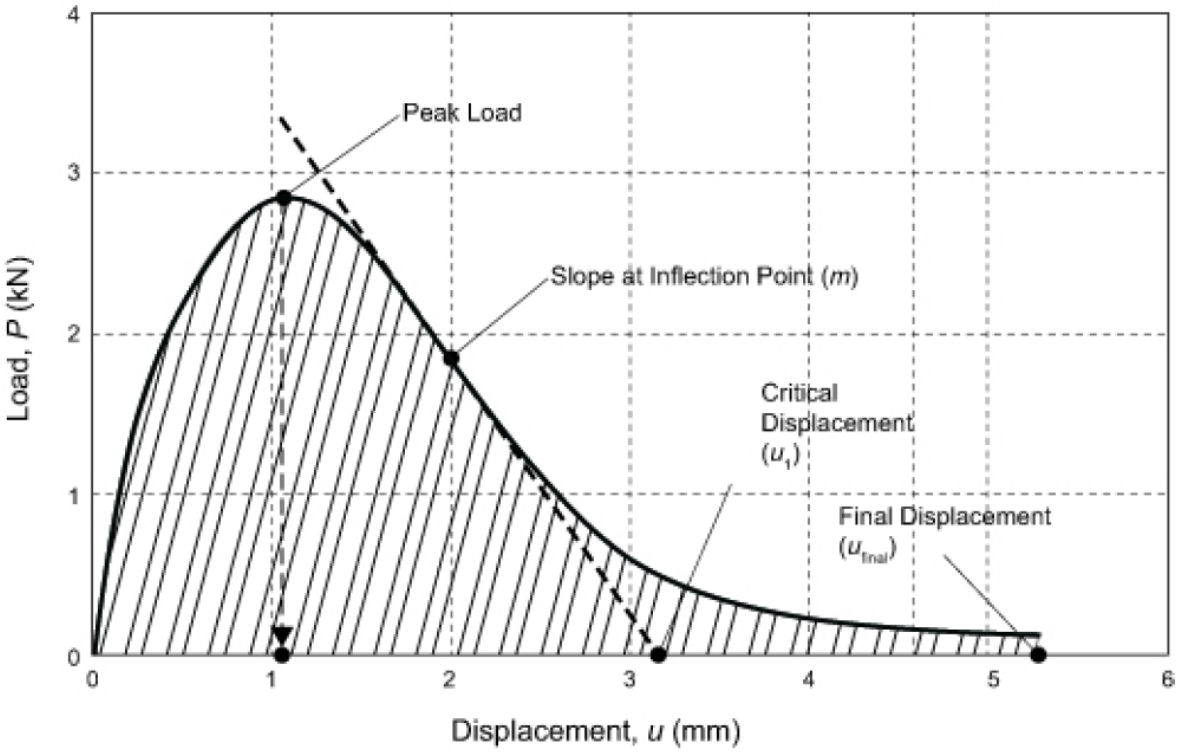

Figure 5-8. SCB-FI Typical Test Curve (AASHTO 2018b)

$$FI = \frac{G_f}{|m|} \times 0.01 \quad (5\text{-}3)$$

Figure 5-9 shows the SCB-FI results for the four samples of GA95P76G75, AV 7%.

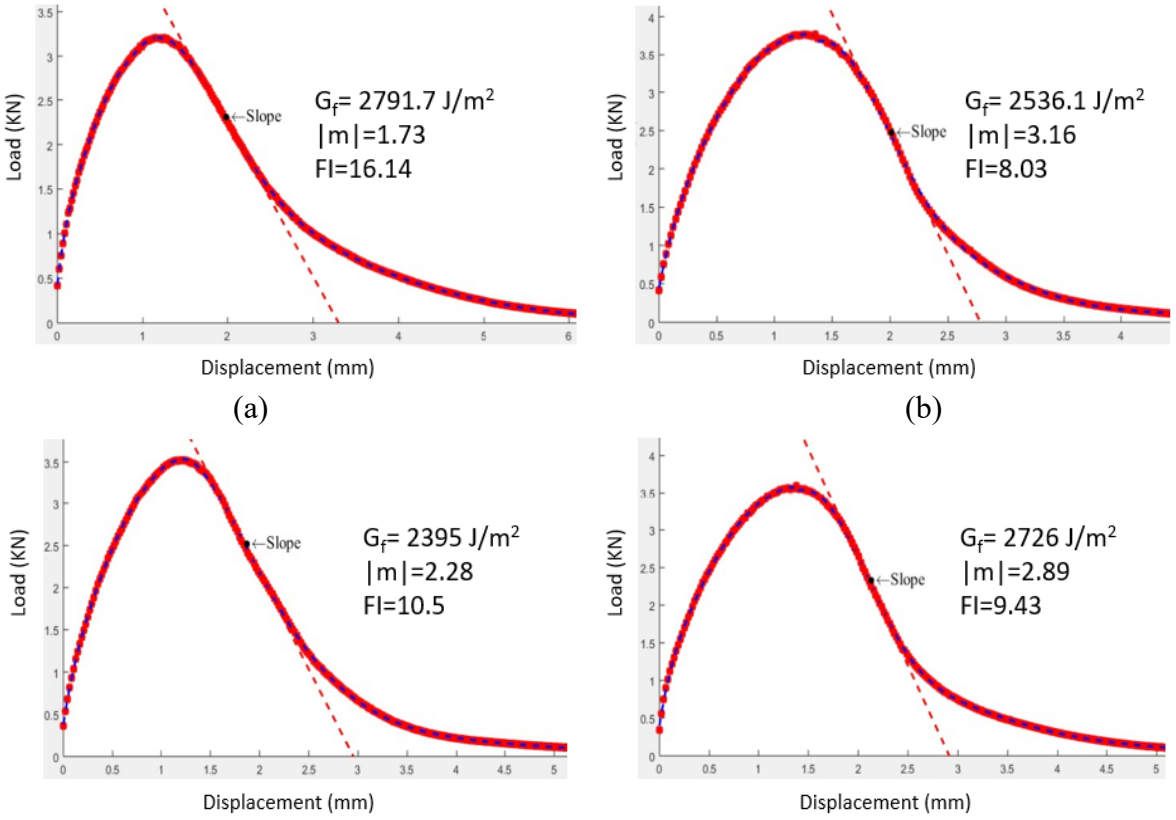

Figure 5-9. SCB-FI Results of GA95P76G75, AV 7% Samples (a) #1, (b) #2, (c) #3, and (d) #4

5.5 APA

APA test was conducted following AASHTO T340 (AASHTO 2010a). It involves the application of continuous passes of heavily loaded steel wheels on 75-mm-thick (2.95 inches) cylindrical specimens at a certain high temperature (64°C) through pressurized (100 psi) rubber hoses. The total number of wheel loading cycles is 8,000 cycles. Figure 5-10 shows the test equipment and the samples (GA95P76G75, AV 7%) before and after the test. The APA rut depth for the samples of GA95P76G75, AV 7% is shown in Figure 5-11.

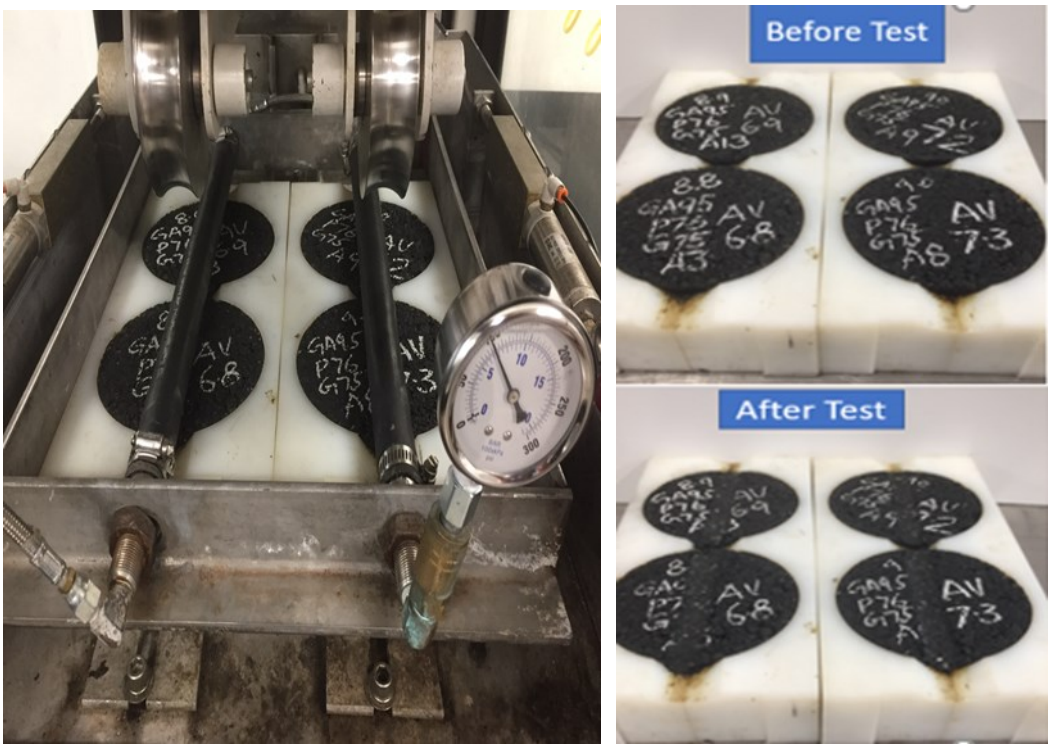

(a) (b)

Figure 5-10. APA (a) Test Equipment and (b) Samples Before and After Test

Figure 5-11 shows the APA results for the samples of GA95P76G75, AV 7%.

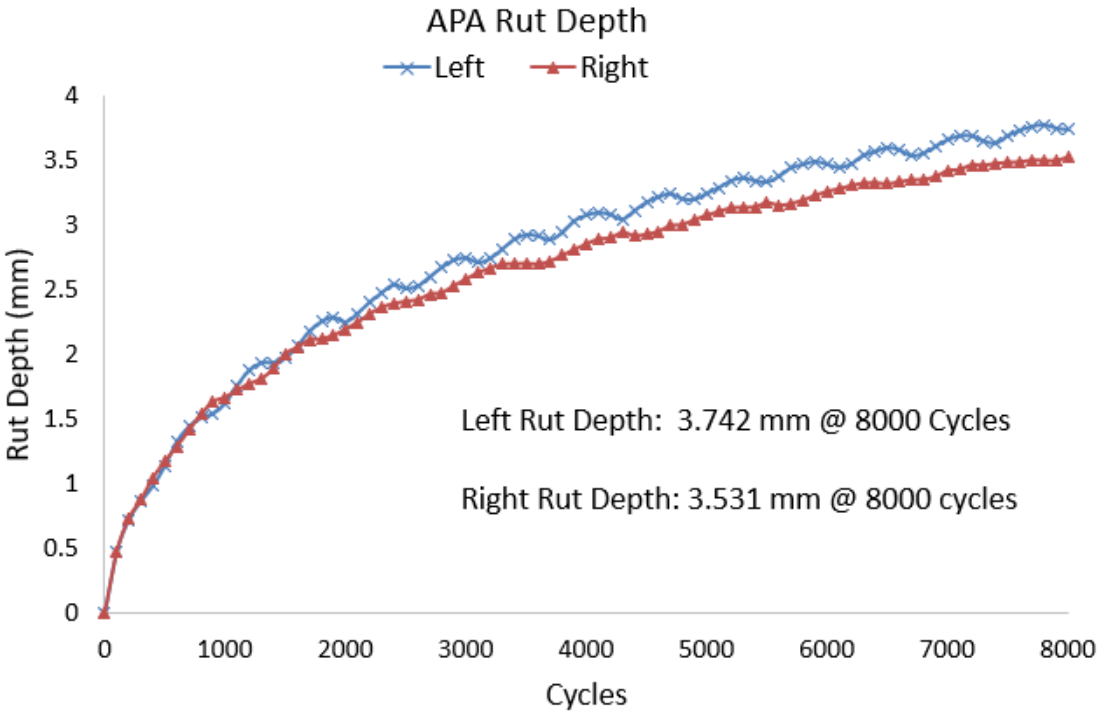

Figure 5-11. APA Results of GA95P76G75, AV 7% Samples

5.6 HWT

The HWT test involves the application of continuous passes of a heavily loaded (705 N or 158 lb) steel wheel directly on 62-mm (2.5 inches)-thick cylindrical asphalt mixture specimens submerged in water at a certain temperature (50°C). The test stops when the number of wheel passes reaches a specified value (usually 20,000 wheel passes), or the rut reaches a certain depth (e.g., 20 mm or 0.79 inches).

The HWT test is conducted underwater; therefore, it can also evaluate the stripping potential of asphalt mixtures (AASHTO 2017c). Since the HWT test results correlated well with field performance, the test has been implemented as a routine rutting test by many DOTs. Figure 5-12 shows the test equipment and the samples (GA95P76G75, AV 7%) before and after the test.

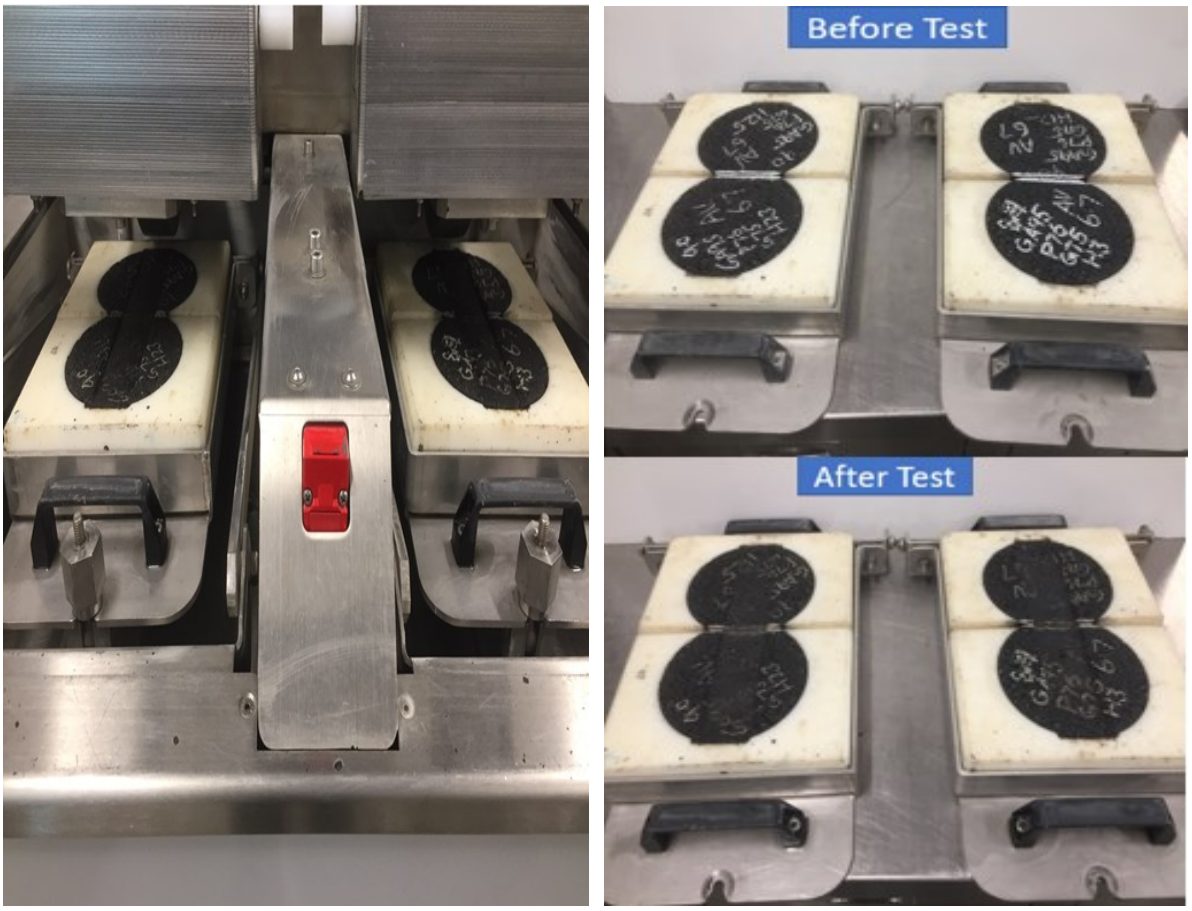

(a) (b)

Figure 5-12. HWT (a) Test Equipment and (b) Samples Before and After Test

Figure 5-13 shows the HWT results for the samples of GA95P76G75, AV 7%. In this study, all Granite SP-9.5 and Granite SP-12.5 mixtures could withstand 20,000 wheel passes without any sign of stripping.

Figure 5-14 shows the HWT result of L95P67G100, AV 7%, an example with stripping. The stripping point, rut depth at stripping point, and the number of passes at 12.5mm rut depth were determined and shown in the figure.

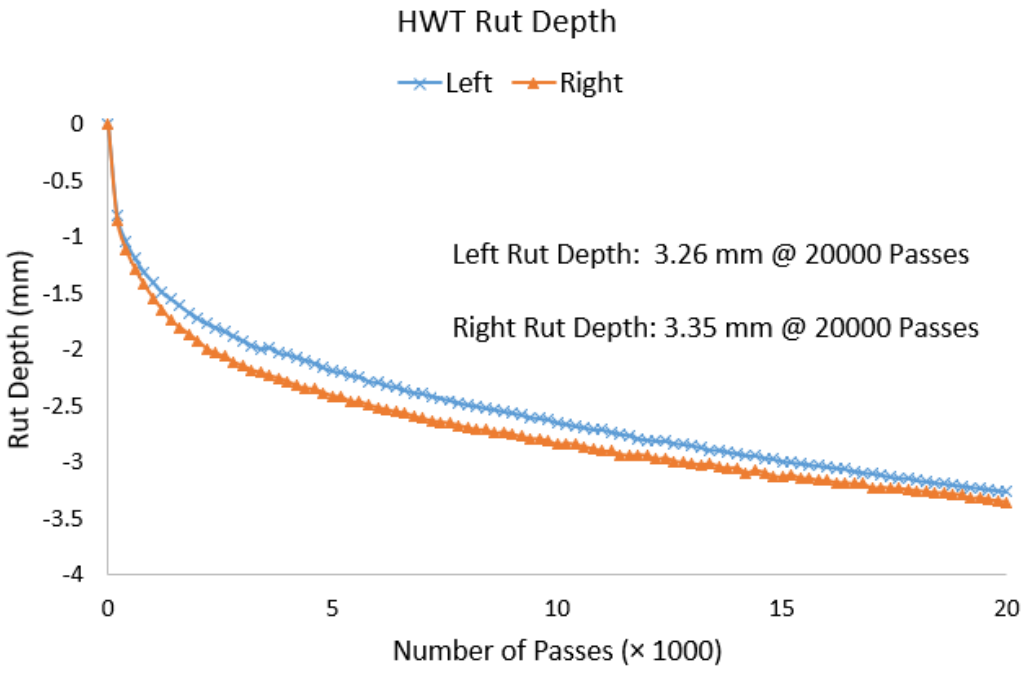

Figure 5-13. HWT Results of GA95P76G75, AV 7% Samples

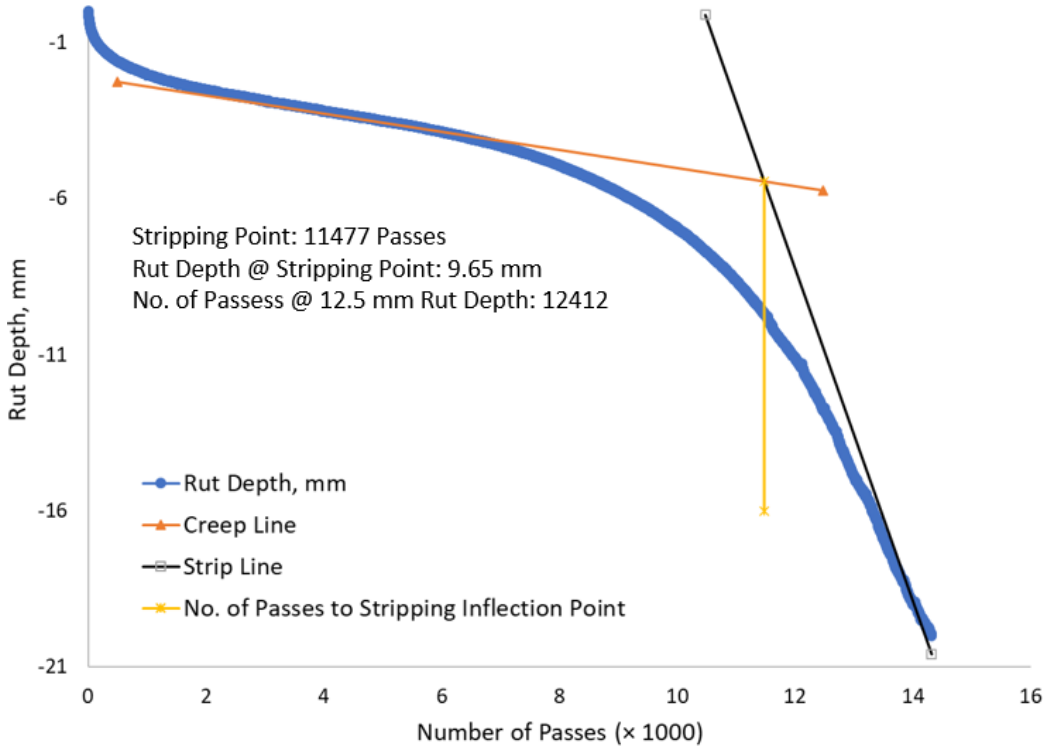

Figure 5-14. HWT Results of L95P67G100, AV 7% Samples

5.7 IDEAL-RT

IDEAL-RT (Zhou et al. 2019a) is used to evaluate the rutting resistance of asphalt mixtures at high temperatures (e.g., 50°C). The rutting tolerance index (RT_{index}) of an asphalt mixture is calculated from the peak load (or shear strength) and is a performance indicator of the rutting resistance of asphalt mixtures. Generally, the higher the RT_{index} value, the better the rutting resistance and, consequently, the smaller the rut depth in the field.

The test loading fixture consists of one upper loading strip and two lower supporting strips to induce shearing force into the specimen. Figure 5-15 shows the test equipment and the samples (GA95P76G75, AV 7%) before and after the test. This figure shows that each sample has two shear cracks after the test.

(a) (b)

Figure 5-15. IDEAL-RT (a) Test Equipment and (b) Samples Before and After Test

The following equations can be used to determine the RT_{index}:

$$RT_{index} = 6.618 \times 10^{-5} \times \frac{\tau_f}{1Pa} \quad (5\text{-}4)$$

$$\tau_f = 0.356 \times \frac{P_{max}}{t \times w} \quad (5\text{-}5)$$

where:

τ_f = shear strength (Pa)
P_{max} = maximum load (N)
t = specimen thickness (m)
w = width of upper loading strip (= 0.0191 m)

Figure 5-16 shows the load-displacement curves and RT_{index} results for the samples of GA95P76G75, AV 7%.

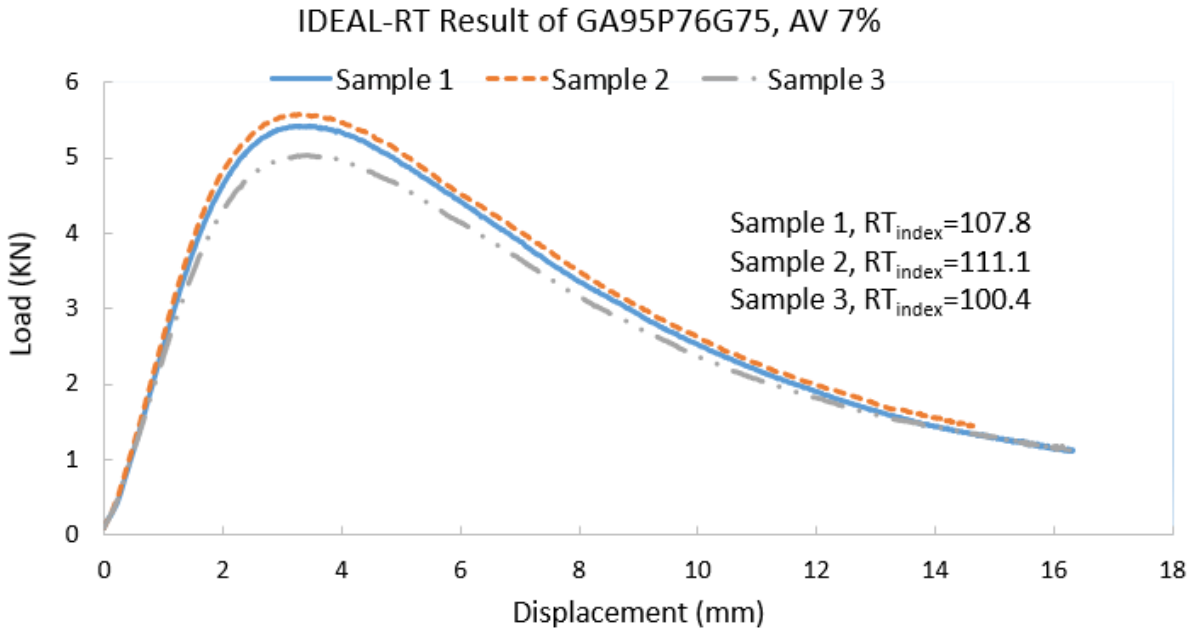

Figure 5-16. IDEAL-RT Result Curves of GA95P76G75, AV 7% Samples

5.8 CAL

The CAL test is the primary test used to evaluate the durability of asphalt mixtures. The test involves placing an SGC specimen in the Los Angeles abrasion drum without steel spheres at a temperature of 25°C and then rotating the drum for 300 revolutions at the rate of 30–33 revolutions/minute. The analysis involves the calculation of mass lost due to abrasion during this process from the difference in specimen mass before and after the test (AASHTO 2018c). More-durable asphalt mixtures usually have lower mass loss compared to less-durable asphalt mixtures. Figure 5-17 shows the test equipment and the samples (GA95P76G75, AV 7%) before and after the test. The corresponding test results are listed in Table 5-2.

(a) (b)

Figure 5-17. CAL (a) Test Equipment and (b) Samples Before and After Test

Table 5-2. CAL Results of GA95P76G75, AV 7% Samples

Sample No.	Weight Before Test (W1), g	Weight After Test (W2), g	W1-W2, g	Mass Loss, %
1	4710.5	4478	232.5	4.94
2	4702.5	4496.5	206	4.38
3	4708.5	4503.5	205	4.35

5.9 Summary

This chapter presented the seven performance tests' sample preparation, test methods, and test data interpretation.

6. TEST RESULTS AND ANALYSIS

This chapter presents the results of each performance test of each mixture. Statistical analysis was performed to compare the performance between SP-9.5 and SP-12.5 mixtures.

6.1 IDEAL-CT Results

Figure 6-1 shows the bar chart of IDEAL-CT results for all mixtures. The height of the rectangular bar shows the average value, and the error bar shows the standard deviation. The rectangular bars filled with diagonal stripes stand for the SP-9.5 mixtures, and the bars filled with solid color stand for the SP-12.5 mixtures. The mixtures in Figure 6-1a are designed at 50 gyrations; Figure 6-1b and Figure 6-1c are designed at 75 and 100 gyrations, respectively. Note that the fewer design gyrations, the higher the mixture's optimum binder content. The ranking of binder content (from high to low) of mixtures in Figure 6-1 is a > b > c.

Overall, the higher the binder content, the more crack-resistant the mixture and the higher the CT_{index} value. This trend is clearly exhibited in Figure 6-1 by comparing the corresponding mixtures among Figure 6-1a, b, and c.

The t-test analysis was performed to determine if the SP-9.5 and SP-12.5 mixtures were significantly different in IDEAL-CT test data. Figure 6-1 shows Limestone SP-9.5 mixtures have higher CT_{index} values (better crack resistance) than Limestone SP-12.5 mixtures. On the contrary, most Granite SP-12.5 mixtures have higher CT_{index} values (better crack resistance) than Granite SP-9.5 mixtures. Thus, the granite and limestone mixtures need to be separate for the t-test analysis since the mixture performance has an opposite trend of change when the aggregate type is different. The other mixture factors, such as binder PG, design gyrations, and AV, were combined during the analysis since no opposite trend of change was observed for these factors.

Table 6-1 shows the CT_{index} values and the paired t-test p-values based on the two-tailed distribution. If the determined p-value is less than 0.05, it would be concluded that there is a significant difference between the two groups in terms of the given performance test.

The p-value is 0.08045 (larger than 0.05) for granite mixtures, which means the Granite SP-9.5 mixtures are not statistically different from Granite SP-12.5 mixtures in terms of IDEAL-CT test performance.

The p-value is 6.7835e-6 (smaller than 0.05) for limestone mixtures, which means the Limestone SP-9.5 mixtures are statistically different from (in this case, better than) Limestone SP-12.5 mixtures in terms of IDEAL-CT test performance. The CT_{index} values of Limestone SP-9.5 mixtures are larger than the corresponding Limestone SP-12.5 mixtures.

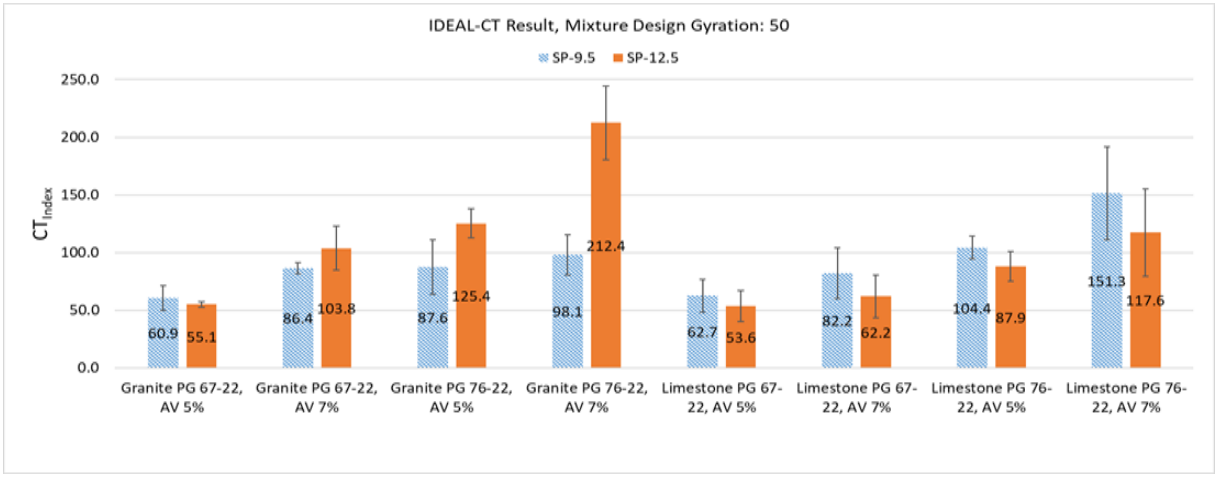

(a)

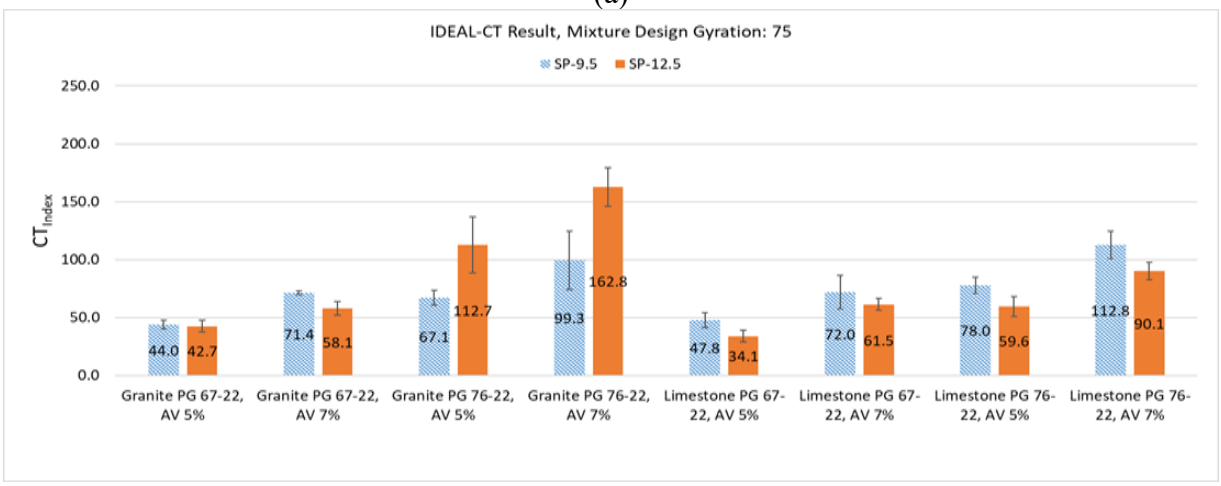

(b)

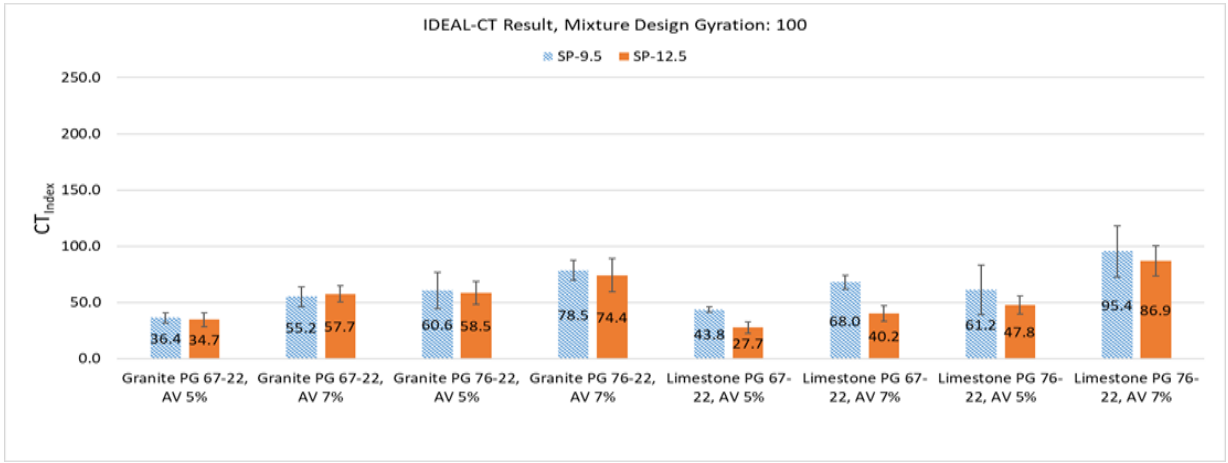

(c)

Figure 6-1. IDEAL-CT Results of Mixtures at (a) 50, (b) 75, and (c) 100 Design Gyrations

Table 6-1. Paired t-test Analysis of IDEAL-CT (CT_{index}) Results

Mixture Factor	SP-9.5	SP-12.5	p-value
Granite PG 67-22, AV 5%, Gyration 50	60.9	55.1	0.08045
Granite PG 67-22, AV 7%, Gyration 50	86.4	103.8	
Granite PG 76-22, AV 5%, Gyration 50	87.6	125.4	
Granite PG 76-22, AV 7%, Gyration 50	98.1	212.4	
Granite PG 67-22, AV 5%, Gyration 75	44.0	42.7	
Granite PG 67-22, AV 7%, Gyration 75	71.4	58.1	
Granite PG 76-22, AV 5%, Gyration 75	67.1	112.7	
Granite PG 76-22, AV 7%, Gyration 75	99.3	162.8	
Granite PG 67-22, AV 5%, Gyration 100	36.4	34.7	
Granite PG 67-22, AV 7%, Gyration 100	55.2	57.7	
Granite PG 76-22, AV 5%, Gyration 100	60.6	58.5	
Granite PG 76-22, AV 7%, Gyration 100	78.5	74.4	
Limestone PG 67-22, AV 5%, Gyration 50	62.7	53.6	*6.7835e-6*
Limestone PG 67-22, AV 7%, Gyration 50	82.2	62.2	
Limestone PG 76-22, AV 5%, Gyration 50	104.4	87.9	
Limestone PG 76-22, AV 7%, Gyration 50	151.3	117.6	
Limestone PG 67-22, AV 5%, Gyration 75	47.8	34.1	
Limestone PG 67-22, AV 7%, Gyration 75	72.0	61.5	
Limestone PG 76-22, AV 5%, Gyration 75	78.0	59.6	
Limestone PG 76-22, AV 7%, Gyration 75	112.8	90.1	
Limestone PG 67-22, AV 5%, Gyration 100	43.8	27.7	
Limestone PG 67-22, AV 7%, Gyration 100	68.0	40.2	
Limestone PG 76-22, AV 5%, Gyration 100	61.2	47.8	
Limestone PG 76-22, AV 7%, Gyration 100	95.4	86.9	

6.2 UF-IDT Results

Figure 6-2 and Figure 6-3 show the bar charts of the UF-IDT results—ER and DCSE, respectively. Similar to Figure 6-1, the rectangular bars filled with diagonal stripes stand for the SP-9.5 mixtures, and the bars filled with solid color stand for the SP-12.5 mixtures. The mixtures of 50, 75, and 100 design gyrations are shown in figures with subtitles a, b, and c, respectively. No standard deviation was determined since the DCSE and ER were determined based on a "trimming average process" of deformation data. Thus, no error bar could be plotted.

Higher ER values or DCSE values indicate higher cracking resistance of mixtures. The paired t-test analysis was conducted to determine if the SP-9.5 and SP-12.5 mixtures were significantly different in UF-IDT test data. The granite mixtures and limestone mixtures were analyzed separately. The other mixture factors, such as binder PG, design gyrations, and AV, were combined during the analysis since no opposite trend of change was observed for these factors. Table 6-2 and Table 6-3 show the ER and DCSE values and their paired t-test p-values based on two-tailed distribution.

According to the ER results, the p-value is 7.3623e-4 (smaller than 0.05) for granite mixtures, which means the Granite SP-9.5 mixtures are statistically different from (in this case, better than) Granite SP-12.5 mixtures. The ER values of Granite SP-9.5 mixtures are larger than the corresponding Granite SP-12.5 mixtures. The p-value is 0.2825 (larger than 0.05) for limestone mixtures, which means the Limestone SP-9.5 mixtures are not statistically different from Limestone SP-12.5 mixtures.

According to the DCSE results, the p-value is 0.0817 and 0.1963 for granite and limestone mixtures, respectively. Both values are larger than 0.05, which means SP-9.5 mixtures are not statistically different from SP-12.5 mixtures in terms of DCSE results, whether the aggregate type is granite or limestone.

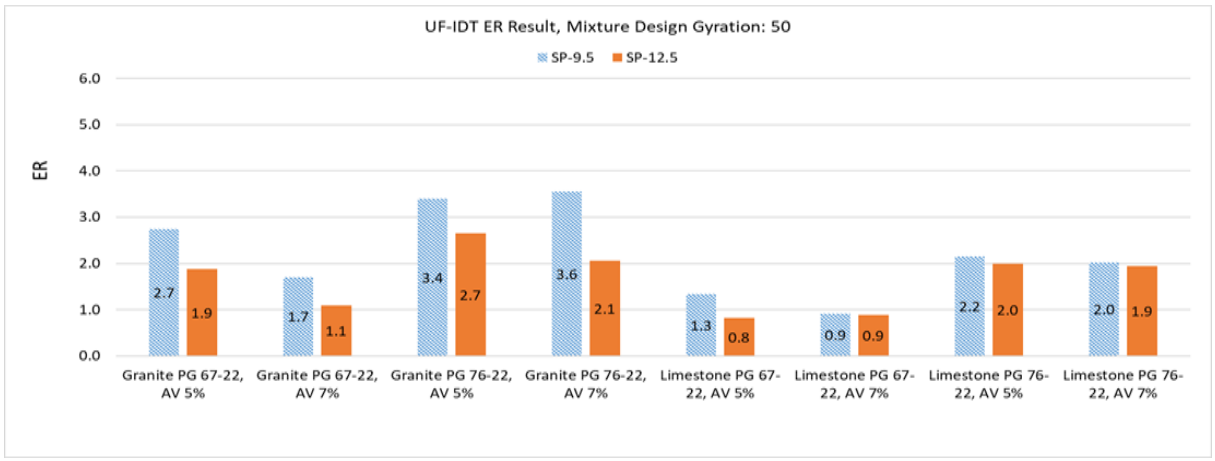

(a)

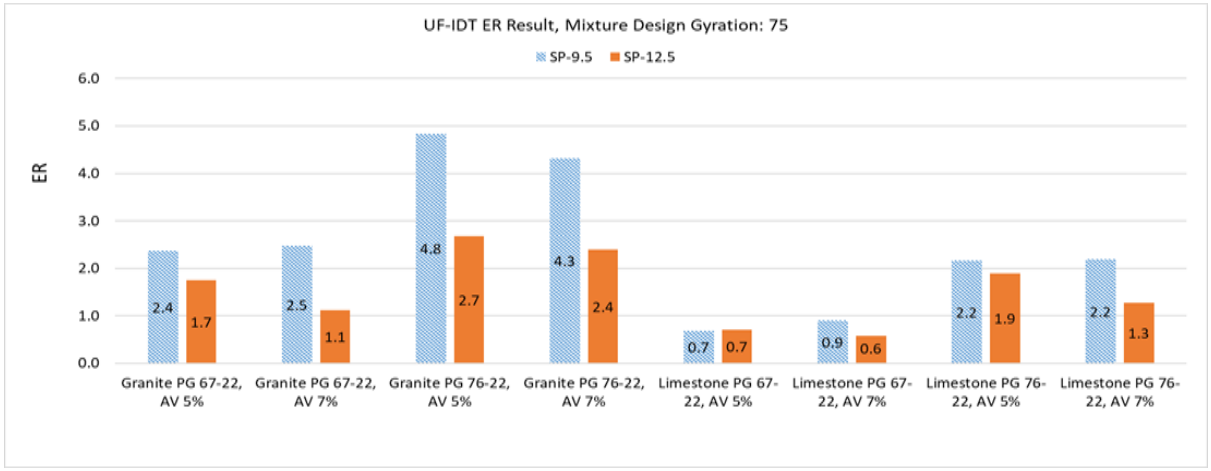

(b)

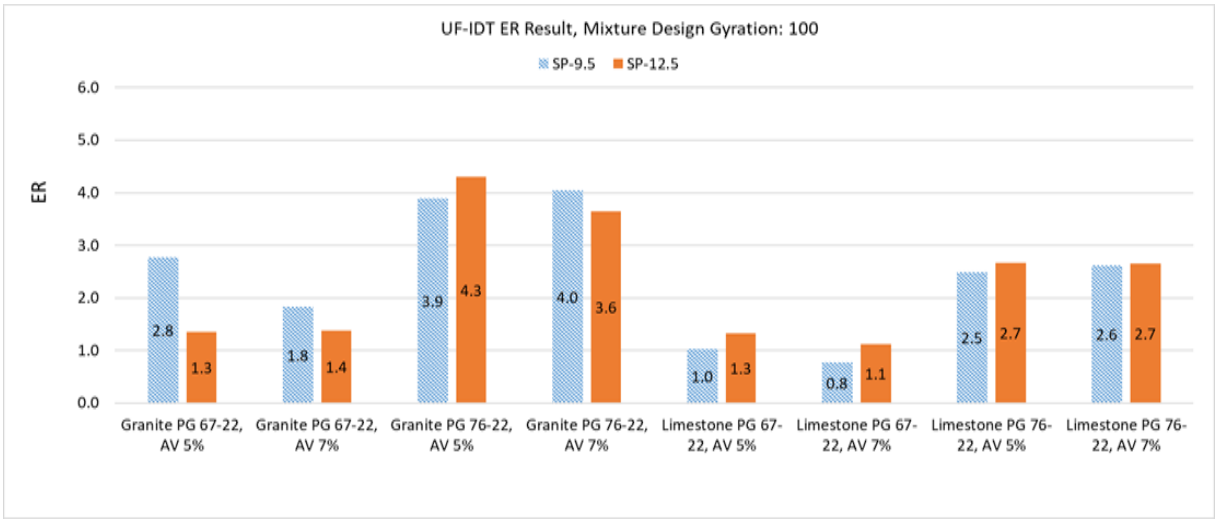

(c)

Figure 6-2. UF-IDT ER Results of Mixtures at (a) 50, (b) 75, and (c) 100 Design Gyrations

Table 6-2. Paired t-test Analysis of UF-IDT (ER) Results

Mixture Factor	SP-9.5	SP-12.5	p value
Granite PG 67-22, AV 5%, Gyration 50	2.7	1.9	
Granite PG 67-22, AV 7%, Gyration 50	1.7	1.1	
Granite PG 76-22, AV 5%, Gyration 50	3.4	2.7	
Granite PG 76-22, AV 7%, Gyration 50	3.6	2.1	
Granite PG 67-22, AV 5%, Gyration 75	2.4	1.7	
Granite PG 67-22, AV 7%, Gyration 75	2.5	1.1	*7.3623e-4*
Granite PG 76-22, AV 5%, Gyration 75	4.8	2.7	
Granite PG 76-22, AV 7%, Gyration 75	4.3	2.4	
Granite PG 67-22, AV 5%, Gyration 100	2.8	1.3	
Granite PG 67-22, AV 7%, Gyration 100	1.8	1.4	
Granite PG 76-22, AV 5%, Gyration 100	3.9	4.3	
Granite PG 76-22, AV 7%, Gyration 100	4.0	3.6	
Limestone PG 67-22, AV 5%, Gyration 50	1.3	0.8	
Limestone PG 67-22, AV 7%, Gyration 50	0.9	0.9	
Limestone PG 76-22, AV 5%, Gyration 50	2.2	2.0	
Limestone PG 76-22, AV 7%, Gyration 50	2.0	1.9	
Limestone PG 67-22, AV 5%, Gyration 75	0.7	0.7	
Limestone PG 67-22, AV 7%, Gyration 75	0.9	0.6	0.2825
Limestone PG 76-22, AV 5%, Gyration 75	2.2	1.9	
Limestone PG 76-22, AV 7%, Gyration 75	2.2	1.3	
Limestone PG 67-22, AV 5%, Gyration 100	1.0	1.3	
Limestone PG 67-22, AV 7%, Gyration 100	0.8	1.1	
Limestone PG 76-22, AV 5%, Gyration 100	2.5	2.7	
Limestone PG 76-22, AV 7%, Gyration 100	2.6	2.7	

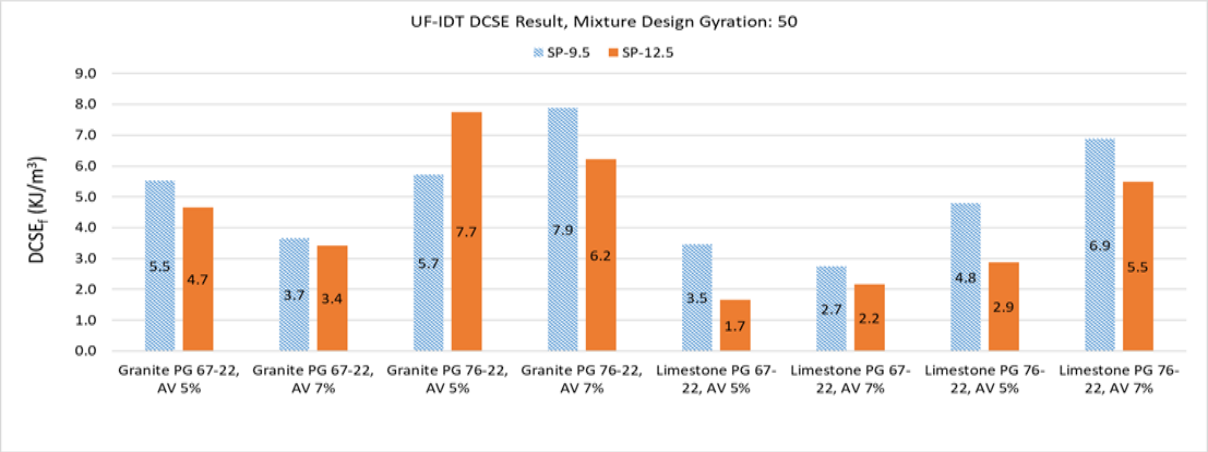

(a)

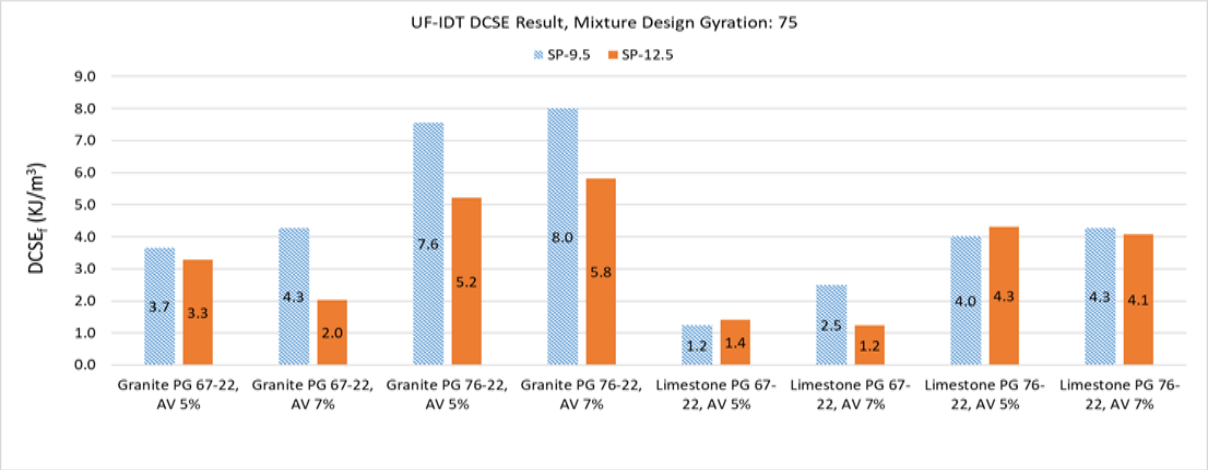

(b)

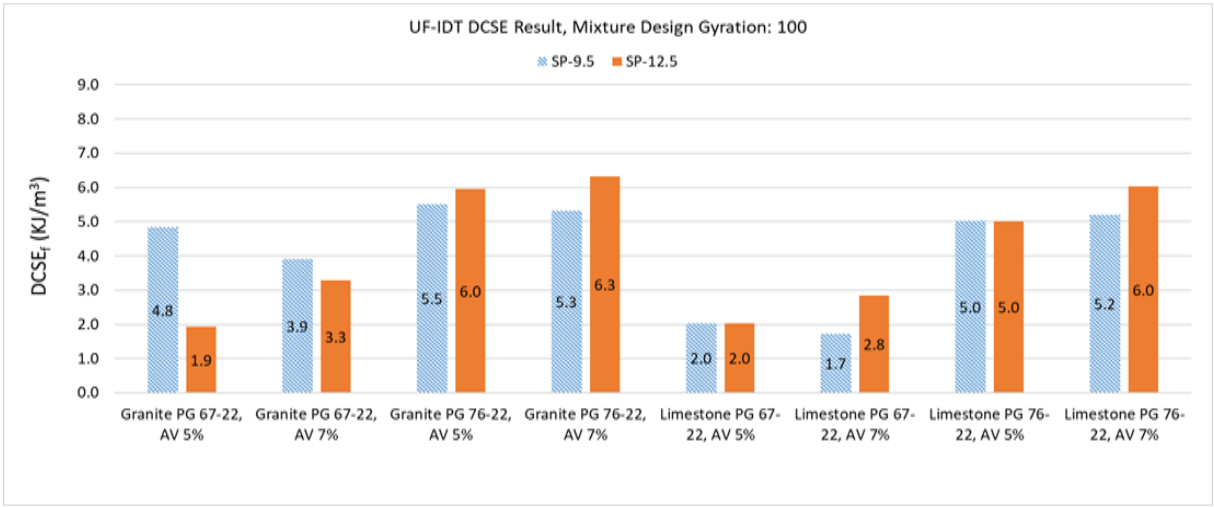

(c)

Figure 6-3. UF-IDT DCSE Results of Mixtures at (a) 50, (b) 75, and (c) 100 Design Gyrations

Table 6-3. Paired t-test Analysis of UF-IDT (DCSE) Results

Mixture Factors	SP-9.5	SP-12.5	p value
Granite PG 67-22, AV 5%, Gyration 50	5.5	4.7	
Granite PG 67-22, AV 7%, Gyration 50	3.7	3.4	
Granite PG 76-22, AV 5%, Gyration 50	5.7	7.7	
Granite PG 76-22, AV 7%, Gyration 50	7.9	6.2	
Granite PG 67-22, AV 5%, Gyration 75	3.7	3.3	
Granite PG 67-22, AV 7%, Gyration 75	4.3	2.0	0.0817
Granite PG 76-22, AV 5%, Gyration 75	7.6	5.2	
Granite PG 76-22, AV 7%, Gyration 75	8.0	5.8	
Granite PG 67-22, AV 5%, Gyration 100	4.8	1.9	
Granite PG 67-22, AV 7%, Gyration 100	3.9	3.3	
Granite PG 76-22, AV 5%, Gyration 100	5.5	6.0	
Granite PG 76-22, AV 7%, Gyration 100	5.3	6.3	
Limestone PG 67-22, AV 5%, Gyration 50	3.5	1.7	
Limestone PG 67-22, AV 7%, Gyration 50	2.7	2.2	
Limestone PG 76-22, AV 5%, Gyration 50	4.8	2.9	
Limestone PG 76-22, AV 7%, Gyration 50	6.9	5.5	
Limestone PG 67-22, AV 5%, Gyration 75	1.2	1.4	
Limestone PG 67-22, AV 7%, Gyration 75	2.5	1.2	0.1963
Limestone PG 76-22, AV 5%, Gyration 75	4.0	4.3	
Limestone PG 76-22, AV 7%, Gyration 75	4.3	4.1	
Limestone PG 67-22, AV 5%, Gyration 100	2.0	2.0	
Limestone PG 67-22, AV 7%, Gyration 100	1.7	2.8	
Limestone PG 76-22, AV 5%, Gyration 100	5.0	5.0	
Limestone PG 76-22, AV 7%, Gyration 100	5.2	6.0	

6.3 SCB-FI Results

Figure 6-4 shows the bar chart of SCB-FI results for all mixtures. Again, the rectangular bars filled with diagonal stripes stand for the SP-9.5 mixtures, and the bars filled with solid color stand for the SP-12.5 mixtures. The mixtures of 50, 75, and 100 design gyrations are shown in figures with subtitles a, b, and c, respectively.

Higher FI values indicate higher cracking resistance of mixtures. The paired t-test analysis was conducted to determine if the SP-9.5 and SP-12.5 mixtures were significantly different in SCB-FI test data. The granite mixtures and limestone mixtures were analyzed separately. The other mixture factors, such as binder PG, design gyrations, and AV, were combined during the analysis since no opposite trend of change was observed for these factors. Table 6-4 shows the FI values and paired t-test p-values based on two-tailed distribution.

According to the FI results, the p-value is 0.0137 (smaller than 0.05) for granite mixtures, which means the Granite SP-9.5 mixtures are statistically different from (in this case, worse than) Granite SP-12.5 mixtures in terms of SCB-FI test performance. Overall, the FI values of Granite SP-9.5 mixtures are smaller than Granite SP-12.5 mixtures.

The p-value is 4.4369e-4 (smaller than 0.05) for limestone mixtures, which means the Limestone SP-9.5 mixtures are statistically different from (in this case, better than) Limestone SP-12.5 mixtures according to the SCB-FI test. The FI values of Limestone SP-9.5 mixtures are larger than the corresponding Limestone SP-12.5 mixtures.

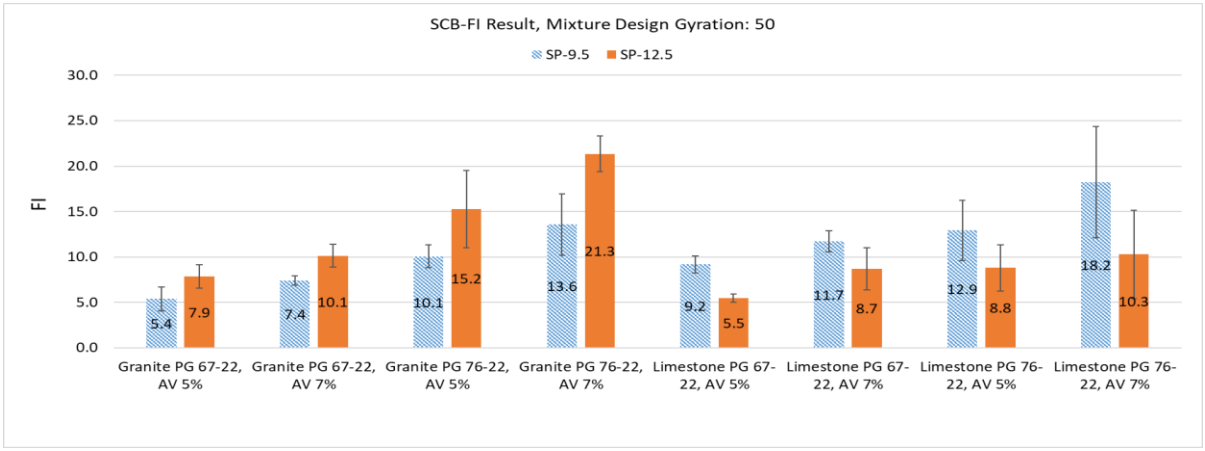

(a)

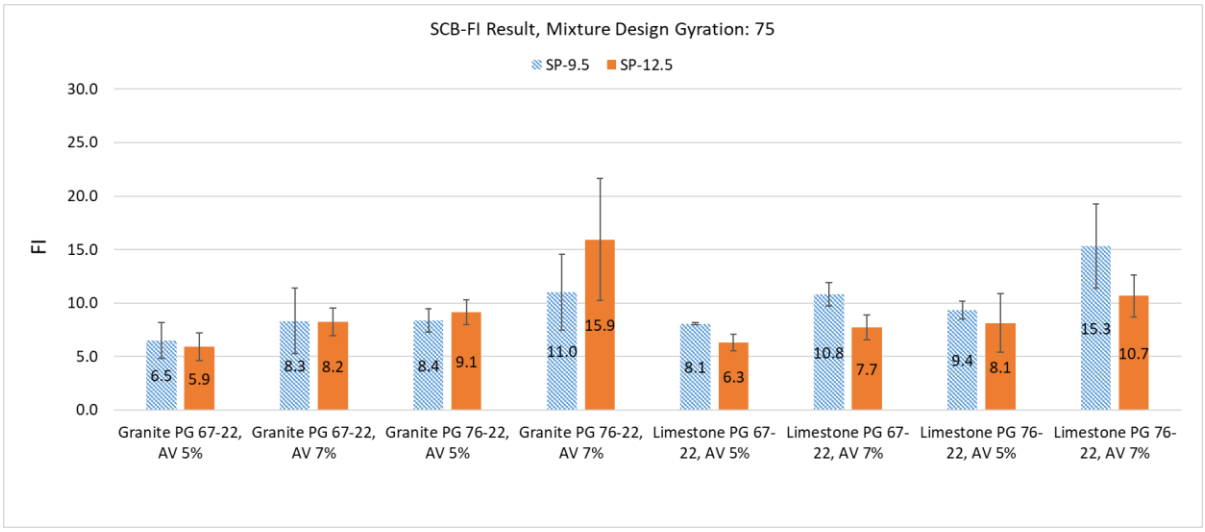

(b)

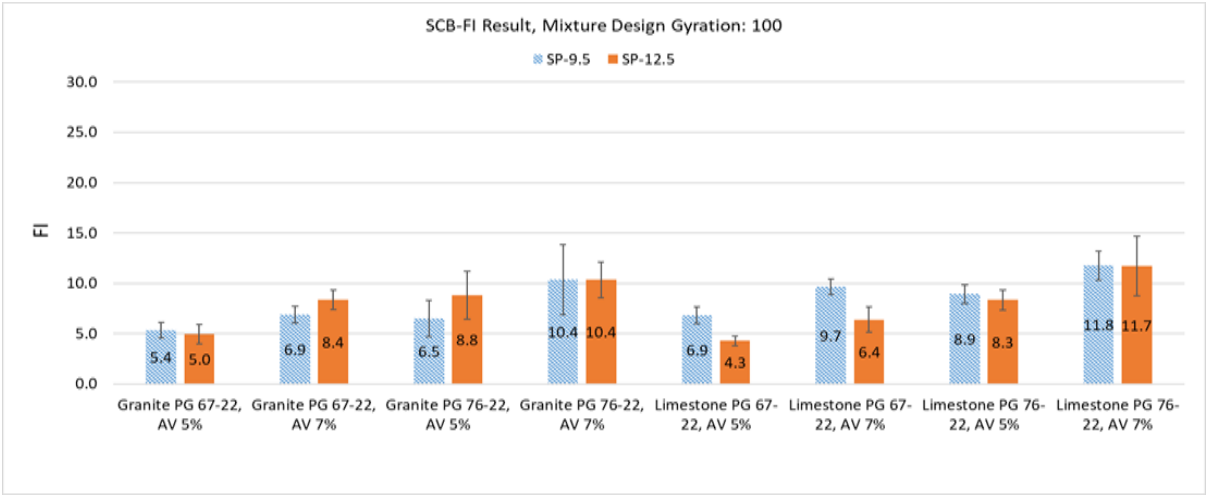

(c)

Figure 6-4. SCB-FI Results of Mixtures at (a) 50, (b) 75, and (c) 100 Design Gyrations

Table 6-4. Paired t-test Analysis of SCB-FI Results

Mixture Factor	SP-9.5	SP-12.5	p-value
Granite PG 67-22, AV 5%, Gyration 50	5.4	7.9	
Granite PG 67-22, AV 7%, Gyration 50	7.4	10.1	
Granite PG 76-22, AV 5%, Gyration 50	10.1	15.2	
Granite PG 76-22, AV 7%, Gyration 50	13.6	21.3	
Granite PG 67-22, AV 5%, Gyration 75	6.5	5.9	
Granite PG 67-22, AV 7%, Gyration 75	8.3	8.2	*0.0137*
Granite PG 76-22, AV 5%, Gyration 75	8.4	9.1	
Granite PG 76-22, AV 7%, Gyration 75	11.0	15.9	
Granite PG 67-22, AV 5%, Gyration 100	5.4	5.0	
Granite PG 67-22, AV 7%, Gyration 100	6.9	8.4	
Granite PG 76-22, AV 5%, Gyration 100	6.5	8.8	
Granite PG 76-22, AV 7%, Gyration 100	10.4	10.4	
Limestone PG 67-22, AV 5%, Gyration 50	9.2	5.5	
Limestone PG 67-22, AV 7%, Gyration 50	11.7	8.7	
Limestone PG 76-22, AV 5%, Gyration 50	12.9	8.8	
Limestone PG 76-22, AV 7%, Gyration 50	18.2	10.3	
Limestone PG 67-22, AV 5%, Gyration 75	8.1	6.3	
Limestone PG 67-22, AV 7%, Gyration 75	10.8	7.7	*4.4369e-4*
Limestone PG 76-22, AV 5%, Gyration 75	9.4	8.1	
Limestone PG 76-22, AV 7%, Gyration 75	15.3	10.7	
Limestone PG 67-22, AV 5%, Gyration 100	6.9	4.3	
Limestone PG 67-22, AV 7%, Gyration 100	9.7	6.4	
Limestone PG 76-22, AV 5%, Gyration 100	8.9	8.3	
Limestone PG 76-22, AV 7%, Gyration 100	11.8	11.7	

6.4 APA Results

Figure 6-5 shows the bar chart of APA results with the rut depths at 8,000 cycles for all mixtures. Similarly, the rectangular bars filled with diagonal stripes stand for the SP-9.5 mixtures, and the bars filled with solid color stand for the SP-12.5 mixtures. The mixtures of 50, 75, and 100 design gyrations are shown in figures with subtitles a, b, and c, respectively.

Higher rut depths indicate lower rutting resistance of mixtures. The paired t-test analysis was conducted to determine if the SP-9.5 and SP-12.5 mixtures were significantly different in APA test data. The granite mixtures and limestone mixtures were analyzed separately. The other mixture factors, such as binder PG, design gyrations, and AV, were combined during the analysis since no opposite trend of change was observed for these factors. Table 6-5 shows the APA rut depths and their paired t-test p-values based on two-tailed distribution.

According to the APA results, the p-value is 0.2123 (larger than 0.05) for granite mixtures, which means the Granite SP-9.5 mixtures are not statistically different from Granite SP-12.5 mixtures in terms of rutting performance.

The p-value is 8.5406e-3 (smaller than 0.05) for limestone mixtures, which means the Limestone SP-9.5 mixtures are statistically different from (in this case, worse than) Limestone SP-12.5 mixtures in terms of APA rutting performance. The APA rut depths of Limestone SP-9.5 mixtures are larger than the corresponding Limestone SP-12.5 mixtures.

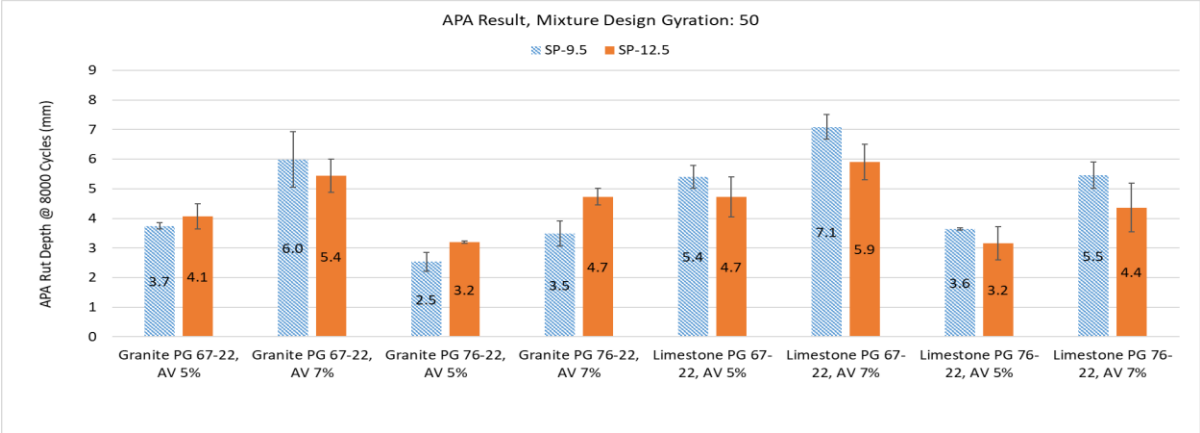

(a)

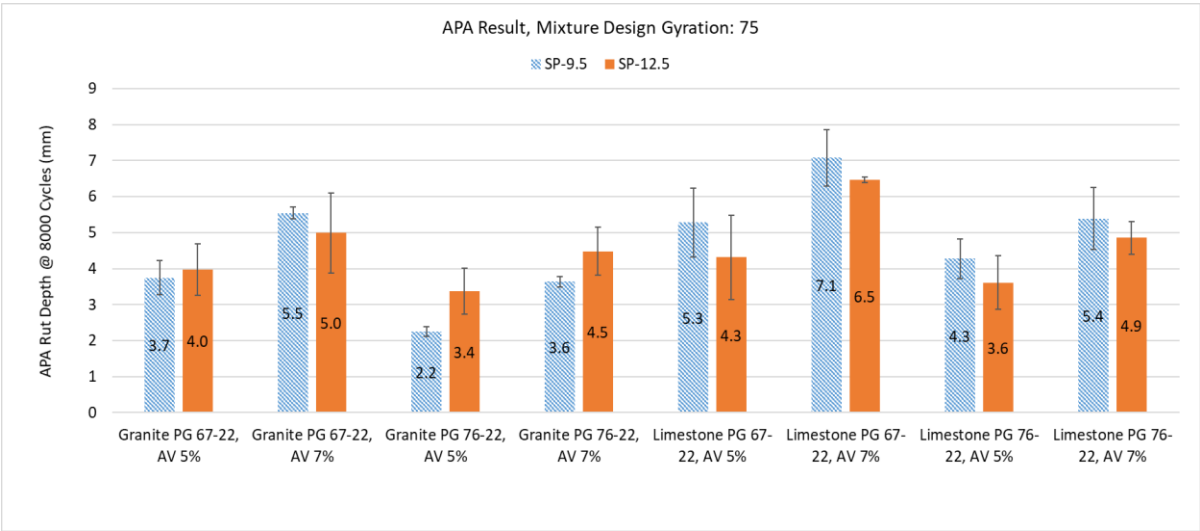

(b)

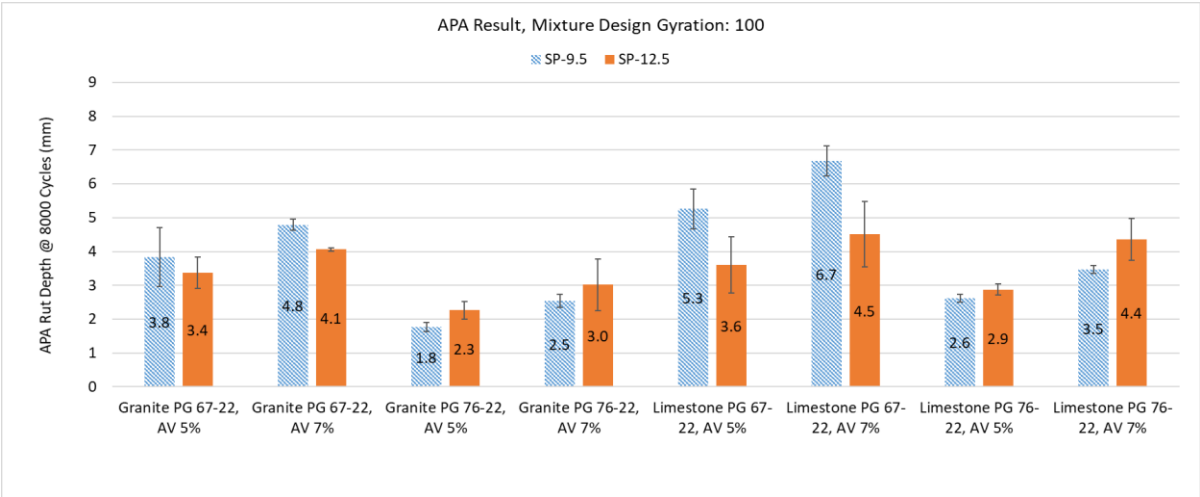

(c)

Figure 6-5. APA Results of Mixtures at (a) 50, (b) 75, and (c) 100 Design Gyrations

Table 6-5. Paired t-test Analysis of APA Results

Mixture Factor	SP-9.5	SP-12.5	p-value
Granite PG 67-22, AV 5%, Gyration 50	3.7	4.1	0.2123
Granite PG 67-22, AV 7%, Gyration 50	6.0	5.4	
Granite PG 76-22, AV 5%, Gyration 50	2.5	3.2	
Granite PG 76-22, AV 7%, Gyration 50	3.5	4.7	
Granite PG 67-22, AV 5%, Gyration 75	3.7	4.0	
Granite PG 67-22, AV 7%, Gyration 75	5.5	5.0	
Granite PG 76-22, AV 5%, Gyration 75	2.2	3.4	
Granite PG 76-22, AV 7%, Gyration 75	3.6	4.5	
Granite PG 67-22, AV 5%, Gyration 100	3.8	3.4	
Granite PG 67-22, AV 7%, Gyration 100	4.8	4.1	
Granite PG 76-22, AV 5%, Gyration 100	1.8	2.3	
Granite PG 76-22, AV 7%, Gyration 100	2.5	3.0	
Limestone PG 67-22, AV 5%, Gyration 50	5.4	4.7	*8.5406e-3*
Limestone PG 67-22, AV 7%, Gyration 50	7.1	5.9	
Limestone PG 76-22, AV 5%, Gyration 50	3.6	3.2	
Limestone PG 76-22, AV 7%, Gyration 50	5.5	4.4	
Limestone PG 67-22, AV 5%, Gyration 75	5.3	4.3	
Limestone PG 67-22, AV 7%, Gyration 75	7.1	6.5	
Limestone PG 76-22, AV 5%, Gyration 75	4.3	3.6	
Limestone PG 76-22, AV 7%, Gyration 75	5.4	4.9	
Limestone PG 67-22, AV 5%, Gyration 100	5.3	3.6	
Limestone PG 67-22, AV 7%, Gyration 100	6.7	4.5	
Limestone PG 76-22, AV 5%, Gyration 100	2.6	2.9	
Limestone PG 76-22, AV 7%, Gyration 100	3.5	4.4	

6.5 HWT Results

Figure 6-6 shows the bar chart of HWT results for all mixtures. Since the HWT tests stopped before 15,000 passes for many limestone mixtures, the rut depth at 10,000 passes was selected as the parameter. The rectangular bars filled with diagonal stripes stand for the SP-9.5 mixtures, and the bars filled with solid color stand for the SP-12.5 mixtures. The mixtures of 50, 75, and 100 design gyrations are shown in figures with subtitles a, b, and c, respectively.

Higher rut depths indicate lower rutting resistance of mixtures. The paired t-test analysis was conducted to determine if the SP-9.5 and SP-12.5 mixtures were significantly different in HWT test data. The granite mixtures and limestone mixtures were analyzed separately. The other mixture factors, such as binder PG, design gyrations, and AV, were combined during the analysis since no opposite trend of change was observed for these factors. Table 6-6 shows the HWT rut depths and paired t-test p-values based on two-tailed distribution.

According to the HWT results, the p-value is 0.1362 (larger than 0.05) for granite mixtures, which means the Granite SP-9.5 mixtures are not statistically different from Granite SP-12.5 mixtures in terms of rutting performance.

The p-value is 4.7819e-3 (smaller than 0.05) for limestone mixtures, which means the Limestone SP-9.5 mixtures are statistically different from (in this case, worse than) Limestone SP-12.5 mixtures in terms of HWT rutting performance. The HWT rut depths of Limestone SP-9.5 mixtures are larger than the corresponding Limestone SP-12.5 mixtures.

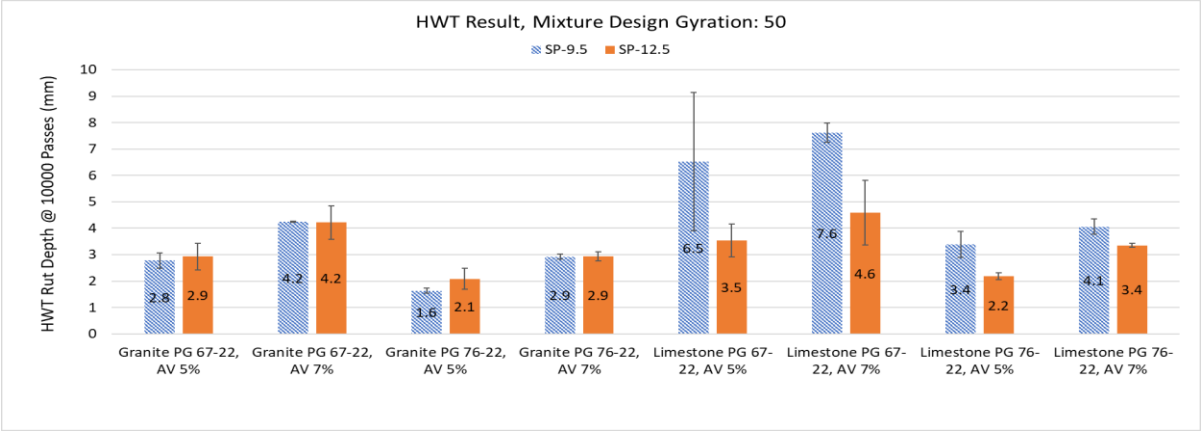

(a)

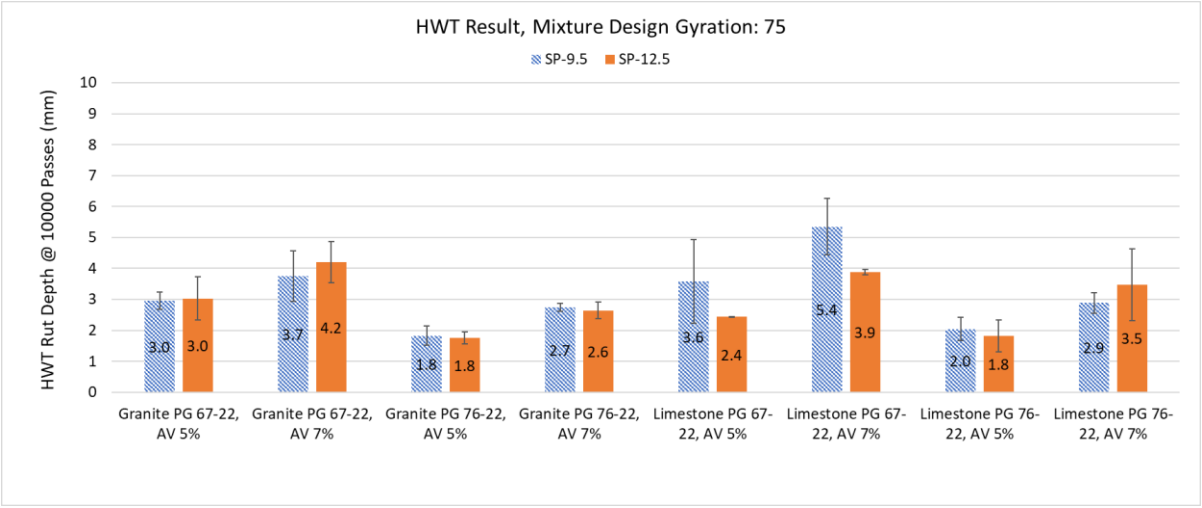

(b)

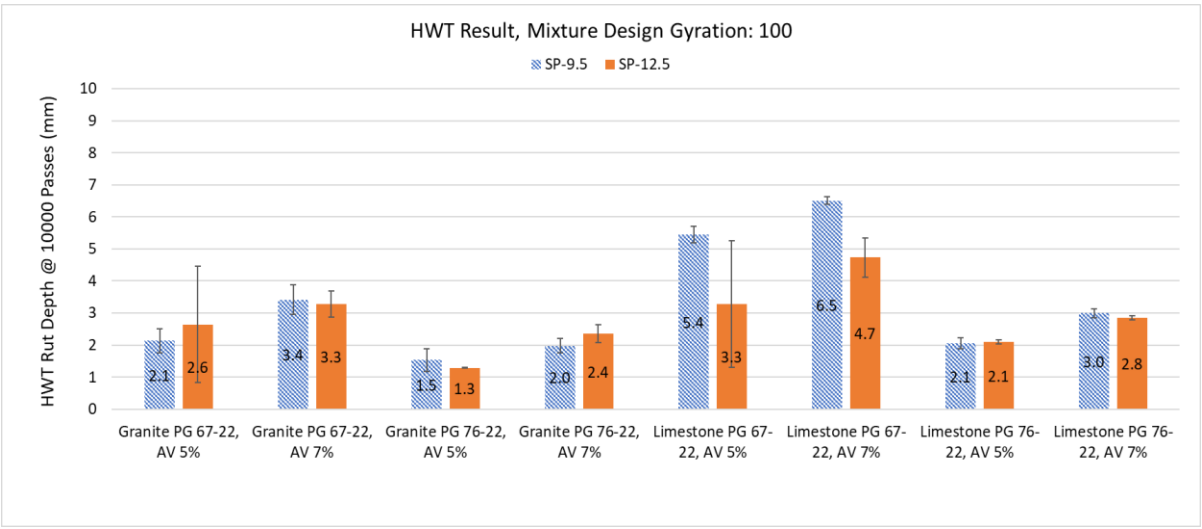

(c)

Figure 6-6. HWT Results of Mixtures at (a) 50, (b) 75, and (c) 100 Design Gyrations

Table 6-6. Paired t-test Analysis of HWT Results

Mixture Factor	SP-9.5	SP-12.5	p-value
Granite PG 67-22, AV 5%, Gyration 50	2.8	2.9	
Granite PG 67-22, AV 7%, Gyration 50	4.2	4.2	
Granite PG 76-22, AV 5%, Gyration 50	1.6	2.1	
Granite PG 76-22, AV 7%, Gyration 50	2.9	2.9	
Granite PG 67-22, AV 5%, Gyration 75	3.0	3.0	
Granite PG 67-22, AV 7%, Gyration 75	3.7	4.2	0.1362
Granite PG 76-22, AV 5%, Gyration 75	1.8	1.8	
Granite PG 76-22, AV 7%, Gyration 75	2.7	2.6	
Granite PG 67-22, AV 5%, Gyration 100	2.1	2.6	
Granite PG 67-22, AV 7%, Gyration 100	3.4	3.3	
Granite PG 76-22, AV 5%, Gyration 100	1.5	1.3	
Granite PG 76-22, AV 7%, Gyration 100	2.0	2.4	
Limestone PG 67-22, AV 5%, Gyration 50	6.5	3.5	
Limestone PG 67-22, AV 7%, Gyration 50	7.6	4.6	
Limestone PG 76-22, AV 5%, Gyration 50	3.4	2.2	
Limestone PG 76-22, AV 7%, Gyration 50	4.1	3.4	
Limestone PG 67-22, AV 5%, Gyration 75	3.6	2.4	
Limestone PG 67-22, AV 7%, Gyration 75	5.4	3.9	*4.7819e-3*
Limestone PG 76-22, AV 5%, Gyration 75	2.0	1.8	
Limestone PG 76-22, AV 7%, Gyration 75	2.9	3.5	
Limestone PG 67-22, AV 5%, Gyration 100	5.4	3.3	
Limestone PG 67-22, AV 7%, Gyration 100	6.5	4.7	
Limestone PG 76-22, AV 5%, Gyration 100	2.1	2.1	
Limestone PG 76-22, AV 7%, Gyration 100	3.0	2.8	

6.6 IDEAL-RT Results

Figure 6-7 shows the bar chart of IDEAL-RT results (RTindex) for all mixtures. The rectangular bars filled with diagonal stripes stand for the SP-9.5 mixtures, and the bars filled with solid color stand for the SP-12.5 mixtures. The mixtures of 50, 75, and 100 design gyrations are shown in figures with subtitles a, b, and c, respectively.

Higher RT_{index} values indicate higher rutting resistance of mixtures. The paired t-test analysis was conducted to determine if the SP-9.5 and SP-12.5 mixtures were significantly different in IDEAL-RT test data. The granite mixtures and limestone mixtures were analyzed separately. The other mixture factors, such as binder PG, design gyrations, and AV, were combined during the analysis since no opposite trend of change was observed for these factors. Table 6-7 shows the RT_{index} values and paired t-test p-values based on two-tailed distribution.

According to the IDEAL-RT results, the p-value is 0.019 (smaller than 0.05) for granite mixtures, which means the Granite SP-9.5 mixtures are statistically different from (in this case, better than) Granite SP-12.5 mixtures in terms of rutting performance. The RT_{index} values of Granite SP-9.5 mixtures are larger than the corresponding Granite SP-12.5 mixtures.

The p-value is 0.211 (larger than 0.05) for limestone mixtures, which means the Limestone SP-9.5 mixtures are not statistically different from Limestone SP-12.5 mixtures in terms of IDEAL-RT rutting performance.

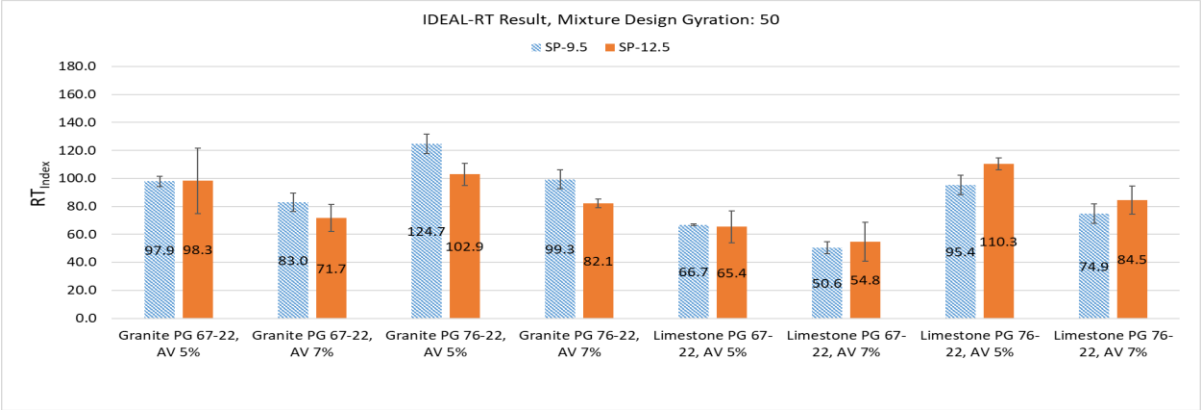

(a)

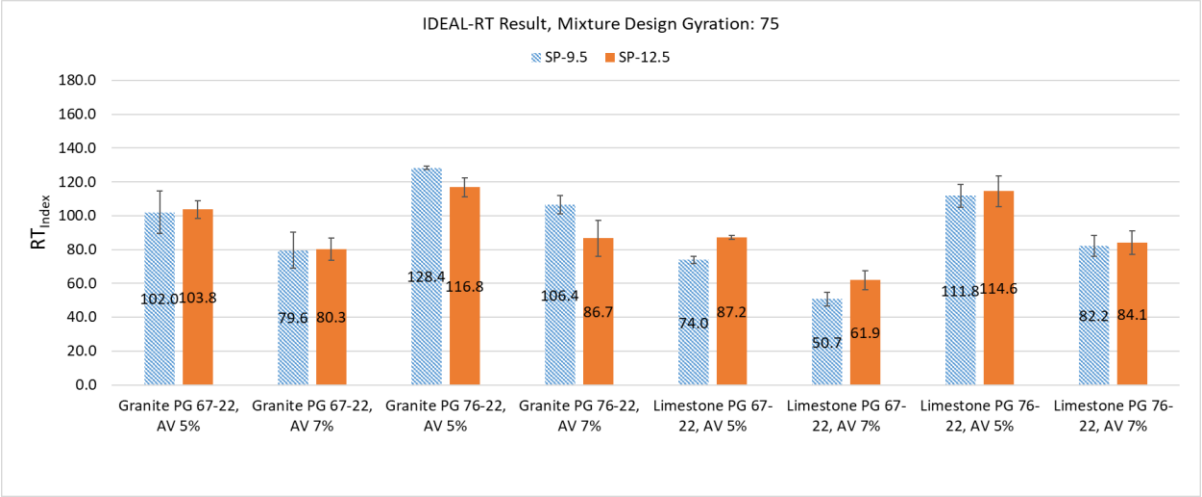

(b)

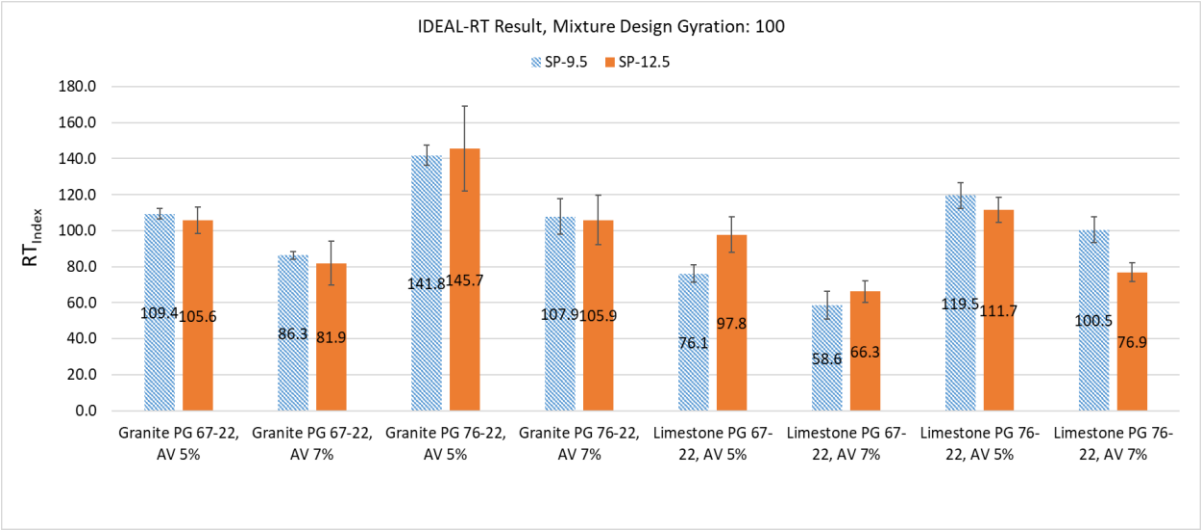

(c)

Figure 6-7. IDEAL-RT Results of Mixtures at (a) 50, (b) 75, and (c) 100 Design Gyrations

Table 6-7. Paired t-test Analysis of IDEAL-RT (RT_{index}) Results

Mixture Factor	SP-9.5	SP-12.5	p-value
Granite PG 67-22, AV 5%, Gyration 50	97.9	98.3	
Granite PG 67-22, AV 7%, Gyration 50	83.0	71.7	
Granite PG 76-22, AV 5%, Gyration 50	124.7	102.9	
Granite PG 76-22, AV 7%, Gyration 50	99.3	82.1	
Granite PG 67-22, AV 5%, Gyration 75	102.0	103.8	
Granite PG 67-22, AV 7%, Gyration 75	79.6	80.3	
Granite PG 76-22, AV 5%, Gyration 75	128.4	116.8	*0.0190*
Granite PG 76-22, AV 7%, Gyration 75	106.4	86.7	
Granite PG 67-22, AV 5%, Gyration 100	109.4	105.6	
Granite PG 67-22, AV 7%, Gyration 100	86.3	81.9	
Granite PG 76-22, AV 5%, Gyration 100	141.8	145.7	
Granite PG 76-22, AV 7%, Gyration 100	107.9	105.9	
Limestone PG 67-22, AV 5%, Gyration 50	66.7	65.4	
Limestone PG 67-22, AV 7%, Gyration 50	50.6	54.8	
Limestone PG 76-22, AV 5%, Gyration 50	95.4	110.3	
Limestone PG 76-22, AV 7%, Gyration 50	74.9	84.5	
Limestone PG 67-22, AV 5%, Gyration 75	74.0	87.2	
Limestone PG 67-22, AV 7%, Gyration 75	50.7	61.9	
Limestone PG 76-22, AV 5%, Gyration 75	111.8	114.6	0.2110
Limestone PG 76-22, AV 7%, Gyration 75	82.2	84.1	
Limestone PG 67-22, AV 5%, Gyration 100	76.1	97.8	
Limestone PG 67-22, AV 7%, Gyration 100	58.6	66.3	
Limestone PG 76-22, AV 5%, Gyration 100	119.5	111.7	
Limestone PG 76-22, AV 7%, Gyration 100	100.5	76.9	

6.7 CAL Results

Figure 6-8 shows the bar chart of CAL results (mass loss percent) for all mixtures. The rectangular bars filled with diagonal stripes stand for the SP-9.5 mixtures, and the bars filled with solid color stand for the SP-12.5 mixtures. The mixtures of 50, 75, and 100 design gyrations are shown in figures with subtitles a, b, and c, respectively.

Smaller mass loss values indicate better durability of mixtures. The paired t-test analysis was conducted to determine if the SP-9.5 and SP-12.5 mixtures were significantly different in CAL test data. The granite mixtures and limestone mixtures were analyzed separately. The other mixture factors, such as binder PG, design gyrations, and AV, were combined during the analysis since no opposite trend of change was observed for these factors. Table 6-8 shows the mass loss values and their paired t-test p-values based on two-tailed distribution.

According to the CAL results, the p-value is 0.019 (smaller than 0.05) for granite mixtures, which means the Granite SP-9.5 mixtures are statistically different from (in this case, better than) Granite SP-12.5 mixtures in terms of durability. The mass loss values of Granite SP-9.5 mixtures are smaller than the corresponding Granite SP-12.5 mixtures.

The p-value is 1.6105e-4 (smaller than 0.05) for limestone mixtures, which means the Limestone SP-9.5 mixtures are statistically different from (in this case, better than) Limestone SP-12.5 mixtures in terms of durability. The mass loss values of Limestone SP-9.5 mixtures are smaller than the corresponding Limestone SP-12.5 mixtures.

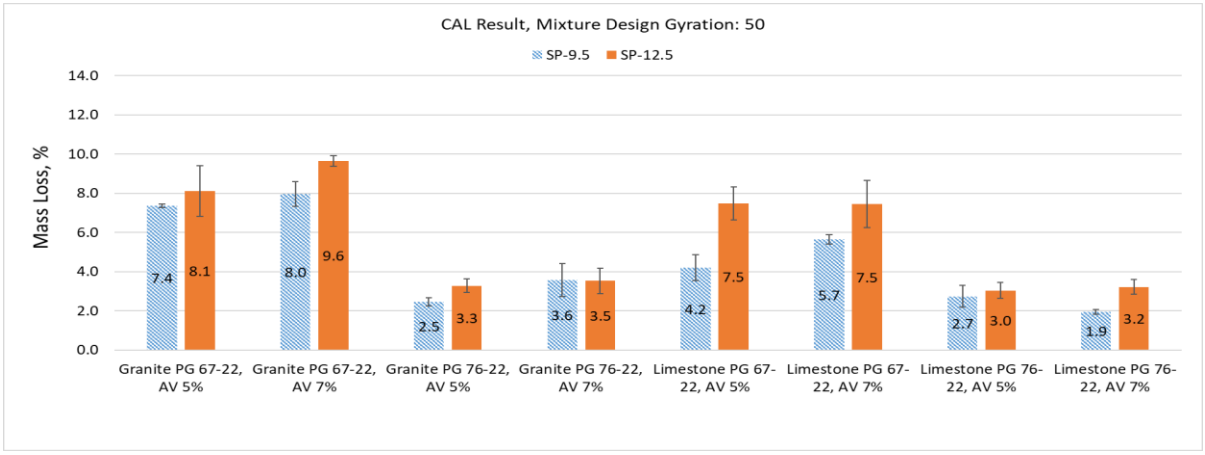
CAL Result, Mixture Design Gyration: 50
SP-9.5
SP-12.5
Mass Loss, %
14.0
12.0
10.0
8.0
6.0
4.0
2.0
0.0
7.4
8.1
8.0
9.6
2.5
3.3
3.6
3.5
4.2
7.5
5.7
7.5
2.7
3.0
1.9
3.2
Granite PG 67-22, AV 5%
Granite PG 67-22, AV 7%
Granite PG 76-22, AV 5%
Granite PG 76-22, AV 7%
Limestone PG 67-22, AV 5%
Limestone PG 67-22, AV 7%
Limestone PG 76-22, AV 5%
Limestone PG 76-22, AV 7%

(a)

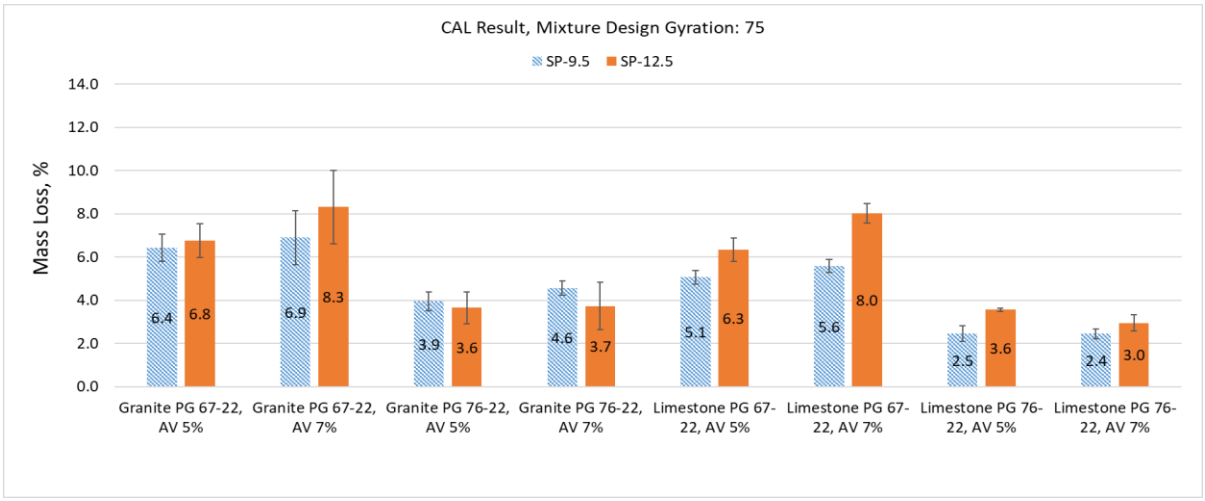
CAL Result, Mixture Design Gyration: 75
SP-9.5
SP-12.5
Mass Loss, %
14.0
12.0
10.0
8.0
6.0
4.0
2.0
0.0
6.4
6.8
6.9
8.3
3.9
3.6
4.6
3.7
5.1
6.3
5.6
8.0
2.5
3.6
2.4
3.0
Granite PG 67-22, AV 5%
Granite PG 67-22, AV 7%
Granite PG 76-22, AV 5%
Granite PG 76-22, AV 7%
Limestone PG 67-22, AV 5%
Limestone PG 67-22, AV 7%
Limestone PG 76-22, AV 5%
Limestone PG 76-22, AV 7%

(b)

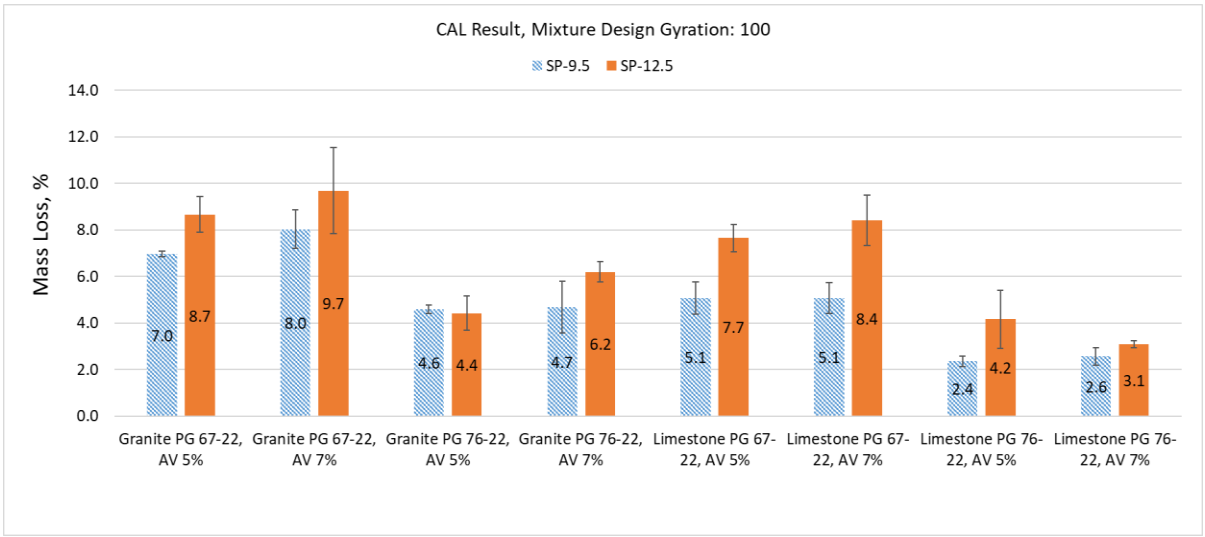
CAL Result, Mixture Design Gyration: 100
SP-9.5
SP-12.5
Mass Loss, %
14.0
12.0
10.0
8.0
6.0
4.0
2.0
0.0
7.0
8.7
8.0
9.7
4.6
4.4
4.7
6.2
5.1
7.7
5.1
8.4
2.4
4.2
2.6
3.1
Granite PG 67-22, AV 5%
Granite PG 67-22, AV 7%
Granite PG 76-22, AV 5%
Granite PG 76-22, AV 7%
Limestone PG 67-22, AV 5%
Limestone PG 67-22, AV 7%
Limestone PG 76-22, AV 5%
Limestone PG 76-22, AV 7%

(c)

Figure 6-8. CAL Results of Mixtures at (a) 50, (b) 75, and (c) 100 Design Gyrations

Table 6-8. Paired t-test Analysis of CAL (Mass Loss, %) Results

Mixture Factor	SP-9.5	SP-12.5	p-value
Granite PG 67-22, AV 5%, Gyration 50	7.4	8.1	
Granite PG 67-22, AV 7%, Gyration 50	8.0	9.6	
Granite PG 76-22, AV 5%, Gyration 50	2.5	3.3	
Granite PG 76-22, AV 7%, Gyration 50	3.6	3.5	
Granite PG 67-22, AV 5%, Gyration 75	6.4	6.8	
Granite PG 67-22, AV 7%, Gyration 75	6.9	8.3	
Granite PG 76-22, AV 5%, Gyration 75	3.9	3.6	*0.0190*
Granite PG 76-22, AV 7%, Gyration 75	4.6	3.7	
Granite PG 67-22, AV 5%, Gyration 100	7.0	8.7	
Granite PG 67-22, AV 7%, Gyration 100	8.0	9.7	
Granite PG 76-22, AV 5%, Gyration 100	4.6	4.4	
Granite PG 76-22, AV 7%, Gyration 100	4.7	6.2	
Limestone PG 67-22, AV 5%, Gyration 50	4.2	7.5	
Limestone PG 67-22, AV 7%, Gyration 50	5.7	7.5	
Limestone PG 76-22, AV 5%, Gyration 50	2.7	3.0	
Limestone PG 76-22, AV 7%, Gyration 50	1.9	3.2	
Limestone PG 67-22, AV 5%, Gyration 75	5.1	6.3	
Limestone PG 67-22, AV 7%, Gyration 75	5.6	8.0	
Limestone PG 76-22, AV 5%, Gyration 75	2.5	3.6	*1.6105e-4*
Limestone PG 76-22, AV 7%, Gyration 75	2.4	3.0	
Limestone PG 67-22, AV 5%, Gyration 100	5.1	7.7	
Limestone PG 67-22, AV 7%, Gyration 100	5.1	8.4	
Limestone PG 76-22, AV 5%, Gyration 100	2.4	4.2	
Limestone PG 76-22, AV 7%, Gyration 100	2.6	3.1	

6.8 Summary of the t-test Analysis Comparing SP-9.5 and SP-12.5 Mixtures

Table 6-9 summarizes the paired t-test results. Below are the findings from the table:

- For granite mixtures, the p-values are 0.08045 and 0.08017 for IDEAL-CT and UF-IDT DCSE results, respectively. Thus, Granite SP-9.5 mixtures have statistically equivalent cracking resistance to Granite SP-12.5 mixtures in IDEAL-CT and UF-IDT DCSE results.
- Granite SP-9.5 mixtures have statistically better cracking resistance than Granite SP-12.5 mixtures in UF-IDT ER results according to the p-value (7.3623e-4) and the ER values.
- Granite SP-9.5 mixtures have statistically worse cracking resistance than Granite SP-12.5 mixtures in SCB-FI results according to the p-value (0.0137) and the FI values. Note this conclusion is the opposite of the conclusion made from the UF-IDT ER results.
- Since three indexes (CT_{index}, DCSE, ER) show that Granite SP-9.5 mixtures have equivalent or better cracking performance than Granite SP-12.5 and only one index (FI) shows the contrary, the researchers lean to the conclusion that Granite SP-9.5 mixtures have equivalent cracking resistance to Granite SP-12.5 mixtures.
- Granite SP-9.5 mixtures have statistically equivalent or better rutting resistance than Granite SP-12.5 mixtures in APA, HWT, and IDEAL-RT test results. The p-values are 0.2123 (APA rut depth at 8,000 cycles), 0.1362 (HWT rut depth at 10,000 passes), and 0.019 (RT_{index}), respectively.
- Granite SP-9.5 mixtures have statistically better durability than Granite SP-12.5 mixtures in Cantabro test results according to the p-value (0.019) and the mass loss values.
- Limestone SP-9.5 mixtures have statistically equivalent or better cracking resistance than Limestone SP-12.5 mixtures in IDEAL-CT, UF-IDT (ER and DCSE), and SCB-FI test results. The p-values are 6.7835e-6 (CT_{index}), 0.2825 (UF-IDT ER), 0.1963 (UF-IDT DCSE), and 4.4369e-4 (FI).
- Limestone SP-9.5 mixtures have statistically worse rutting resistance than Limestone SP-12.5 mixtures in APA and HWT test results. The p-values are 8.5406e-3 (APA rut depth at 8,000 cycles) and 4.78e-3 (HWT rut depth at 10,000 passes).
- Limestone SP-9.5 mixtures have statistically equivalent rutting resistance to Limestone SP-12.5 mixtures in IDEAL-RT tests according to the p-value (0.211) and the RT_{index} values.
- Limestone SP-9.5 mixtures have statistically better durability than Limestone SP-12.5 mixtures in CAL results according to the p-value (1.61e-4) and the mass loss values.

In general, Granite SP-9.5 mixtures show equivalent or better performance (rutting, cracking, and durability) than Granite SP-12.5 mixtures. Limestone SP-9.5 mixtures show equivalent or better performance (cracking and durability) than Granite SP-12.5 mixtures. The major concern is Limestone SP-9.5 mixtures that show worse rutting performance than Limestone SP-12.5 mixtures in both APA and HWT results.

Table 6-9. Paired t-test Analysis Summary

Mixture Aggregate	Performance Test	Mixture Property Evaluated	Parameter	p-value	Is the difference statistically significant?
Granite	IDEAL-CT	Cracking	CT_{index}	0.08045	No
	UF-IDT	Cracking	ER	*7.3623E-04*	Yes (SP-9.5 is better)
			DCSE	0.0817	No
	SCB-FI	Cracking	FI	*0.0137*	Yes (SP-12.5 is better)
	APA	Rutting	Rut Depth @ 8,000 Cycles	0.2123	No
	HWT	Rutting	Rut Depth @ 10,000 Passes	0.1362	No
	IDEAL-RT	Rutting	RT_{index}	*0.0190*	Yes (SP-9.5 is better)
	CAL	Durability	Mass Loss %	*0.0190*	Yes (SP-9.5 is better)
Limestone	IDEAL-CT	Cracking	CT_{index}	*6.7835E-06*	Yes (SP-9.5 is better)
	UF-IDT	Cracking	ER	0.2825	No
			DCSE	0.1963	No
	SCB-FI	Cracking	FI	*4.4369E-04*	Yes (SP-9.5 is better)
	APA	Rutting	Rut Depth @ 8,000 Cycles	*8.5406E-03*	Yes (SP-12.5 is better)
	HWT	Rutting	Rut Depth @ 10,000 Passes	*4.78E-03*	Yes (SP-12.5 is better)
	IDEAL-RT	Rutting	RT_{index}	0.211	No
	CAL	Durability	Mass Loss %	*1.61E-04*	Yes (SP-9.5 is better)

6.9 Impact of Binder Type on the Rutting Performance Comparison Between Limestone SP-9.5 And SP-12.5 Mixtures

The researchers further investigated the rutting performance of limestone mixtures by separating the binder types (PG 67-22 and PG 76-22) and making corresponding t-test analyses. Table 6-10, Table 6-11, and Table 6-12 show the results. The difference between Limestone SP-9.5 and Limestone SP-12.5 mixtures is mainly due to the binder PG 67-22. The difference between the Limestone PG 67-22 SP-9.5 mixtures and the Limestone PG 67-22 SP-12.5 mixtures is statistically significant for all three performance tests (APA, HWTT, and IDEAL-RT). The p-values are 4.4546e-3, 1.2643e-3, and 0.033 in APA, HWTT, and IDEAL-RT results, respectively. On the other hand, no significant differences were found between Limestone PG

76-22 SP-9.5 mixtures and Limestone PG 76-22 SP-12.5 mixtures. The p-values are larger than 0.05 in APA, HWTT, and IDEAL-RT results, such as 0.4019, 0.3262, and 0.9512, respectively.

Table 6-10. Paired t-test Analysis of APA Results for Limestone Mixture by Separating the Binder Type

Mixture Factor	SP-9.5	SP-12.5	p-value
Limestone PG 67-22, AV 5%, Gyration 50	5.4	4.7	*4.4546e-3*
Limestone PG 67-22, AV 7%, Gyration 50	7.1	5.9	
Limestone PG 67-22, AV 5%, Gyration 75	5.3	4.3	
Limestone PG 67-22, AV 7%, Gyration 75	7.1	6.5	
Limestone PG 67-22, AV 5%, Gyration 100	5.3	3.6	
Limestone PG 67-22, AV 7%, Gyration 100	6.7	4.5	
Limestone PG 76-22, AV 5%, Gyration 50	3.6	3.2	0.4019
Limestone PG 76-22, AV 7%, Gyration 50	5.5	4.4	
Limestone PG 76-22, AV 5%, Gyration 75	4.3	3.6	
Limestone PG 76-22, AV 7%, Gyration 75	5.4	4.9	
Limestone PG 76-22, AV 5%, Gyration 100	2.6	2.9	
Limestone PG 76-22, AV 7%, Gyration 100	3.5	4.4	

Table 6-11. Paired t-test Analysis of HWT Results for Limestone Mixture by Separating the Binder Type

Mixture Factor	SP-9.5	SP-12.5	p-value
Limestone PG 67-22, AV 5%, Gyration 50	6.5	3.5	
Limestone PG 67-22, AV 7%, Gyration 50	7.6	4.6	
Limestone PG 67-22, AV 5%, Gyration 75	3.6	2.4	*1.2643e-3*
Limestone PG 67-22, AV 7%, Gyration 75	5.4	3.9	
Limestone PG 67-22, AV 5%, Gyration 100	5.4	3.3	
Limestone PG 67-22, AV 7%, Gyration 100	6.5	4.7	
Limestone PG 76-22, AV 5%, Gyration 50	3.4	2.2	
Limestone PG 76-22, AV 7%, Gyration 50	4.1	3.4	
Limestone PG 76-22, AV 5%, Gyration 75	2.0	1.8	0.3262
Limestone PG 76-22, AV 7%, Gyration 75	2.9	3.5	
Limestone PG 76-22, AV 5%, Gyration 100	2.1	2.1	
Limestone PG 76-22, AV 7%, Gyration 100	3.0	2.8	

Table 6-12. Paired t-test Analysis of IDEAL-RT Results for Limestone Mixture by Separating the Binder Type

Mixture Factor	SP-9.5	SP-12.5	p-value
Limestone PG 67-22, AV 5%, Gyration 50	66.7	65.4	
Limestone PG 67-22, AV 7%, Gyration 50	50.6	54.8	
Limestone PG 67-22, AV 5%, Gyration 75	74.0	87.2	*0.0330*
Limestone PG 67-22, AV 7%, Gyration 75	50.7	61.9	
Limestone PG 67-22, AV 5%, Gyration 100	76.1	97.8	
Limestone PG 67-22, AV 7%, Gyration 100	58.6	66.3	
Limestone PG 76-22, AV 5%, Gyration 50	95.4	110.3	
Limestone PG 76-22, AV 7%, Gyration 50	74.9	84.5	
Limestone PG 76-22, AV 5%, Gyration 75	111.8	114.6	0.9512
Limestone PG 76-22, AV 7%, Gyration 75	82.2	84.1	
Limestone PG 76-22, AV 5%, Gyration 100	119.5	111.7	
Limestone PG 76-22, AV 7%, Gyration 100	100.5	76.9	

Thus, only Limestone PG 67-22 SP-9.5 mixtures show worse rutting performance than SP-12.5 mixtures. Figure 6-9 and Figure 6-10 show the rut depth curve comparison examples between Limestone PG 67-22 mixtures and Limestone PG 76-22 mixtures, respectively.

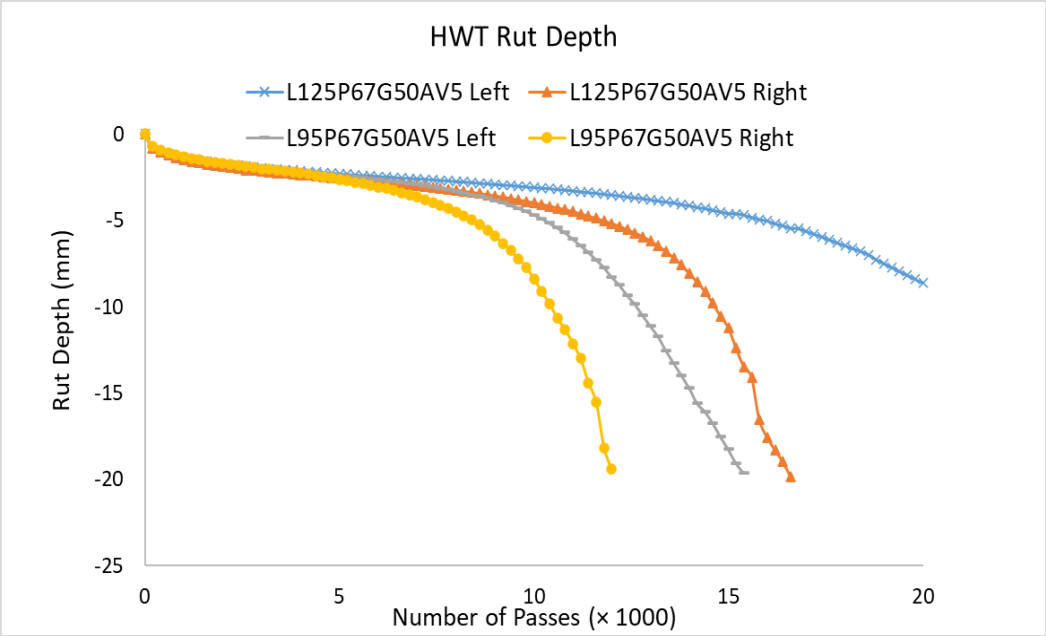

(a)

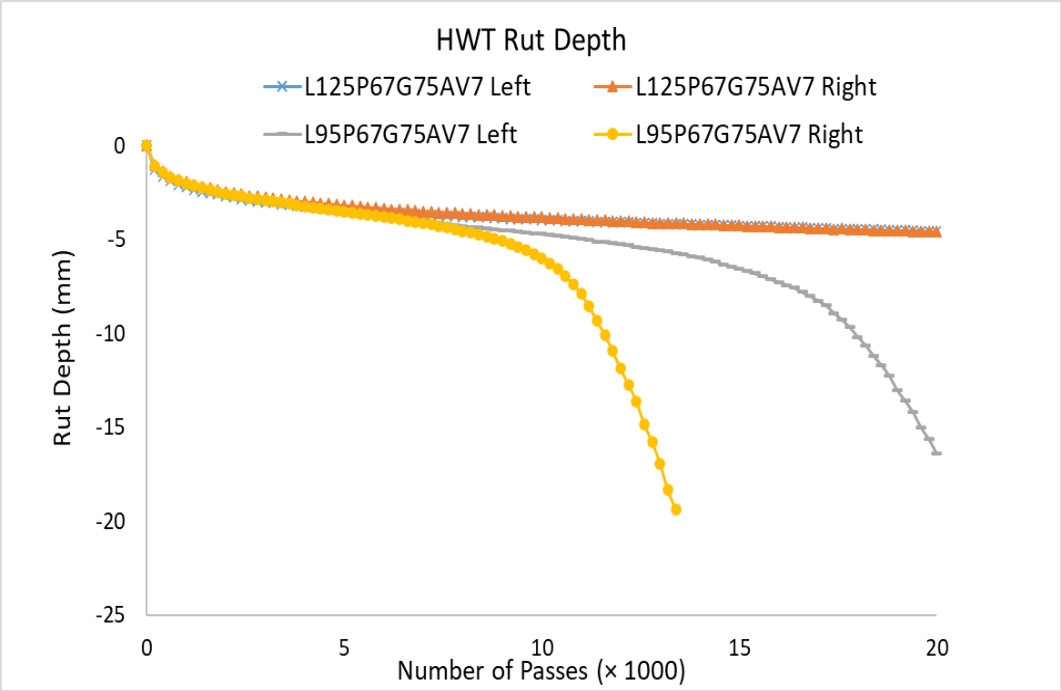

(b)

Figure 6-9. Rut Depth Curve Comparison between Limestone PG 67-22 SP-9.5 and SP-12.5 Mixtures (a) Gyration 50, AV5 and (b) Gyration 75, AV7

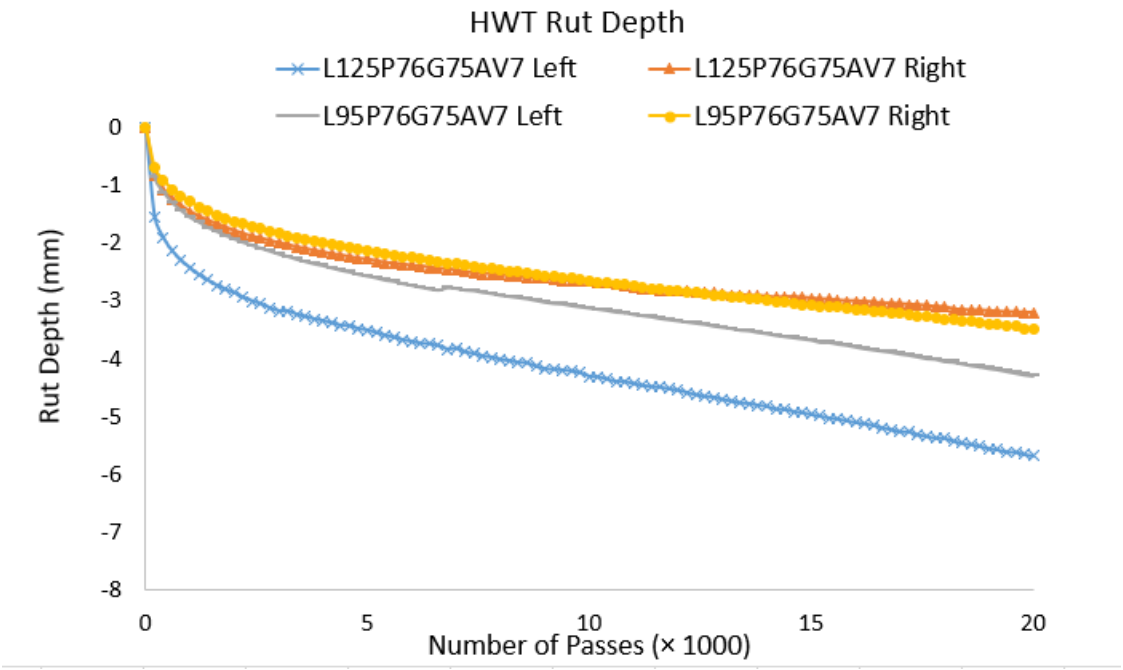

Figure 6-10. Rut Depth Curve Comparison between Limestone PG 76-22 SP-9.5 and SP-12.5 Mixtures

Table 6-13 lists the stripping inflection point, the rut depth at the stripping inflection point, and the number of passes at 12.5 mm rut depth for Limestone PG 67-22 SP-9.5 and SP-12.5 mixtures. In general, the SP-9.5 mixtures developed stripping at an earlier time and a deeper rut depth than SP-12.5 mixtures. The table shows that the numbers of passes at 12.5 mm rut depth for most of the Limestone PG 67-22 SP-9.5 mixtures are less than 14,000 cycles, while SP-12.5 mixtures are more than 20,000 passes.

Table 6-13. Rut Depths and Stripping Points of Limestone PG 67-22 SP-9.5 and SP-12.5 Mixtures

Mixture Factors	AV, %	Sample Location	Stripping Inflection Point		Rut Depth @ Stripping Inflection Point, mm		No. of Passes @ 12.5 mm Rut Depth	
			SP-12.5	SP-9.5	SP-12.5	SP-9.5	SP-12.5	SP-9.5
Limestone, PG 67-22, Gyration 50	5	Left	16087	11999	5.12	8.26	> 20000	13376
		Right	13245	9690	6.53	7.38	15236	11080
	7	Left	17341	11107	5.21	10.08	> 20000	11932
		Right	15993	10907	6.79	9.69	> 20000	11670
Limestone, PG 67-22, Gyration 75	5	Left	13591	11498	2.79	8.04	> 20000	12598
		Right	15379	16340	3.2	6.22	> 20000	18408
	7	Left	NA	11384	NA	9.26	> 20000	12140
		Right	NA	17030	NA	8.29	> 20000	18848
Limestone, PG 67-22, Gyration 100	5	Left	16264	10393	3.32	8.29	> 20000	11350
		Right	12021	12968	6.34	8.59	14458	13968
	7	Left	10499	11477	5.42	9.65	14691	12412
		Right	15875	11412	5.21	9.14	> 20000	12104

Figure 6-11 shows the specimen photos of Limestone PG 67-22 Gyration 75 mixtures before and after the HWT test. The SP-9.5 samples show much deeper rut depths than the SP-12.5 samples.

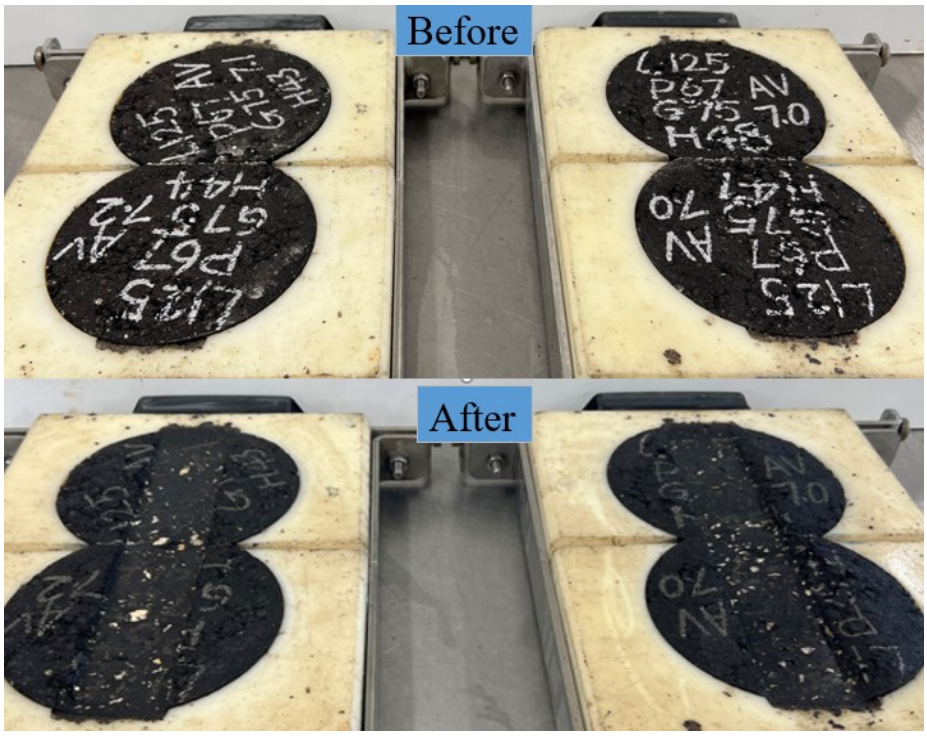

(a)

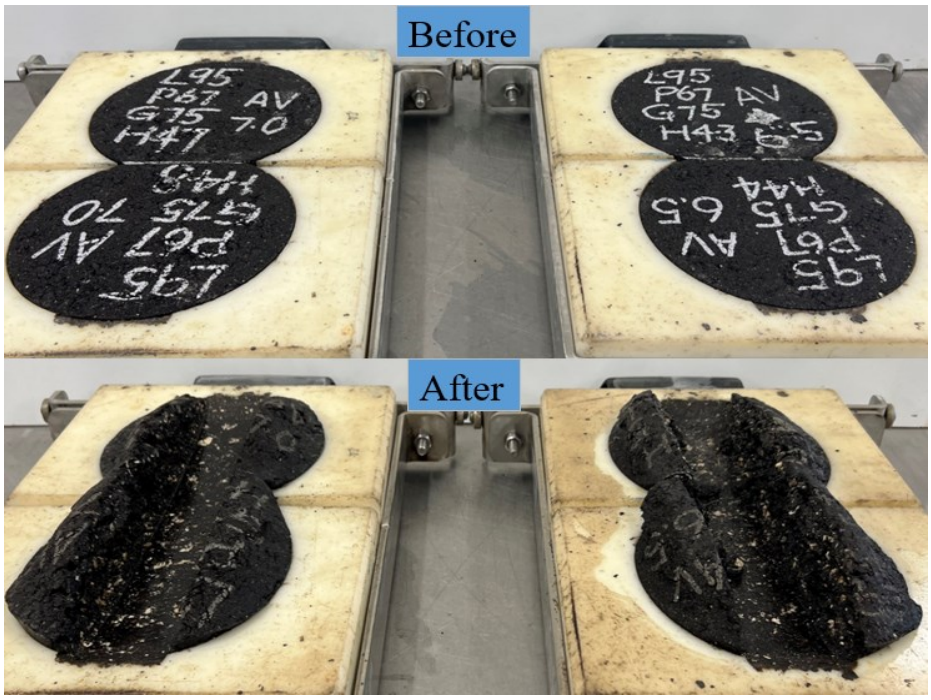

(b)

Figure 6-11. Specimen Photos Before and After HWT Test of Limestone PG 67-22, Gyration 75 Mixtures (a) SP-12.5 and (b) SP-9.5

6.10 Impact of AV and Gyration on the Rutting Performance Comparison Between Limestone SP-9.5 And SP-12.5 Mixtures

The researchers also investigated the rutting performance of limestone mixtures by separating the AV (5% and 7%) and the Gyration (50, 75, and 100) and making corresponding t-test analyses and comparisons. Table 6-14, Table 6-15, Table 6-16, Table 6-17, Table 6-18, and Table 6-19 show the results. Overall it confirms that only limestone SP-9.5 mixtures with PG 67-22 binder show worse rutting performance than the corresponding SP-12.5 mixtures. In addition, according to the p-values, the difference between SP-9.5 and SP-12.5 mixtures at AV 7% is relatively less significant than the difference between SP-9.5 and SP-12.5 mixtures at AV 5%. The difference between Limestone SP-9.5 and SP-12.5 mixtures at Gyration 100 is less significant than that between SP-9.5 and SP-12.5 mixtures at Gyration 50. Below are the tables and corresponding interpretations.

Table 6-14. Paired t-test Analysis of APA Results for Limestone Mixture by Separating the AV and Binder Type

Mixture Factor	SP-9.5	SP-12.5	p-value 1	p-value 2
Limestone PG 67-22, AV 5%, Gyration 50	5.4	4.7		
Limestone PG 67-22, AV 5%, Gyration 75	5.3	4.3		0.0617
Limestone PG 67-22, AV 5%, Gyration 100	5.3	3.6	*0.0402*	
Limestone PG 76-22, AV 5%, Gyration 50	3.6	3.2		
Limestone PG 76-22, AV 5%, Gyration 75	4.3	3.6		0.4017
Limestone PG 76-22, AV 5%, Gyration 100	2.6	2.9		
Limestone PG 67-22, AV 7%, Gyration 50	7.1	5.9		
Limestone PG 67-22, AV 7%, Gyration 75	7.1	6.5		0.1023
Limestone PG 67-22, AV 7%, Gyration 100	6.7	4.5	0.1175	
Limestone PG 76-22, AV 7%, Gyration 50	5.5	4.4		
Limestone PG 76-22, AV 7%, Gyration 75	5.4	4.9		0.7240
Limestone PG 76-22, AV 7%, Gyration 100	3.5	4.4		

Table 6-14 shows the APA results in two groups separated by different AVs. The p-value 1 is the paired t-test result when the data is divided into two groups based on AV (5% and 7%), and the p-value 2 is the paired test result when the data is further divided based on the binder type (PG 67-22 and PG 76-22). The p-value is 0.0402 (smaller than 0.05) for limestone mixtures with 5% AV, which means the Limestone SP-9.5 AV 5% mixtures are statistically different from (in this case, worse than) Limestone SP-12.5 mixtures. The p-value is 0.1175 (larger than 0.05) for limestone mixtures with 7% AV, which means the Limestone SP-9.5 AV 7% mixtures are not statistically different from Limestone SP-12.5 mixtures.

By further splitting the data based on the binder type, the p-values are 0.0617 (PG 67-22) vs. 0.4017 (PG 76-22) and 0.1023 (PG 67-22) vs. 0.7240 (PG 76-22), which shows the difference between PG 67-22 SP-9.5 and SP-12.5 mixtures is relatively more significant than the difference between PG 76-22 SP-9.5 and SP-12.5 mixtures.

Table 6-15. Paired t-test Analysis of HWT Results for Limestone Mixture by Separating the AV and Binder Type

Mixture Factor	SP-9.5	SP-12.5	p-value 1	p-value 2
Limestone PG 67-22, AV 5%, Gyration 50	6.5	3.5	*0.0412*	0.0596
Limestone PG 67-22, AV 5%, Gyration 75	3.6	2.4		
Limestone PG 67-22, AV 5%, Gyration 100	5.4	3.3		
Limestone PG 76-22, AV 5%, Gyration 50	3.4	2.2		0.3448
Limestone PG 76-22, AV 5%, Gyration 75	2.0	1.8		
Limestone PG 76-22, AV 5%, Gyration 100	2.1	2.1		
Limestone PG 67-22, AV 7%, Gyration 50	7.6	4.6	0.0921	*0.0483*
Limestone PG 67-22, AV 7%, Gyration 75	5.4	3.9		
Limestone PG 67-22, AV 7%, Gyration 100	6.5	4.7		
Limestone PG 76-22, AV 7%, Gyration 50	4.1	3.4		0.8370
Limestone PG 76-22, AV 7%, Gyration 75	2.9	3.5		
Limestone PG 76-22, AV 7%, Gyration 100	3.0	2.8		

Table 6-15 shows the HWT results in two groups separated by different AVs. The p-value 1 is the paired t-test result when the data is divided into two groups based on AV (5% and 7%), and the p-value 2 is the paired test result when the data is further divided based on the binder type (PG 67-22 and PG 76-22). The p-value is 0.0412 (smaller than 0.05) for limestone mixtures with 5% AV, which means the Limestone SP-9.5 AV 5% mixtures are statistically different from (in this case, worse than) Limestone SP-12.5 mixtures. The p-value is 0.0921 (larger than 0.05) for limestone mixtures with 7% AV, which means the Limestone SP-9.5 AV 7% mixtures are not statistically different from Limestone SP-12.5 mixtures.

By further splitting the data based on the binder type, the p-values are 0.0596 (PG 67-22) vs. 0.3448 (PG 76-22) and 0.0483 (PG 67-22) vs. 0.8370 (PG 76-22), which shows the difference between PG 67-22 SP-9.5 and SP-12.5 mixtures is relatively more significant than the difference between PG 76-22 SP-9.5 and SP-12.5 mixtures.

Table 6-16. Paired t-test Analysis of Ideal-RT Results for Limestone Mixture by Separating the AV and Binder Type

Mixture Factor	SP-9.5	SP-12.5	p-value 1	p-value 2
Limestone PG 67-22, AV 5%, Gyration 50	66.7	65.4		
Limestone PG 67-22, AV 5%, Gyration 75	74.0	87.2		0.2378
Limestone PG 67-22, AV 5%, Gyration 100	76.1	97.8	0.1735	
Limestone PG 76-22, AV 5%, Gyration 50	95.4	110.3		
Limestone PG 76-22, AV 5%, Gyration 75	111.8	114.6		0.6672
Limestone PG 76-22, AV 5%, Gyration 100	119.5	111.7		
Limestone PG 67-22, AV 7%, Gyration 50	50.6	54.8		
Limestone PG 67-22, AV 7%, Gyration 75	50.7	61.9		0.0624
Limestone PG 67-22, AV 7%, Gyration 100	58.6	66.3	0.7402	
Limestone PG 76-22, AV 7%, Gyration 50	74.9	84.5		
Limestone PG 76-22, AV 7%, Gyration 75	82.2	84.1		0.7279
Limestone PG 76-22, AV 7%, Gyration 100	100.5	76.9		

Table 6-16 shows the IDEAL-RT results in two groups separated by different AVs. The p-value 1 is the paired t-test result when the data is divided into two groups based on AV (5% and 7%), and the p-value 2 is the paired test result when the data is further divided based on the binder type (PG 67-22 and PG 76-22). The p-value is 0.1735 for limestone mixtures with 5% AV and 0.7402 for limestone mixtures with 7% AV, which means the Limestone SP-9.5 (AV 5% and 7%) are not statistically different from Limestone SP-12.5 mixtures. The difference between 7% AV SP-9.5 and SP-12.5 mixtures is relatively less significant than the difference between 5% AV SP-9.5 and SP-12.5 mixtures since 0.7402 is larger than 0.1735. This trend is consistent with the observations in the APA and HWT test results.

By further splitting the data based on the binder type, the p-values are 0.2378 (PG 67-22) vs. 0.0.6672 (PG 76-22) and 0.0624 (PG 67-22) vs. 0.7279 (PG 76-22), which shows the difference between PG 67-22 SP-9.5 and SP-12.5 mixtures is relatively more significant than the difference between PG 76-22 SP-9.5 and SP-12.5 mixtures.

According to Table 6-14, Table 6-15, and Table 6-16, the difference between SP-9.5 and SP-12.5 mixtures at AV 7% is relatively less significant than that between SP-9.5 and SP-12.5 mixtures at AV 5% when data for both binder grades are combined. When separating the data by binder grade, there is no apparent conclusion that the rutting performance of SP-9.5 mixtures with PG 67-22 binder performed differently by air void level (5% vs. 7%). The analysis of the further splitting data based on binder type confirms that only limestone SP-9.5 mixtures with PG 67-22 binder show worse rutting performance than the corresponding SP-12.5 mixtures.

Table 6-17. Paired t-test Analysis of APA Results for Limestone Mixture by Separating the Gyration Level

Mixture Factor	SP-9.5	SP-12.5	p-value
Limestone PG 67-22, AV 5%, Gyration 50	5.4	4.7	*0.0139*
Limestone PG 67-22, AV 7%, Gyration 50	7.1	5.9	
Limestone PG 76-22, AV 5%, Gyration 50	3.6	3.2	
Limestone PG 76-22, AV 7%, Gyration 50	5.5	4.4	
Limestone PG 67-22, AV 5%, Gyration 75	5.3	4.3	*0.0054*
Limestone PG 67-22, AV 7%, Gyration 75	7.1	6.5	
Limestone PG 76-22, AV 5%, Gyration 75	4.3	3.6	
Limestone PG 76-22, AV 7%, Gyration 75	5.4	4.9	
Limestone PG 67-22, AV 5%, Gyration 100	5.3	3.6	0.4341
Limestone PG 67-22, AV 7%, Gyration 100	6.7	4.5	
Limestone PG 76-22, AV 5%, Gyration 100	2.6	2.9	
Limestone PG 76-22, AV 7%, Gyration 100	3.5	4.4	

Table 6-17 shows the APA results in three groups separated by different gyrations. The p-values are 0.0139, 0.0054, and 0.4341 for limestone mixtures with Gyrations 50, 75, and 100, respectively. The Limestone SP-9.5 (Gyration 50 or 75) mixtures are statistically different from the corresponding SP-12.5 mixtures. The difference between the SP-9.5 Gyration 100 and the corresponding SP-12.5 mixtures is not statistically significant.

Table 6-18. Paired t-test Analysis of HWT Results for Limestone Mixture by Separating the Gyration

Mixture Factor	SP-9.5	SP-12.5	p-value
Limestone PG 67-22, AV 5%, Gyration 50	6.5	3.5	*0.0458*
Limestone PG 67-22, AV 7%, Gyration 50	7.6	4.6	
Limestone PG 76-22, AV 5%, Gyration 50	3.4	2.2	
Limestone PG 76-22, AV 7%, Gyration 50	4.1	3.4	
Limestone PG 67-22, AV 5%, Gyration 75	3.6	2.4	0.3177
Limestone PG 67-22, AV 7%, Gyration 75	5.4	3.9	
Limestone PG 76-22, AV 5%, Gyration 75	2.0	1.8	
Limestone PG 76-22, AV 7%, Gyration 75	2.9	3.5	
Limestone PG 67-22, AV 5%, Gyration 100	5.4	3.3	0.1673
Limestone PG 67-22, AV 7%, Gyration 100	6.5	4.7	
Limestone PG 76-22, AV 5%, Gyration 100	2.1	2.1	
Limestone PG 76-22, AV 7%, Gyration 100	3.0	2.8	

Table 6-18 shows the HWT results in three groups separated by different gyrations. The p-values are 0.0458, 0.3177, and 0.1673 for limestone mixtures with Gyrations 50, 75, and 100, respectively. The Limestone SP-9.5 Gyration 50 mixtures are statistically different from the corresponding SP-12.5 mixtures. The difference between the SP-9.5 (Gyration 75 or Gyration 100) and the corresponding SP-12.5 mixtures is not statistically significant.

Table 6-19. Paired t-test Analysis of IDEAL-RT Results for Limestone Mixture by Separating the Gyration

Mixture Factor	SP-9.5	SP-12.5	p-value
Limestone PG 67-22, AV 5%, Gyration 50	66.7	65.4	0.1451
Limestone PG 67-22, AV 7%, Gyration 50	50.6	54.8	
Limestone PG 76-22, AV 5%, Gyration 50	95.4	110.3	
Limestone PG 76-22, AV 7%, Gyration 50	74.9	84.5	
Limestone PG 67-22, AV 5%, Gyration 75	74.0	87.2	0.0861
Limestone PG 67-22, AV 7%, Gyration 75	50.7	61.9	
Limestone PG 76-22, AV 5%, Gyration 75	111.8	114.6	
Limestone PG 76-22, AV 7%, Gyration 75	82.2	84.1	
Limestone PG 67-22, AV 5%, Gyration 100	76.1	97.8	0.9619
Limestone PG 67-22, AV 7%, Gyration 100	58.6	66.3	
Limestone PG 76-22, AV 5%, Gyration 100	119.5	111.7	
Limestone PG 76-22, AV 7%, Gyration 100	100.5	76.9	

Table 6-19 shows the IDEAL-RT results in three groups separated by different gyrations. The p-values are 0.1451, 0.0861, and 0.9619 for limestone mixtures with Gyrations 50, 75, and 100, respectively. The difference between the SP-9.5 and the corresponding SP-12.5 mixture at Gyration 50, 75, or 100 is not statistically significant in terms of IDEAL-RT results.

According to Table 6-17, Table 6-18, and Table 6-19, the difference between Limestone SP-9.5 and SP-12.5 mixtures at Gyration 100 is less significant than that between SP-9.5 and SP-12.5 mixtures at Gyration 50.

6.11 Summary

In general, only Limestone PG 67-22 SP-9.5 mixtures show worse rutting performance than the corresponding SP-12.5 mixtures. Other SP-9.5 mixtures, such as Granite (PG 67-22 or PG 76-22) and Limestone PG 76-22, show equivalent or better performance (rutting, cracking, and durability) than the corresponding SP-12.5 mixtures.

The researchers also performed the t-test analyses for the granite mixtures' performances (rutting, cracking, and durability) by separating the binder types (PG 67-22 and PG 76-22), the AVs (5% and 7%), and the Gyrations (50, 75, and 100). The previous conclusion, “Granite SP-9.5 mixtures show equivalent or better performance than Granite SP-12.5 mixtures,” was confirmed by these analyses.

7. CONCLUSIONS AND RECOMMENDATIONS

This project's main objective is to compare the performance of SP-9.5 with SP-12.5 asphalt mixtures and then determine if SP-9.5 mixtures were at least equivalent to SP-12.5 mixtures in terms of cracking and rutting resistance, including durability. The researchers executed a full factorial experiment to achieve this goal. The experimental design included the following factors:

- Two gradation types: SP-9.5 and SP-12.5.
- Two aggregate types: Georgia granite and Florida limestone.
- Two binder grades: PG 67-22 and PG 76-22.
- Three design numbers of gyrations targeting 4 percent AV: 50, 75, and 100.
- Two compaction levels: 93 percent and 95 percent G_{mm}.
- Seven performance tests: IDEAL-CT, UF-IDT, SCB-FI, APA, HWT, IDEAL-RT, and CAL.

The researchers fabricated and tested 24 mixture designs (i.e., two gradation types × two aggregate types × two binder grades × three design gyrations). The mixture design details, such as the trial binder contents and their corresponding G_{mm} and G_{mb} values for each mixture, can be found in Appendix A: Mixture Design Data Sheets.

Two compaction levels were specified for each of the 24 mixtures and seven performance tests—93 percent G_{mm} (7 percent AV) and 95 percent G_{mm} (5 percent AV) when molding performance samples. The researchers prepared the samples and conducted each performance test according to their specifications and data interpretation methods. The test results were summarized in tables and bar charts. Statistical analysis was performed to compare the performance between SP-9.5 and SP-12.5 mixtures.

Below are the conclusions and recommendations according to the test results and the paired t-test analyses.

7.1 Conclusions

- Granite SP-9.5 mixtures have statistically equivalent cracking resistance to the corresponding Granite SP-12.5 mixtures, according to IDEAL-CT and UF-IDT DCSE results.
- Granite SP-9.5 mixtures have statistically better cracking resistance than the corresponding Granite SP-12.5 mixtures, according to UF-IDT ER results.
- Granite SP-9.5 mixtures have statistically worse cracking resistance than the corresponding Granite SP-12.5 mixtures, according to SCB-FI results.
- Since three indexes (CT_{index}, DCSE, ER) show that Granite SP-9.5 mixtures have equivalent or better cracking performance than Granite SP-12.5 and only one index (FI) shows the contrary, the researchers lean to the conclusion that Granite SP-9.5 mixtures have equivalent cracking resistance to Granite SP-12.5 mixtures.

- Granite SP-9.5 mixtures have statistically equivalent or better rutting resistance than the corresponding Granite SP-12.5 mixtures, according to APA, HWT, and IDEAL-RT test results.
- Granite SP-9.5 mixtures have statistically better durability than the corresponding Granite SP-12.5 mixtures, according to CAL results.
- Limestone SP-9.5 mixtures have statistically equivalent or better cracking resistance than the corresponding Limestone SP-12.5 mixtures, according to IDEAL-CT, UF-IDT (ER and DCSE), and SCB-FI test results.
- Limestone SP-9.5 PG 67-22 mixtures have statistically worse rutting resistance than the corresponding Limestone SP-12.5 PG 67-22 mixtures, according to APA, HWT, and IDEAL-RT results.
- Limestone SP-9.5 PG 76-22 mixtures have statistically equivalent rutting resistance to the corresponding Limestone SP-12.5 PG 67-22 mixtures, according to APA, HWT, and IDEAL-RT results.
- Limestone SP-9.5 mixtures have statistically better durability than the corresponding Limestone SP-12.5 mixtures, according to CAL results.

In general, only Limestone SP-9.5 PG 67-22 mixtures show worse rutting performance than the corresponding SP-12.5 mixtures. Other SP-9.5 mixtures, such as Granite (PG 67-22 or PG 76-22) and Limestone (PG 76-22), show equivalent or better performance (rutting, cracking, and durability) than the corresponding SP-12.5 mixtures.

7.2 Recommendations

The most updated FDOT specification, *Standard Specification for Road and Bridge Construction* (FDOT 2022a), specifies the traffic levels and the corresponding gyratory compaction requirements for mixture designs, as seen in Table 7-1.

Table 7-1. Gyratory Compaction Requirements

Traffic Level	N_{design} Number of Gyrations
B	65
C	75
E	100

Note that previous versions of this specification included traffic levels A and D. Traffic Level A is now combined with B, and Traffic Level D is now combined with E.

The *Flexible Pavement Design Manual* (FDOT 2022b) specifies “The appropriate Traffic Level is to be shown for structural friction courses FC-9.5 and FC-12.5. For Traffic Levels B, and C, PG 76-22 should be called for in the friction course. For Traffic Level E, PG 76-22 or High Polymer should be called for in the friction course. Note that, as with SP-9.5, FC-9.5 should not be used for Traffic Level E.”

According to the findings of this research, only the rutting performance of Limestone SP-9.5 PG 67-22 mixtures is a concern. If the binder is PG 76-22, the SP-9.5 mixtures have equivalent or better performance (rutting, cracking, and durability) than the corresponding SP-12.5 mixtures. Since the manual required PG 76-22 or high polymer for Traffic Level E, the statement, “Note that, as with SP-9.5, FC-9.5 should not be used for Traffic Level E” is not necessary and is proposed to be removed. Similar limitations, for example, “Type SP-9.5—Do not use for Traffic Level E applications” in the specification (FDOT 2022a) section 334-1.4.1, are also proposed to be removed.

REFERENCES

AASHTO (2020a). *AASHTO T 27 Sieve Analysis of Fine and Coarse Aggregate*, Washington, DC.

AASHTO (2020b). *AASHTO T 304 Uncompacted Void Content of Fine Aggregate*, Washington, DC.

AASHTO (2020c). *AASHTO T 11 Standard Method of Test for Materials Finer Than 75-µm (No. 200) Sieve in Mineral Aggregates by Washing*, Washington, DC.

AASHTO (2019a). *AASHTO TP 133-19 Standard Method of Test for Determining the Damage Characteristic Curve and Failure Criterion Using Small Specimens in the Asphalt Mixture Performance Tester (AMPT) Cyclic Fatigue Test*, Washington, DC.

AASHTO (2019b). *AASHTO M 332 Performance-Graded Asphalt Binder Using Multiple Stress Creep Recovery (MSCR) Test*, Washington, DC.

AASHTO (2018a). *AASHTO TP 107-18 Standard Method of Test for Determining the Damage Characteristic Curve and Failure Criterion Using the Asphalt Mixture Performance Tester (AMPT) Cyclic Fatigue Test*, Washington, DC.

AASHTO (2018b). *AASHTO TP 124-18 Standard Method of Test for Determining the Fracture Potential of Asphalt Mixtures Using the Flexibility Index Test (FIT)*, Washington, DC.

AASHTO (2018c). *AASHTO TP 108-14 Standard Method of Test for Determining the Abrasion Loss of Asphalt Mixture Specimens*, Washington, DC.

AASHTO (2017a). *AASHTO M 323 Standard Specification for Superpave Volumetric Mix Design*, Washington, DC.

AASHTO (2017b). *AASHTO R 35 Superpave Volumetric Design for Asphalt Mixtures*, Washington, DC.

AASHTO (2017c). *AASHTO T 324 Standard Method of Test for Hamburg Wheel-Track Testing of Compacted Asphalt Mixtures*, Washington, DC.

AASHTO (2017d). *AASHTO T 321 Standard Method of Test for Determining the Fatigue Life of Compacted Asphalt Mixtures Subjected to Repeated Flexural Bending*, Washington, DC.

AASHTO (2017e). *AASHTO T 378 Standard Method of Test for Determining the Dynamic Modulus and Flow Number for Asphalt Mixtures Using the Asphalt Mixture Performance Tester (AMPT)*, Washington, DC.

AASHTO (2017f). *AASHTO T 84 Specific Gravity and Absorption of Fine Aggregate*, Washington, DC.

AASHTO (2016a). *AASHTO T 320 Standard Method of Test for Determining the Permanent Shear Strain and Stiffness of Asphalt Mixtures Using the Superpave Shear Tester (SST)*, Washington, DC.

AASHTO (2016b). *AASHTO R 76 Standard Practice for Reducing Samples of Aggregate to Testing Size*, Washington, DC.

AASHTO (2016c). *AASHTO T 313 Standard Method of Test for Determining the Flexural Creep Stiffness of Asphalt Binder Using the Bending Beam Rheometer (BBR)*, Washington, DC.

AASHTO (2016d). *AASHTO T 315 Standard Method of Test for Determining the Rheological Properties of Asphalt Binder Using a Dynamic Shear Rheometer (DSR)*, Washington, DC

AASHTO (2015a). *AASHTO TP 116-15 Standard Method of Test for Rutting Resistance of Asphalt Mixtures Using Incremental Repeated Load Permanent Deformation (iRLPD)*, Washington, DC.

AASHTO (2015b). *AASHTO TP 105-13 Standard Method of Test for Determining the Fracture Energy of Asphalt Mixtures Using the Semicircular Bend Geometry (SCB)*, Washington, DC.

AASHTO (2014). *AASHTO T 305 Standard Method of Test for Determination of Draindown Characteristics in Uncompacted Asphalt Mixtures*, Washington, DC.

AASHTO (2010a). *AASHTO T 340 Standard Method of Test for Determining Rutting Susceptibility of Hot Mix Asphalt (HMA) Using the Asphalt Pavement Analyzer (APA)*, Washington, DC.

AASHTO (2010b). *AASHTO T 246 Standard Method of Test for Resistance to Deformation and Cohesion of Hot Mix Asphalt (HMA) by Means of Hveem Apparatus*, Washington, DC.

Abdulshafi, A.A. and K. Majidzadra (1985). J-Integral and Cyclic Plasticity Approach to Fatigue of Asphaltic Mixtures, *TRR,* Transportation Research Board, No. 1034, pp. 112–123.

Ahlrich, R.C. (1996). *Influence of Aggregate Gradation and Particle Shape/Texture on Permanent Deformation of Hot Mix Asphalt Pavements*, Army Engineer Waterways Experiment Station, Vicksburg MS Geotechnical Lab.

Ahmad, J., M.Y. Abdul Rahman, M.R. Hainin, M. Hossain (2012). Comparative evaluation of hot-mix asphalt design methods, *International Journal of Pavement Engineering*, VOL. 13, pp. 89–97. https://doi.org/10.1080/10298436.2011.565765

ALDOT (2018). *Standard Specifications for Highway Construction,* Montgomery, AL.

ALDOT (2016). *ALDOT-384 Superpave Mix Design Procedure for Asphalt Mixtures*, Montgomery, AL.

ALDOT (2008a). *ALDOT-395 Stone Matrix Asphalt Mix Design*, Montgomery, AL.

ALDOT (2008b). *ALDOT-361 Resistance of Compacted Hot-Mix Asphalt to Moisture Induced Damage*, Montgomery, AL.

ALDOT (2001). *ALDOT-401 Rutting Susceptibility Determination of Asphalt Paving Mixtures Using the Asphalt Pavement Analyzer*, Montgomery, AL.

ALDOT (1999). *ALDOT-259 Open-Graded Asphalt Concrete Friction Course Design Method*, Montgomery, AL.

Ali, U.M. (2018). *Evaluating the Cracking Resistance of a Superpave 5 mix and a Conventional Superpave Mix Using the Illinois Flexibility Index Test*, University of Illinois at Urbana-Champaign, IL.

Al-Qadi, I.L., H. Ozer, and J. Lambros (2019). *Development of the Illinois Flexibility Index Test*, *Relationship Between Laboratory Cracking Tests and Field Performance of Asphalt Mixtures,* Transportation Research Circular, Transportation Research Board, Washington, DC, pp. 31–50.

Al-Qadi, I.L., H. Ozer, J. Lambros, A. El Khatib, P. Singhvi, T. Khan, J. Rivera-Perez, and B. Doll (2015). *Testing Protocols to Ensure Performance of High Asphalt Binder Replacement Mixes Using RAP and RAS*, No. FHWA-ICT-15-017, Illinois Center for Transportation, Urbana, IL.

Al-Qadi, I.L., S. Wu, D.L. Lippert, H. Ozer, M.K. Barry, and F.R. Safi (2017). Impact of high recycled mixed on HMA overlay crack development rate, *Road Materials and Pavement Design*, No. 18, pp. 311–327.

Anderson, D.A., G.A. Huber, D.E. Walker, and X. Zhang (2000). Mixture Testing, Analysis, and Field Performance of the Pilot Superpave Projects: The 1992 SPS-9 Mixtures, *Journal of the Association of Asphalt Paving Technologists*, No. 69, 177–211.

Arámbula-Mercado, E., S. Caro, C.A.R. Torres, P. Karki, M. Sánchez-Silva, and E.S. Park (2019). *Evaluation of FC-5 with PG 76-22 HP to Reduce Raveling*, FDOT Project Report BE287, Texas A&M Transportation Institute, College Station, TX.

Arámbula-Mercado, E., R.A. Hill, S. Caro, L. Manrique, E.S. Park, and E. Fernando (2016). *Understanding Mechanisms of Raveling to Extend Open Graded Friction Course (OGFC) Service Life*, Report No. FDOT-BDR74-977-04, Texas A&M Transportation Institute, College Station, TX.

Asphalt Institute (2015). *MS-2 Asphalt Mix Design Methods*, 7th ed. Asphalt Institute.

ASTM (2019). *ASTM D8225 Standard Test Method for Determination of Cracking Tolerance Index of Asphalt Mixture Using the Indirect Tensile Cracking Test at Intermediate Temperature*, ASTM International, West Conshohocken, PA.

ASTM (2018). *ASTM D8237 Standard Test Method for Determining Fatigue Failure of Asphalt-Aggregate Mixtures with the Four-Point Beam Fatigue Device*, ASTM International, West Conshohocken, PA.

ASTM (2016). *ASTM D8044 Standard Test Method for Evaluation of Asphalt Mixture Cracking Resistance using the Semi-Circular Bend Test (SCB) at Intermediate Temperatures*, ASTM International, West Conshohocken, PA.

ASTM (2015). *ASTM D1560 Standard Test Methods for Resistance to Deformation and Cohesion of Asphalt Mixtures by Means of Hveem Apparatus*, ASTM International, West Conshohocken, PA.

Azari, H. and A. Mohseni (2013). Permanent Deformation Characterization of Asphalt Mixtures by Using Incremental Repeated Load Testing, *Transportation Research Record*, No. 2373, 134–142. https://doi.org/10.3141/2373-14

Barry, M.K. (2016). *An Analysis of Impact Factors on the Illinois Flexibility Index Test,* Thesis, University of Illinois at Urbana-Champaign, Urbana, IL.

Batioja-Alvarez, D., J. Lee, and J.E. Haddock (2019). Understanding the Illinois Flexibility Index Test (I-FIT) using Indiana Asphalt Mixtures, *Transportation Research Record*, https://doi.org/10.1177/0361198119841282

Baumgardner, G.L., J.M. Hemsley, W. Jordan, and I.L. Howard (2012). Laboratory evaluation of asphalt mixtures containing dry added ground tire rubber and a processing aid, *Journal of The Association of Asphalt Paving Technologists,* No. 81, pp. 507–539.

Bonaquist, R. (2012). *Evaluation of Flow Number (FN) as a Discriminating HMA Mixture Property*, Final Report No. WHRP 12-01, Advanced Asphalt Technologies, LLC, Sterling, VA.

Button, J.W., D. Perdomo, and R.L. Lytton (1990). Influence of Aggregate on Rutting in Asphalt Concrete Pavements, *TRR*, Transportation Research Board, No. 1259, pp. 141–152.

Chehab, G.R. (2002). *Characterization of asphalt concrete in tension using a viscoelastoplastic model*, PhD Dissertation, North Carolina State University, Raleigh, NC.

Choubane, B., S. Gokhale, G. Sholar, and H. Moseley (2006). Evaluation of Coarse- and Fine-Graded Superpave Mixtures under Accelerated Pavement Testing. *Transportation Research Record*, No. 1974, pp. 120–127.

Chowdhury, A. and J.W. Button (2002). *Evaluation of Superpave Shear Test Protocols*, Report No. FHWA/TX-02/1819-1, Texas A&M Transportation Institute, College Station, TX.

Cooley, L.A., J.W. Brumfield, R.B. Mallick, W.S. Mogawer, M. Partl, L. Poulikakos, and G. Hicks (2009). *Construction and maintenance practices for permeable friction courses*,

No. NCHRP Report 640, National Cooperative Highway Research Program, Washington, DC.
Cox, B.C., B.T. Smith, I.L. Howard, and R.S. James (2017). State of Knowledge for Cantabro Testing of Dense Graded Asphalt, *Journal of Materials in Civil Engineering*, No. 29, 04017174. https://doi.org/10.1061/(ASCE)MT.1943-5533.0002020
Deacon, J.A. (1965). *Fatigue of Asphalt Concrete. Institute of Transportation and Traffic Engineering*, University of California.
Doyle, J. and I.L. Howard (2016). Characterization of Dense-Graded Asphalt with the Cantabro Test, *Journal of Testing and Evaluation*, No. 44, pp. 77–88. https://doi.org/10.1520/JTE20140212
Doyle, J.D. and I.L. Howard (2011). *Evaluation of the Cantabro Durability Test for Dense Graded Asphalt*, Proceedings of Geo-Frontiers 2011, Advances in Geotechnical Engineering Geotechnical Special Publication No. 211, ASCE, Reston, VA, pp. 4563–4572. https://doi.org/10.1061/41165(397)467
FDOT (2022a). *Standard Specifications for Road and Bridge Construction*, Tallahassee, FL.
FDOT (2022b). *Flexible Pavement Design Manual*, Tallahassee, FL.
FDOT (2020). *Standard Specifications for Road and Bridge Construction*, Tallahassee, FL.
Fwa, T.F., H.R. Pasindu and G.P. Ong (2012). Critical Rut Depth for Pavement Maintenance Based on Vehicle Skidding and Hydroplaning Consideration, *Journal of Transportation Engineering*, No. 138, pp. 423–429.
GDOT (2020a). *GDT 114 Determining Optimum Asphalt Content for Open-graded Bituminous Paving Mixtures*, Atlanta, GA.
GDOT (2020b). *GDT 56 Heat Stable Anti-Strip Additive*, Atlanta, GA.
GDOT (2020c). *GDT 115 Determining Rutting Susceptibility Using The Loaded Wheel Tester*, Atlanta, GA.
GDOT (2019). *Standard Operating Procedure (SOP) 2: Control of Superpave Bituminous Mixture Designs*, Atlanta, GA.
GDOT (2018). *Interdepartment Correspondence: Criteria for Use of Asphaltic Concrete Layer and Mix Types*, Atlanta, GA.
GDOT (2013). *Standard Specifications for Construction of Transportation Systems*, Atlanta, GA.
GDOT (2011a). *GDT 1 Measurement of Water Permeability of Compacted Asphalt Paving Mixtures*, Atlanta, GA.
GDOT (2011b). *GDT 66 Evaluating the Moisture Susceptibility of Bituminous Mixtures by Diametral Tensile Splitting*, Atlanta, GA.
Germann, F.P.and R.L. Lytton (1979). *Methodology for predicting the reflection cracking life of asphalt concrete overlays*, Interim Report. Texas A&M University, College Station, TX.
Golalipour, A., E. Jamshidi, Y. Niazi, Z. Afsharikia, and M. Khadem (2012). Effect of Aggregate Gradation on Rutting of Asphalt Pavements, *Procedia—Social and Behavioral Sciences*, No. 53, pp. 440–449.
Greene, J. and B. Choubane (2016). *Thickness and Binder Type Evaluation of a 4.75 mm Asphalt Mixture using Accelerated Pavement Testin*, Report No. FL/DOT/SMO/16-578, Florida Department of Transportation, Gainesville, FL.
Hernandez-Fernandez, N., B.S. Underwood and A. Ossa-Lopez (2020). Simulation of the asphalt concrete stiffness degradation using simplified viscoelastic continuum damage model, *International Journal of Fatigue*, https://doi.org/10.1016/j.ijfatigue.2020.105850

Huber, G. (2013). *History of Asphalt Mix Design in North America*, Asphalt Magazine, Vol. 28.
Kandhal, P.S. and L. Cooley (2002). Coarse- Versus Fine-Graded Superpave Mixtures: Comparative Evaluation of Resistance to Rutting, *Transportation Research Record*, No. 1789, pp. 216–224, https://doi.org/10.3141/1789-24
Kandhal, P.S. and L.A., Cooley (2003). *Accelerated Laboratory Rutting Tests: Evaluation of the Asphalt Pavement Analyzer*, Final Report No. NCHRP Report 508, National Center for Asphalt Technology, Auburn, AL.
Karki, P., A. Bhasin, and B.S. Underwood (2016). Fatigue performance prediction of asphalt composites subjected to cyclic loading with intermittent rest periods, *TRR*, Transportation Research Board, No. 2576, pp. 72–82. https://doi.org/10.3141/2576-08
Karki, P., R. Li, and A. Bhasin (2014). Quantifying overall damage and healing behavior of asphalt materials using continuum damage approach, *International Journal of Pavement Engineering*, No. 16, pp. 350–362.
Karki, P., L. Meng, S. Im, C. Estakhri, and F. Zhou (2019). Re-refined engine oil bottom: Detection and upper limits in asphalt binders and seal coat binders, Final Report No. FHWA/TX-18/0-6881-1, Texas A&M Transportation Institute, College Station, TX.
Kaseer, F., F. Yin, E. Arámbula-Mercado, A. Epps Martin, J.S. Daniel, and S. Salari (2018). Development of an index to evaluate the cracking potential of asphalt mixtures using the semi-circular bending test, *Construction and Building Materials*, No. 167, pp. 286–298. https://doi.org/10.1016/j.conbuildmat.2018.02.014
Kim, M., L.N. Mohammad and M.A. Elseifi (2012). Characterization of Fracture Properties of Asphalt Mixtures as Measured by Semicircular Bend Test and Indirect Tension Test, *Transportation Research Record*, No. 2296, pp. 115–124.
Kim, Y.R., Y.C. Lee, and H.J. Lee (1995). Correspondence principle for characterization of asphalt concrete, *Journal of Materials in Civil Engineering*, No. 7, pp. 59–68.
Kingham, R.I. (1972). *Failure Criteria from AASHO Road Test Data*, Proceedings of the Third International Conference on the Structural Design of Asphalt Pavements, London, UK, pp. 656–669.
Kutay, M.E., N.H. Gibson, and J.S. Youtcheff (2008). Conventional and viscoelastic continuum damage (VECD)-based fatigue analysis of polymer modified asphalt pavements, *Journal of the Association of Asphalt Paving Technologists*, No. 77, pp. 395–434.
LaDOTD (2018). *Supplemental Specifications Part V—Asphalt Pavements*, Baton Rouge, LA.
LaDOTD (2016). *Standard Specifications for Roads and Bridges*, Baton Rouge, LA.
Lai, J.S. (1986). *Development of a Simplified Test Method to Predict Rutting Characteristics of Asphalt Mixes*, GDOT Research Project 8502, Georgia Institute of Technology, Atlanta, GA.
Little, D.N. and K. Mahboub (1985). Engineering Properties of First Generation Plasticized Sulfur Binders and Low Temperature Fracture Evaluation of Plasticized Sulfur Paving Mixtures, *Transportation Research Record*, Transportation Research Board, No. 1034, pp. 103–111.
Lytton, R.L., J. Uzan, E.G. Fernando, R. Roque, D.R. Hiltunen, and S.M. Stoffels (1993). *Development and validation of performance prediction models and specifications for asphalt binders and paving mixes*, No. SHRP-A-357, National Research Council, Washington, DC.

Ma, W. (2014). *Proposed Improvements to Overlay Test for Determining Cracking Resistance of Asphalt Mixtures*, Thesis, Auburn University, Auburn, AL.
MDOT (2017). *Standard Specifications for Road and Bridge Construction*, Jackson, MS.
MDOT (2010a). *MT-78 Volumetric Design of Hot Bituminous Paving Mixtures Using The Superpave Gyratory Compactor*, Materials Division Inspection, Testing and Certification Manual, Jackson, MS.
MDOT (2010b). *MT-83 Mix Design of Open Graded Friction Course Hot Mix Asphalt,* Materials Division Inspection, Testing and Certification Manual, Jackson, MS.
MDOT (2010c). MT-80 *Volumetric Mix Design Procedure for Stone Matrix Asphalt*, Materials Division Inspection, Testing and Certification Manual, Jackson, MS.
MDOT (2010d). *MT-82 Drain down Testing of Stone Matrix Asphalt Mixtures*, Materials Division Inspection, Testing and Certification Manual, Jackson, MS.
MDOT (2010e). *MT-84 Permeability of Open Graded Friction Course Asphalt Mixtures*, Materials Division Inspection, Testing and Certification Manual, Jackson, MS.
MDOT (2010f.) *MT-85 Abrasion Testing of Open Graded Friction Course Asphalt Mixture*, Materials Division Inspection, Testing and Certification Manual, Jackson, MS.
MDOT (2010g). *MT-63 Resistance of Bituminous Paving Mixtures to Stripping (Vacuum Saturation Method)*, Materials Division Inspection, Testing and Certification Manual, Jackson, MS.
MDOT (2010h). *MT-59 Determination of Loss of Coating of HMA (Boiling Water Test)*, Materials Division Inspection, Testing and Certification Manual, Jackson, MS.
Mogawer, W., J.S. Daniel, and A.J. Austerman (2010). *Relating Hot Mix Asphalt Pavement Density to Performance*, No. NETCR76, The New England Transportation Consortium, Fall River, MA.
Mogawer, W.S., A.J. Austerman, J.S. Daniel, F. Zhou, and T. Bennert (2011). Evaluation of the effects of hot mix asphalt density on mixture fatigue performance, rutting performance and MEPDG distress predictions, *International Journal of Pavement Engineering*, No. 12, pp. 161–175, https://doi.org/10.1080/10298436.2010.546857
Monismith, C.L., K.E. Secor, and E.W. Blackmer (1961). Asphaltic mixture behaviour in repeated flexure, *Journal of AAPT*, No. 30, pp. 188–222.
Monismith, C.L. and A.A. Tayebali (1994). *Permanent Deformation Response of Asphalt Aggregate Mixes*, No. SHRP A-415, Strategic Highway Research Program, Washington, DC.
Mull, M.A., K. Stuart, and A. Yehia (2002). Fracture resistance characterization of chemically modified crumb rubber asphalt pavement, *Journal of Materials Science*, No.37, pp. 557–566, https://doi.org/10.1023/A:1013721708572
NAPA (2002). IS-115: *Design, Construction, and Maintenance of Open-Graded Asphalt Friction Courses*, Lanham, MD.
NCHRP (2011). *A Manual for Design of Hot Mix Asphalt with Commentary*, No. NCHRP Report 673, Transportation Research Board, Washington DC.
Nekkanti, H., B.J., Putman, B., Danish (2019). Influence of Aggregate Gradation and Nominal Maximum Aggregate Size on the Performance Properties of OGFC Mixtures, *Transportation Research Record*, No. 2673, pp. 240–245.
Ozer, H., I.L. Al-Qadi, J. Lambros, A. El-Khatib, P. Singhvi, and B. Doll (2016a). Development of the fracture-based flexibility index for asphalt concrete cracking potential using

modified semi-circle bending test parameters, *Construction and Building Materials*, No. 115, pp. 390–401.

Ozer, H., I.L. Al-Qadi, P. Singhvi, T. Khan, J. Rivera-Perez, and A. El-Khatib (2016b). Fracture Characterization of Asphalt Mixtures with High Recycled Content Using Illinois Semicircular Bending Test Method and Flexibility Index, *Transportation Research Record*, Transportation Research Board, No. 2575, pp. 130–137.

Powell, R. (2006). *Predicting Field Performance on the NCAT Pavement Test Track*, PhD Dissertation, Auburn University, Auburn, AL.

Romero, P. and W. Mogawer (1998). Evaluation of the Superpave Shear testing Using 19-mm Mixtures from the Federal Highway Administration's Accelerated Loading Facility, *Journal of the Association of Asphalt Paving Technologists*, No. 67, pp. 573–601.

Roque R.(2015). *Draft AASHTO Tensile Creep Compliance, Tensile Failure Limits and Energy Ratio of Asphalt Mixtures Using the Superpave Indirect Tension (IDT) Test.*

Roque, R., B. Birgisson, C. Drakos, and B. Dietrich (2004). Development and Field Evaluation of Energy-Based Criteria for Top-down Cracking Performance of Hot Mix Asphalt, *Journal of the Association of Asphalt Paving Technologist*, No. 73, pp. 229–260.

SCDOT (2019a). *Supplemental Specification for Open-Graded Friction Course*, Columbia, SC.

SCDOT (2019b). *SC-T-90 Standard Method of Test for Determining Drain-Down Characteristics in an Uncompacted Asphalt Mixture*, Columbia, SC.

SCDOT (2018a). *SC-M-402 Supplemental Technical Specification for Hot-Mix Asphalt Material Properties*, Columbia, SC.

SCDOT (2018b). *SC-T-70 Laboratory Determination of Moisture Susceptibility Based on Retained Strength of Asphalt Concrete Mixture*, Columbia, SC.

SCDOT (2013). *SC-T-127 Standard Method of Test for Abrasion Resistance of Open Graded Friction Course (OGFC) Mixtures*, Columbia, SC.

SCDOT (2007). *Specifications for Highway Construction*, Columbia, SC.

Schapery, R.A. (1984). Correspondence principles and a generalized J integral for large deformation and fracture analysis of viscoelastic media, *International Journal of Fracture,* No. 25, pp. 195–223.

Tavakol, M., M. Hossain, and B. Heptig (2018). Minimum Virgin Binder Content Needed in Recycled Superpave Mixtures to Resist Fatigue Cracking and Moisture Damage, *Journal of Materials in Civil Engineering*, https://doi.org/10.1061/(ASCE)MT.1943-5533.0002314

Tayebali, A.A., J.A. Deacon, J.S. Coplantz, F.N. Finn, and C.L. Monismith (1994). *Fatigue Response of Asphalt-Aggregate Mixes, Part II: Extended Test Program*, No. SHRP-A-404, National Research Council, Washington, DC.

Tayebali, A.A., N.P. Khosla, G.A. Malpass and H.F. Waller (1999). Evaluation of Superpave Repeated Shear at Constant Height Test to Predict Rutting Potential of Mixes: Performance of Three Pavement Sections in North Carolina, *Transportation Research Record*, No. 1681, pp. 97–105, https://doi.org/10.3141/1681-12

Taylor, A.J. (2018). *Cracking Group Experiment-Laboratory Results*, National Center for Asphalt Technology, http://www.pavetrack.com/180327/23.pdf

TDOT (2015). *Standard Specifications for Road and Bridge Construction*, Nashville, TN.

Timm, D.H., G.A. Sholar, J. Kim, and J.R. Willis (2009). Forensic Investigation and Validation of Energy Ratio Concept, *Transportation Research Record*, No. 2127, pp. 43–51. https://doi.org/10.3141/2127-06

Tsai, B.W., A. Fan, J.T. Harvey, and C.L. Monismith (2012). *Improved Methodology for Mix Design of Open-Graded Friction Courses*, No. UCPRC-RR-2013-06, University of California Pavement Research Center.

TxDOT (2017). Tex-248-F Test Procedure for Overlay Test, Austin, TX.

Underwood, B.S., C. Baek, and Y.R., Kim, 2012. Simplified Viscoelastic Continuum Damage Model as Platform for Asphalt Concrete Fatigue Analysis, *Transportation Research Record*, No. 2296, pp. 36–45. https://doi.org/10.3141/2296-04

Underwood, B.S. and Y.R. Kim (2012). Simplified viscoelastic continuum damage model as an asphalt concrete fatigue analysis platform, *Transportation Research Record*, Transportation Research Board, No. 2296, pp. 36–45.

Underwood, B.S., Y.R. Kim, and M.N. Guddati (2010). Improved calculation method of damage parameter in viscoelastic continuum damage model, *International Journal of Pavement Engineering*, No. 11, pp. 459–476.

Underwood, S. and A. Braham (2019). *Fatigue or Not Fatigue: That is The Question—A White Paper*, DOI:10.13140/RG.2.2.13898.41921/1

Walubita, L.F., A.N. Faruk, G. Das, H.A. Tanvir, J. Zhang, and T. Scullion (2012a). *The Overlay Tester: A Sensitivity Study to Improve Repeatability and Minimize Variability in the Test Results*, Technical Report No. FHWA/TX-12/0-6607-1, Texas A&M Transportation Institute, College Station, TX.

Walubita, L.F., J. Zhang, G. Das, X. Hu, C. Mushota, A.E. Alvarez, and T. Scullion (2012b). Hot-Mix Asphalt Permanent Deformation Evaluated by Hamburg Wheel Tracking, Dynamic Modulus, and Repeated Load Tests, *Transportation Research Record*, Transportation Research Board, No. 2296, pp. 46–56.

Walubita, L.F., J. Zhang, A.N. Faruk, A.E. Alvarez, and T. Scullion (2014). Laboratory Hot-Mix Asphalt Performance Testing: Asphalt Mixture Performance Tester Versus Universal Testing Machine, *Transportation Research Record*, No. 2447, pp. 61–73.

Wang, Y.D., B.S. Underwood, and Y.R. Kim (2020). Development of a fatigue index parameter, Sapp, for asphalt mixes using viscoelastic continuum damage theory, *International Journal of Pavement Engineering*, pp. 1–15.

West, R., C. Rodezno, F. Leiva, and A. Taylor (2018a). *Regressing Air Voids for Balanced HMA Mix Design*, Wisconsin DOT No. 0092-16– 06, National Center for Asphalt Technology at Auburn University, Auburn, AL.

West, R., C. Rodezno, F. Leiva, and F. Yin (2018b). *Development of a Framework for Balanced Mix Design*, No. Final Report NCHRP 20-07/Task 406, National Center for Asphalt Technology, Auburn, AL.

West, R., D. Timm, B. Powell, M. Heitzman, N. Tran, C. Rodezno, D. Watson, F. Leiva, and A. Vargas (2018c). *Phase VI (2015-2018) NCAT Test Track Findings*, No. NCAT Draft Report 18-04, National Center for Asphalt Technology (NCAT), Auburn, AL.

Williams, R.C. and B.D., Prowell (1999). Comparison of Laboratory Wheel-Tracking Test Results with WesTrack Performance, *Transportation Research Record*, Transportation Research Board, No. 1681, pp. 121–128.

Willis, J.R., C. Rodezno, A. Taylor, and N. Tran (2014). *Evaluation of a Rubber-Modified Mixture in Alabama*, Interim Report No. NCAT Report 14-03, National Center for Asphalt Technology (NCAT), Auburn, AL.

Witczak, M.W., K. Kaloush, T. Pellinen, M. El-Basyouny, and H. Von Quintus (2002). *Simple Performance Test for Superpave Mix Design*, No. NCHRP Report 465, Transportation Research Board, Washington DC.

Wu, Z., L. Mohammad, L. Wang, and M. Mull (2005). Fracture Resistance Characterization of Superpave Mixtures Using the Semi-Circular Bending Test, *Journal of ASTM International*, No. 2, pp. 1–15. https://doi.org/10.1520/JAI12264

Xie, Z., J. Shen, M. Earnest, B. Li, and M. Jackson (2015). Fatigue Performance Evaluation of Rubberized Porous European Mixture by Simplified Viscoelastic Continuum Damage Model, *Transportation Research Record*, No. 2506, pp. 90–99.

Yan, Y., R. Roque, C. Cocconcelli, M. Bekoe, and G., Lopp (2017). Evaluation of cracking performance for polymer-modified asphalt mixtures with high RAP content, *Road Materials and Pavement Design*, No. 18, pp. 450–470.

Zhang, J., A.E. Alvarez, S.I. Lee, A. Torres, and L.F. Walubita (2013). Comparison of flow number, dynamic modulus, and repeated load tests for evaluation of HMA permanent deformation, *Construction and Building Materials*, No. 44, pp. 391–398.

Zhou, F., B., Crockford, J. Zhang, S. Hu, J. Epps, and L. Sun (2019a). *Development and Validation of an Ideal Shear Rutting Test for Asphalt Mix Design and QC/QA*, Presented at AAPT Annual Meeting, Ft. Worth, TX.

Zhou, F, S. Im, and S. Hu (2019b). *Development and Validation of the IDEAL Cracking Test*, Relationship Between Laboratory Cracking Tests and Field Performance of Asphalt Mixtures, Transportation Research Circular, Transportation Research Board, Washington, DC., pp. 1–21.

Zhou, F., S. Im, S. Hu, D. Newcomb, and T., Scullion (2017a). Selection and Preliminary Evaluation of Laboratory Cracking Tests for Routine Asphalt Mix Designs, *Road Materials and Pavement Design*, No. 18, pp. 62–86.

Zhou, F., S. Im, L. Sun, and T. Scullion (2017b). Development of an IDEAL cracking test for asphalt mix design and QC/QA, *Road Materials and Pavement Design*, No. 18, pp. 405–427. https://doi.org/10.1080/14680629.2017.1389082

Zhou, F. and T. Scullion (2005). *Overlay Tester: A Rapid Performance Related Crack Resistance Test*, Final Report No. FHWA/TX-05/0-4467-2, Texas A&M Transportation Institute, College Station, TX.

Zhou, F. and T. Scullion (2003). *Upgraded Overlay Tester and Its Application to Characterize Reflection Cracking Resistance of Asphalt Mixtures*, Technical Report No. FHWA/TX-04/0-4467-1, Texas A&M Transportation Institute, College Station, TX.

APPENDIX A. MIXTURE DESIGN DATA SHEETS

This appendix presents the design data sheets for the 24 mixtures.

P_b	G_{mb} @ N_{des}	G_{mm}	V_a	VMA	VFA	P_{be}	$P_{0.075}$ / P_{be}	%G_{mm} @ N_{ini}	%G_{mm} @ N_{max}
5.0	2.403	2.572	6.6	16.3	60	4.2	1.3		
5.5	2.440	2.542	4.0	15.4	74	4.8	1.1		
6.0	2.466	2.521	2.2	15.0	85	5.4	1.0		

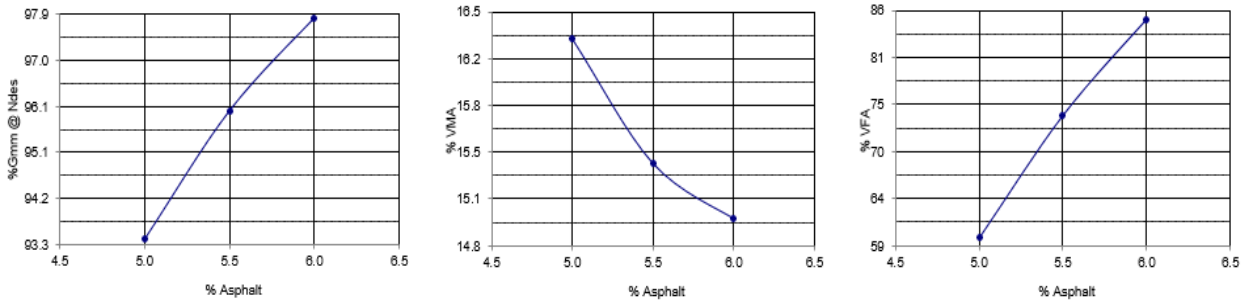

Figure A-1. Design Data Sheet of Granite SP-9.5 PG 67-22 at 50 Gyrations

P_b	G_{mb} @ N_{des}	G_{mm}	V_a	VMA	VFA	P_{be}	$P_{0.075}$ / P_{be}	%G_{mm} @ N_{ini}	%G_{mm} @ N_{max}
5.0	2.429	2.572	5.6	15.4	64	4.2	1.3		
5.5	2.457	2.542	3.4	14.9	77	4.8	1.1		
6.0	2.486	2.521	1.4	14.3	90	5.4	1.0		

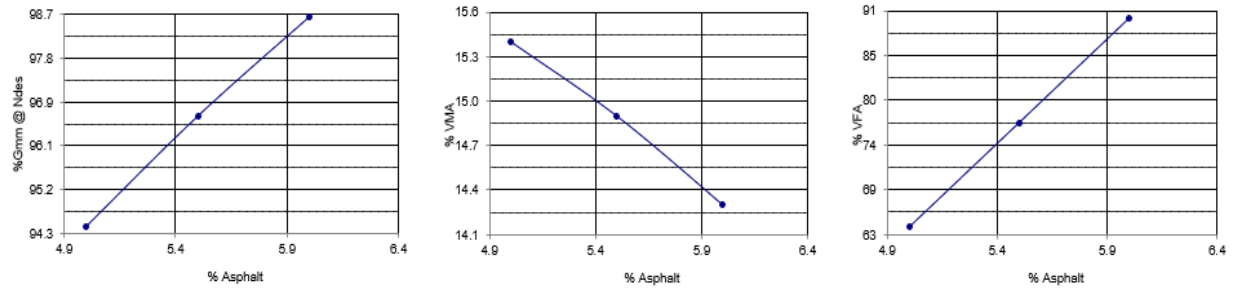

Figure A-2. Design Data Sheet of Granite SP-9.5 PG 67-22 at 75 Gyrations

P_b	G_{mb} @ N_{des}	G_{mm}	V_a	VMA	VFA	P_{be}	$P_{0.075}$ / P_{be}	%G_{mm} @ N_{ini}	%G_{mm} @ N_{max}
5.0	2.442	2.572	5.1	14.9	66	4.2	1.3		
5.5	2.466	2.542	3.0	14.5	79	4.8	1.1		
6.0	2.503	2.521	0.7	13.7	95	5.4	1.0		

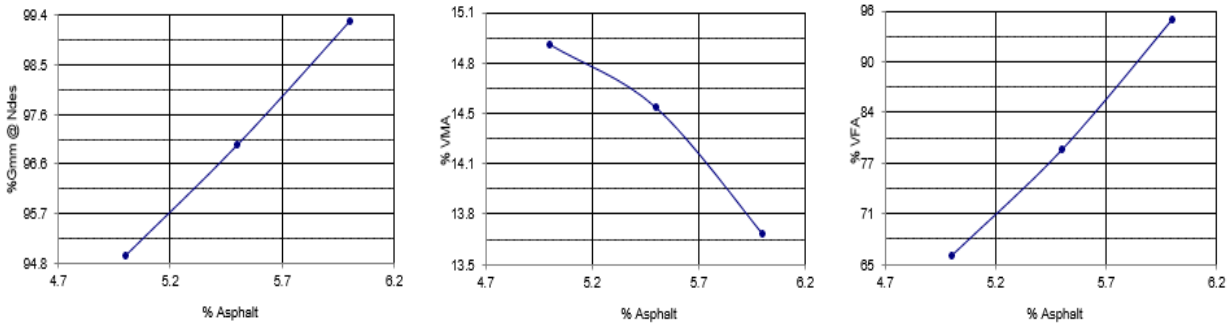

Figure A-3. Design Data Sheet of Granite SP-9.5 PG 67-22 at 100 Gyrations

P_b	G_{mb} @ N_{des}	G_{mm}	V_a	VMA	VFA	P_{be}	$P_{0.075}$ / P_{be}	%G_{mm} @ N_{ini}	%G_{mm} @ N_{max}
4.7	2.417	2.578	6.3	15.6	60	4.0	0.9		
5.2	2.444	2.554	4.3	15.1	72	4.5	0.8		
5.7	2.468	2.532	2.5	14.7	83	5.1	0.7		

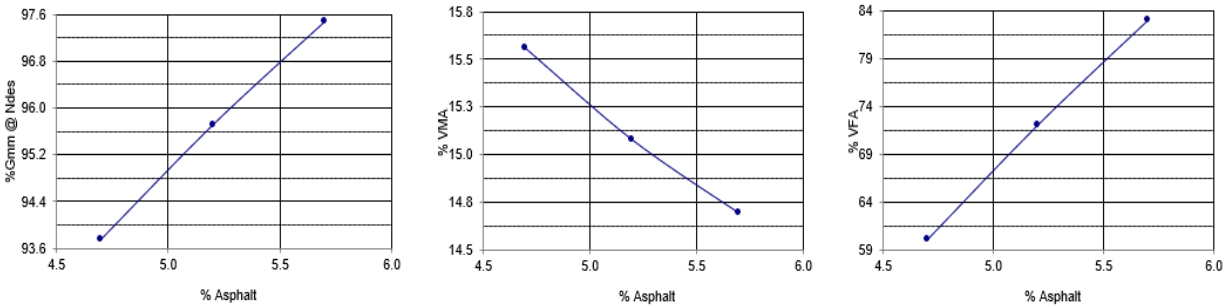

Figure A-4. Design Data Sheet of Granite SP-12.5 PG 67-22 at 50 Gyrations

P_b	G_{mb} @ N_{des}	G_{mm}	V_a	VMA	VFA	P_{be}	$P_{0.075}$ / P_{be}	%G_{mm} @ N_{ini}	%G_{mm} @ N_{max}
4.7	2.435	2.578	5.6	14.9	62	4.0	0.9		
5.2	2.460	2.554	3.7	14.5	74	4.5	0.8		
5.7	2.475	2.532	2.2	14.4	85	5.1	0.7		

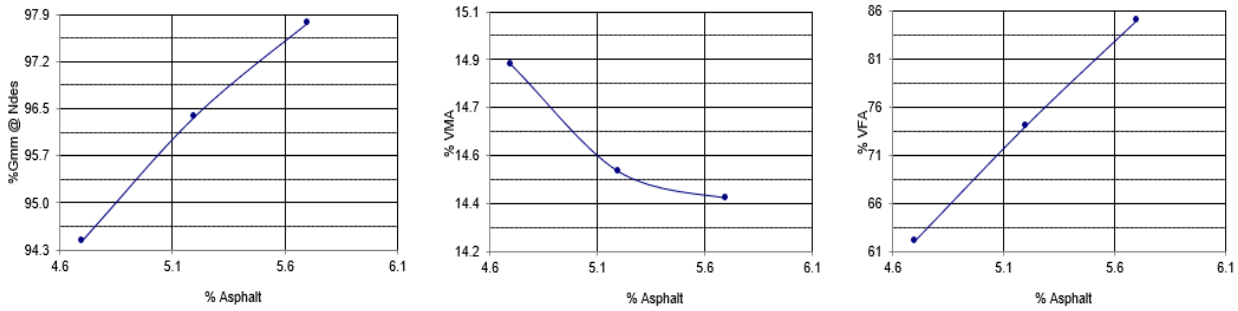

Figure A-5. Design Data Sheet of Granite SP-12.5 PG 67-22 at 75 Gyrations

P_b	G_{mb} @ N_{des}	G_{mm}	V_a	VMA	VFA	P_{be}	$P_{0.075}$ / P_{be}	%G_{mm} @ N_{ini}	%G_{mm} @ N_{max}
4.7	2.452	2.578	4.9	14.3	66	4.0	0.9		
5.2	2.473	2.554	3.2	14.1	77	4.5	0.8		
5.7	2.490	2.532	1.6	13.9	88	5.1	0.7		

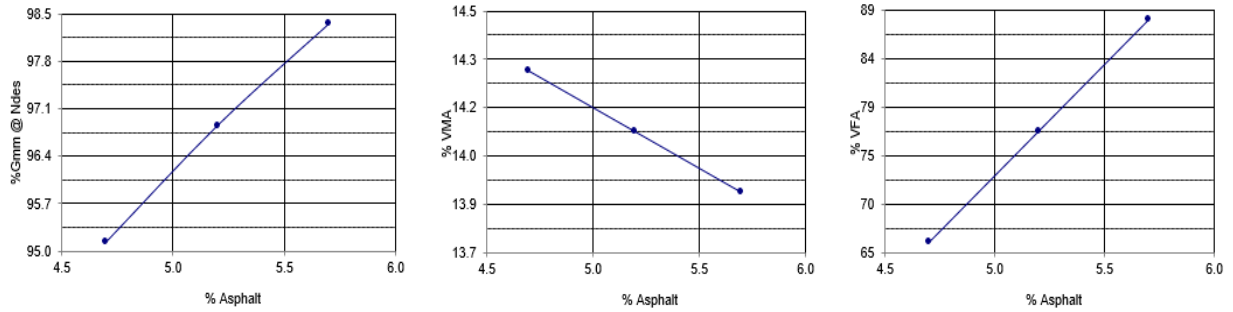

Figure A-6. Design Data Sheet of Granite SP-12.5 PG 67-22 at 100 Gyrations

P_b	G_{mb} @ N_{des}	G_{mm}	V_a	VMA	VFA	P_{be}	$P_{0.075}$ / P_{be}	%G_{mm} @ N_{ini}	%G_{mm} @ N_{max}
6.5	2.221	2.359	5.8	16.8	65	5.1	0.7		
7.0	2.242	2.336	4.0	16.5	76	5.7	0.6		
7.5	2.256	2.327	3.0	16.4	82	6.1	0.6		

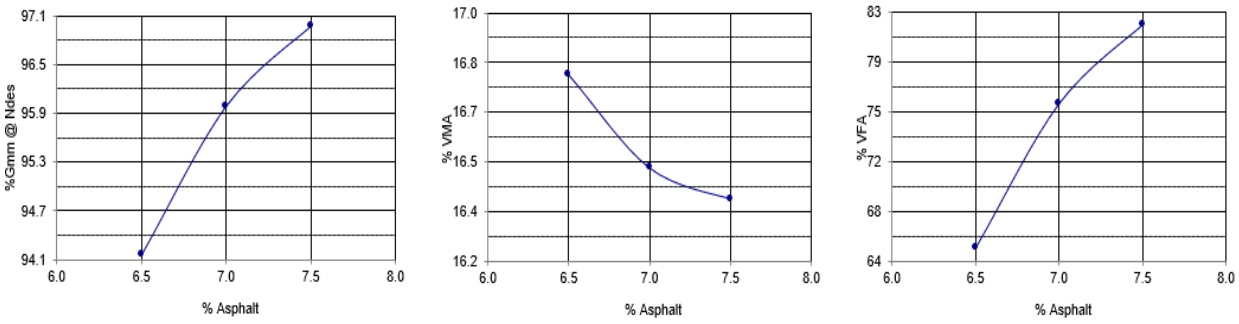

Figure A-7. Design Data Sheet of Limestone SP-9.5 PG 67-22 at 50 Gyrations

P_b	G_{mb} @ N_{des}	G_{mm}	V_a	VMA	VFA	P_{be}	$P_{0.075}$ / P_{be}	%G_{mm} @ N_{ini}	%G_{mm} @ N_{max}
6.5	2.238	2.359	5.1	16.2	69	5.1	0.7		
7.0	2.251	2.336	3.6	16.2	78	5.7	0.6		
7.5	2.262	2.327	2.8	16.2	83	6.1	0.6		

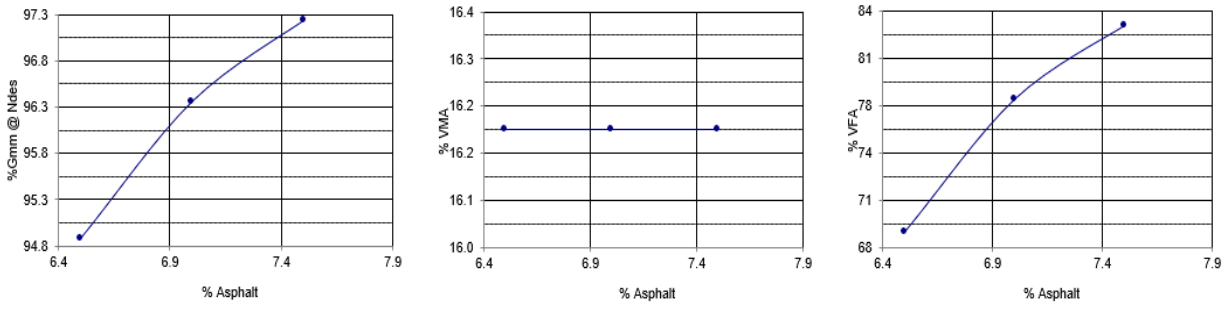

Figure A-8. Design Data Sheet of Limestone SP-9.5 PG 67-22 at 75 Gyrations

P_b	G_{mb} @ N_{des}	G_{mm}	V_a	VMA	VFA	P_{be}	$P_{0.075}$ / P_{be}	%G_{mm} @ N_{ini}	%G_{mm} @ N_{max}
6.5	2.241	2.359	5.0	16.1	69	5.1	0.7		
7.0	2.259	2.336	3.3	15.9	79	5.7	0.6		
7.5	2.269	2.327	2.5	16.0	84	6.1	0.6		

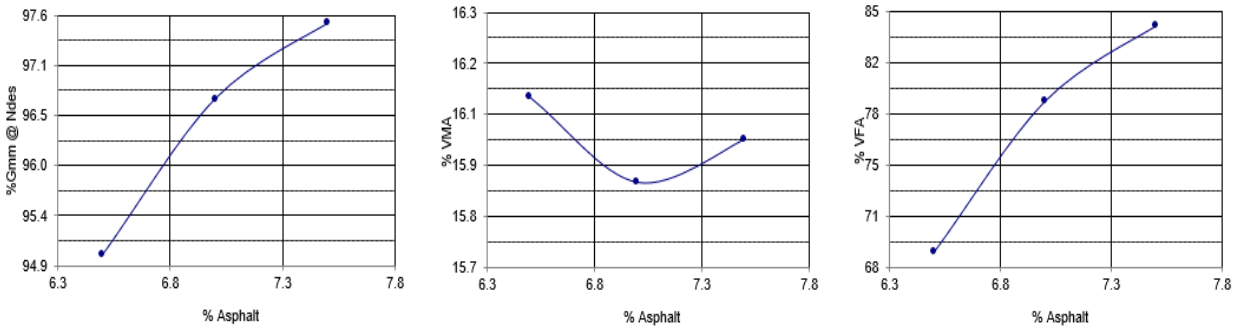

Figure A-9. Design Data Sheet of Limestone SP-9.5 PG 67-22 at 100 Gyrations

P_b	G_{mb} @ N_{des}	G_{mm}	V_a	VMA	VFA	P_{be}	$P_{0.075}$ / P_{be}	%G_{mm} @ N_{ini}	%G_{mm} @ N_{max}
5.5	2.232	2.385	6.4	14.6	56	3.8	0.9		
6.0	2.249	2.361	4.7	14.5	68	4.5	0.8		
6.5	2.265	2.343	3.3	14.3	77	5.0	0.7		

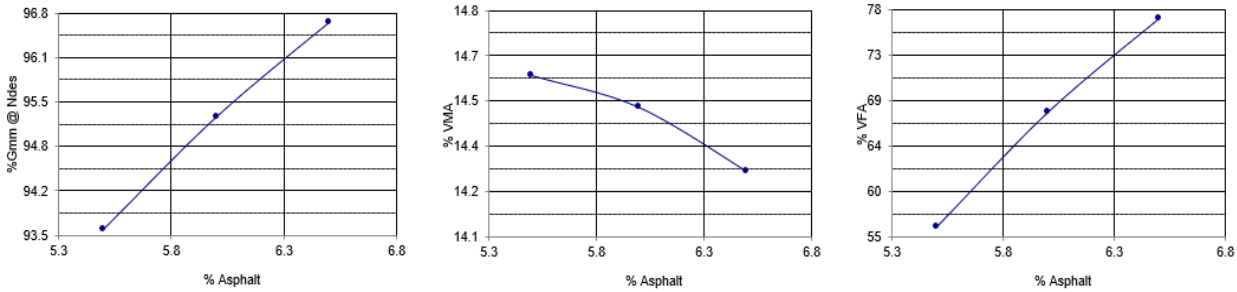

Figure A-10. Design Data Sheet of Limestone SP-12.5 PG 67-22 at 50 Gyrations

P_b	G_{mb} @ N_{des}	G_{mm}	V_a	VMA	VFA	P_{be}	$P_{0.075}$ / P_{be}	$\%G_{mm}$ @ N_{ini}	$\%G_{mm}$ @ N_{max}
5.5	2.246	2.385	5.8	14.1	59	3.8	0.9		
6.0	2.260	2.361	4.3	14.0	69	4.5	0.8		
6.5	2.275	2.343	2.9	13.9	79	5.0	0.7		

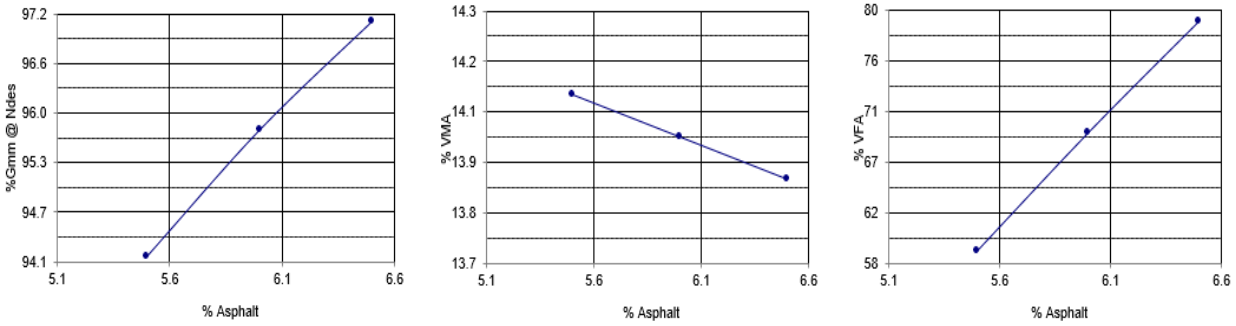

Figure A-11. Design Data Sheet of Limestone SP-12.5 PG 67-22 at 75 Gyrations

P_b	G_{mb} @ N_{des}	G_{mm}	V_a	VMA	VFA	P_{be}	$P_{0.075}$ / P_{be}	$\%G_{mm}$ @ N_{ini}	$\%G_{mm}$ @ N_{max}
5.5	2.255	2.385	5.4	13.8	61	3.8	0.9		
6.0	2.267	2.361	4.0	13.8	71	4.5	0.8		
6.5	2.287	2.343	2.4	13.5	82	5.0	0.7		

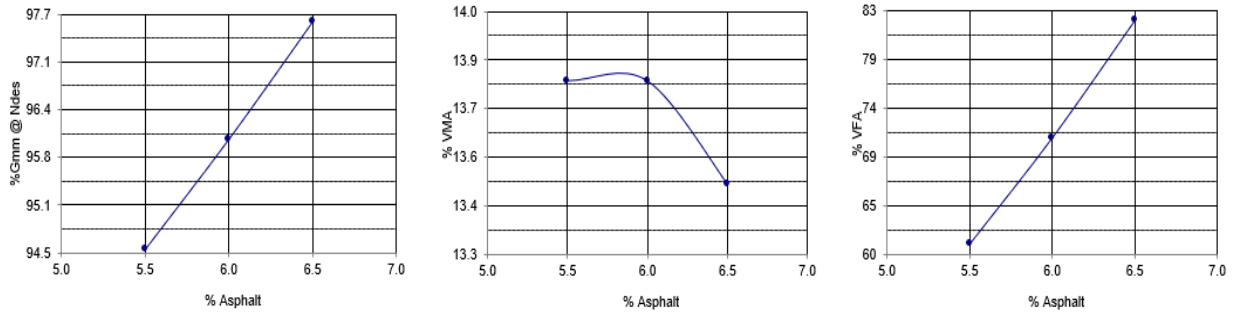

Figure A-12. Design Data Sheet of Limestone SP-12.5 PG 67-22 at 100 Gyrations

P_b	G_{mb} @ N_{des}	G_{mm}	V_a	VMA	VFA	P_{be}	$P_{0.075}$ / P_{be}	$\%G_{mm}$ @ N_{ini}	$\%G_{mm}$ @ N_{max}
5.0	2.409	2.567	6.2	16.1	61	4.2	1.3		
5.5	2.424	2.545	4.8	16.0	70	4.8	1.1		
6.0	2.445	2.521	3.0	15.7	81	5.3	1.0		

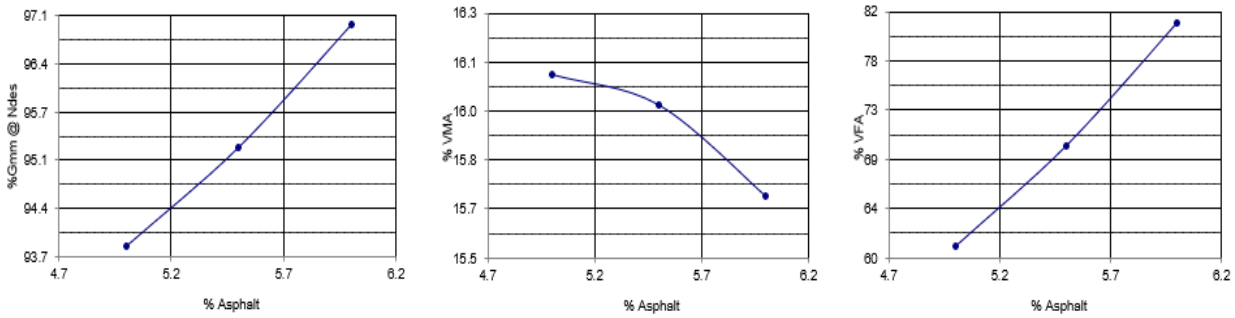

Figure A-13. Design Data Sheet of Granite SP-9.5 PG 76-22 at 50 Gyrations

P_b	G_{mb} @ N_{des}	G_{mm}	V_a	VMA	VFA	P_{be}	$P_{0.075}$ / P_{be}	$\%G_{mm}$ @ N_{ini}	$\%G_{mm}$ @ N_{max}
4.8	2.410	2.576	6.5	15.9	59	4.0	1.4		
5.3	2.443	2.553	4.3	15.2	72	4.6	1.2		
5.8	2.432	2.531	3.9	16.0	76	5.1	1.1		

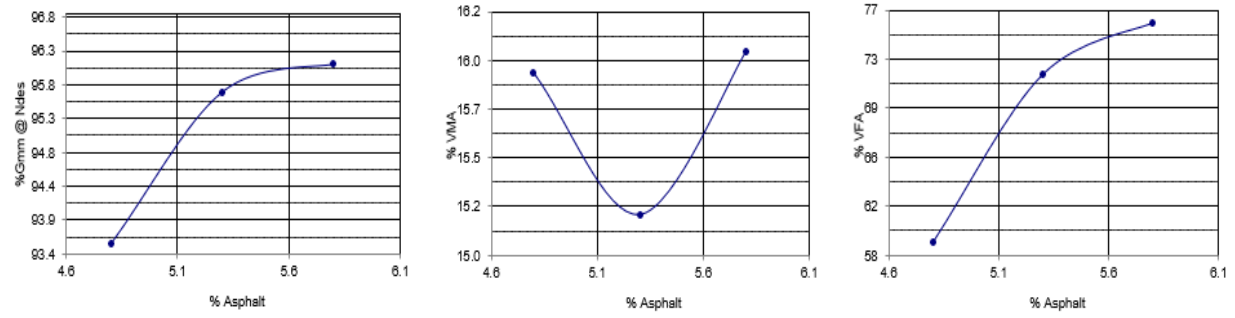

Figure A-14. Design Data Sheet of Granite SP-9.5 PG 76-22 at 75 Gyrations

P_b	G_{mb} @ N_{des}	G_{mm}	V_a	VMA	VFA	P_{be}	$P_{0.075}$ / P_{be}	%G_{mm} @ N_{ini}	%G_{mm} @ N_{max}
4.8	2.429	2.576	5.7	15.2	63	4.0	1.4		
5.3	2.450	2.553	4.0	14.9	73	4.6	1.2		
5.8	2.473	2.531	2.3	14.6	84	5.1	1.1		

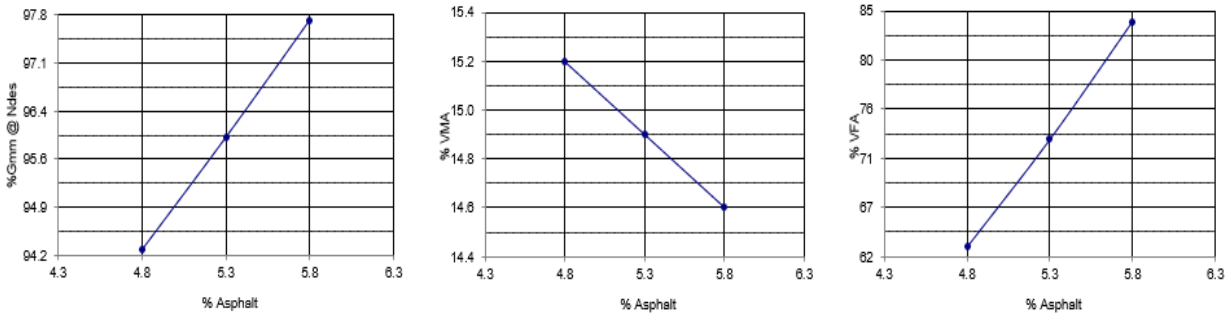

Figure A-15. Design Data Sheet of Granite SP-9.5 PG 76-22 at 100 Gyrations

P_b	G_{mb} @ N_{des}	G_{mm}	V_a	VMA	VFA	P_{be}	$P_{0.075}$ / P_{be}	%G_{mm} @ N_{ini}	%G_{mm} @ N_{max}
5.0	2.401	2.565	6.4	16.4	61	4.3	0.8		
5.5	2.425	2.545	4.7	16.0	71	4.8	0.8		
6.0	2.450	2.520	2.8	15.6	82	5.4	0.7		

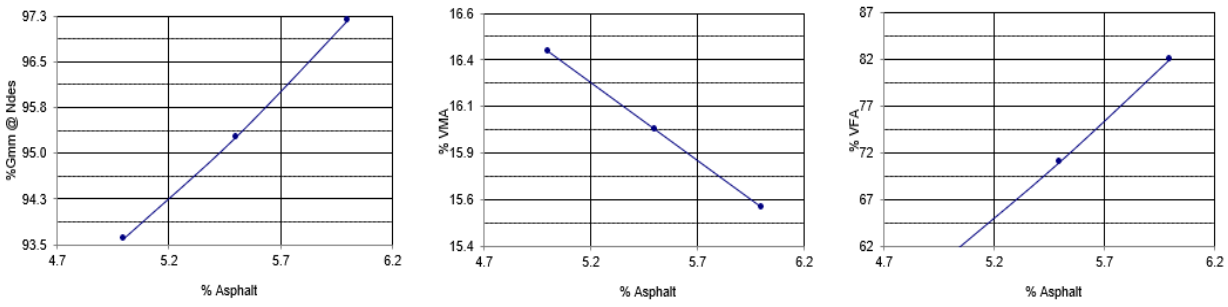

Figure A-16. Design Data Sheet of Granite SP-12.5 PG 76-22 at 50 Gyrations

P_b	G_{mb} @ N_{des}	G_{mm}	V_a	VMA	VFA	P_{be}	$P_{0.075}$ / P_{be}	%G_{mm} @ N_{ini}	%G_{mm} @ N_{max}
4.8	2.416	2.573	6.1	15.7	61	4.1	0.9		
5.3	2.431	2.553	4.8	15.6	69	4.6	0.8		
5.8	2.453	2.533	3.2	15.3	79	5.1	0.7		

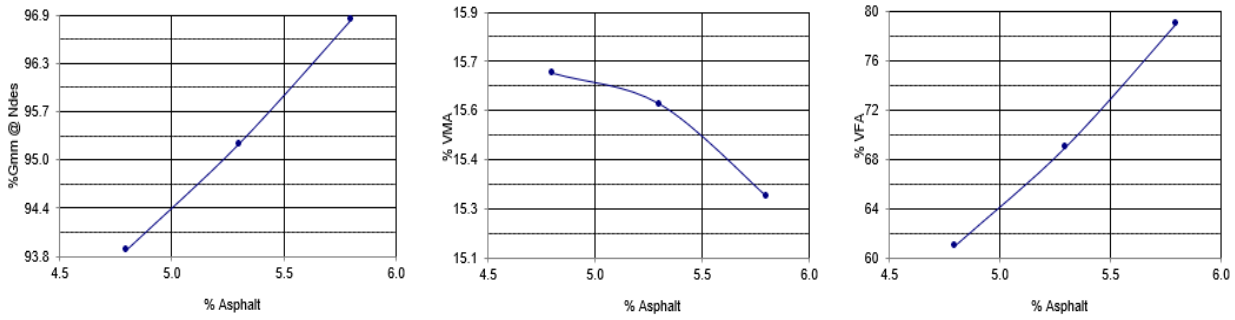

Figure A-17. Design Data Sheet of Granite SP-12.5 PG 76-22 at 75 Gyrations

P_b	G_{mb} @ N_{des}	G_{mm}	V_a	VMA	VFA	P_{be}	$P_{0.075}$ / P_{be}	%G_{mm} @ N_{ini}	%G_{mm} @ N_{max}
4.8	2.430	2.575	5.6	15.2	63	4.1	0.9		
5.3	2.466	2.551	3.3	14.4	77	4.6	0.8		
5.8	2.482	2.532	2.0	14.3	86	5.1	0.7		

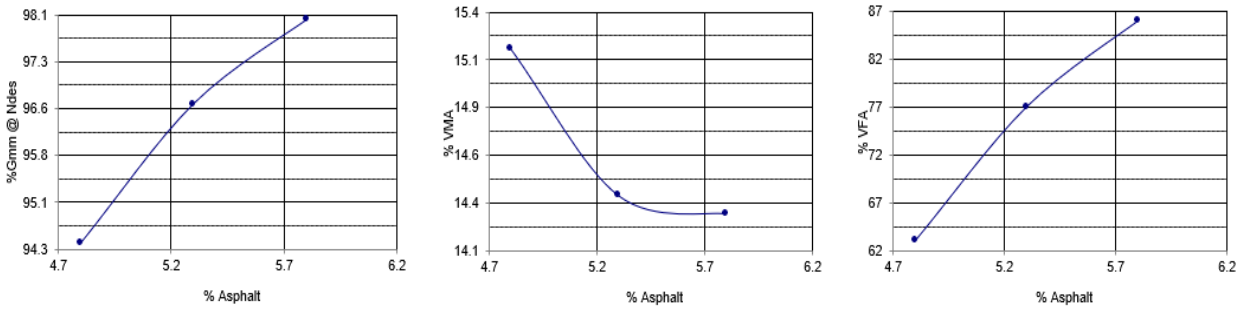

Figure A-18. Design Data Sheet of Granite SP-12.5 PG 76-22 at 100 Gyrations

P_b	G_{mb} @ N_{des}	G_{mm}	V_a	VMA	VFA	P_{be}	$P_{0.075}$ / P_{be}	%G_{mm} @ N_{ini}	%G_{mm} @ N_{max}
6.5	2.217	2.353	5.8	17.0	66	5.2	0.7		
7.0	2.234	2.332	4.2	16.8	75	5.8	0.6		
7.5	2.247	2.318	3.1	16.8	82	6.3	0.6		

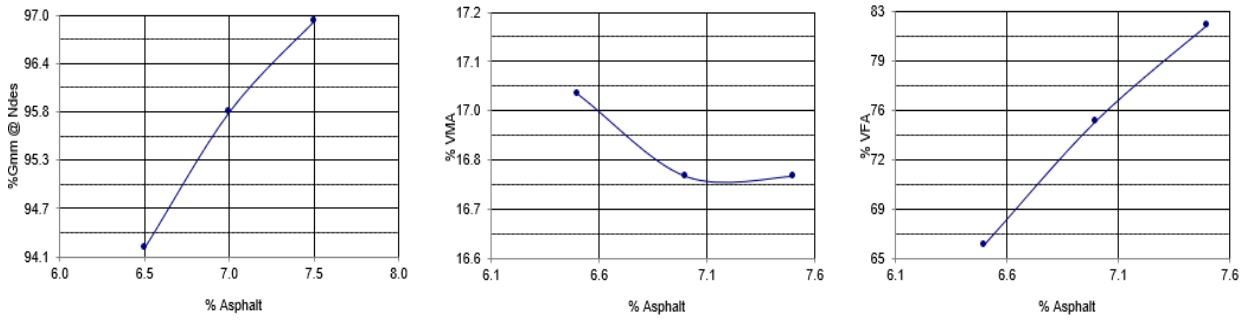

Figure A-19. Design Data Sheet of Limestone SP-9.5 PG 76-22 at 50 Gyrations

P_b	G_{mb} @ N_{des}	G_{mm}	V_a	VMA	VFA	P_{be}	$P_{0.075}$ / P_{be}	%G_{mm} @ N_{ini}	%G_{mm} @ N_{max}
6.6	2.228	2.354	5.3	16.7	68	5.2	0.7		
7.1	2.247	2.328	3.5	16.4	79	5.9	0.6		
7.6	2.262	2.316	2.3	16.3	86	6.3	0.6		

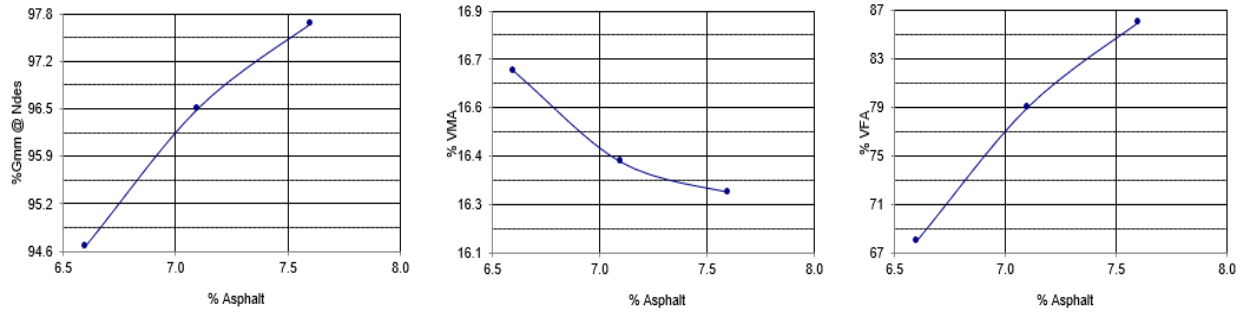

Figure A-20. Design Data Sheet of Limestone SP-9.5 PG 76-22 at 75 Gyrations

P_b	G_{mb} @ N_{des}	G_{mm}	V_a	VMA	VFA	P_{be}	$P_{0.075}$ / P_{be}	%G_{mm} @ N_{ini}	%G_{mm} @ N_{max}
6.5	2.235	2.353	5.0	16.3	69	5.2	0.7		
7.0	2.255	2.332	3.3	16.0	79	5.8	0.6		
7.5	2.269	2.318	2.2	16.0	86	6.3	0.6		

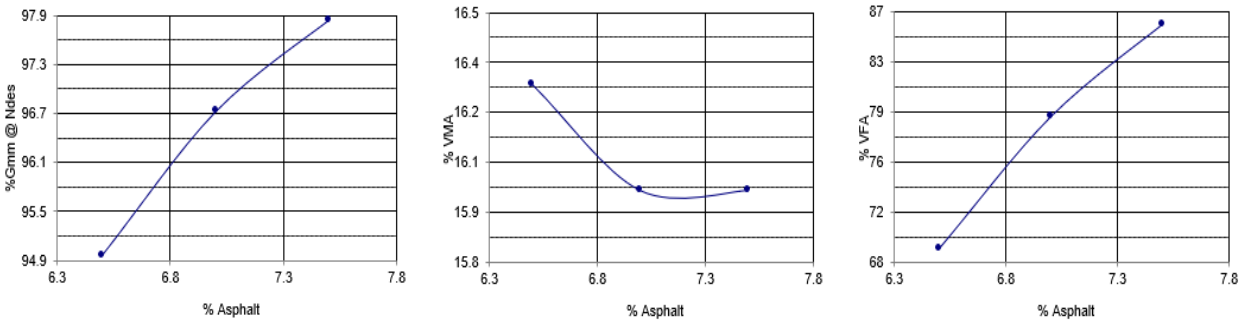

Figure A-21. Design Data Sheet of Limestone SP-9.5 PG 76-22 at 100 Gyrations

P_b	G_{mb} @ N_{des}	G_{mm}	V_a	VMA	VFA	P_{be}	$P_{0.075}$ / P_{be}	%G_{mm} @ N_{ini}	%G_{mm} @ N_{max}
6.0	2.238	2.364	5.3	14.9	64	4.4	0.7		
6.5	2.261	2.339	3.3	14.5	77	5.1	0.6		
7.0	2.260	2.323	2.7	14.9	82	5.6	0.5		

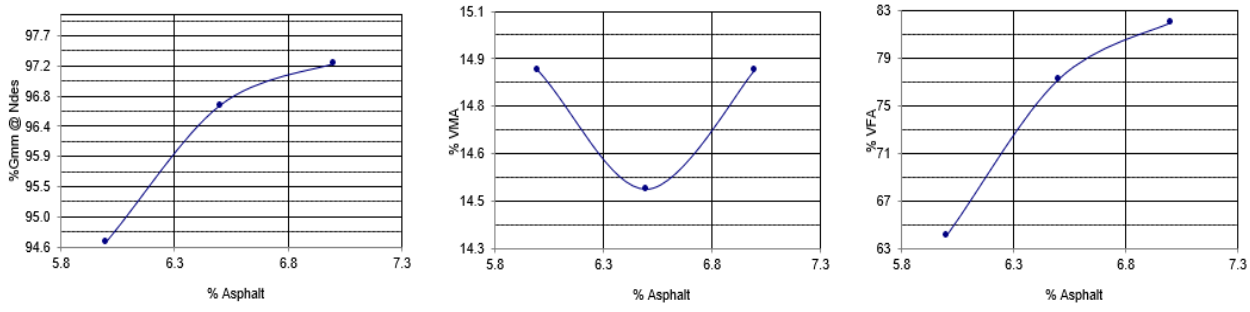

Figure A-22. Design Data Sheet of Limestone SP-12.5 PG 76-22 at 50 Gyrations

P_b	G_{mb} @ N_{des}	G_{mm}	V_a	VMA	VFA	P_{be}	$P_{0.075}$ / P_{be}	%G_{mm} @ N_{ini}	%G_{mm} @ N_{max}
6.0	2.253	2.364	4.7	14.3	67	4.4	0.7		
6.5	2.265	2.339	3.1	14.3	78	5.1	0.6		
7.0	2.272	2.323	2.2	14.5	85	5.6	0.5		

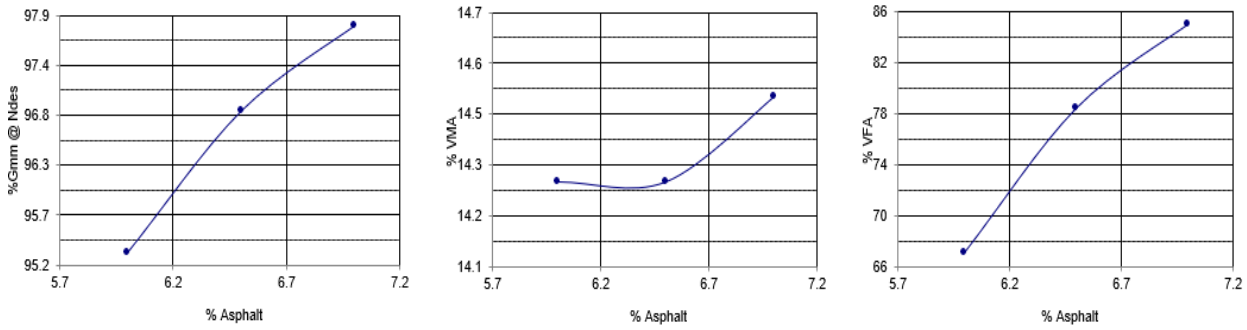

Figure A-23. Design Data Sheet of Limestone SP-12.5 PG 76-22 at 75 Gyrations

P_b	G_{mb} @ N_{des}	G_{mm}	V_a	VMA	VFA	P_{be}	$P_{0.075}$ / P_{be}	%G_{mm} @ N_{ini}	%G_{mm} @ N_{max}
6.0	2.258	2.364	4.5	14.1	68	4.4	0.7		
6.5	2.277	2.339	2.6	13.8	81	5.1	0.6		
7.0	2.278	2.323	1.9	14.3	87	5.6	0.5		

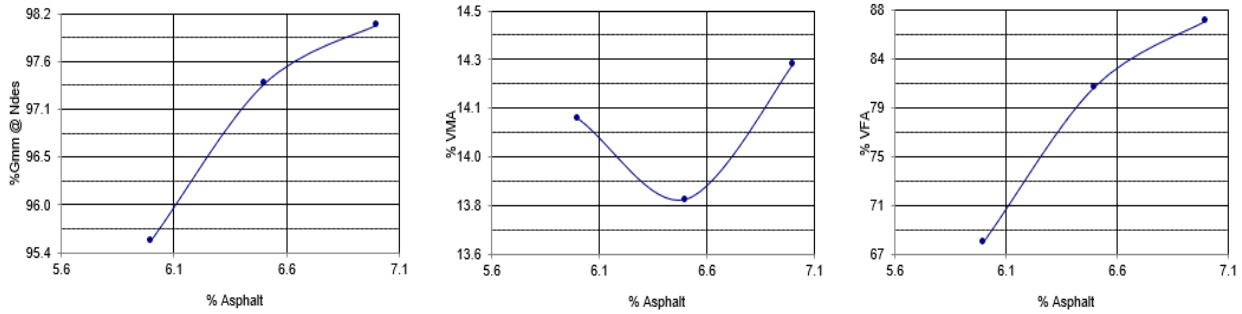

Figure A-24. Design Data Sheet of Limestone SP-12.5 PG 76-22 at 100 Gyrations